1871
ИнБЮМ – IBSS

ISSN 2499-9768 print

МОРСКОЙ БИОЛОГИЧЕСКИЙ ЖУРНАЛ

MARINE BIOLOGICAL JOURNAL

Vol. 10 No. 3

2025

ZOOLOGICAL INSTITUTE OF RAS
A. O. KOVALEVSKY INSTITUTE OF BIOLOGY OF THE SOUTHERN SEAS OF RAS

МОРСКОЙ БИОЛОГИЧЕСКИЙ ЖУРНАЛ

MARINE BIOLOGICAL JOURNAL

2025 Vol. 10 No. 3

Established in February 2016 SCIENTIFIC JOURNAL *4 issues per year*

CONTENTS

Scientific communications

Notes

1871
ИнБЮМ – IBSS

Морской биологический журнал
Marine Biological Journal
2025, vol. 10, no. 3, pp. 3–10
https://marine-biology.ru

SCIENTIFIC COMMUNICATIONS

UDC 594-111.11:[551.464.6:546.221.1]

ERYTHROID CELLS IN THE HEMOLYMPH OF A BIVALVE *ANADARA KAGOSHIMENSIS* (TOKUNAGA, 1906) UNDER HYDROGEN SULFIDE LOADING: FLOW CYTOMETRY AND LIGHT MICROSCOPY

© 2025 **Yu. Bogdanovich[1], A. Soldatov[1,2], N. Shalagina[1], and V. Rychkova[1]**

[1]A. O. Kovalevsky Institute of Biology of the Southern Seas of RAS, Sevastopol, Russian Federation

[2]Sevastopol State University, Sevastopol, Russian Federation

E-mail: *alekssoldatov@yandex.ru*

Received 25.02.2025; revised 25.02.2025;
accepted 12.08.2025.

The imbalance between organic matter oxidation and oxygen supply mediates the formation of time-stable redox zones in the water column. On the shelf, this typically occurs due to the absence of thorough vertical convection and the formation of localized decomposition zones. The functional mechanisms of the resistance of certain benthic organisms to such conditions are of particular interest. In this work, we study a bivalve *Anadara kagoshimensis* (Tokunaga, 1906) known for its tolerance to hydrogen sulfide contamination. Using flow cytometry and light microscopy, we examined the effect of hydrogen sulfide loading on morphofunctional characteristics of its erythroid cells under experimental conditions. The analysis was carried out on adult specimens with a shell height of 23–34 mm. The control group of molluscs was kept in an aquarium with an oxygen concentration of 7.0–8.2 mg $O_2 \cdot L^{-1}$ (normoxia). For the experimental group, oxygen content was first lowered to 0.1 mg $O_2 \cdot L^{-1}$ for 2 h (*via* nitrogen bubbling); then, Na_2S was added to water to a final concentration of 6 mg $S^{2-} \cdot L^{-1}$. Exposure to hydrogen sulfide revealed a significant increase in the volume of erythroid cells in *A. kagoshimensis* hemolymph (more than 40%, $p < 0.01$) accompanied by a substantial rise in fluorescence intensity of rhodamine 123 (R123) and 2′-7′-dichlorofluorescein-diacetate (DCF-DA) (2–3-fold, $p < 0.01$). This evidences for enhanced oxidative processes within cells and their possible lysis. The latter one may facilitate the release of hematin-containing granules, and hematin is capable of neutralizing sulfides. The observed response seems to be an adaptive one. A rise in values of side scatter and SYBR Green I fluorescence reflects an increase in abundance of granular inclusions within red blood cells under hydrogen sulfide loading and a gain in the functional activity of their nuclei.

Keywords: *Anadara kagoshimensis*, hydrogen sulfide, hemolymph, erythroid cells, morphology, flow cytometry

A Pacific bivalve *Anadara kagoshimensis* (Tokunaga, 1906) was first recorded off the coast of the Caucasus in 1968 [Kiseleva, 1992]. Currently, its abundant populations are primarily registered along the Caucasian and Romanian coasts of the Black Sea [Revkov, 2016]. This mollusc is actively colonizing the Sea of Azov shelf [Zhivoglyadova et al., 2021], and it has already become one of the dominant benthic forms [Revkov, 2016]. Such a rapid expansion of the Sea of Azov–Black Sea region is attributed to the species adaptive plasticity, particularly the ability to survive under low oxygen levels and hydrogen sulfide contamination.

Specialized studies have shown that *A. kagoshimensis* can maintain high energy levels in its tissues under acute hypoxia [Cortesi et al., 1992]. At the same time, the intensity of aerobic metabolism in its tissues is much lower compared to that of other bivalves [Andreenko et al., 2009]. The mollusc is resistant to hydrogen sulfide in water [Miyamoto, Iwanaga, 2017], and this is partly attributed to the presence of hematin-containing granules in its hemolymph cells [Holden et al., 1994; Vismann, 1993]. The density of these inclusions was shown to increase noticeably under experimental hydrogen sulfide loading [Soldatov et al., 2018].

Certain effects have also been revealed in the response of *A. kagoshimensis* cellular systems to hypoxia and presence of hydrogen sulfide [Soldatov et al., 2018, 2021]. Those primarily concern the functional morphology of cells: volume, specific surface area, and nuclear–cytoplasmic ratios. The present research continues earlier studies.

We aimed at assessing the effect of hydrogen sulfide on functional characteristics of erythroid cells in *Anadara kagoshimensis* hemolymph under *in vivo* experimental conditions using flow cytometry and light microscopy.

MATERIAL AND METHODS

Adult *A. kagoshimensis* specimens were studied. Bivalves were sampled in the Laspi Bay (the Crimea). Shell height ranged 23 to 34 mm (measured from the hinge to the valve edge).

Experimental design. The molluscs were divided into two groups: the control and the experimental ones. The control group was kept at an oxygen concentration of 7.0–8.2 mg $O_2 \cdot L^{-1}$. In the experimental group, oxygen content was lowered to 0.1 mg $O_2 \cdot L^{-1}$ for 2 h (*via* nitrogen bubbling); then, Na_2S was added to water to a final concentration of 6 mg $S^{2-} \cdot L^{-1}$. The presence of sulfide ions increased water alkalinity, and it was compensated by using 0.1 N HCl. Values of pH were stabilized at 8.2–8.3. Molluscs of both groups were kept under these conditions for 48 h. Water temperature was of +17…+20 °C.

Oxygen levels were monitored with a portable dissolved oxygen meter DO Meter ST300D (Ohaus, the USA). Values of pH were measured with a pocket pH-meter InoLab pH 720 (Germany). Sulfide ion concentration in water was determined potentiometrically with a sulfide-selective MSBS sensor (the Netherlands).

Hemolymph sampling. Hemolymph was sampled *via* syringe puncture of the extrapallial space. Heparin (Richter, Hungary) served as an anticoagulant. The obtained sample was divided into two parts. The first one was used to prepare smears. The second part was washed *via* centrifugation three times [500 g, 5 minutes, +4 °C, Eppendorf 5424 R refrigerated centrifuge (Germany)] to remove plasma. The cells were resuspended in sterile seawater. The obtained samples were used for cytometric studies.

Flow cytometry. A part of the erythrocyte suspension was stained with SYBR Green I (Sigma Aldrich, the USA). The final concentration in the sample was of 10 μM; the incubation in the dark lasted for 40 min. The fluorescence of this DNA dye was analyzed in the FL1 channel (excitation at 497 nm, emission at 521 nm). The pattern of distribution of cells in the suspension was classified based on their relative size: by forward scatter (FS) and side scatter (SS).

The spontaneous production of reactive oxygen species by erythrocytes was assessed by fluorescence of 2',7'-dichlorodihydrofluorescein diacetate (DCF-DA, Sigma Aldrich). Thus, 1 mL of the erythrocyte suspension was incubated with 10 μL of DCF-DA solution for 40 min in the dark. The final dye concentration in the sample was of 10 μM. Its fluorescence was analyzed in the FL1 channel (excitation at 485 nm, emission at 525 nm).

Changes in the mitochondrial membrane potential of erythrocytes were monitored by fluorescence intensity of cells stained with rhodamine 123 (R123) (Molecular Probes, the USA). Erythrocytes were R123-stained for 40 min. The dye concentration in the sample was of 2.5 μM. Fluorescence intensity was measured in the FL1 channel (excitation at 508 nm, emission at 528 nm).

All measurements were carried out on a Cytomics FC 500 flow cytometer (Beckman Coulter, the USA) equipped with a single-phase argon laser (wavelength of 488 nm).

Light microscopy. The part of the hemolymph used to prepare smears was stained by the combined Pappenheim method (May–Grünwald + Romanowsky–Giemsa) [Zolotnitskaya, 1987]. Then, this part was used to assess the morphometric characteristics of red blood cells. Under a Biomed PR-2 Lum light microscope (magnification 100×, China–Russia) equipped with a Levenhuk C NG Series camera, large and small diameters of cells (C_1 and C_2, respectively) and their nuclei (N_1 and N_2) were measured from photographs (ImageJ 1.44p software). The sample size was 100 cells *per* smear. Based on obtained values and using established algorithms, mean cell volume (V_c) [Houchin et al., 1958], nuclear volume (V_n) [Tască, 1976], and nuclear–cytoplasmic ratio (NCR) were calculated:

$$V_c = 0.7012 \cdot \left(\frac{C_1 + C_2}{2}\right)^2 \cdot h + V_n \,,$$

$$V_n = \frac{\pi \cdot N_1 \cdot N_2^2}{6} \,,$$

$$NCR = \frac{V_n}{V_c} \,.$$

Statistical processing. Data are presented as $M \pm m$. Statistical comparisons were made using the Mann–Whitney U test. Difference was considered significant at $p < 0.05$. The data were processed and visualized in MS Office Excel 2010. Sample sizes are shown in the graphs.

RESULTS

Flow cytometry. The analysis of forward scatter (FS) and side scatter (SS) in suspensions of erythroid cells under hydrogen sulfide loading revealed an increase in both parameters (Fig. 1). In the case of SS, the differences were statistically significant ($p < 0.001$).

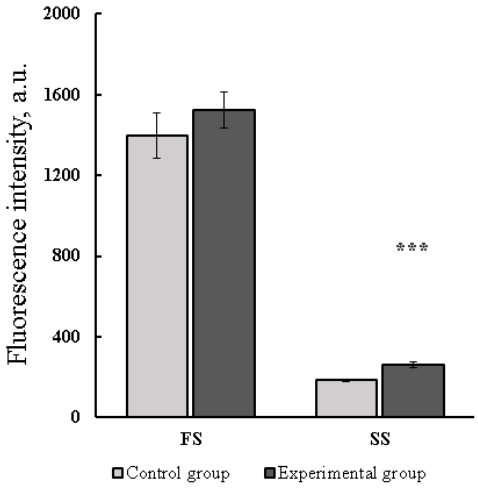

Fig. 1. Parameters of forward scatter (FS) and side scatter (SS) of suspensions of erythroid cells in *Anadara kagoshimensis* hemolymph under hydrogen sulfide loading (***, $p < 0.001$)

A noticeable rise in fluorescence intensity in the presence of H_2S was observed for SYBR Green I, R123, and DCF-DA as well (Fig. 2): 1.7-fold ($p < 0.05$), 1.9-fold ($p < 0.01$), and 3.2-fold ($p < 0.001$), respectively.

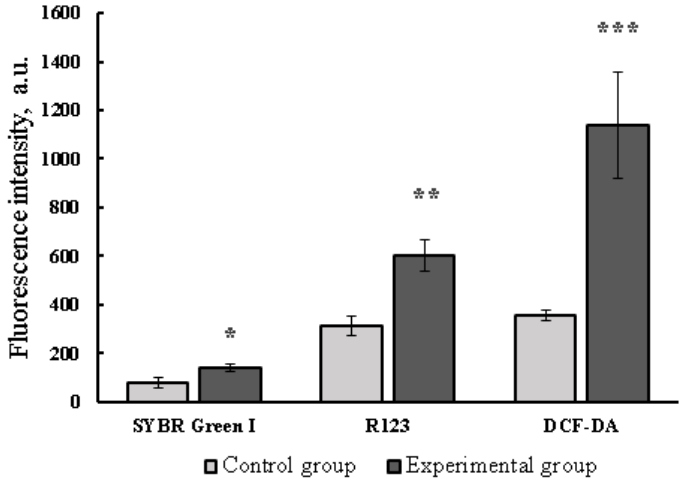

Fig. 2. Fluorescence intensity of SYBR Green I, R123, and DCF-DA suspensions of erythroid cells in *Anadara kagoshimensis* hemolymph under hydrogen sulfide loading (*, $p < 0.05$; **, $p < 0.01$; ***, $p < 0.001$)

Morphometry of erythroid cells. As revealed, under hydrogen sulfide loading, there was an increase in cell volume and the number of granular inclusions in cells (Fig. 3). It was confirmed by morphometric data. Longitudinal and transverse axes of erythroid cells (C_1 and C_2) were increased by 20–21% ($p < 0.05$ for C_2) (Fig. 4). There was a boost in cell volume as well: by more than 40% ($p < 0.01$). Nuclei exhibited similar changes, but those were weakly expressed ($p > 0.05$) (Fig. 5). The calculation of NCR also revealed no statistically significant shifts: the values for the control group were of (0.120 ± 0.020), and for the experimental one, (0.090 ± 0.004).

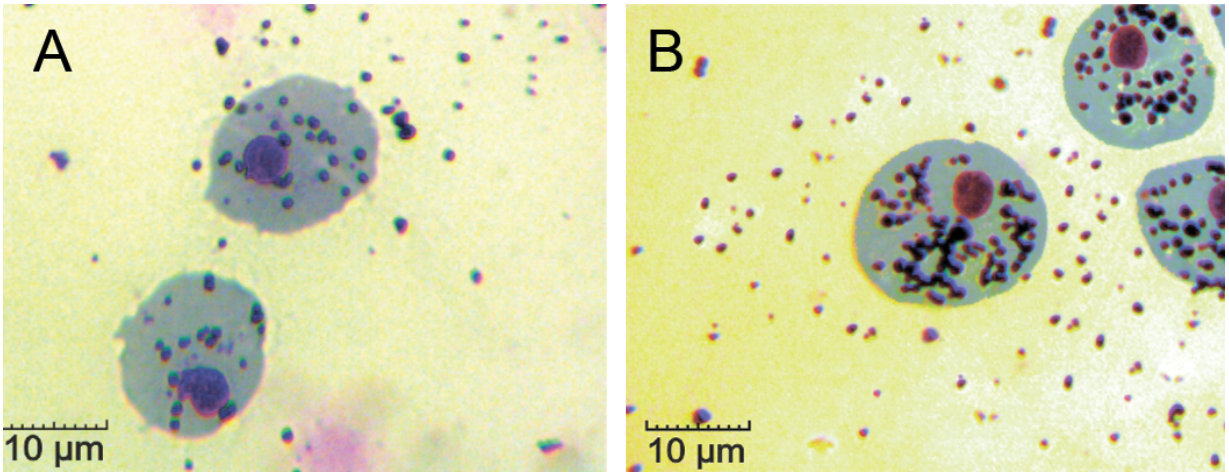

Fig. 3. Erythroid cells in *Anadara kagoshimensis* hemolymph (A, normoxia; B, hydrogen sulfide contamination)

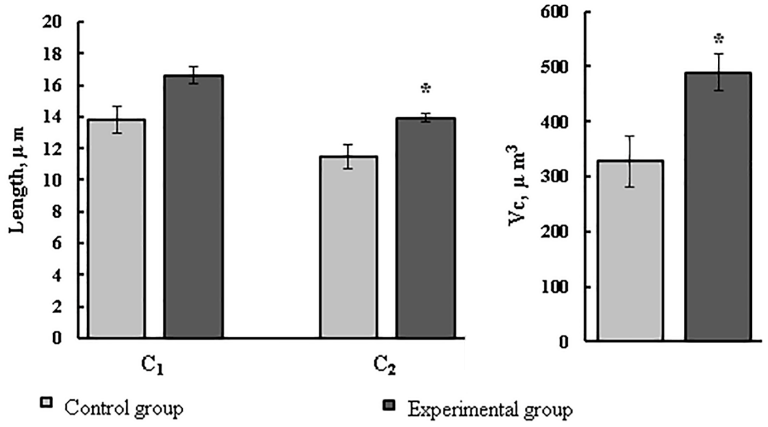

Fig. 4. Morphometric characteristics of erythroid cells in *Anadara kagoshimensis* hemolymph under normoxia and hydrogen sulfide loading (C_1, large cell diameter; C_2, small cell diameter; V_c, cell volume; *, $p < 0.01$)

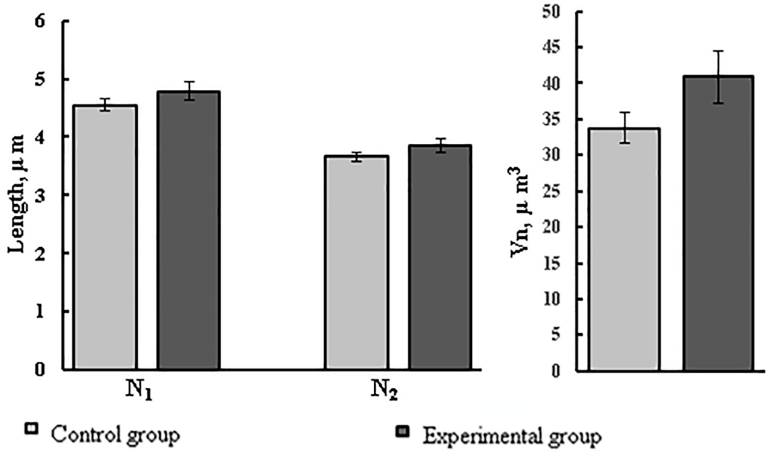

Fig. 5. Morphometric characteristics of nuclei of erythroid cells in *Anadara kagoshimensis* hemolymph under normoxia and hydrogen sulfide loading (N_1, large nucleus diameter; N_2, small nucleus diameter; V_n, nucleus volume)

DISCUSSION

The results of our experiment showed that hydrogen sulfide loading induced distinct alterations in erythroid cells of *A. kagoshimensis* hemolymph: an increase in cell volume, a rise in SS of cell suspensions, and a boost in fluorescence intensity of SYBR Green I, R123, and DCF-DA.

Typically, the presence of hydrogen sulfide in marine environment co-occurs with acute hypoxia, with the latter one known to induce erythrocyte swelling [Holk, 1996; Nikinmaa et al., 1987]. Earlier, we observed similar responses in *A. kagoshimensis* under both hypoxia alone and its combined effect with hydrogen sulfide [Soldatov et al., 2018]. In fish erythrocytes, hypoxia activates Na^+/H^+ antiporters [Salama, Nikinmaa, 1990; Val et al., 1997]. This reaction is further amplified by catecholamines (*e. g.*, adrenaline and noradrenaline), and their production can be enhanced under experimental loading. Nuclear erythrocytes were shown to contain β-adrenergic receptors through which hormones stimulate cAMP production in cells [Salama, Nikinmaa, 1990; Val et al., 1997]; typically, this results in a cell volume increase by 5–6% only [Nikinmaa et al., 1987]. Importantly, in our study, cell volume rose by more than 40%. This often precedes the apoptosis characterized by production of cell fragments called apoptotic bodies [Manskikh, 2007]. Our previous studies documented lysis of erythroid cells in *A. kagoshimensis* under hydrogen sulfide loading [Soldatov et al., 2018]. This reaction seemed to be an adaptive one, as it was accompanied by the release of granular inclusions capable of neutralizing sulfides [Holden et al., 1994; Vismann, 1993].

The observed rise in SS we recorded aligns well with the increased cytoplasmic granularity of erythroid cells, as visually confirmed earlier in hydrogen sulfide–exposed *A. kagoshimensis* [Soldatov et al., 2018]. These granules contain hematin [Vismann, 1993] which reacts with sulfides to form sulfur:

$$2Fe^{3+} + 3S^{2-} \rightarrow Fe_2S_3 \,,$$
$$2Fe_2S_3 + 3O_2 = Fe_2O_3 + 6S^0 \,.$$

Given that sulfur accumulation has been recorded in other marine invertebrates exposed to sulfides [Powell et al., 1980], similar reactions may occur in *A. kagoshimensis* hemolymph.

The increase in SYBR Green I fluorescence intensity in *A. kagoshimensis* erythrocytes in the presence of hydrogen sulfide we registered is currently difficult to interpret, since the mechanism of interaction between this fluorochrome and DNA molecule is not fully known. However, several authors suggest that in most cases, this phenomenon reflects enhanced functional activity of the cell nucleus [Cerca et al., 2011]. Given that the volume of nuclei in *A. kagoshimensis* erythroid cells increased under H_2S loading alongside with cytoplasmic granularity of the cell, we may reasonably accept this perspective as a working hypothesis.

A significant rise in R123 and DCF-DA fluorescence in erythroid cells of the mollusc's hemolymph under hydrogen sulfide loading we observed indicates an increase in mitochondrial membrane potential and levels of reactive oxygen species. Overall, this evidences for a substantial intensification of oxidative processes within cells which would likely lead to their lysis. The previously noted excessive increase in cell volume seems to reflect this process. The destruction of these cells is accompanied by the release of hematin-containing granular inclusions, and hematin is capable of neutralizing sulfides in *A. kagoshimensis* hemolymph. This response appears to be an adaptive mechanism specific to red blood cells. In other somatic tissues (gills, hepatopancreas, and foot muscle), it is virtually absent [Soldatov et al., 2022].

Conclusion. Experimental findings revealed as follows: under hydrogen sulfide loading, the volume of erythroid cells in *Anadara kagoshimensis* hemolymph significantly increased and was accompanied by a substantial rise in R123 and DCF-DA fluorescence. This indicates enhanced oxidative processes in cells and their possible lysis. The latter one seems to facilitate the release of hematin-containing granular inclusions, and hematin is capable of neutralizing sulfides. This observed response appears to have an adaptive significance. An increase in side scatter and SYBR Green I fluorescence evidences for a higher number of granular inclusions in erythroid cells in the presence of hydrogen sulfide, as well as elevated functional activity of their nuclei.

This work was carried out within the framework of IBSS state research assignment "Functional, metabolic, and molecular genetic mechanisms of marine organism adaptation to conditions of extreme ecotopes of the Black Sea, the Sea of Azov, and other areas of the World Ocean" (No. 124030100137-6).

REFERENCES

1. Andreenko T. I., Soldatov A. A., Golovina I. V. Adaptive reorganization of metabolism in bivalve mollusk (*Anadara inaequivalvis* Bruguiere) under experimental anoxia. *Dopovidi Natsional'noi akademii nauk Ukrainy*, 2009, no. 7, pp. 155–160. (in Russ.). https://repository.marine-research.ru/handle/299011/14288
2. Zhivoglyadova L. A., Revkov N. K., Frolenko L. N., Afanasyev D. F. The expansion of the bivalve mollusk *Anadara kagoshimensis*

(Tokunaga, 1906) in the Sea of Azov. *Rossiiskii zhurnal biologicheskikh invazii*, 2021, vol. 14, no. 1, pp. 83–94. (in Russ.). https://doi.org/10.35885/1996-1499-2021-14-1-83-94

3. Zolotnitskaya R. P. Metody gematologicheskikh issledovanii. In: *Laboratornye metody issledovaniya v klinike* : spravochnik / V. V. Menshikov (Ed.). Moscow : Meditsina, 1987, pp. 106–148. (in Russ.)
4. Kiseleva M. I. Sravnitel'naya kharakteristika donnykh soobshchestv u poberezh'ya Kavkaza. In: *Mnogoletnie izmeneniya zoobentosa Chernogo morya* / V. E. Zaika (Ed.). Kyiv : Naukova dumka, 1992, pp. 84–99. (in Russ.). https://repository.marine-research.ru/handle/299011/5644
5. Manskikh V. N. Pathways of cell death and their biological importance. *Tsitologiya*, 2007, vol. 49, no. 11, pp. 909–915. (in Russ.). https://elibrary.ru/mpvsgr
6. Revkov N. K. Colonization's features of the Black Sea basin by recent invader *Anadara kagoshimensis* (Bivalvia: Arcidae). *Marine Biological Journal*, 2016, vol. 1, no. 2, pp. 3–17. (in Russ.). https://doi.org/10.21072/mbj.2016.01.2.01
7. Cerca F., Trigo G., Correia A., Cerca N., Azeredo J., Vilanova M. SYBR Green as a fluorescent probe to evaluate the biofilm physiological state of *Staphylococcus epidermidis*, using flow cytometry. *Canadian Journal of Microbiology*, 2011, vol. 57, no. 10, pp. 850–856. https://doi.org/10.1139/w11-078
8. Cortesi P., Cattani O., Vitali G., Carpené E., de Zwaan A., van den Thillart G., Roos J., van Lieshout G., Weber R. E. Physiological and biochemical responses of the bivalve *Scapharca inaequivalvis* to hypoxia and cadmium exposure: Erythrocytes versus other tissues. In: *Marine Coastal Eutrophication* : proceedings of an International Conference, Bologna, Italy, 21–24 March, 1990. Amsterdam, the Netherlands : Elsevier, 1992, pp. 1041–1054. https://doi.org/10.1016/B978-0-444-89990-3.50090-0
9. Holden J. A., Pipe R. K., Quaglia A., Ciani G. Blood cells of the arcid clam, *Scapharca inaequivalvis*. *Journal of the Marine Biological Association of the United Kingdom*, 1994, vol. 74, iss. 2, pp. 287–299. https://doi.org/10.1017/S0025315400039333
10. Holk K. Effects of isotonic swelling on the intracellular Bohr factor and the oxygen affinity of trout and carp blood. *Fish Physiology and Biochemistry*, 1996, vol. 15, pp. 371–375. https://doi.org/10.1007/BF01875579
11. Houchin D. N., Munn J. I., Parnell B. L. A method for the measurement of red cell dimensions and calculation of mean corpuscular volume and surface area. *Blood*, 1958, vol. 13, no. 12, pp. 1185–1191. https://doi.org/10.1182/blood.V13.12.1185.1185
12. Miyamoto Y., Iwanaga C. Effects of sulphide on anoxia-driven mortality and anaerobic metabolism in the ark shell *Anadara kagoshimensis*. *Journal of the Marine Biological Association of the United Kingdom*, 2017, vol. 97, iss. 2, pp. 329–336. https://doi.org/10.1017/S0025315416000412
13. Nikinmaa M., Cech J. J., Ryhänen L., Salama A. Red cell function of carp (*Cyprinus carpio*) in acute hypoxia. *Experimental Biology*, 1987, vol. 47, iss. 1, pp. 53–58.
14. Powell E. N., Crenshaw M. A., Rieger R. W. Adaptations to sulfide in sulfide-system meiofauna. End-products of sulfide detoxification in three turbellarians and a gastrotrich. *Marine Ecology Progress Series*, 1980, vol. 2, no. 2, pp. 169–177.
15. Salama A., Nikinmaa M. Effect of oxygen tension on catecholamine-induced formation of cAMP and on swelling of carp red blood cells. *American Journal of Physiology – Cell Physiology*, 1990, vol. 259, iss. 5, pt 1, pp. C723–C726. https://doi.org/10.1152/ajpcell.1990.259.5.c723
16. Soldatov A. A., Golovina I. V., Kolesnikova E. E., Sysoeva I. V., Sysoev A. A. Effect of hydrogen sulfide loading on the activity of energy metabolism enzymes and the adenylate system in tissues of the *Anadara kagoshimensis* clam. *Inland Water Biology*, 2022, vol. 15, no. 5, pp. 632–640. https://doi.org/10.1134/S1995082922050194
17. Soldatov A., Kukhareva T., Morozova V., Richkova V., Andreyeva A., Bashmakova A. Morphometric parameters of erythroid hemocytes

of alien mollusc *Anadara kagoshimensis* under normoxia and anoxia. *Ruthenica, Russian Malacological Journal*, 2021, vol. 31, no. 2, pp. 77–86. https://doi.org/10.35885/ruthenica.2021.31(2).3

18. Soldatov A. A., Kukhareva T. A., Andreeva A. Y., Efremova E. S. Erythroid elements of hemolymph in *Anadara kagoshimensis* (Tokunaga, 1906) under conditions of the combined action of hypoxia and hydrogen sulfide contamination. *Russian Journal of Marine Biology*, 2018, vol. 44, iss. 6, pp. 452–457. https://doi.org/10.1134/S1063074018060111
19. Tască C. *Introducere în morfologia cantitativă cito-histologică.* Bucuresti : Editură Academiei Republicii Socialiste România, 1976, 182 p.
20. Val A. L., De Menezes G. C., Wood C. M. Red blood cell adrenergic responses in Amazonian teleosts. *Journal of Fish Biology*, 1997, vol. 52, iss. 1, pp. 83–93. https://doi.org/10.1111/j.1095-8649.1998.tb01554.x
21. Vismann B. Hematin and sulfide removal in hemolymph of the hemoglobin-containing bivalve *Scapharca inaequivalvis*. *Marine Ecology Progress Series*, 1993, vol. 98, pp. 115–122. http://doi.org/10.3354/meps098115

ЭРИТРОИДНЫЕ ЭЛЕМЕНТЫ ГЕМОЛИМФЫ ДВУСТВОРЧАТОГО МОЛЛЮСКА *ANADARA KAGOSHIMENSIS* (TOKUNAGA, 1906) В УСЛОВИЯХ СЕРОВОДОРОДНОЙ НАГРУЗКИ: ПРОТОЧНАЯ ЦИТОМЕТРИЯ И СВЕТОВАЯ МИКРОСКОПИЯ

Ю. В. Богданович[1], А. А. Солдатов[1,2], Н. Е. Шалагина[1], В. Н. Рычкова[1]

[1]ФГБУН ФИЦ «Институт биологии южных морей имени А. О. Ковалевского РАН», Севастополь, Российская Федерация

[2]Севастопольский государственный университет, Севастополь, Российская Федерация

E-mail: *alekssoldatov@yandex.ru*

Нарушение баланса между окислением органического вещества и поступлением кислорода приводит к формированию в водной толще устойчивых во времени редокс-зон. На шельфе это обычно происходит вследствие отсутствия сквозной вертикальной конвекции и образования локальных зон гниения мёртвого органического вещества. Функциональные аспекты устойчивости ряда бентосных организмов к подобным условиям представляют определённый интерес. В настоящей работе исследован двустворчатый моллюск *Anadara kagoshimensis* (Tokunaga, 1906), способный переносить условия сероводородного заражения. При помощи методов проточной цитометрии и световой микроскопии экспериментально изучено влияние сероводородной нагрузки на морфофункциональные характеристики эритроидных элементов моллюска. Работа выполнена на взрослых особях с высотой раковины 23–34 мм. Контрольную группу *A. kagoshimensis* содержали в аквариуме с концентрацией кислорода 7,0–8,2 мг $O_2 \cdot л^{-1}$ (нормоксия). У опытной группы сначала в течение 2 ч понижали уровень кислорода до 0,1 мг $O_2 \cdot л^{-1}$ (барботаж воды азотом). Затем в воду вносили Na_2S до финальной концентрации 6 мг $S^{2-} \cdot л^{-1}$. При наличии сероводорода выявлен значительный рост объёма эритроидных элементов гемолимфы анадары (более 40 %, $p < 0{,}01$), происходящий на фоне существенного повышения величины флуоресценции родамина 123 (R123) и 2′-7′-дихлорфлуоресцеин-диацетата (DCF-DA) (2–3 раза, $p < 0{,}01$), что отражает усиление окислительных процессов в клетках и их возможный лизис. Последний позволяет освобождать гранулы, содержащие гематин, который способен нейтрализовать сульфиды. Отмеченная реакция, по-видимому, имеет адаптивное значение. Рост величин бокового светорассеяния и флуоресценции SYBR Green I отражает увеличение числа гранулярных включений в клетках красной крови при наличии сероводорода и повышение функциональной активности их ядер.

Ключевые слова: *Anadara kagoshimensis*, сероводород, гемолимфа, эритроидные элементы, морфология, проточная цитометрия

1871
ИнБЮМ – IBSS

Морской биологический журнал
Marine Biological Journal
2025, vol. 10, no. 3, pp. 11–19
https://marine-biology.ru

UDC 595.371-14(262.5)

MORPHOLOGY OF *STENOTHOE* CF. *TERGESTINA* (NEBESKI, 1881) (CRUSTACEA, AMPHIPODA, STENOTHOIDAE), RECENT INVADER TO THE BLACK SEA

© 2025 **V. Grintsov**

A. O. Kovalevsky Institute of Biology of the Southern Seas of RAS, Sevastopol, Russian Federation
E-mail: *vgrintsov@gmail.com*

Received 14.02.2025; revised 26.02.2025;
accepted 12.08.2025.

The relevance of research on species new to regions is governed by their interaction with species of local ecosystems, as it may be negative in some instances. The aim of this work is to clarify the morphology and variability of some parameters of body and appendages of adult males and females of *Stenothoe* cf. *tergestina* which is similar to *Stenothoe tergestina* (Nebeski, 1881) but has some morphological differences not allowing to classify them as different species. Methods of morphology investigations and analysis under both light and electron microscopes were used. A detailed description of adult *S.* cf. *tergestina* females and males, their appendages, and the sex structure of the population from fouling of constructions of a mussel-and-oyster farm near Sevastopol is provided. New data on the discovered taxon were comparatively analyzed with similar data from other habitats to clarify the species affiliation. The variability of several morphological traits was revealed. The length of females in the populations exceeded the length of males. The finding of individuals on various substrates evidences for high adaptability of the species to this habitat.

Keywords: Amphipoda, Black Sea, *Stenothoe* cf. *tergestina*, morphology

Since 1999, in the Black Sea, several Amphipoda species have been recorded previously unknown in this region [Grintsov, 2003a, b, 2009a, b, 2010, 2011, 2018, 2021].

The relevance of research on species new to regions is mediated by their interaction with species of local ecosystems, as it may be negative in some instances. To date, three species of the genus *Stenothoe* Dana, 1852 have been reported for the Black Sea: *Stenothoe monoculoides* (Montagu, 1813) [Greze, 1977, 1985], *Stenothoe marina* (Spence Bate, 1857) [Grintsov, Sezgin, 2011], and *Stenothoe* cf. *tergestina* [Grintsov, 2024]. *S. marina* is distributed along the coast of Turkey. *S. monoculoides* inhabits the entire Black Sea area. Since 2018, we register *S.* cf. *tergestina* in high abundance (males, females, and juveniles) on structures of a mussel-and-oyster farm (the outer roadstead of Sevastopol). These amphipods occur within a depth range of 0–10 m in all seasons.

The aim of this work is to clarify the morphology and variability of some body and appendage parameters of adult *Stenothoe* cf. *tergestina* males and females.

MATERIAL AND METHODS

Periphyton was sampled manually in 2018–2024 from constructions of the mussel-and-oyster farm located on the outer roadstead of Sevastopol, from a depth of 0–5 m.

Periphyton was kept in freshwater for 10 min and separated from the substrate. The resulting wash was filtered through a mill sieve with a mesh size of 0.5 mm and fixed with 96% ethanol. In a laboratory, amphipods were identified under a light binocular microscope MBS-9 (Russia) at a magnification of 8 × 2 and 8 × 4 and a microscope Mikmed-5 (Russia) at 10 × 4 and 10 × 10. Species-specific features were analyzed [Greze, 1985; Grintsov, Sezgin, 2011; Krapp-Schickel, 1993]. Measurements were carried out with an eyepiece micrometer for MBS-9. Micrographs of the habitus and body details of adult Amphipoda males and females were taken under a scanning electron microscope (hereinafter SEM) Hitachi SU3500 (Japan) by the author of the work and the head of the IBSS microscopy laboratory V. Lishaev.

During late August–early September 2024, ratios of juveniles and adults of this amphipod, as well as males and females, were determined in 35 samples; 981 ind. were analyzed. In total, more than 10,000 ind. of *S.* cf. *tergestina* have been studied since 2018.

Morphological variability was assessed on 30 adult males and females. The following traits were analyzed: the body length (in mm), the ratio of antenna I length and antenna II length (LAI/LAII), the ratio of the length of the stalk of antenna II and the length of its flagellum (LAIISt/LAIIFl), the ratio of the maximum width of coxal plates II and III (CoxII/CoxIII), and the ratio of the telson length and the uropod III length (LTl/LUIII). All ratios were calculated for the left side of the body. The arithmetic mean, standard deviation, minimum value, and maximum value were determined as well.

RESULTS AND DISCUSSION

Description of *Stenothoe* cf. *tergestina* morphology. Female (Fig. 1), length 4.50 mm, 6 eggs.

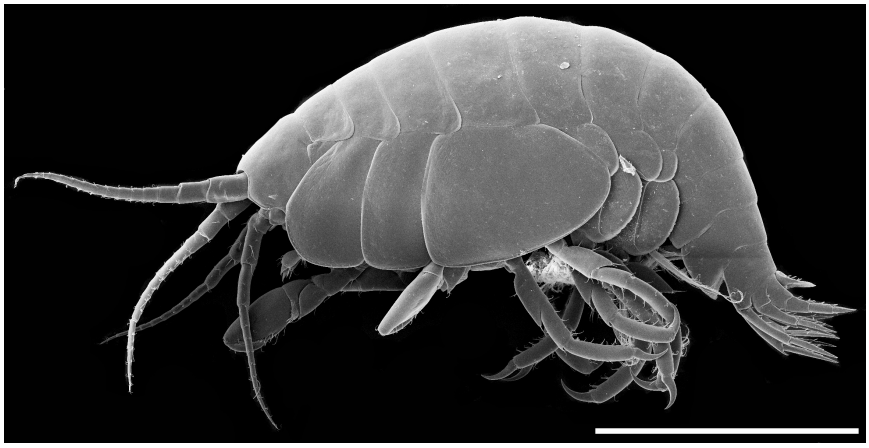

Fig. 1. Habitus of an adult *Stenothoe* cf. *tergestina* female (a scanning electron microscope). Scale line is 1 mm; from [Grintsov, 2024]

Head. Rostrum small. Eyes 0.15 mm, 3.33 times shorter than head length. Rounded, white in ethanol. Interantennal lobes trapezoidal.

Antenna I. Length 1.40 mm. Peduncle: ratio of lengths of 1 : 2 : 3 segments (articles) – 1.0 : 0.8 : 0.5; thickness of segments decreases successively from the 1st to the 3rd one; the 1st segment slightly narrows distally; a seta extero-laterally, a spine ventro-distally; the 2nd segment cylindrical, setae intero-laterally and distally, spines ventrally; the 3rd segment cylindrical, setae distally. Flagellum longer than peduncle, includes 14 segments; segments with setae and aesthetasc sensillae distally.

Antenna II. Length 1.40 mm. Peduncle: ratio of lengths of 3 : 4 : 5 segments – 0.5 : 1.0 : 1.0; the 3rd segment almost round, inflated, with curved spines intero-ventrally; the 4th segment cylindrical, slightly curved, spines extero-laterally, intero-laterally, and distally; the 5th segment slightly curved, spines and setae extero-laterally, intero-laterally, and distally. Flagellum longer than peduncle, includes 15 segments, segments with setae distally.

Mouthparts. Epistome and labrum. Labrum with a deep notch on ventral margin (Fig. 2A).

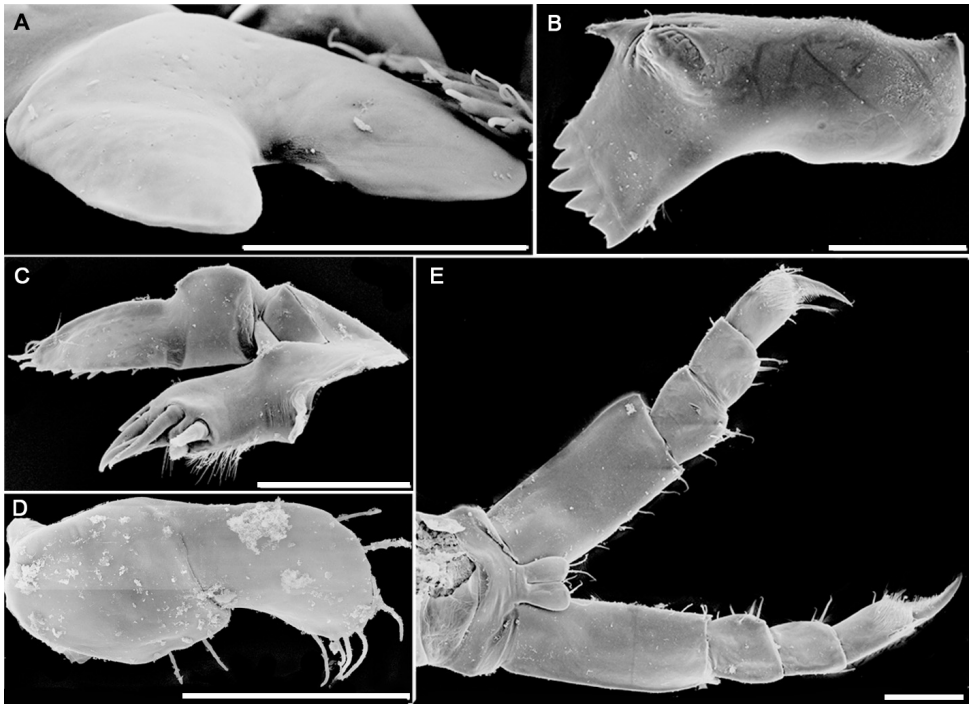

Fig. 2. Mouthparts of an adult *Stenothoe* cf. *tergestina* female (a scanning electron microscope). A, upper lip; B, right mandible; C, maxilla I; D, maxilla II; E, maxilliped. Scale lines are 0.1 mm; original photo

Right and left mandibles (Fig. 2B). Cutting edge with 6 denticles. Additional plate short, with 4 denticles. Row of denticles with 2 setae. Molar in the form of a small tubercle with setae. Labium. Inner and outer lobes fused and pubescent distally. Maxilla I (Fig. 2C). Inner lobe small, rounded, with 1 long seta; outer lobe several times larger than inner lobe, with strong spines distally. Palp 2-articulate, the 2nd segment twice longer than the 1st; the 2nd segment of palp with setae and spines along margin. Maxilla II (Fig. 2D). Inner lobe almost not expressed. Outer lobe convex along margin, with setae. Maxillipeds (Fig. 2E). Inner lobes small, much smaller than the 1st segment of palp, with 2 setae distally. No outer lobes. Palp 4-articulate, the 4th segment claw-like. Ratio of lengths of 1 : 2 : 3 : 4 segments – 1.0 : 1.0 : 1.2 : 1.0; the 1st, 2nd, and 3rd segments with setae along inner margin. Pereon. Width of segments increases from the 1st to the 7th one. Cuticular structures not expressed.

Gnathopod I (Fig. 3A). Coxal plate small, almost completely hidden by coxal plate II, rectangular in shape, with sparse small setae on ventral margin. Basipodite 1.1 times longer than ischium, propodus slightly narrowed in middle part, anterior margin proximally convex, subdistally with a notch, middle part of posterior margin straight; a tiny seta intero-distally. Ischium equal to merus in length, curved. A small seta in middle part of posterior margin. Merus 0.8 times as long as carpus; posterodistally forms a lobe with a brush of tiny setae at distal end and several larger setae and spines. Carpus 0.4 times as long as propodus, convex at anterior margin and with a small lobe posterodistally; setae and spines distally

on a lobe. Propodus twice as long as claw, subtly trapezoidal; anterior margin convex, with several setae, posterior margin straight, shorter than anterior margin, inner plane with several setae. Claw-side palmar margin slightly convex, with spines and setae, the largest spines are locking. Claw equal to claw-side palmar margin, with several setae.

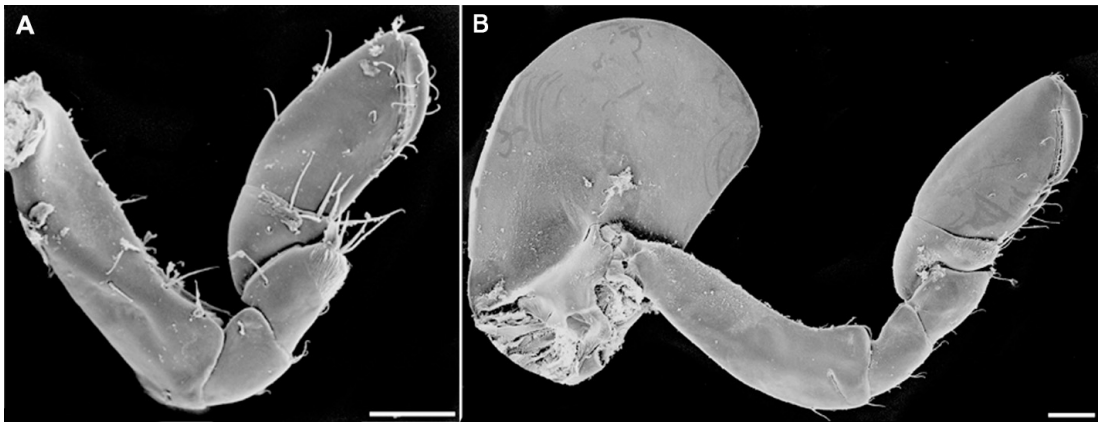

Fig. 3. Gnathopodes of an adult *Stenothoe* cf. *tergestina* female (a scanning electron microscope). A, gnathopod I; B, gnathopod II. Scale lines are 0.1 mm; original photo

Gnathopod II (Fig. 3B). Larger than gnathopod I. Coxal plate elongated dorsoventrally, widens ventrally, anterior and ventral margins convex, posterior concave, small spines posterodistally. Basipodite twice as long as ischium + carpus, widens distally, curved toward distal end, anterior margin weakly convex proximally, concave distally, posterior margin straight proximally, convex distally, setae posterodistally and distally. Ischium 0.9 times as long as merus, curved, anterior margin concave, posterior margin convex; one seta in middle part and one distally on posterior margin. Merus slightly larger than carpus, forms a triangular lobe along entire posterior margin, posterior margin convex; setae in posterodistal angle of posterior margin. Carpus 0.4 times as long as propodus, anterior margin convex, posterior margin with a narrow long lobe; 2 setae and 1 spine at distal end of lobe. Propodus 1.8 times the length of claw, oval, anterior margin convex proximally and straighter distally, posterior margin uniformly convex, with a small notch proximally; anterior margin with setae distally, posterior margin with setae and spines. Claw-side palmar margin about 0.5 times the length of inner margin, uniformly convex, with setae and spines, the largest spines are locking. Claw equal to claw-side palmar margin; setae on outer and inner margins, a denticle at distal end.

Pereopod III (Fig. 4A). Coxal plate III rectangular, elongated dorsoventrally, anterior and ventral margins convex, posterior margin concave; small spines along posterior margin. Basipodite 0.8 as long as ischium – propodus, curved, widening distally, anterior margin proximally convex, distally concave, posterior margin convex, setae in distal half of posterior margin, a seta entero-distally. Ischium 0.7 as long as merus, curved, anterior margin proximally concave, distally convex, posterior margin convex; setae in middle part of posterior margin. Merus equal to carpus in length, anterior margin forms a convex lobe, with its distal end not reaching middle part of carpus, a lobe ends in 3 different-sized spines, a seta in proximal part of a lobe; posterior margin convex proximally and concave distally, a seta in middle part of margin and distally. Carpus 0.7 as long as propodus, convex along anterior margin and straight along posterior one; spines along posterior margin and distally. Propodus 1.7 times the length of claw, slightly curved, convex along anterior margin and concave along posterior one; small setae along anterior margin and developed spines along posterior margin. Claw with no cuticular structures.

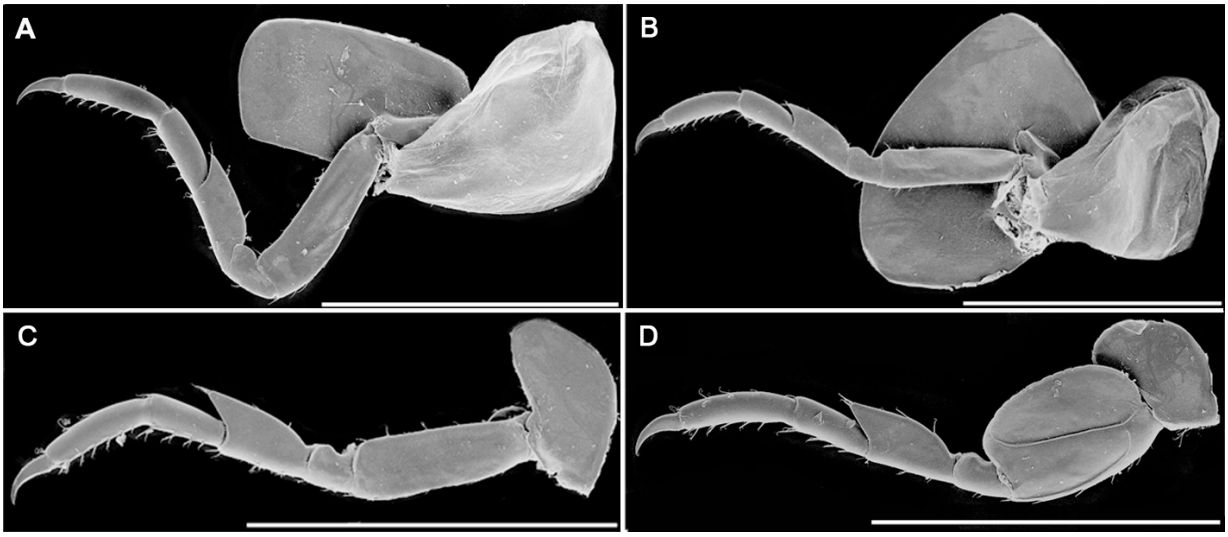

Fig. 4. Pereopodes of an adult *Stenothoe* cf. *tergestina* female (a scanning electron microscope). A, pereopod III; B, pereopod IV; C, pereopod V; D, pereopod VI. Scale lines are 1 mm; original photo

Pereopod IV (Fig. 4B). Similar in size to pereopod III. Coxal plate IV the largest, trapezoidal, width exceeds height; anterior, ventral, and posterior margins convex, with no cuticular structures. Basipodite equal to ischium + carpus in length, straight, not widen distally, spines distally and along posterior margin, especially in its distal half. Ischium + claw same as in pereopod III, but with more massive spines.

Pereopod V (Fig. 4C). Slightly longer than pereopod IV. Coxal plate V bilobed, posterior lobe longer and thinner, anterior lobe slightly convex, with setae. Basipodite + merus as in pereopod IV, but cuticular structures more developed. Carpus widens distally, armature similar to that of pereopod IV, but more massive; propodus + claw similar to those of pereopod IV, but cuticular structures more massive.

Pereopod VI (Fig. 4D). Slightly longer than pereopod V. Behind, coxal plate VI forms oval-elongated lobe with small spines along anterior margin. Basipodite equal to ischium + merus in length, convex along anterior margin; along posterior margin, forms a convex lobe, finely scalloped along margin and reaching a third of ischium; short, strong spines along anterior margin. Ischium 0.5 as long as merus, convex along anterior margin, with a proximal notch along posterior margin; spines along anterior margin. Merus equal to carpus in length, anterior margin straight, a convex lobe on posterior margin, with distal end of a lobe not reaching middle part of carpus; spines along anterior and posterior margins, the largest at distal end of a lobe. Carpus 0.9 times as long as propodus, widens distally, anterior margin straight, posterior margin convex; spines along anterior margin and distally. Propodus 1.5 times longer than claw, slightly curved; setae along posterior margin, strong spines along anterior margin. Claw with no cuticular structures.

Pereopod VII. Slightly larger than pereopod VI. Behind, coxal plate VII forms a small, irregularly rounded lobe. Basipodite 0.9 times as long as ischium + propodus, a lobe on posterior margin reaches half of the length of ischium. Rest of morphology and cuticular structures similar to those of pereopod VI.

Pleone (see Fig. 1). All segments of pleone equal in width. Epimeral plate I the smallest, ventrally convex. Epimeral plate II medium-sized, ventral margin convex, posterior margin almost straight. Epimeral plate III the largest, ventral margin convex, an outgrowth formed ventro-distally, posterior margin concave.

Urosome (see Fig. 1). The 1st segment significantly wider than other ones. Cuticular structures not expressed.

Uropod I (Fig. 5A, UI). Longer than uropod III. Peduncle longer than rami; spines extero-dorsally and distally, a small denticle formed distally below rami. Rami equal in length and pointed terminally, spines only dorsally, no terminal spines.

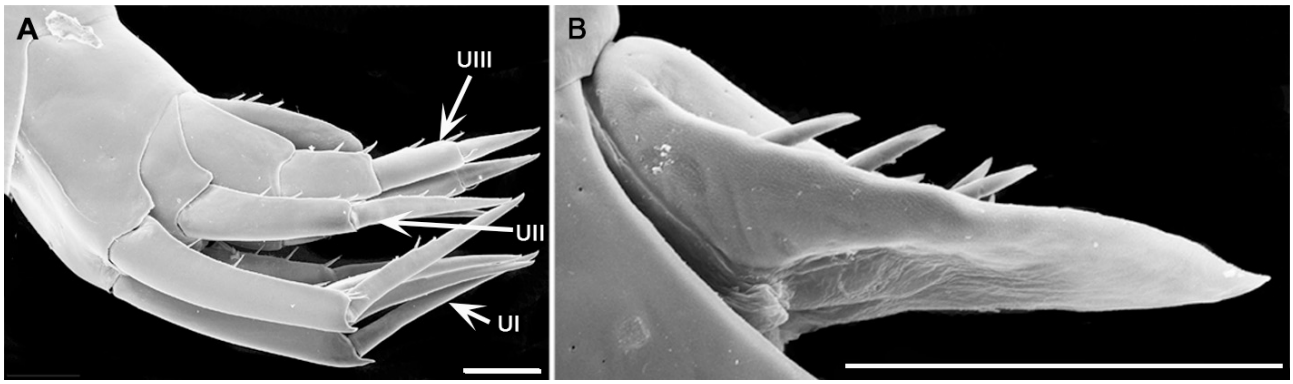

Fig. 5. Pereopodes of an adult *Stenothoe* cf. *tergestina* female (a scanning electron microscope). A, urosome with uropodes; B, telson (lateral view); UI–UIII, uropodes I–III. Scale lines are 0.1 mm; original photo

Uropod II (Fig. 5A, UII). Peduncle equal in length to inner ramus, spines extero-dorsally. Outer branch slightly shorter than inner one, both branches pointed terminally, with spines dorsally, no terminal spines.

Uropod III (Fig. 5A, UIII). Slightly shorter than uropod II. Peduncle shorter than single ramus, tapering distally, with strong spines dorsally. Ramus with 2 segments of equal length, the 1st segment with spines dorsally, the 2nd segment pointed at end and with no cuticular structures.

Telson (Fig. 5B). Entire, tapering distally, with convex margins and strong spines along margins.

Male (Fig. 6A), length 3.00 mm (distinctive sexual characteristics).

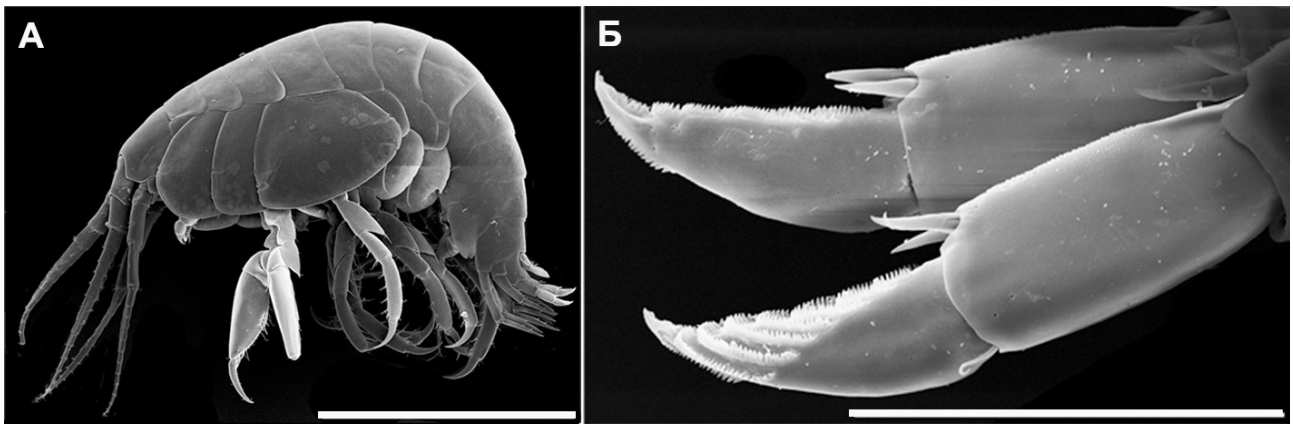

Fig. 6. Habitus (A) and rami of uropodes III (B) of a *Stenothoe* cf. *tergestina* male (a scanning electron microscope). Scale lines are 1 mm (A) and 0.1 mm (B); from [Grintsov, 2024]

Gnathopod II. Propodus equal to basipodite or slightly longer.

Uropod III (Fig. 6B). The second terminal segment of ramus with a different shape than in females: sharply swollen proximally and sharply tapering distally. Dorsally with a notch covered with rows of tiny hairs.

Analysis of individual variability of several traits showed as follows: the ratio of the length of the stalk of antenna II and the length of its flagellum (LAIISt/LAIIFl) is subject to higher variability in both adult males and adult females (Table 1). Analysis of Pearson's paired correlation between the length of an individual and the studied ratios revealed no significant correlations in either females or males. Besides the above-mentioned ratio (LAIISt/LAIIFl), the ratio of the lengths of antenna I and antenna II is noteworthy. In some females, antenna I predominates in length, in others, antenna II (see Table 1), although in general, antenna I prevails in length. In males, either antennae are equal or antenna I predominates (Table 1).

Table 1. Values of individual variability of morphological traits in adult *Stenothoe* cf. *tergestina* males and females

Morphological trait	Males	Females
Body length	2.15–3.25 2.72 ± 0.28	2.50–4.35 3.06 ± 0.47
LAI/LAII	1.00–1.41 1.16 ± 0.09	0.89–1.56 1.16 ± 0.15
LAIISt/LAIIFl	0.44–1.05 0.72 ± 0.12	0.50–1.38 0.75 ± 0.17
CoxII/CoxIII	1.05–1.39 1.24 ± 0.07	1.02–1.50 1.15 ± 0.09
LTl/LUIII	0.52–0.77 0.64 ± 0.06	0.46–0.67 0.57 ± 0.06

Note: the range of values (min–max) is above the line; the mean ± standard deviation is below the line. Abbreviations are explained in "Material and Methods" section.

Ecology. The species was found on various substrates of the marine farm structures: in oyster cages, on ropes, fastening elements, buoys, in Bivalvia druses, on Hydrozoa and Bryozoa colonies, and among several macrophytes. *S.* cf. *tergestina* settlements are female-dominated. The analysis of 35 samples (646 females and 335 males; 981 adult individuals in total) showed that females prevailed in 30 samples, the abundance of males and females was equal in 3 samples, and males predominated in 2 samples. In the overwhelming majority of the samples (30 out of 35), adult amphipods prevailed (981 adult individuals and 406 juveniles).

Conclusion. Clarifying the morphology of adult *Stenothoe* cf. *tergestina* females and males allows for comparing its representatives found on structures of a marine farm with individuals of various species of this genus from other habitats. For adults of both sexes, variability of several morphological traits was revealed reflecting the degree of their variability; this can be useful in comparative studies on the morphology of the genus *Stenothoe*. The analysis of the sex structure of adult individuals uncovered the predominance of females in settlements, and the investigation of the size composition of the population showed that the length of females exceeded that of males. The results of the study evidence for a high degree of adaptability of representatives of this taxon: those are capable of living in various communities and inhabiting different types of substrates.

This work was carried out within the framework of IBSS state research assignment "Comprehensive study of the functioning mechanisms of marine biotechnological complexes with the aim of obtaining bioactive substances from hydrobionts" (No. 124022400152-1).

REFERENCES

1. Greze I. I. *Amfipody Chernogo morya i ikh biologiya.* Kyiv : Naukova dumka, 1977, 154 p. (in Russ.). https://repository.marine-research.ru/handle/299011/5661
2. Greze I. I. *Vysshie rakoobraznye.* Iss. 5: *Bokoplavy.* Kyiv : Naukova dumka, 1985, 172 p. (Fauna Ukrainy ; vol. 26). (in Russ.). https://repository.marine-research.ru/handle/299011/1471
3. Grintsov V. A. New data on morphology, biology and ecology of the amphipod *Jassa* spp. (Amphipoda, Ishyroceridae) from the Black Sea. *Vestnik zoologii*, 2003a, vol. 37, no. 2, pp. 73–76. (in Russ.). https://elibrary.ru/dtmkup
4. Grintsov V. A. On the first find of *Orchestia platensis* (Amphipoda, Talitridae), a species new for Ukrainian fauna in Crimean shore. *Vestnik zoologii*, 2003b, vol. 37, no. 3, pp. 42. (in Russ.). https://elibrary.ru/zoqfsl
5. Grintsov V. A. *Parhyale taurica* sp. nov. (Amphipoda, Hyalidae) – the new species from the Crimea coastal zone (Black Sea). *Byulleten' Moskovskogo obshchestva ispytatelei prirody. Otdel biologicheskii*, 2009a, vol. 114, iss. 2, pp. 73–76. (in Russ.). https://elibrary.ru/pnfhvx
6. Grintsov V. A. *Ampelisca sevastopoliensis* sp. n. (Amphipoda, Ampeliscidae) – new species from coastal zone of Crimea (Black Sea). *Byulleten' Moskovskogo obshchestva ispytatelei prirody. Otdel biologicheskii*, 2011, vol. 116, iss. 1, pp. 67–69. (in Russ.). https://elibrary.ru/plvqbz
7. Grintsov V. A new amphipod species *Echinogammarus karadagiensis* sp. n. (Amphipoda, Gammaridae) from Crimean coasts (Black Sea, Ukraine). *Vestnik zoologii*, 2009b, vol. 43, no. 2, pp. 23–26. https://elibrary.ru/xkirkl
8. Grintsov V. On finding *Dexamine thea* (Amphipoda, Dexaminidae) in the Ukrainian territorial waters (Crimea, Black Sea). *Vestnik zoologii*, 2010, vol. 44, no. 3, pp. 281–283. https://elibrary.ru/vdstwc
9. Grintsov V. A. On finding of *Monocorophium insidiosum* Crawford, 1937 (Amphipoda, Corophiidae) in the coastal waters of Crimea (Black Sea), a new species for this region. *Marine Biological Journal*, 2018, vol. 3, no. 2, pp. 33–39. https://doi.org/10.21072/mbj.2018.03.2.02
10. Grintsov V., Sezgin M. *Manual for Identification of Amphipoda from the Black Sea.* Sevastopol : Digit Print, 2011, 151 p., 379 ill. https://repository.marine-research.ru/handle/299011/1472
11. Grintsov V. A. First finding of *Centraloecetes* cf. *neapolitanus* (Schiecke, 1978) (Ischyroceridae, Amphipoda) in coastal zone of Sevastopol (Crimea, Black Sea). *Trudy Karadagskoi nauchnoi stantsii imeni T. I. Vyazemskogo – prirodnogo zapovednika RAN*, 2021, no. 2 (18), pp. 3–11. https://doi.org/10.21072/eco.2021.18.01
12. Grintsov V. A. The first record of *Stenothoe* cf. *tergestina* (Nebeski, 1881) (Crustacea, Amphipoda, Stenothoidae) in the Black Sea. *Biology Bulletin*, 2024, vol. 51, no. 7, pp. 2034–2038. https://doi.org/10.1134/S1062359024700547
13. Krapp-Schickel G. Genus *Stenothoe* Dana, 1852. The Amphipoda of the Mediterranean. *Mémoires de l'Institut océanographique.* Monaco, 1993, vol. 13, no. 3, pp. 692–709.

МОРФОЛОГИЯ *STENOTHOE* CF. *TERGESTINA* (NEBESKI, 1881) (CRUSTACEA, AMPHIPODA, STENOTHOIDAE), НЕДАВНЕГО ВСЕЛЕНЦА В ЧЁРНОЕ МОРЕ

В. А. Гринцов

ФГБУН ФИЦ «Институт биологии южных морей имени А. О. Ковалевского РАН»,
Севастополь, Российская Федерация
E-mail: *vgrintsov@gmail.com*

Актуальность исследований новых для регионов видов обусловлена их взаимодействием с видами местных экосистем, которое порой может иметь негативный характер. Цель настоящей работы — уточнить морфологию и вариабельность нескольких параметров тела и конечностей взрослых самцов и самок *Stenothoe* cf. *tergestina*, который сходен с *Stenothoe tergestina* (Nebeski, 1881), но имеет ряд морфологических различий, не позволяющих отнести их к разным видам. Для выполнения поставленных задач использованы методы анализа морфологии с применением световой и электронной микроскопии. Приведено детальное описание взрослых самок и самцов *S.* cf. *tergestina*, их конечностей, а также половой структуры популяции из обрастаний конструкций мидийно-устричной фермы вблизи Севастополя. Новые данные по обнаруженному таксону проанализированы в сравнении со сведениями из других местообитаний, что позволяет уточнить его видовую принадлежность. Выявлена вариабельность ряда морфологических признаков. В популяциях длина самок превышала длину самцов. Обнаружение особей на различных субстратах указывает на высокую приспособленность вида к данному местообитанию.

Ключевые слова: амфиподы, Чёрное море, *Stenothoe* cf. *tergestina*, морфология

1871
ИнБЮМ – IBSS

Морской биологический журнал
Marine Biological Journal
2025, vol. 10, no. 3, pp. 20–30
https://marine-biology.ru

UDC 582.261.1-114.3:57.043

THE EFFECT OF TEMPERATURE ON THE GROWTH OF TWO SPECIES OF *PSEUDO-NITZSCHIA* H. PERAGALLO (BACILLARIOPHYTA) IN LABORATORY CULTURES ISOLATED FROM THE SEA OF JAPAN

© 2025 **A. Zinov and I. Stonik**

A. V. Zhirmunsky National Scientific Center of Marine Biology, FEB RAS, Vladivostok, Russian Federation
E-mail: *innast2004@mail.ru*

Received 03.12.2024; revised 30.01.2025;
accepted 12.08.2025.

Diatoms of the genus *Pseudo-nitzschia* H. Peragallo, 1900, known as producers of the neurotoxic domoic acid, regularly cause algal blooms in the Russian Far Eastern seas. Temperature is an important factor affecting diatom blooms; however, its effect on the growth of this group of microalgae from the Sea of Japan has not been sufficiently studied. In this regard, growth characteristics of two diatom species were investigated in laboratory culture within the temperature range of +5 to +20 °C. The test involved direct counting in a Nageotte chamber. Cell density, growth rates, and generation time were evaluated. As found, the maximum average density of *P. fraudulenta* reached 2.2×10^5 cells·L^{-1} on the 16th day of the experiment at +18 °C. For this species, at +18 °C, the growth rate (0.11–0.16 div.·day^{-1}) remained relatively high, and the generation time (4.4–6.7 days) was relatively low for most of the test. The maximum mean density of *P. hasleana*, 5×10^5 cells·L^{-1}, was recorded on the 16th day of the experiment at +17 °C. For this species, high growth rate (0.2–0.92 div.·day^{-1}) and low generation time (0.8–3.6 days) were recorded at +17 °C from the 2nd to the 10th day of the test. The average densities of *P. fraudulenta* and *P. hasleana* were statistically significantly higher at +17 °C and +18 °C, respectively, than at the other temperatures studied (Tukey's test, $p < 0.05$). As recorded, when *P. fraudulenta* clones were grown at +10, +16, and +18 °C, and when *P. hasleana* clones were cultured at +14, +17, and +20 °C, their cells remained viable and continued to divide. When the cultivation temperature for *P. fraudulenta* and *P. hasleana* was lowered to +5 and +7 °C, respectively, division slowed down dramatically, and cell density was statistically significantly lower than at higher temperatures (Tukey's test, $p < 0.05$). Ranges of tolerant temperature during *P. fraudulenta* and *P. hasleana* cultivation were found to be within +10…+18 °C and +14…+17 °C, respectively. The revealed lower temperature tolerance limits for the two species during cultivation (+10 and +14 °C) corresponded to water temperatures under which *P. fraudulenta* and *P. hasleana* blooms were observed in the natural environment (+6…+16 and +10…+16 °C, respectively). The study demonstrated the broad adaptive potential of the investigated species to temperature changes.

Keywords: *Pseudo-nitzschia fraudulenta*, *Pseudo-nitzschia hasleana*, laboratory cultivation, temperature, Sea of Japan

Diatoms of the genus *Pseudo-nitzschia* H. Peragallo, 1900 are a dominant taxon of toxic planktonic microalgae in the northwestern Sea of Japan: those account for 75–98% of the total phytoplankton density during bloom seasons [Orlova et al., 2008]. They are known as potential producers of neurotoxic domoic acid [Bates et al., 2018; Liu et al., 2021; Zhou et al., 2024] and belong to one of the most

numerous groups of toxic phytoplankton regularly causing algal blooms in the Far Eastern seas of Russia [Stonik, 2021; Stonik, Orlova, 2018; Stonik et al., 2011, 2019]. Temperature plays a decisive role in the metabolic processes of Bacillariophyta and other microalgae, affects photosynthesis and nutrient absorption, and mediates enzymatic processes in cells [Claquin et al., 2008; Davison et al., 1991; Klochkova, Lelekov, 2022; Kuzmin, 2025; Raven, Geider, 1988]. Thus, temperature is a significant factor of the occurrence and development of diatom blooms [Fu et al., 2012; Ryabushko et al., 2008]. Two species, *Pseudo-nitzschia fraudulenta* (Cleve) Hasle, 1993 and *Pseudo-nitzschia hasleana* Lundholm, 2012, are regularly recorded in Peter the Great Bay (the Sea of Japan) as an important component of phytoplankton involved in the formation of water blooms [Stonik, Orlova, 2018; Stonik, Zinov, 2023; Stonik et al., 2008]. However, environmental factors, primarily temperature, driving the abundance and physiological state of *Pseudo-nitzschia* spp. from the Sea of Japan have not been sufficiently studied.

In this regard, the aim of the work is to investigate under experimental conditions the effect of temperature on the dynamics of density, division rate, and generation time in laboratory cultures of *Pseudo-nitzschia fraudulenta* and *P. hasleana*: diatoms isolated from waters of the Russian sector of the Sea of Japan.

MATERIAL AND METHODS

The object of the study is unialgal cultures of diatoms of the genus *Pseudo-nitzschia* isolated from Peter the Great Bay, Sea of Japan. *P. fraudulenta* culture (clone MBRU-PF-16) was isolated from the Amur Bay (N43.2°, E131.91°) in November 2016 at water temperature of +5.2 °C. *P. hasleana* culture (clone MBRU-PH-18) was isolated from the Patrokl Bay of the Ussuri Bay (N43.07°, E131.96°) in November 2018 at water temperature of +6.8 °C. The cultures are maintained in the "Marine Biobank" core facility at NSCMB FEB RAS [2024].

The cultures were grown on f/2 nutrient medium [Guillard, Ryther, 1962]. Before the experiment, both clones were pre-adapted to studied temperatures for four days. Cultures at the exponential growth stage were used as an inoculum. For the test, the cultures were transferred to Erlenmeyer flasks (250 mL) with a culture suspension volume of 200 mL; the light flux intensity was of 3,500 lux, and photoperiod was 12 h : 12 h (light : darkness). *P. fraudulenta* culture was grown at +5, +10, +16, and +18 °C; *P. hasleana* culture, at +7, +14, +17, and +20 °C (in three flasks at each value). Binder KBW 400 climate chambers (Germany) were used to create the required temperature conditions. Illumination in the chambers was provided by daylight fluorescent lamps. The intensity of the luminous flux was measured with a UNI-T mini UT383 00-00007443 light meter (UNI-T, China). The experiments were performed in triplicate.

The cell density was estimated by direct counting in a 0.05-mL Nageotte counting chamber under an Olympus BX41 light microscope (Japan) at 20× magnification. Cells were counted every two days. Samples for quantitative analysis were taken in triplicate 2–3 h after the end of the dark period, and the suspension was thoroughly mixed and fixed with Utermöhl's solution [Fedorov, 1979].

The specific growth rate of the culture was calculated based on cell concentration data by the formula [Zaika, 1972]:

$$\mu = \frac{\ln X_1 - \ln X_0}{T_1 - T_0},$$

where X_1 and X_0 are concentration values corresponding to the time of growth T_1 and T_0.

The cell density doubling time (generation time) was estimated by the formula [Jones et al., 1963]:

$$g = \frac{\ln 2}{\mu} = \frac{0.693}{\mu},$$

where g is the generation time;

μ is the specific growth rate.

A test for a reliable relationship between temperature, age of the culture, and cell density was performed using a two-factor analysis of variance. Data on cell density, growth rate, and generation time depending on temperature were subjected to a one-factor analysis of variance. For multiple comparisons of means, Tukey test was applied. All calculations were performed in Statistica 7.0 [StatSoft, 2025].

RESULTS

As revealed using a two-factor analysis of variance, both factors considered in the experiment, temperature and age of culture, and their interaction were statistically significant ($p < 0.001$) and affected *Pseudo-nitzschia* spp. cell density (Table 1).

Table 1. Results of a two-factor analysis of variance on the effect of *Pseudo-nitzschia fraudulenta* and *P. hasleana* cultivation conditions on cell density

Factor	*F*		*p*
	Pseudo-nitzschia fraudulenta	*Pseudo-nitzschia hasleana*	
	942.3	12,764.37	0.00
Temperature	373.7	477.33	0.00
Age of the culture	42.8	1,238.92	0.00

Note: all values of the correlation coefficients, the Fisher's criterion (*F*) and probability (*p*), were significant.

The dynamics of *P. fraudulenta* and *P. hasleana* density under cultivation conditions at different temperatures is shown in Fig. 1.

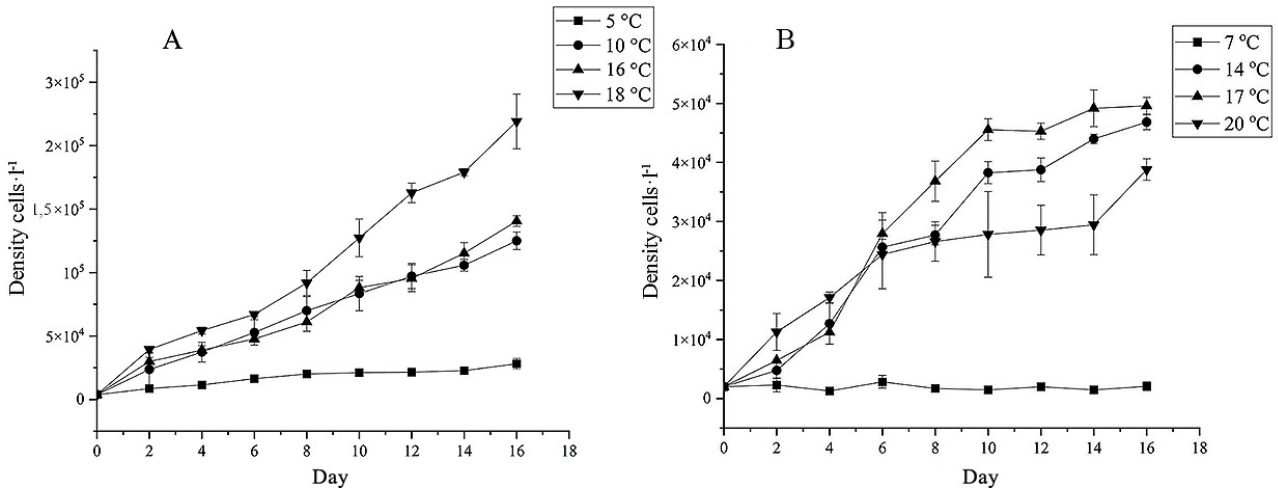

Fig. 1. Dynamics of cell densities of *Pseudo-nitzschia fraudulenta* cells (A) and *P. hasleana* cells (B) at different temperature (the means and standard deviations are given)

Pseudo-nitzschia fraudulenta. The initial cell density in the experiment was 3.7×10^3 cells·L^{-1}. Throughout the test, there was an increase in total cell density in a range of temperatures +10 to +18 °C (Fig. 1A). The maximum mean density (2.2×10^5 cells·L^{-1}) was recorded on the 16th day of the experiment at +18 °C, and the minimum one (8.6×10^3 cells·L^{-1}) was registered on the 2nd day at +5 °C. When the cultivation temperature was reduced to +5 °C, the mean density was 2.8×10^4 cells·L^{-1} on the day 16; it is approximately an order of magnitude lower than at the end of the test at +18 °C. The mean cell density at +18 °C was statistically significantly higher (Tukey test, $p < 0.05$) than at other temperature values throughout the experiment. From the 4th day of cultivation and until the end of the test, there were no statistically significant differences between the mean density values at +10 and +16 °C (Fig. 1A, Table 2).

Table 2. Statistically significant differences between *Pseudo-nitzschia fraudulenta* cell abundance curves at different temperature based on the Tukey matrix at $p < 0.05$

Day	Temperature, °C			
	+5	+10	+16	+18
2	+10, +16, +18	+5, +16, +18	+5, +10, +18	+5, +10, +16
4	+10, +16, +18	+5, +18	+5, +18	+5, +10, +16
6	+10, +16, +18	+5, +18	+5, +18	+5, +10, +16
8	+10, +16, +18	+5, +18	+5, +18	+5, +10, +16
10	+10, +16, +18	+5, +18	+5, +18	+5, +10, +16
12	+10, +16, +18	+5, +18	+5, +18	+5, +10, +16
14	+10, +16, +18	+5, +18	+5, +18	+5, +10, +16
16	+10, +16, +18	+5, +18	+5, +18	+5, +10, +16

The mean growth rates during cultivation at +5 °C (0.1–0.18 div.·day^{-1}) and +10 °C (0.14–0.23 div.·day^{-1}) were higher than at other temperatures from day 2 to days 6–8. From the 8th to the 14th day, the growth rates dropped reaching a minimum (0.01 div.·day^{-1}) against the backdrop of the maximum generation time (40.5 days) on days 10–12 at +5 °C (Table 3).

Table 3. Growth rate (div.·day^{-1}) and generation time (days) during *Pseudo-nitzschia fraudulenta* cultivation at different temperature

Days	+5 °C		+10 °C		+16 °C		+18 °C	
	μ	g	μ	g	μ	g	μ	g
2–4	0.14 ± 0.063	5.5 ± 1.902	0.23 ± 0.067	3.3 ± 0.631	0.13 ± 0.011	5.3 ± 0.234	0.16 ± 0.016	4.4 ± 0.267
4–6	0.18 ± 0.051	4.1 ± 1.070	0.17 ± 0.056	4.2 ± 1.187	0.1 ± 0.024	6.9 ± 1.464	0.11 ± 0.015	6.7 ± 1.039
6–8	0.1 ± 0.051	9.2 ± 5.016	0.14 ± 0.056	6.4 ± 4.450	0.12 ± 0.024	6.1 ± 2.258	0.16 ± 0.015	4.7 ± 1.520
8–10	0.03 ± 0.051	35.1 ± 17.094	0.09 ± 0.056	11.4 ± 5.253	0.11 ± 0.024	6.4 ± 1.340	0.16 ± 0.015	4.5 ± 1.548
10–12	0.01 ± 0.004^{b,c}	40.5 ± 2.428$^{a–c}$	0.08 ± 0.031	10.5 ± 5.477^{a}	0.11 ± 0.020^{b}	6.4 ± 1.240^{b}	0.12 ± 0.037^{c}	5.9 ± 2.141^{c}
12–14	0.03 ± 0.004^{b,c}	31.5 ± 12.416	0.04 ± 0.031	16.6 ± 2.056	0.1 ± 0.020^{b}	7.8 ± 2.554	0.05 ± 0.037^{c}	15.8 ± 5.026
14–16	0.1 ± 0.004^{b,c}	11 ± 5.004	0.08 ± 0.031	8.7 ± 2.199	0.1 ± 0.020^{b}	7.4 ± 2.112	0.1 ± 0.037^{c}	7.7 ± 2.535

Note: the values of growth rates and generation time are provided in the columns μ and g, respectively, with confidence intervals. Footnotes to the means mark results that are statistically significantly different (Tukey's test, $p < 0.05$) under the following cultivation conditions: +5 and +10 °C (a); +5 and +16 °C (b); +5 and +18 °C (c).

Cultivation at +16 and +18 °C revealed relatively high growth rates (0.11–0.16 div.·day^{-1}) and low values of generation time (4.4–6.9 days) during most of the experiment, from the 2nd to the 12th day (Table 3). On days 12–14 at +16…+18 °C, a decrease in the growth rate and a rise in the generation time were recorded compared to the values in the previous periods of cultivation (from day 2 to day 12) (Table 3).

A slight increase in the growth rate at the end of the test, on the 14–16th days, at +5, +10, and +18 °C was noticeably lower than the values in the first half of the experiment (Table 3). On days 10–14 of cultivation, statistically significant differences in the mean growth rates (Tukey test, $p < 0.05$) at +5 and +16 °C, as well as at +5 and +18 °C, were registered. The growth rates at +5 °C were noticeably lower during most of the test than at a higher temperature (Table 3), and this determined the low cell density in the experiment at +5 °C (Fig. 1A).

Pseudo-nitzschia hasleana. The initial cell density in the test was 2 × 10^3 cells·L^{-1}. Throughout the experiment on *P. hasleana* culturing, we revealed a rise in the total cell density in the temperature range +14 to +20 °C (Fig. 1B).

The maximum mean density (5 × 10^5 cells·L^{-1}) was recorded on day 16 at +17 °C, and the minimum mean density (1.3 × 10^3 cells·L^{-1}) was noted on day 4 at +7 °C. At cultivation temperature of +7 °C, on the 6th day of the experiment, the cell density increased to 2.8 × 10^3 cells·L^{-1}, and then it dropped; only on the 12th day, it rose to 2 × 10^3 cells·L^{-1} and remained at this level until the end of the test (Fig. 1B). The differences in the mean density values at all studied temperature values (+7, +14, +17, and +20 °C) were statistically significant (Tukey test, $p < 0.05$) only on days 10–12 of the experiment (Table 4).

Table 4. Statistically significant differences between *Pseudo-nitzschia hasleana* cell abundance curves at different temperature based on the Tukey matrix at $p < 0.05$

Day	Temperature, °C			
	+7	+14	+17	+20
2	+17, +20	+20	+7, +20	+7, +14, +17
4	+14, +17, +20	+7	+7	+7
6	+14, +17, +20	+7	+7, +20	+7, +17
8	+14, +17, +20	+7, +17	+7, +14, +20	+7, +17
10	+14, +17, +20	+7, +17, +20	+7, +14, +20	+7, +14, +17
12	+14, +17, +20	+7, +17, +20	+7, +14, +20	+7, +14, +17
14	+14, +17, +20	+7, +20	+7, +20	+7, +14, +17
16	+14, +17, +20	+7	+7, +20	+7, +17

The mean cell density at +17 °C was noticeably higher (Tukey test, $p < 0.05$) than that for all other temperature values on the 8–12th days of the test (Table 4). On days 14–16, no statistically significant differences were found between the mean density at +14 and +17 °C (Fig. 1B, Table 4).

When *P. hasleana* was cultured at +14, +17, and +20 °C, high growth rates were recorded during the first half of the experiment, and at 7 °C, during the second half (Table 5).

Thus, at a temperature of +14 °C, the highest growth rates (0.73–0.98 div.·day^{-1}) were registered from the 2nd to the 6th day. From days 6–8 to 8–10, the values decreased from 0.54 to 0.32 div.·day^{-1}. From the 10th to the 12th day and until the end of the experiment, the growth rate at this temperature

was relatively low, with a minimum (0.01 div.·day^{-1}) on the 10–12th day (Table 5). High growth rates (0.2–0.92 div.·day^{-1}) were noted at +17 °C from day 2 to day 10, and at +20 °C, from day 2 to day 8 (0.2–0.47 div.·day^{-1}). From the 10th day until the end of the test, the growth rates at +14, +17, and +20 °C dropped dramatically compared to the values in the first part of the experiment (Table 5). The exceptions were relatively high growth rate (0.19 div.·day^{-1}) and long generation time (5.1 days) on days 14–16th at +20 °C.

Table 5. Growth rate (div.·day^{-1}) and generation time (days) during *Pseudo-nitzschia hasleana* cultivation at different temperature

Days	+7 °C		+14 °C		+17 °C		+20 °C	
	μ	g	μ	g	μ	g	μ	g
2–4	0.08 ± 0.003$^{a–c}$	8.7 ± 0.347$^{a–c}$	0.98 ± 0.075^{a,d,e}	0.7 ± 0.054^{a}	0.54 ± 0.164^{b,d,e}	1.4 ± 0.506^{b}	0.47 ± 0.130^{c,e}	1.6 ± 0.447^{c}
4–6	0.05 ± 0.023$^{a–c}$	15.5 ± 5.613$^{a–c}$	0.73 ± 0.240^{a}	1.0 ± 0.283^{a}	0.92 ± 0.159^{b}	0.8 ± 0.138^{b}	0.20 ± 0.097^{c}	4.0 ± 1.876^{c}
6–8	0.07 ± 0.001^{b,c}	9.8 ± 0.200$^{b–e}$	0.54 ± 0.031$^{a,d–e}$	6.4 ± 2.368$^{d.e}$	0.28 ± 0.033^{b,d}	2.5 ± 0.323^{b,d}	0.22 ± 0.050^{c,e}	3.3 ± 0.888^{c,e}
8–10	0.16 ± 0.001^{b,c}	4.8 ± 2.086	0.32 ± 0.031^{d,e}	2.1 ± 0.089^{e}	0.20 ± 0.033^{b,d}	3.6 ± 1.167	0.08 ± 0.010^{c,e}	11.4 ± 5.949^{e}
10–12	0.15 ± 0.049$^{a–c}$	4.9 ± 1.796^{a}	0.01 ± 0.008^{a}	7.2 ± 1.190^{a}	0.02 ± 0.016^{b}	18.3 ± 3.928	0.06 ± 0.017^{c}	12.1 ± 3.136
12–14	0.25 ± 0.049$^{a–c}$	2.9 ± 0.464$^{b.c}$	0.14 ± 0.008^{a}	5.3 ± 1.942	0.07 ± 0.016^{b}	12.1 ± 5.488^{b}	0.06 ± 0.017^{c}	11.0 ± 1.865^{c}
14–16	0.31 ± 0.049^{a,b}	2.3 ± 0.464^{b,c}	0.04 ± 0.017^{a}	9.7 ± 1.942	0.01 ± 0.020^{b}	8.1 ± 5.488^{b}	0.19 ± 0.123	5.1 ± 1.865^{c}

Note: the values of growth rates and generation time are provided in the columns μ and g, respectively, with confidence intervals. Footnotes to the means mark results that are statistically significantly different (Tukey's test, $p < 0.05$) under the following cultivation conditions: +7 and +14 °C (a); +7 and +17 °C (b); +7 and +20 °C (c); +14 and +17 °C (d); +14 and +20 °C (e).

Cultivation at +7 °C showed as follow: from the 2nd to the 8th day, the growth rates remained relatively low (0.05–0.08 div.·day^{-1}), and the generation time was high (8.7–15.5 days). Only on days 8–10, the growth rates began to rise (Table 5). Throughout most of the test at +7 °C, the growth rates were statistically significantly lower (Tukey test, $p < 0.05$) than at a higher temperature, and this mediated the low density at the minimum temperature investigated (Fig. 1B).

DISCUSSION

Our data show that *P. fraudulenta* and *P. hasleana* are capable of remaining in a viable state throughout the experiment and actively divide within the temperature ranges of +10…+18 °C and +14…+20 °C, respectively. The mean cell density of *P. fraudulenta* at +18 °C was statistically significantly higher than at other values (Tukey test, $p < 0.05$) throughout the test (Fig. 1A, Table 2). The mean cell density of *P. hasleana* at +17 °C was noticeably higher (Tukey test, $p < 0.05$) than that at other temperatures on days 8–12 (Fig. 1B, Table 4). At a temperature tolerant for *P. fraudulenta* and *P. hasleana* cultivation, in most cases, the growth rates at the end of the experiment (from the 10–12th to 14–16th days) were lower, and the generation time was higher than during the previous part of the test, despite small peaks on the 14–16th day at +18 °C for *P. fraudulenta* and at +20 °C for *P. hasleana* (Tables 3, 5).

This indicated a slowdown in cell growth towards the end of the experiment. It can be assumed as follows: on days 14–16, due to the release of nutrients resulting from the decomposition of dying cells and the effect of bacterial exometabolites, which can promote the growth of microalgae, small secondary peaks in density and growth rate were recorded. Due to the low growth rates and longer generation time, the mean cell density of *P. fraudulenta* and *P. hasleana* when cultured at +5 and +7 °C, respectively, was significantly lower than that at a higher temperature (Tukey test, $p < 0.05$) (Fig. 1A and B).

So, the ranges of tolerant temperatures for *P. fraudulenta* and *P. hasleana* cultivation were +10 to +18 °C and +14 to +20 °C, respectively. The optimal temperatures for the development of these species in culture were +18 and +17 °C, respectively. Since the clones we studied were isolated from the natural environment at relatively low water temperatures (about +5…+7 °C), *P. fraudulenta* and *P. hasleana* appear to be adapted to surviving in a wide range of temperatures. This is consistent with the available literature data on the widespread distribution of these species in plankton at high, low, and temperate latitudes [Bates et al., 2018].

Literature data support our findings on the development of the investigated species in a wide range of temperature for cultivation. According to previous studies, for *P. fraudulenta* isolates from different areas of the World Ocean, the optimal ranges of water temperatures for growth were +10…+15 °C [Ayache et al., 2021; Fehling et al., 2006; Gai et al., 2018; Thessen et al., 2009] and +18.5…+26.5 °C [Delegrange et al., 2018]. Other authors reported a temperature of (20.8 ± 0.8) °C for a *P. fraudulenta* clone from coastal waters of France [Claquin et al., 2008]. In the North Atlantic, *P. fraudulenta* vegetation began at a water temperature of +9…+14.4 °C [Hasle, 1965]. Importantly, this did not differ much from our data on the species blooms in Peter the Great Bay (Sea of Japan) within the temperature range of +6…+16 °C [Stonik et al., 2008]. As for *P. hasleana*, according to literature data, water temperature favorable for its development off the coast of Australia exceeded +16 °C [Ajani et al., 2013]. Water blooms caused by *Pseudo-nitzschia calliantha* Lundholm, Moestrup & Hasle, 2003 and *P. hasleana* in Peter the Great Bay were previously registered by us at water temperature of +10…+16 °C [Stonik, Zinov, 2023]. Thus, lower limits of temperature conditions for culturing two species we revealed (+10 and +14 °C) are consistent with the parameters of water temperature in the natural environment (Peter the Great Bay, Sea of Japan) at which blooms of *P. fraudulenta* (+6…+16 °C) and *P. hasleana* (+10…+16 °C) were observed.

The occurrence of high adaptive capabilities of *Pseudo-nitzschia* species in relation to temperature, along with high genetic variability in natural populations of this genus [Evans et al., 2005], suggest that *P. fraudulenta* and *P. hasleana* may gain advantages for growth in a relatively wide range of water temperatures, +10…+18 °C and +14…+20 °C, respectively, in Russian waters of the Sea of Japan. The obtained data can be used to predict blooms of the analyzed species in the study area.

Conclusions. When *Pseudo-nitzschia fraudulenta* clones were grown at temperatures of +10, +16, and +18 °C, and *Pseudo-nitzschia hasleana* clones were grown at +14, +17, and +20 °C, cells remained in a viable state and continued to divide. When the cultivation temperature of *P. fraudulenta* and *P. hasleana* was lowered to +5 and +7 °C, respectively, division slowed down dramatically.

The ranges of tolerable temperatures during *P. fraudulenta* and *P. hasleana* cultivation were +10 to +18 °C and +14 to +20 °C, respectively. The revealed lower limits of the range of temperatures for cultivation of these two species (+10 and +14 °C) are consistent with the parameters of water temperature in the natural environment, Peter the Great Bay (Sea of Japan), under which blooms of *P. fraudulenta* (+6…+16 °C) and *P. hasleana* (+10…+16 °C) were observed.

The work was carried out within the framework of NSCMB FEB RAS state research assignment "Dynamics of marine ecosystems, adaptation of marine organisms and communities to changes in the habitat" (No. 121082600038-3).

Acknowledgments. The authors express their deep gratitude to N. Aizdaicher (NSCMB FEB RAS) for her useful consultations during the work.

REFERENCES

1. Zaika V. E. *Specific Production of Aquatic Invertebrates.* Kyiv : Naukova dumka, 1972, 147 p. (in Russ.). https://repository.marine-research.ru/handle/299011/1127
2. Klochkova V. S., Lelekov A. S. Study of the temperature effect on the specific growth rate of *Arthrospira platensis* culture. *Trudy Karadagskoi nauchnoi stantsii imeni T. I. Vyazemskogo – prirodnogo zapovednika RAN*, 2022, no. 1 (21), pp. 40–50. (in Russ.). https://doi.org/10.21072/eco.2022.21.05
3. Kuzmin D. V. *Razrabotka platformy po polucheniyu biologicheski aktivnykh soedinenii iz fotosinteziruyushchikh mikroorganizmov* : avtoref. dis. … d-ra biol. nauk : 1.5.6 / Vserossiiskii nauchno-issledovatel'skii institut sel'skokhozyaistvennoi biotekhnologii. Dolgoprudny, 2025, 47 p. (in Russ.)
4. *Marine Biobank. Resource Collection. Core Shared Research Facility* / National Scientific Center of Marine Biology, Far Eastern Branch, Russian Academy of Sciences : [site]. Vladivostok, 2024. (in Russ.). URL: https://marbank.dvo.ru/index.php/ru/ [accessed: 25.11.2024].
5. Ryabushko L. I., Besiktepe S., Ediger D., Yilmaz D., Zenginer A., Ryabushko V. I., Lee R. I. Toxic diatom of *Pseudo-nitzschIa calliantha* Lundholm, Moestrup et Hasle from the Black Sea: Morphology, taxonomy, ecology. *Morskoj ekologicheskij zhurnal*, 2008, vol. 7, no. 3, pp. 51–60. (in Russ.). https://repository.marine-research.ru/handle/299011/973
6. Stonik I. V., Orlova T. Y. Domoic acid–producing diatoms of the genus *Pseudo-nitzschia* H. Peragallo, 1900 (Bacillariophyta) from the North Pacific. *Biologiya morya*, 2018, vol. 44, no. 5, pp. 299–306. (in Russ.). https://doi.org/10.1134/S0134347518050017
7. Fedorov V. D. *O metodakh izucheniya fitoplanktona i ego aktivnosti* : [uchebnoe posobie]. Moscow : Izd-vo Mosk. un-ta, 1979, 167 p. (in Russ.)
8. Ajani P., Murray S., Hallegraef G., Brett S., Armand L. First reports of *Pseudo-nitzschia micropora* and *P. hasleana* (Bacillariaceae) from the Southern Hemisphere: Morphological, molecular and toxicological characterization. *Phycological Research*, 2013, vol. 61, iss. 3, pp. 237–248. https://doi.org/10.1111/pre.12020
9. Ayache N., Lundholm N., Gai F., Hervé F., Amzil Z., Caruana A. Impacts of ocean acidification on growth and toxin content of the marine diatoms *Pseudo-nitzschia australis* and *P. fraudulenta*. *Marine Environmental Research*, 2021, vol. 169, art. no. 105380 (9 p.). https://doi.org/10.1016/j.marenvres.2021.105380
10. Bates S., Hubbard A., Lundholm N., Montresor M. *Pseudo-nitzschia*, *Nitzschia*, and domoic acid: New research since 2011. *Harmful Algae*, 2018, vol. 79, pp. 3–43. https://doi.org/10.1016/j.hal.2018.06.001
11. Claquin P., Probert I., Lefebvre S., Véron B. Effects of temperature on photosynthetic parameters and TEP production in eight species of marine microalgae. *Aquatic Microbial*

Ecology, 2008, vol. 51, no. 1, pp. 1–11. https://doi.org/10.3354/ame01187

12. Davison I. R., Greene R. M., Podolak E. J. Temperature acclimation of respiration and photosynthesis in the brown alga *Laminaria saccharina*. *Marine Biology*, 1991, vol. 110, iss. 3, pp. 449–454. https://doi.org/10.1007/bf01344363
13. Delegrange A., Lefebvre A., Gohin F., Courcot L., Vincent D. *Pseudo-nitzschia* sp. diversity and seasonality in the southern North Sea, domoic acid levels and associated phytoplankton communities. *Estuarine, Coastal and Shelf Science*, 2018, vol. 214, pp. 194–206. https://doi.org/10.1016/j.ecss.2018.09.030
14. Evans K. M., Kuhn S. F., Hayes P. K. High levels of genetic diversity and low levels of genetic differentiation in North Sea *Pseudo-nitzschia pungens* (Bacillariophyceae) populations. *Journal of Phycology*, 2005, vol. 41, iss. 3, pp. 506–514. https://doi.org/10.1111/j.1529-8817.2005.00084.x
15. Fehling J., Davidson K., Bolch C., Tett P. Seasonality of *Pseudo-nitzschia* spp. (Bacillariophyceae) in western Scottish waters. *Marine Ecology Progress Series*, 2006, vol. 323, pp. 91–105. https://doi.org/10.3354/meps323091
16. Fu F. X., Tatters A. O., Hutchins D. A. Global change and the future of harmful algal blooms in the ocean. *Marine Ecology Progress Series*, 2012, vol. 470, pp. 207–233. https://doi.org/10.3354/meps10047
17. Gai F. F., Hedemand C. K., Louw D. C., Grobler K., Krock B., Moestrup Ø., Lundholm N. Morphological, molecular and toxigenic characteristics of Namibian *Pseudo-nitzschia* species – including *Pseudo-nitzschia bucculenta* sp. nov. *Harmful Algae*, 2018, vol. 76, pp. 80–95. https://doi.org/10.1016/j.hal.2018.05.003
18. Guillard R. R. L., Ryther J. H. Studies of marine planktonic diatoms. I. *Cyclotella nana* Hustedt, and *Detonula confervacea* (Cleve) Gran. *Canadian Journal of Microbiology*, 1962, vol. 8, no. 2, pp. 229–239. https://doi.org/10.1139/m62-029
19. Hasle G. R. *Nitzschia* and *Fragilariopsis* species studied in the light and electron microscopes. II. The group *Pseudo-nitzschia*. *Skrifter utgitt av det Norske Videnskaps-Akademi i Oslo. Matematisk-Naturvitenskapelig Klasse Ny Serie*, 1965, vol. 18, pp. 1–45.
20. Jones R. F., Speen H. L., Kury W. Studies on the growth of the red alga *Porphyridium cruentum*. *Physiologia Plantarum*, 1963, vol. 16, iss. 3, pp. 636–643. https://doi.org/10.1111/j.1399-3054.1963.tb08342.x
21. Liu C., Ji Y., Zhang L., Qiu J., Wang Z., Liu L., Zhuang Y., Chen T., Li Y., Niu B., Li A. Spatial distribution and source of biotoxins in phytoplankton from the South China Sea, China. *Journal of Hazardous Materials*, 2021, vol. 418, art. no. 126285 (10 p.). https://doi.org/10.1016/j.jhazmat.2021.126285
22. Orlova T. Yu., Stonik I. V., Aizdaicher N. A., Bates S. S., Léger C., Fehling J. Toxicity, morphology and distribution of *Pseudonitzschia calliantha*, *P. multistriata* and *P. multiseries* (Bacillariophyta) from the northwestern Sea of Japan. *Botanica Marina*, 2008, vol. 51, no. 4, pp. 297–306. https://doi.org/10.1515/bot.2008.035
23. Raven J. A., Geider R. J. Temperature and algal growth. *New Phytologist*, 1988, vol. 110, no. 4, pp. 441–461. https://doi.org/10.1111/j.1469-8137.1988.tb00282.x
24. *StatSoft* : [site]. Moscow, 2025. URL: https://statsoftai.ru/ [accessed: 25.01.2025].
25. Stonik I. V. Long-term variations in species composition of bloom-forming toxic

Pseudo-nitzschia diatoms in the northwestern Sea of Japan during 1992–2015. *Journal of Marine Science and Engineering*, 2021, vol. 9, iss. 6, art. no. 568 (13 p.). https://doi.org/10.3390/jmse9060568

26. Stonik I. V., Orlova T. Y., Chikalovets I. V., Aizdaicher N. A., Aleksanin A. I., Kachur V. A., Morozova T. V. *Pseudo-nitzschia* species (Bacillariophyceae) and the domoic acid concentration in *Pseudo-nitzschia* cultures and bivalves from the northwestern Sea of Japan, Russia. *Nova Hedwigia*, 2019, Bd 108, Heft 1–2, S. 73–93. https://doi.org/10.1127/nova_hedwigia/2018/0502
27. Stonik I. V., Orlova T. Yu., Begun A. A. Potentially toxic diatoms *Pseudo-nitzschia fraudulenta* and *P. calliantha* from Russian waters of East/Japan Sea and Sea of Okhotsk. *Ocean Science Journal*, 2008, vol. 43, iss. 1, pp. 25–30. https://doi.org/10.1007/BF03022428
28. Stonik I. V., Orlova T. Yu., Lundholm N. Diversity of *Pseudo-nitzschia* H. Peragallo from the western North Pacific. *Diatom Research*, 2011, vol. 26, iss. 1, pp. 121–134. https://doi.org/10.1080/0269249x.2011.573706
29. Stonik I. V., Zinov A. A. Changes in the composition of bloom-forming toxic *Pseudo-nitzschia* diatoms in surface waters in Ussuri Bay, northwestern Sea of Japan, during the autumn seasons of 2017–2022. *Journal of Marine Science and Engineering*, 2023, vol. 11, iss. 5, art. no. 1024 (14 p.). https://doi.org/10.3390/jmse11051024
30. Thessen A. E., Bowers H. A., Stoecker D. K. Intra- and interspecies differences in growth and toxicity of *Pseudo-nitzschia* while using different nitrogen sources. *Harmful Algae*, 2009, vol. 8, iss. 5, pp. 792–810. https://doi.org/10.1016/j.hal.2009.01.003
31. Zhou C.-Y., Pan C.-G., Peng F.-J., Zhu R.-J., Hu J.-J., Yu K. Simultaneous determination of trace marine lipophilic and hydrophilic phycotoxins in various environmental and biota matrices. *Marine Pollution Bulletin*, 2024, vol. 203, art. no. 116444 (8 p.). https://doi.org/10.1016/j.marpolbul.2024.116444

ВОЗДЕЙСТВИЕ ТЕМПЕРАТУРЫ НА РОСТ ДВУХ ВИДОВ *PSEUDO-NITZSCHIA* H. PERAGALLO (BACILLARIOPHYTA) В ЛАБОРАТОРНЫХ КУЛЬТУРАХ, ИЗОЛИРОВАННЫХ ИЗ ЯПОНСКОГО МОРЯ

А. А. Зинов, И. В. Стоник

Национальный научный центр морской биологии имени А. В. Жирмунского ДВО РАН,
Владивосток, Российская Федерация
E-mail: *innast2004@mail.ru*

Диатомовые водоросли рода *Pseudo-nitzschia* H. Peragallo, 1900, продуцирующие нейротоксичную домоевую кислоту, нередко интенсивно размножаются в дальневосточных морях России, что вызывает цветения воды. Температура известна как важный фактор, влияющий на развитие диатомей, однако его воздействие на рост этой группы микроводорослей из Японского моря исследовано недостаточно. Изучены особенности роста в лабораторной культуре двух видов диатомей — *Pseudo-nitzschia fraudulenta* (Cleve) Hasle, 1993 и *Pseudo-nitzschia hasleana* Lundholm, 2012 — в диапазоне температуры от +5 до +20 °C. Методом прямого подсчёта в камере Нажотта оценены плотность клеток, темпы роста и время генерации. Установлено, что максимальная средняя плотность клеток *P. fraudulenta* достигала $2{,}2 \times 10^5$ кл.·л$^{-1}$ на 16-е сутки опыта

при +18 °C. Для этого вида при +18 °C темпы роста (0,11–0,16 дел.·сут$^{-1}$) оставались относительно высокими, а время генерации (4,4–6,7 сут) — относительно низким в течение большей части эксперимента. Максимальная средняя плотность клеток *P. hasleana*, 5×10^5 кл.·л$^{-1}$, отмечена на 16-е сутки опыта при +17 °C. Для этого вида высокие темпы роста (0,2–0,92 дел.·сут$^{-1}$) и низкое время генерации (0,8–3,6 сут) зарегистрированы при +17 °C с 2-х по 10-е сутки эксперимента. Средняя плотность клеток *P. fraudulenta* при +18 °C оказалась статистически достоверно выше, чем при других изученных значениях температуры (тест Тьюки, $p < 0,05$) на протяжении всего опыта. Средняя плотность клеток *P. hasleana* при +17 °C была статистически значимо выше (тест Тьюки, $p < 0,05$) таковой при других температурах на 8–12-е сутки эксперимента. Установлено, что при выращивании клонов *P. fraudulenta* при +10, +16 и +18 °C и клонов *P. hasleana* при +14, +17 и +20 °C клетки оставались в жизнеспособном состоянии и продолжали делиться. При понижении температуры культивирования *P. fraudulenta* и *P. hasleana* до +5 и +7 °C соответственно деление резко замедлялось, а плотность клеток была статистически значимо ниже, чем при более высокой температуре (тест Тьюки, $p < 0,05$). Установлены диапазоны толерантной температуры при выращивании диатомей — от +10 до +18 °C для *P. fraudulenta* и от +14 до +17 °C для *P. hasleana*. Выявленные нижние границы температурных условий для культивирования двух видов (+10 и +14 °C) согласуются с параметрами температуры воды в природной среде, при которых отмечены цветения *P. fraudulenta* (+6…+16 °C) и *P. hasleana* (+10…+16 °C). Показаны широкие адаптивные возможности изученных видов по отношению к температуре.

Ключевые слова: *Pseudo-nitzschia fraudulenta*, *Pseudo-nitzschia hasleana*, лабораторное культивирование, температура, Японское море

1871
ИнБЮМ – IBSS

Морской биологический журнал
Marine Biological Journal
2025, vol. 10, no. 3, pp. 31–46
https://marine-biology.ru

UDC 591.524.11(282.257.6.05)

MACROZOOBENTHOS OF THE SUSUYA RIVER ESTUARY (SAKHALIN ISLAND): II. BOTTOM COMMUNITIES AND DISTRIBUTION OF KEY SPECIES

© 2025 **V. Labay, E. Korneev, E. Abramova, O. Berezova, A. Vodop'janova, K. Kostyuchenko, O. Sharlay, and T. Shpilko**

Sakhalin Branch of the Russian Federal Research Institute of Fisheries and Oceanography (SakhNIRO), Yuzhno-Sakhalinsk, Russian Federation
E-mail: *v.labaj@yandex.ru*

Received 09.10.2023; revised 28.04.2024; accepted 12.08.2025.

Communities of macrozoobenthos and their characteristics in river estuaries of Sakhalin Island have not been studied properly. The composition of bottom communities in most estuaries of short rivers on the island is very limited in contrast with that of estuaries of other rivers in the Russian Far East. The Susuya River estuary – a full-sized one compared to estuaries of small rivers of the island – was surveyed in September 2022. The aim of the work is to describe major patterns of distribution of bottom communities, their structure, key species, and trophic characteristics of macrozoobenthos along the salinity gradient in the full-size Susuya River estuary on Sakhalin Island. Bottom communities of the estuary were identified by cluster and ordination analysis. The main communities, trophic characteristics, and distribution features of key macrozoobenthic species along the Susuya River estuary are described. Data on major patterns of distribution of macrozoobenthic communities, key species, and trophic groupings in the Susuya River estuary are provided. In total, 11 communities of macrozoobenthos were identified and united into five types: a community of the riffle separating the estuary from above, communities of the δ-chorohaline zone, communities of the middle estuary oligohaline zone, communities of the lower estuary polyhaline–mesohaline zone, and a community of the river mouth. The community of the water's edge is confined to the river mouth and to the polyhaline–mesohaline zone. The main communities of the estuary are *Corbicula japonica*, *Macoma balthica*, and *Fluviocingula nipponica* + *Macoma balthica*. Environmental factors most affecting the distribution of key macrozoobenthic species are the water salinity and, to a lesser extent, the depth. The type of sediment is not a determining factor.

Keywords: estuary, macrozoobenthos, bottom community, trophic characteristics, Sakhalin Island

Estuaries are zones, where river freshwater mixes with seawater; there, polyhaline, mesohaline (brackish), and oligohaline (freshened) parts are allocated [Aladin, 1988; Aladin, Plotnikov, 2013; Khlebovich, 1974, 1989]. Features of hydrological characteristics of estuaries determine shifts in key macrobenthos species and the development of unique bottom communities there. Ultrafast sedimentation of suspended and dissolved mineral and organic matter in the zone of the effect of the 'marginal filter' results in frequent changes in the trophic groups of benthos within the limited area of the estuary [Lisitsyn, 1994]. For the same reason, estuary ecosystems are characterized by increased productivity [Kolpakov, 2018; Saf'yanov, 1987].

Communities of macrozoobenthos and their characteristics in river estuaries of Sakhalin Island have not been sufficiently studied [Labay et al., 2022; Watercourses of Sakhalin Island, 2015]. In the most properly analyzed estuary, that of the Manuy River, typical of major short rivers on the island, the composition of benthic communities is very limited compared to that of estuaries of other rivers in the Russian Far East [Labay et al., 2022].

In September 2022, the Susuya River estuary, full-sized in comparison with estuaries of short rivers on the island, was surveyed. The material of the study formed the basis of this work.

The aim of the work is to describe the main patterns of distribution of benthic communities, their structure, key species, and trophic characteristics of macrozoobenthos along the salinity gradient in the full-sized estuary of the Susuya River on Sakhalin Island.

MATERIAL AND METHODS

The methods for macrozoobenthos sampling and processing have been described by us earlier, as well as the volume of collected data [Labay et al., 2024].

For the identification of benthic communities and ordination constructions, we used the Q index (cal·m^{-2}·h^{-1}) reflecting species abundance. It is equivalent to the energy expenditure of all individuals of the *i*-th species on respiration [Vilenkin, Vilenkina, 1979]:

$$Q = k \cdot B_i^{0.75} \cdot N_i^{0.25} ,$$

where B_i (g·m^{-2}) and N_i (ind.·m^{-2}) are the specific biomass and density of the *i*-th species *per* 1 m^2, respectively.

The *k* coefficient is taken to be 0.178 for Polychaeta; 0.115 for Oligochaeta; 0.126 for Gastropoda; 0.089 for Bivalvia; 0.302 for Amphipoda; 0.133 for Cumacea, Isopoda, Mysida, and Decapoda; 0.189 for Diptera; and 0.115 for Agnatha [Alimov et al., 2013; Golubkov, 2000].

Clustering of benthic stations when describing communities of benthic hydrobionts was carried out according to the similarity index introduced by J. Czekanowski [Czekanowski, 1909; Sörensen, 1948]:

$$C_{1,2} = 2\sum (MIN_{x_{1i},x_{2i}})/(\sum x_{1i} + \sum x_{2i}) ,$$

where x_{1i} and x_{2i} are abundance values of the *i*-th species (Q) at conditional stations 1 and 2, respectively.

Benthic stations were united into a community if the index value exceeded 40%. This value corresponds to the condition that the biomass or Q of the dominant species is at least 10% of the total one, with an occurrence frequency of 100%. Clustering of the original matrices was performed by the unweighted pair group method with arithmetic mean [Duran, Odell, 1977].

To describe bottom communities, the following parameters were used: number of species (S); specific abundance (density) (N, ind.·m^{-2}); biomass (B, g·m^{-2}); relative species abundance (N, % of total macrozoobenthic abundance); relative species biomass (B, % of total macrozoobenthic biomass); and frequency of occurrence (FO, %). The community structure was analyzed using the density index [Brotskaya, Zenkevich, 1939] or the relativity coefficient [Kuznetsov, 1963]:

$$RC = B \cdot FO ,$$

where B is the relative biomass (%) or Q (%);

FO is the frequency of occurrence (%).

When structuring communities, we took into account the proportion of each species (form) in the mean total macrozoobenthic biomass, FO, and RC. A species was considered dominant if the RC value was in the range of 1,000–10,000. Bottom communities are named according to their dominant species.

The main patterns of benthic distribution are described using ordination graphs constructed by the principal component analysis [Kalinina, Soloviev, 2003] with the Statistica software (v. 8).

For comparative procedures, the Shannon diversity index (entropy index) (I, bit·species^{-1}) was used [Shannon, 1948; Shannon, Weaver, 1949], separately for density (I_N) and biomass (I_B). Also, the ABC method (abundance/biomass comparison method) [Warwick, 1986] by the ABC index [Meire, Dereu, 1990] was applied.

The feeding type of individual macrozoobenthic species was determined based on literature data [Izvekova, 1980; Kanaya et al., 2008; Konstantinov, 1959; Macdonald et al., 2010; Nielsen et al., 1995; Riisgård, 1991; Toba, Sato, 2013; Vedel, Riisgård, 1993]. The following nomenclature was used for the feeding type: Br, browser; De, deposit feeder; Dt, detritus feeder; Gr, grazer; Pr, predator; Sc, scavenger; Sp, suctorial parasite; and Su, suspension feeder (filter feeder). Some species feature a combination of several feeding types, and this is reflected in a mixed characteristic, for example Dt, Br, Sc, or Dt, Su, or De, Su.

RESULTS AND DISCUSSION

The key communities. According to the dendrogram of the similarity of benthic stations, 8 clusters were identified (provided that sta. 34 was combined with cluster 29–14), and also 3 separate stations comparable with bottom communities (Fig. 1).

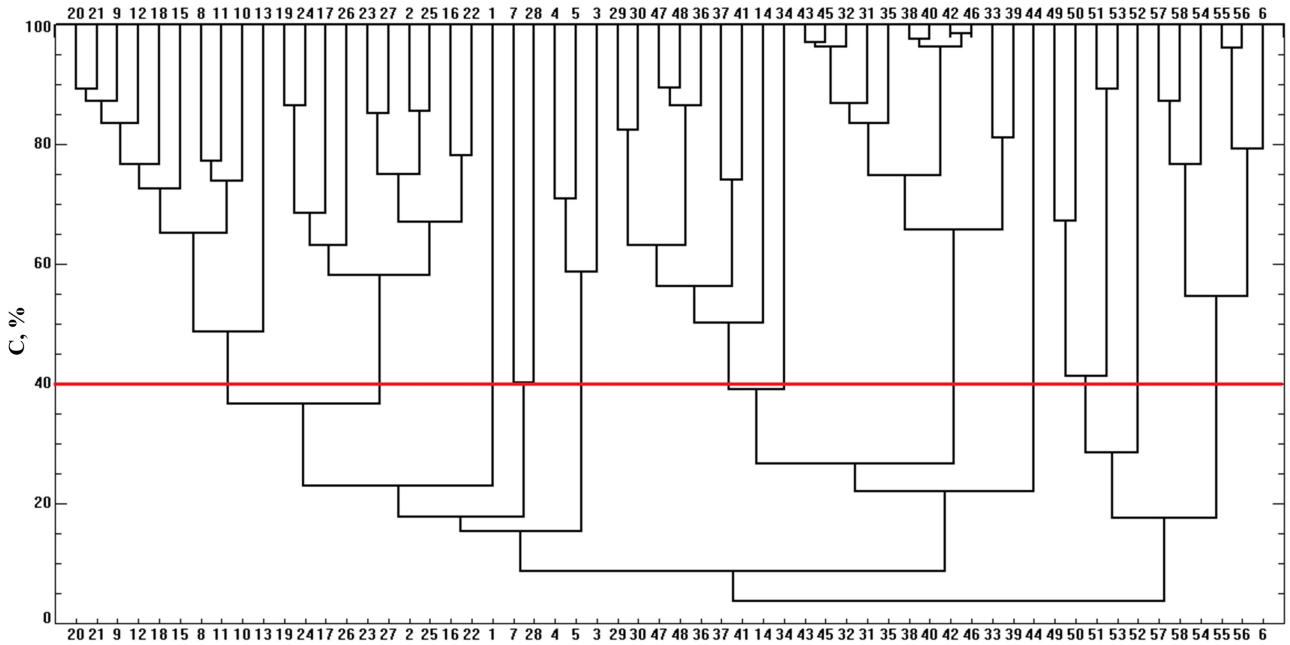

Fig. 1. Dendrogram of the similarity for macrozoobenthos sampled at various stations

Cluster 4, 5, 3, (6) identifies a benthic community dominated by the brush-clawed shore crab *Hemigrapsus takanoi* Asakura & Watanabe, 2005 (74.5% of the total biomass). Subdominants in this community are a gastropod *Fluviocingula nipponica* Kuroda & Habe, 1954 and a bivalve *Macoma balthica* (Linnaeus, 1758) (together, 10.4% of the total biomass). The community is localized in the polyhaline estuary zone (Table 1, Fig. 2). The second cluster, 20, 21, 9, 12, 18, 15, 8, 11, 10, 13, corresponds to the lower estuary polyhaline–mesohaline zone; it is identified as the *Fluviocingula nipponica* + *Macoma balthica* community (predominant species account for 79.5% of the total biomass). Subdominants are polychaetes *Hediste japonica* (Izuka, 1908) and Capitellidae indet. (together, 4.7% of the total biomass). The community is confined to coastal *Zostera* thickets, which is a substrate for a gastropod *F. nipponica*. Both communities are coastal rather than estuarine ones, as their predominant species are common in coastal shallows of Southern Sakhalin [Golikov et al., 1985].

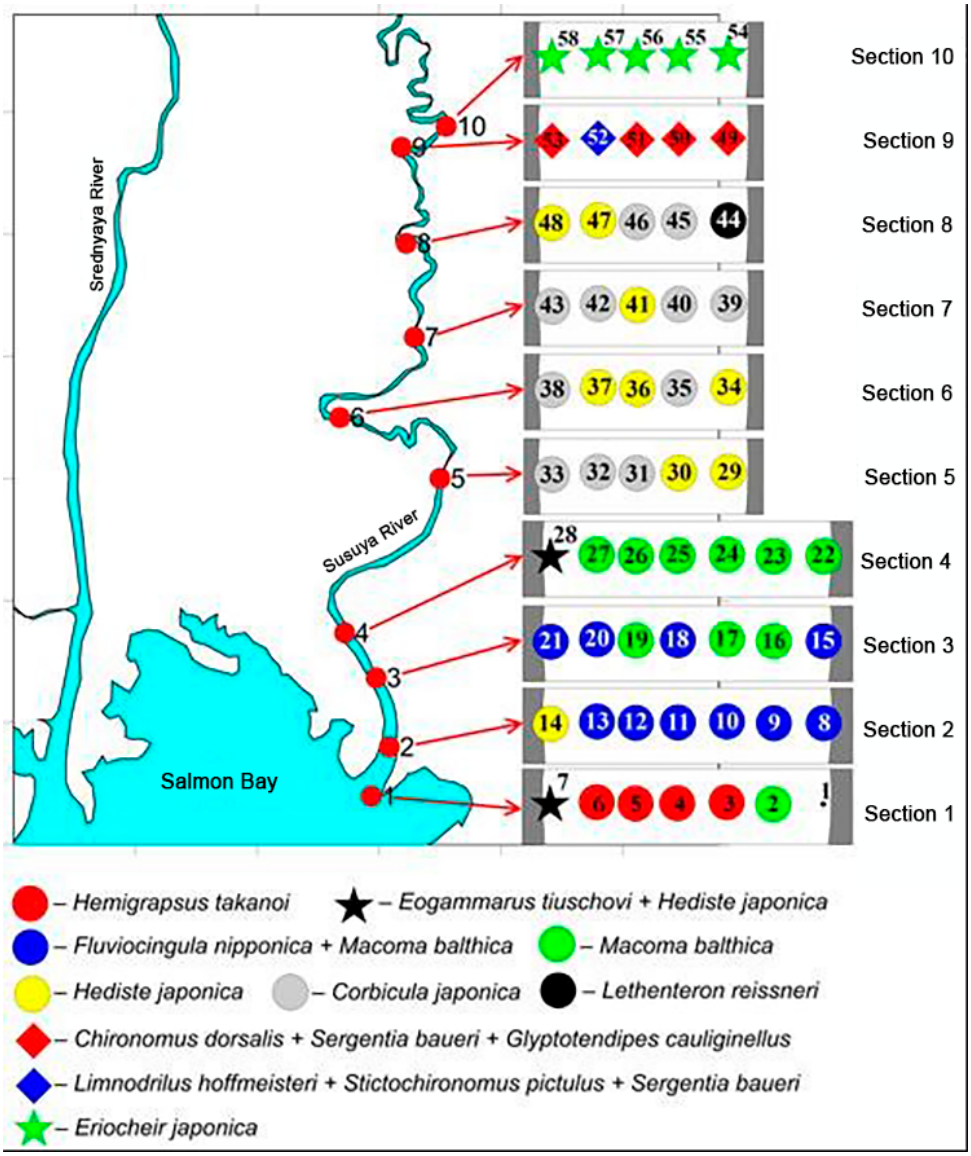

Fig. 2. Location of the major macrobenthic communities in the Susuya River estuary

Table 1. Indicators of macrobenthic abundance in bottom communities of the Susuya River estuary

Parameter		Community (by the dominant species)										
		–	*Eogammarus tiuschovi* + *Hediste japonica*	*Hemigrapsus takanoi*	*Fluviocingula nipponica* + *Macoma balthica*	*Macoma balthica*	*Hediste japonica*	*Corbicula japonica*	*Lethenteron reissneri*	*Chironomus dorsalis* + *Sergentia baueri* + *Glyptotendipes cauliginellus*	*Limnodrilus hoffmeisteri* + *Stictochironomus pictulus* + *Sergentia baueri*	*Eriocheir japonica*
Station numbers		1	7, 28	4, 5, 3, 6	20, 21, 9, 12, 18, 15, 8, 11, 10, 13	19, 24, 17, 26, 23, 27, 2, 25, 16, 22	29, 30, 47, 48, 36, 37, 41, 14, 34	43, 45, 32, 31, 35, 38, 40, 42, 46, 33, 39	44	49, 50, 51, 53	52	57, 58, 54, 55, 56
Depth, m		0.12	0.15–0.4	0.25–0.75	0.1–2	0.5–2.1	0.15–2	0.25–1.8	0.2	0.3–1.6	1.3	0.08–0.15
Sediment type		fine sand, black and grey silt	from siltstone to pebbles with sand	fine sand mixed with siltstone and pebbles	black mud, often mixed with siltstone and fine sand	black silt	black mud, siltstone, sand, clay, pebbles	coarse sand, pebbles, silt	black silt	siltstone, detritus	siltstone, detritus	pebbles, gravel, sand
Salinity, psu		15.2	15.2–24.8	15.2–22.3	18.1–21.7	21.7–25	3.8–11.7	0.6–11.7	0.6	0.1	0.1	0.1
Biotope		mouth	mouth, lower estuary zone (water's edge)	mouth	lower estuary zone	lower estuary zone	middle estuary zone	middle estuary zone	upper estuary zone	upper estuary zone	upper estuary zone	upper estuary zone, riffle
Number of species (S)		12	19	27	27	27	23	24	11	12	7	20
Specific abundance (N), ind.·m^{-2}		350	1,870 ± 243	419 ± 57	5,745 ± 776	2,134 ± 297	1,253 ± 163	1,206 ± 134	1,787	2,940 ± 334	2,040	3,529 ± 336
Biomass (B), g·m^{-2}		0.145	3.27 ± 0.42	6.25 ± 0.98	41.9 ± 4.88	35.1 ± 4.41	17.0 ± 2.69	357 ± 62.6	149.6	3.08 ± 0.293	1.051	23.4 ± 2.78
Biomass (B) of the dominant, %		–	58.4	74.5	79.5	88.4	24.8	98.7	88.4	86.2	77.5	91.7
Biomass (B) of separate groups, %	Ol	0	0.1	0	0.1	0.5	0.02	0.03	0.6	6.0	37.7	4.6
	Po	16.3	25.4	1.8	5.0	2.6	26.2	0.8	9.4	0.5	7.4	1.0
	Ga	23.3	7.6	11.4	59.6	7.5	11.4	0.3	0	0	0	0
	Bi	28.5	0.2	5.5	25.8	88.8	37.7	98.7	0	0	0	0.002
	Am	9.8	44.9	2.2	1.4	0.3	0.4	0.02	0	0	0	0.4
	Is	2.1	5.5	0.7	0.4	0.04	0.9	0.04	0	0	0	0.003
	My	0	1.9	0.01	0.5	0.01	0.3	0.002	0	0.6	0	0.02
	De	0	13.8	78.3	7.2	0.1	22.4	0.2	1.0	0	0	91.7
	Di	0	0.1	0	0.003	0.01	0.1	0.01	0.6	93.0	54.9	2.3
	Ag	0	0	0	0.0	0.0	0	0	88.4	0	0	0
I, bit·species^{-1}	I_N	0.64	1.72	2.20	1.75	1.91	1.86	1.92	1.32	1.40	1.46	1.35
	I_B	2.15	1.87	1.12	1.47	0.57	1.65	0.09	0.45	1.40	1.59	0.40
I_{ABC}, %		17.9	5.8	33.2	14.6	22.6	13.5	19.0	31.2	15.4	7.7	11.8

Note: Ol, Oligochaeta; Po, Polychaeta; Ga, Gastropoda; Bi, Bivalvia; Am, Amphipoda; Is, Isopoda; My, Mysida; De, Decapoda; Di, Diptera; Ag, Agnatha.

Transect 4 in the lower estuary zone, completely filled with mesohaline waters, is occupied by the *Macoma balthica* community identified by cluster 19, 24, 17, 26, 23, 27, 2, 25, 16, 22 (see Fig. 2). This community partially penetrates transect 3 and is also recorded in the littoral of the mouth transect. The dominant species accounts for 84.4% of the total biomass. Another 5.5% cover subdominants: a gastropod *F. nipponica* and a polychaete *H.japonica*. The described community is typical of brackish-water and marine lagoons of Sakhalin Island; sometimes, it is noted on the sea coast [Golikov et al., 1985; Kafanov et al., 2003; Labay, 2009; Labay et al., 2016]. In river estuaries on the island, it was recorded for the first time.

The *Eogammarus tiuschovi* (Derzhavin, 1927) + *Hediste japonica* community was registered at littoral sta. 7 and 28 in the mouth and in the lower estuary zone (Fig. 2). With the proportion of dominant species of 58.4% of the total biomass, it is characterized by a long list of subdominants (6 species; 38.3% of the total biomass). Those are a shrimp *Crangon amurensis* Bražnikov, 1907; an isopod *Gnorimosphaeroma ovatum* (Gurjanova, 1933); an amphipod *Ampithoe lacertosa* Spence Bate, 1858; a mysid *Neomysis awatschensis* (Brandt, 1851); polychaetes Capitellidae indet.; and a gastropod *Assiminea lutea* A. Adams, 1861. At sta. 1, also included in a supercluster of stations covering the mouth and lower estuary zone, there were no dominant species.

Only two bottom communities were localized on transects 5–8 of the middle estuary zone (see Fig. 2). The first one was identified by cluster 29, 30, 47, 48, 36, 37, 41, 14, 34. The community was dominated by a polychaete *H. japonica* (24.8%). A close community with the prevalence of the same species is typical of estuaries on Sakhalin Island [Labay et al., 2022; Watercourses of Sakhalin Island, 2015], but in the Susuya River estuary, the described community is completely different in structure. There, the list of subdominants covers a bivalve *Corbicula japonica* Prime, 1864; a crab *Deiratonotus cristatum* (De Man, 1895); and a gastropod *As. lutea* (together, 65.8% of the total biomass). This community is noted in the entire range of surveyed depths, from the littoral to the waterway, chiefly on fine sand and silt. The driver of its distribution is the water salinity, which is in the range between α- and δ-chorohaline boundaries. The second community is associated with cluster 43, 45, 32, 31, 35, 38, 40, 42, 46, 33, 39; it is characterized by the dominance of a bivalve *C. japonica* (98.7% of the total biomass) and the lack of subdominants. It is localized in a depth range of 0.25–1.8 m, mostly on coarse sand with pebbles and silt. This community is typical of oligohaline areas of lagoons and lagoon lakes of Sakhalin Island, Japan, and Primorye, where it occurs at the optimum water salinity of 1.2–2.5 psu [Baba et al., 1999; Kafanov et al., 2003; Reservoirs of Sakhalin Island, 2014; Water Biota of Tunaicha Lake, 2016; Yavnov, Rakov, 2002]. In river estuaries of Sakhalin Island and the Far East as a whole, this species inhabits sites with a wide salinity range, from almost 0 (nearly freshwater) to 18 psu [Watercourses of Sakhalin Island, 2015; Yavnov, Rakov, 2002]. In the Susuya River estuary, *Corbicula* is characterized by the first type of salinity distribution: in the middle estuary oligohaline zone.

At sta. 44, in the middle estuary oligohaline zone near the shore, the dominance of the Far Eastern brook lamprey *Lethenteron reissneri* (Dybowski, 1869) was recorded. This community, a local one, is typical of the oligohaline part of the estuaries on Sakhalin Island [Labay et al., 2022].

A sharp change in bottom communities is observed in the δ-chorohaline zone, on transect 9. There, two communities with a predominance of chironomids and oligochaetes are localized. The main community is *Chironomus dorsalis* Meigen, 1818 + *Sergentia baueri* Wulker, Kiknadze & Kerkis, 1999 + *Glyptotendipes cauliginellus* (Kieffer, 1913). It occupies most of the reach, from the water's edge to a depth of 1.6 m; it inhabits detritus and siltstone at the river flow speed of 0.01 $m \cdot s^{-1}$ and lower at the time of survey. In contrast to the above-described communities, where molluscs, polychaetes, and decapods

played the main role, there, dipterans prevail (see Table 1). With the proportion of dominant chironomids of 86.2% of the total biomass, this community has a short list of subdominants (3 species; 10.3% of the total biomass). Those are an oligochaete *Limnodrilus hoffmeisteri* f. *typica* Claparede, 1862 and chironomids *Trissopelopia longimana* (Staeger, 1839) and *Paratendipes albimanus* (Meigen, 1804). The second community, *Limnodrilus hoffmeisteri* + *Stictochironomus pictulus* (Meigen, 1830) + *Sergentia baueri*, was recorded in the waterway at a depth of 1.3 m on siltstone with detritus. There, the role of oligochaetes increased to 37.7% of the total biomass, and the proportion of chironomids was 54.9%. The contribution of dominant species to the total biomass was 77.5%. Three subdominant species accounted for 22.3% of the integral biomass: chironomids *Gl. cauliginellus* and *P. albimanus*, as well as a polychaete *H. japonica*. Common characteristics of benthic communities of the transitional δ-chorohaline zone are high density (more than 2,000 ind.·m^{-2}) with low biomass (several g·m^{-2}) and polydominance (three dominant species in each community).

A benthic community uncommon for the lower ritral of Sakhalin Island, with predominance of juveniles of the Japanese mitten crab *Eriocheir japonica* (De Haan, 1835), was recorded at all stations on the riffle separating the Susuya River estuary from above (see Table 1). The community is temporary, and this is due to the life cycle of the dominant species. In Primorye, *Er. japonica* reproduction occurs in brackish water of estuaries at salinity of 5 to 27 psu in May–August; development of planktonic larvae and settling of fry on the bottom is registered during the same period in the adjacent coastal area; and upriver migration of juveniles is in August–October [Kolpakov, Semenkova, 2012]. Therefore, the concentration of juveniles at the first riffle downstream of the Susuya River fits into the life cycle of the Japanese mitten crab. With the onset of winter, the grown crabs leave the riffle, and this leads to a shift in bottom communities.

The *Eriocheir japonica* community is likely to be recorded at the riffle in late summer and early autumn. The density is formed, the same as downstream, mostly by oligochaetes and dipterans (49.7 and 45.6%, respectively), while the biomass basis (91.7%) is formed by decapods represented by one dominant species only. Two subdominant species, an oligochaete *L. hoffmeisteri* and a chironomid *St. pictulus*, account for another 6.4% of the total biomass.

In general, within the Susuya River estuary, five types of benthic communities are identified: the community of the riffle separating the estuary from above (*Eriocheir japonica*); communities of the δ-chorohaline zone (*Chironomus dorsalis* + *Sergentia baueri* + *Glyptotendipes cauliginellus* and *Limnodrilus hoffmeisteri* + *Stictochironomus pictulus* + *Sergentia baueri*); communities of the middle estuary oligohaline zone (*Corbicula japonica*, *Hediste japonica*, and *Lethenteron reissneri*); communities of the lower estuary polyhaline–mesohaline zone (*Fluviocingula nipponica* + *Macoma balthica* and *Macoma balthica*); and the community of the river mouth (*Hemigrapsus takanoi*). The water's edge community (*Eogammarus tiuschovi* + *Hediste japonica*) is confined to the river mouth and the polyhaline zone. The type and location of communities within the estuary are mediated by the salinity regime and the sediment type (the latter is for communities of the upper estuary freshwater zone).

High values of the diversity index by density were observed in communities confined to the mouth and polyhaline–mesohaline and oligohaline zones (1.72–2.20 bit·species^{-1}). In communities located upstream, in the δ-chorohalinicum zone, at salinity of 0.08 to 1.6 psu, a significant decrease in I_N was revealed, down to 1.32–1.46 bit·species^{-1}. This phenomenon is governed by the fact as follows. In communities of the δ-chorohaline zone, the entropy principle with a uniform distribution of the indicator by species is violated. Accordingly, a pronounced structuring by density occurs within the community, when 62–92% fall on 1–3 dominant species.

High values of the diversity index by biomass were recorded for polydominant communities (*Eogammarus tiuschovi* + *Hediste japonica*, *Fluviocingula nipponica* + *Macoma balthica*, *Chironomus dorsalis* + *Sergentia baueri* + *Glyptotendipes cauliginellus*, and *Limnodrilus hoffmeisteri* + *Stictochironomus pictulus* + *Sergentia baueri*) and for communities with a low relative biomass of the dominant species (*Hediste japonica* and the unnamed community). Those seem to be localized in areas transitional to the cores of zones identified by salinity.

The ABC index showed several peaks that fell on communities with dominance of large-sized species, regardless of salinity: *Hemigrapsus takanoi*, *Macoma balthica*, *Corbicula japonica*, and *Lethenteron reissneri* (19–33.2%). In fact, the ABC index marks typical estuary communities corresponding to the cores of the mouth and polyhaline–mesohaline and oligohaline zones. The dynamics of the diversity index by biomass is in antiphase to the dynamics of the ABC index.

Using the ordination analysis according to the principal component method for the station-by-station structure of macrobenthos in the area of action of three main independent factors (together, those account for 58.9% of the variance), four main units of stations were identified (Fig. 3). The compact unit combining sta. 29–33, 35, 38–40, 42, 43, 45, and 46 is characterized by the dominance of a bivalve *C. japonica* and is associated with the above-described community of the same name. The second unit, that of sta. 2, 13, 16, 17, 19, 22–27, includes stations belonging to the *Macoma balthica* community. Sta. 1, 6, 8–12, 14, 15, 18, 20, and 21 are close to a set of stations for the *Fluviocingula nipponica* + *Macoma balthica* community. Remaining stations, where other bottom communities are localized, are concentrated in an area of close-to-zero coordinate values and do not follow the major revealed patterns. The resulting picture confirms the identification of the key benthic communities in the oligohaline, mesohaline, and polyhaline estuary zones affected by varying salinity during tidal phenomena.

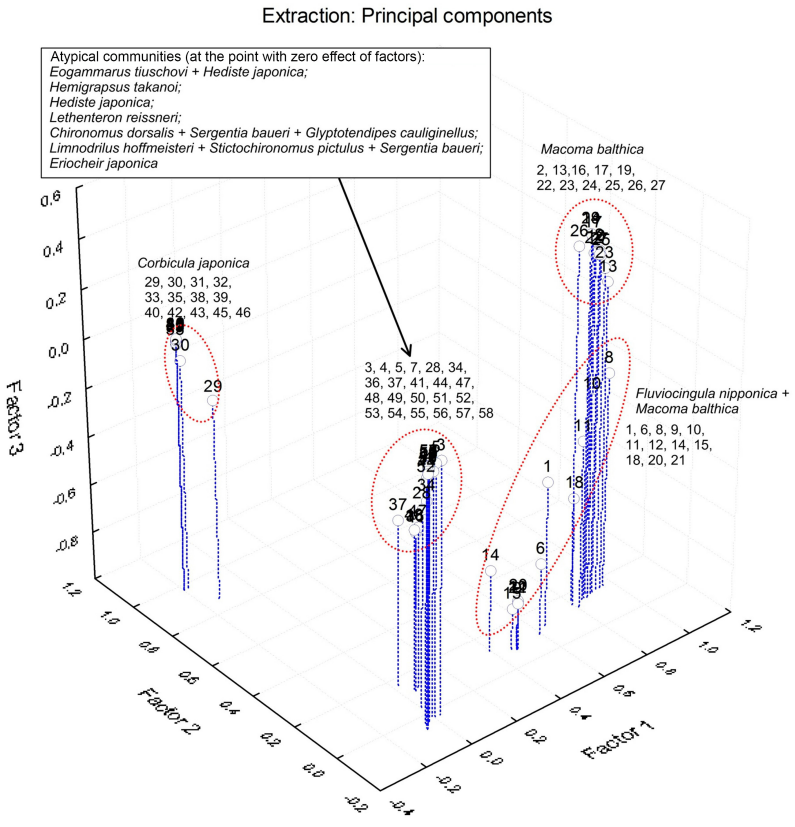

Fig. 3. Principal components analysis (3D ordination) for benthic stations

The correspondence between the distribution of key macrozoobenthic species and the main environmental factors is shown in Fig. 4.

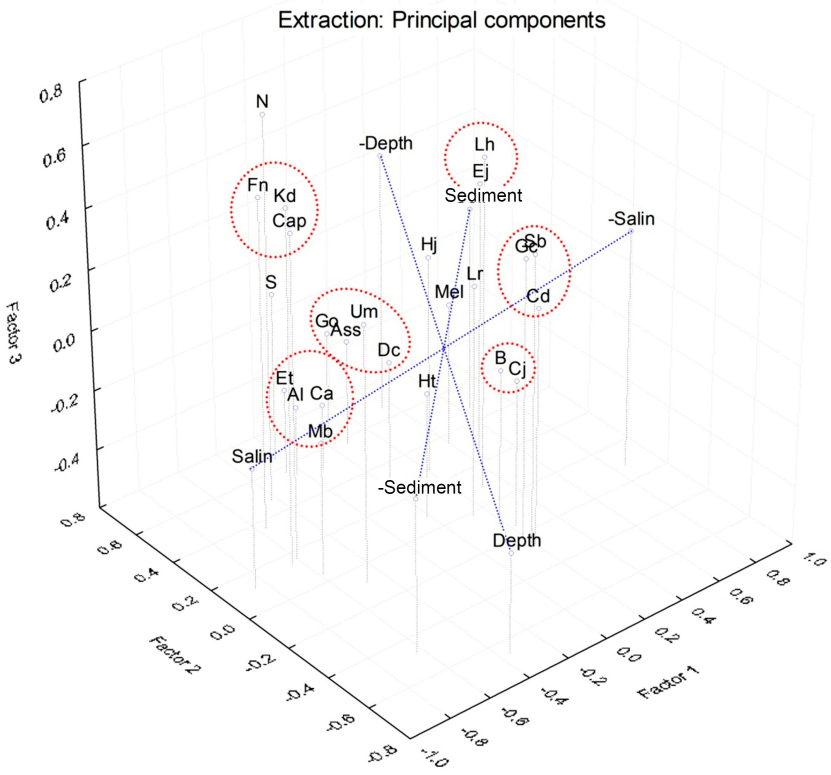

Fig. 4. Principal components analysis (3D ordination) for macrozoobenthic species abundance and biomass and for environmental parameters. Hj, *Hediste japonica*; Cap, Capitellidae; Lh, *Limnodrilus hoffmeisteri*; Fn, *Fluviocingula nipponica*; Ass, *Assiminea lutea*; Mb, *Macoma balthica*; Cj, *Corbicula japonica*; Et, *Eogammarus tiuschovi*; Kd, *Kamaka derzhavini*; Mel, *Melita shimizui* / *Melita* sp.; Al, *Ampithoe lacertosa*; Go, *Gnorimosphaeroma ovatum*; Ej, *Eriocheir japonica*; Ht, *Hemigrapsus takanoi*; Ca, *Crangon amurensis*; Dc, *Deiratonotus cristatum*; Um, *Upogebia major*; Cd, *Chironomus dorsalis*; Sb, *Sergentia baueri*; Gc, *Glyptotendipes cauliginellus*; Lr, *Lethenteron reissneri*. Salin, water salinity; depth, depth studied; sediment, sediment type; S, number of species; N, density; B, biomass

For most species, the distribution of the biomass, as might be expected, is determined by the salinity factor. A separate set in the area of its positive effect (a gain in species biomass with increasing salinity values) is formed by species of the polyhaline–mesohaline zone: *M. balthica*, *E. tiuschovi*, *Am. lacertosa*, and *Cr. amurensis* (Figs 5, 6). The second set, also lying on the segment of salinity in the area of its positive effect, unites species abundant in mesohaline and oligohaline waters: *As. lutea*, *Gn. ovatum*, *D. cristatum*, and *Upogebia major* (De Haan, 1841) (see Figs 5, 6). A negative response to an increase in water salinity is demonstrated by chironomids *C. dorsalis*, *S. baueri*, and *Gl. cauliginellus* abundant in the δ-chorohaline zone (see Fig. 6).

Two groups of species are affected by two abiotic factors: salinity and depth. The first group covers Capitellidae polychaetes, a gastropod *F. nipponica*, and an amphipod *Kamaka derzhavini* Gurjanova, 1951, which are common in the river mouth and adjacent areas. This group shows a positive relationship with salinity and a negative one with depth, *i. e.*, the biomass of these species increases with rising salinity and decreasing depth (see Fig. 5). The second group is represented by one species, *C. japonica*, and features the opposite dependance: a negative relationship with salinity and a positive one with depth (see Fig. 5).

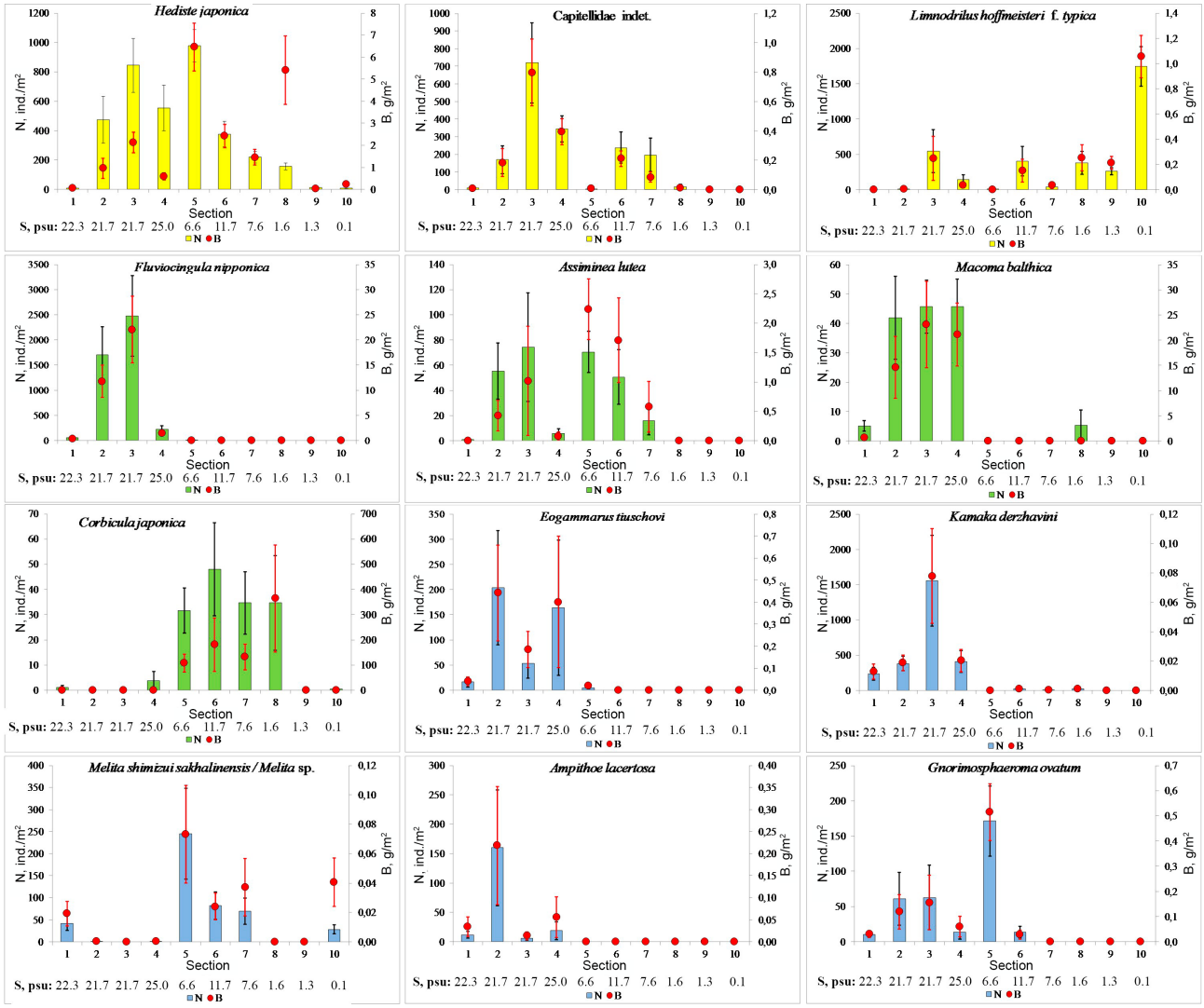

Fig. 5. Distribution of abundant macrozoobenthic species in the Susuya River estuary (Annelida, yellow; Mollusca, green; Amphipoda, blue)

Two species, an oligochaete *L. hoffmeisteri* and a crab *Er. japonica*, are situated far above the area of effect of known environmental factors. Both are abundant in the estuary (see Figs 5, 6). For a crab, such distribution is governed by a biological indicator: the feature of its life cycle.

Other species are located on the 3D plot near the center of the axes (in the area of close-to-zero coordinate values of all three orthogonal factors). Therefore, their distribution in the estuary is subject to other patterns, unknown to us.

Trophic characteristics. Out of 11 trophic groups revealed, only a few form the basis of the biomass on individual transects (Fig. 7). According to the representation of trophic groups, the entire estuary is clearly divided into five areas. The group with a mixed feeding type (detritus feeders, browsers, and scavengers) dominates in macrozoobenthos in the river mouth (94.9% of the total biomass). The biomass is chiefly formed by crabs *H. takanoi* and adult *Er. japonica*, as well as amphipods *E. tiuschovi* and *Eogammarus possjeticus* (Tzvetkova, 1967).

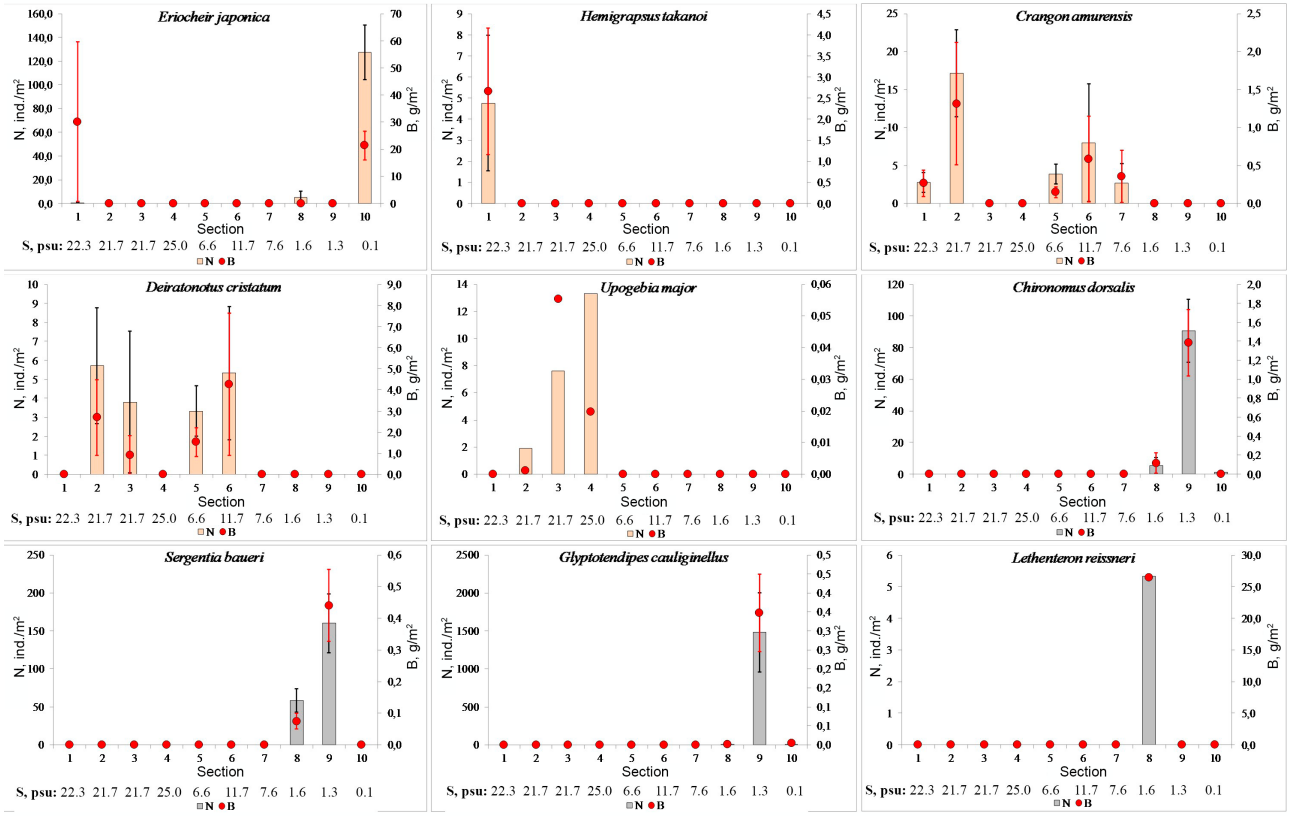

Fig. 6. Distribution of abundant macrozoobenthic species in the Susuya River estuary (Decapoda, light brown; Diptera, grey; Agnatha, grey)

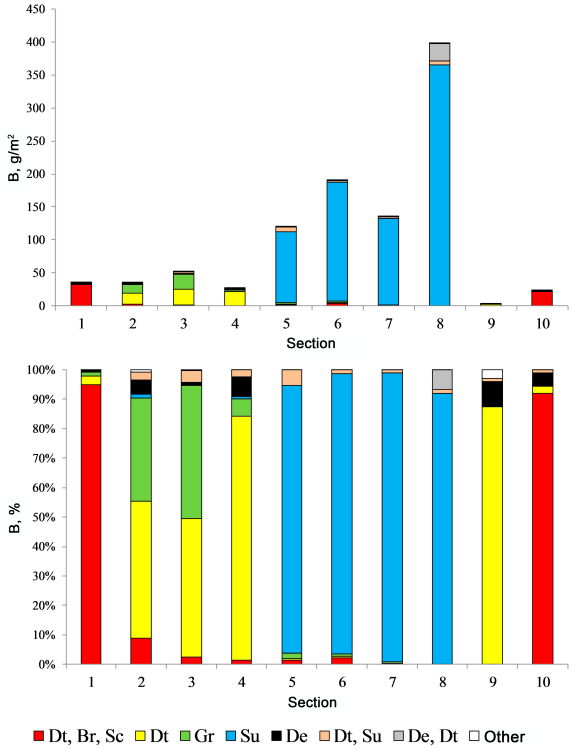

Fig. 7. Spatial distribution of the biomass (B, g·m^{-2}) of macrobenthic trophic groups across the Susuya River estuary (abbreviations are explained in the Table 1 note)

For more than 1.5 km from the mouth, on transects 2–4, the most significant trophic groups are detritus feeders (46.6–82.6% of the total biomass) and grazers (5.9–45.1%). The first ones are represented by a bivalve *M. balthica* (41.2–80.7%), Capitellidae polychaetes, a shrimp *Cr. amurensis*, an amphipod *K. derzhavini*, an isopod *Gn. ovatum*, a mysid *N. awatschensis*, *etc.* The grazers are chiefly epiphytic gastropods *F. nipponica* (5.4–43.1%) and *As. lutea*, an amphipod *Am. lacertosa*, *etc.*

Between transects 4 and 5, another trophic restructuring of the macrozoobenthos occurs (see Fig. 7). At a distance from the mouth, in 3–7 km, on transects 5–8, the biomass is mainly formed by suspension feeders. The key filter feeder in this area is *C. japonica* (90.8–98.1%). The sharp transition from one feeding type to another corresponds to the 'marginal filter' theory and the mean position of a salinity barrier of 5–9 psu during the warm period [Lisitsyn, 1994]. Upstream of this salinity barrier, a large amount of suspended organic matter is recorded in water; it is consumed by suspension feeders. Below the barrier, after ultrafast sedimentation, deposited organic matter predominates; it is available to detritus feeders.

Above the oligohaline zone, in the δ-chorohalinicum zone, on transect 9, on the reach, the leading role is again played by detritus feeders (87.5% of the total biomass) with a significant contribution of deposit feeders (8.5%). There, the biomass of detritus feeders is formed mostly by chironomids: *Ch. dorsalis*, *S. baueri*, *Gl. cauliginellus*, *P. albimanus*, *St. pictulus*, *etc.* Deposit feeders are represented by oligochaetes *L. hoffmeisteri* and *Tubifex tubifex* (O. F. Müller, 1773).

In the area of the river riffle separating the estuary from above, the trophic structure of macrozoobenthos is determined by a group with a mixed feeding type: detritus feeders, browsers, and scavengers (92.0% of the total biomass). This group is represented by juveniles of a crab *Er. japonica* (91.7%) and an amphipod *Eogammarus kygi* (Derzhavin, 1923).

All other trophic groups were not significant.

Conclusion. In the Susuya River estuary, five zones are clearly identified by the distribution of the key communities: the mouth zone, lower estuary polyhaline–mesohaline zone, middle estuary oligohaline zone, upper estuary δ-chorohaline zone, and freshwater zone.

The effect of salinity limits the composition of benthic communities. By cluster analysis, 11 macrozoobenthic communities are identified and united into 5 types: the community of the riffle separating the estuary from above (*Eriocheir japonica*); communities of the δ-chorohaline zone (*Chironomus dorsalis* + *Sergentia baueri* + *Glyptotendipes cauliginellus* and *Limnodrilus hoffmeisteri* + *Stictochironomus pictulus* + *Sergentia baueri*); communities of the middle estuary oligohaline zone (*Corbicula japonica*, *Hediste japonica*, and *Lethenteron reissneri*); communities of the lower estuary polyhaline–mesohaline zone (*Fluviocingula nipponica* + *Macoma balthica* and *Macoma balthica*); and the community of the river mouth (*Hemigrapsus takanoi*). The water's edge community *Eogammarus tiuschovi* + *Hediste japonica* is confined to the river mouth and the polyhaline–mesohaline zone. By the methods of ordination analysis, the communities *Corbicula japonica*, *Macoma balthica*, and *Fluviocingula nipponica* + *Macoma balthica* are identified as the key ones of the estuary.

The major environmental factors affecting the distribution of key macrozoobenthic species are water salinity and, to a lesser extent, depth. The type of sediment is not a determining factor in the area of the effect of salinity.

The estuary is clearly divided into 5 zones by the results of the distribution analysis of the trophic groups of macrobenthos as well. The basis of the macrozoobenthic biomass in the river mouth is formed by a group with a mixed feeding type: detritus feeders, browsers, and scavengers. In the lower

estuary zone, the most significant trophic groups are detritus feeders and grazers. Suspension feeders determine the trophic structure of the middle estuary oligohaline zone. In the δ-chorohalinicum zone, the leading role is again played by detritus feeders with a noticeable contribution of deposit feeders. On the river riffle, the basis of the macrobenthic biomass is formed by a group with a mixed feeding type: detritus feeders, browsers, and scavengers; it is represented by juvenile crabs and amphipods.

The study was not sponsored.

REFERENCES

1. Aladin N. V. The concept of relativity and plurality of barrier salinity zones. *Zhurnal obshchei biologii*, 1988, vol. 49, no. 6, pp. 825–833. (in Russ.)
2. Aladin N. V., Plotnikov I. S. The concept of relativity and plurality of barrier salinity zones and forms of existence of the hydrosphere. *Trudy Zoologicheskogo instituta RAN*, 2013, vol. 317, suppl. S3, pp. 7–21. (in Russ.)
3. Alimov A. F., Bogatov V. V., Golubkov S. M. *Produktsionnaya gidrobiologiya.* Saint Petersburg : Nauka, 2013, 339 p. (in Russ.)
4. Brotskaya V. A., Zenkevich L. A. Kolichestvennyi uchet donnoi fauny Barentseva morya. *Trudy VNIRO*, 1939, vol. 4, pp. 5–126. (in Russ.)
5. Vilenkin B. Ya., Vilenkina M. N. Dykhanie vodnykh bespozvonochnykh. In: *Itogi nauki i tekhniki. Seriya "Zoologiya bespozvonochnykh"*. Moscow : VINITI AN SSSR, 1979, vol. 6, 144 p. (in Russ.)
6. *Water Biota of Tunaicha Lake (Southern Sakhalin) and Conditions of Its Dwelling* / V. S. Labay (Ed.). Yuzhno-Sakhalinsk : Sakhalin Research Institute of Fisheries and Oceanography, 2016, 240 p. (in Russ.)
7. *Reservoirs of Sakhalin Island: From Lagoons to Lakes* / V. S. Labay, I. A. Atamanova, D. S. Zavarzin, et al. ; [G. V. Matyushkov (Ed.)]. Yuzhno-Sakhalinsk : Sakhalinskii oblastnoi kraevedcheskii muzei, 2014, 208 p. (in Russ.)
8. *Watercourses of Sakhalin Island: Life in the Running Water* / V. S. Labay, L. A. Zhivogljadova, A. V. Polteva, et al. ; [G. V. Matyushkov (Ed.)]. Yuzhno-Sakhalinsk : Sakhalinskii oblastnoi kraevedcheskii muzei, 2015, 236 p. (in Russ.)
9. Golikov A. N., Skarlato O. A., Tabunkov V. D. Nekotorye biotsenozy verkhnikh otdelov shel'fa Yuzhnogo Sakhalina i ikh raspredelenie. *Biotsenozy i fauna shel'fa Yuzhnogo Sakhalina* : [sbornik nauchnykh trudov] / A. N. Golikov (Ed.). Leningrad : Nauka, Leningr. otd-nie, 1985, pp. 4–69. (in Russ.)
10. Golubkov S. M. *Funktsional'naya ekologiya lichinok amfibioticheskikh nasekomykh* / A. F. Alimov (Ed.) Saint Petersburg : Zoologicheskii institut RAN, 2000, 294 p. (Trudy Zoologicheskogo instituta ; vol. 284). (in Russ.)
11. Duran B. S., Odell P. L. *Cluster Analysis: A Survey* / transl. from Engl. by E. Z. Demidenko ; A. Ya. Boyarskii (Ed., Introd.). Moscow : Statistika, 1977, 128 p. (in Russ.)
12. Izvekova E. I. Pitanie khironomid. In: *Bentos Uchinskogo vodokhranilishcha*. Moscow : Nauka, 1980, pp. 72–101. (Trudy Vsesoyuznogo gidrobiologicheskogo obshchestva ; vol. 23). (in Russ.)
13. Kalinina V. N., Soloviev V. I. *Vvedenie v mnogomernyi statisticheskii analiz* : uchebnoe posobie dlya studentov vsekh spetsial'nostei. Moscow : Gosudarstvennyi universitet upravleniya, 2003, 66 p. (in Russ.). https://elibrary.ru/qirgcp
14. Kafanov A. I., Labay V. S., Pecheneva N. V. *Biota and Macrobenthic Communities*

of the Northeast Sakhalin Lagoons. Yuzhno-Sakhalinsk : SakhNIRO, 2003, 175 p. (in Russ.). https://elibrary.ru/qkmhzj

15. Kolpakov N. V. *Estuarnye ekosistemy severo-zapadnoi chasti Yaponskogo morya: strukturno-funktsional'naya organizatsiya i bioresursy* / Tikhookeanskii nauchno-issledovatel'skii rybokhozyaistvennyi tsentr. Vladivostok : TINRO-Tsentr, 2018, 428 p. (in Russ.)
16. Kolpakov N. V., Semenkova E. G. *Japanese Mitten Crab of Primorye.* Vladivostok : TINRO-Centre, 2012, 160 p. (in Russ.). https://elibrary.ru/xmwntf
17. Konstantinov A. S. Pitanie lichinok khironomid i nekotorye puti povysheniya kormnosti vodoemov. *Trudy VI soveshchaniya po problemam biologii vnutrennikh vod*. Moscow ; Leningrad : Izd-vo AN SSSR, 1959, pp. 260–269. (in Russ.)
18. Kuznetsov A. P. *Fauna donnykh bespozvonochnykh prikamchatskikh vod Tikhogo okeana i severnykh Kuril'skikh ostrovov.* Moscow : Izd-vo AN SSSR, 1963, 272 p. (in Russ.)
19. Labay V. S. Response of macrozoobenthos of lagoon lake Izmenchivoye (Sakhalin Island) to the discontinuance of water exchange with the sea. *Biologiya morya*, 2009, vol. 35, no. 3, pp. 167–174. (in Russ.). https://elibrary.ru/owkyiv
20. Labay V., Korneev E., Abramova E., Berezova O., Vodop'janova A., Kostyuchenko K., Sharlay O., Shpilko T. Macrozoobenthos of the Susuya River estuary (Sakhalin Island): I. Hydrological characteristics of the estuary, species composition and distribution of macrozoobenthos. *Marine Biological Journal*, 2024, vol. 9, no. 4, pp. 64–80. (in Russ.). https://elibrary.ru/afflnw
21. Labay V. S., Korneev E. S., Abramova E. V., Ushakov A. A., Akhmadeeva E. S. Macrobenthos in the estuary of a typical "salmon" river of Sakhalin Island (on example of the Manuy River). *Izvestiya TINRO*, 2022, vol. 202, no. 3, pp. 640–660. (in Russ.). https://doi.org/10.26428/1606-9919-2022-202-640-660
22. Labay V. S., Kurilova N. V., Shpilko T. S. Seasonal variability of macrozoobenthos in a lagoon with periodic connection to the sea (Lake Ptychje, Southern Sakhalin). *Zoologicheskii zhurnal*, 2016, vol. 95, no. 5, pp. 524–539. (in Russ.). https://doi.org/10.7868/S0044513416050068
23. Lisitsyn A. P. A marginal filter of the oceans. *Okeanologiya*, 1994, vol. 34, no. 5, pp. 735–747. (in Russ.). https://elibrary.ru/yjgohj
24. Saf'yanov G. A. *Estuarii.* Moscow : Mysl', 1987, 189 p. (in Russ.)
25. Khlebovich V. V. *The Critical Salinity of Biological Processes.* Leningrad : Nauka, 1974, 236 p. (in Russ.)
26. Khlebovich V. V. Kriticheskaya solenost' i khorogalinikum: sovremennyi analiz ponyatii. In: *Biologiya solonovatykh vod*. Leningrad : ZIN AN SSSR, 1989, pp. 5–11. (Trudy Zoologicheskogo instituta AN SSSR ; vol. 196). (in Russ.)
27. Yavnov S. V., Rakov P. V. *Korbikula.* Vladivostok : TINRO-Tsentr, 2002, 145 p. (in Russ.)
28. Baba K., Tada M., Kawajiri T., Kuwahara Y. Effects of temperature and salinity on spawning of the brackish water bivalve *Corbicula japonica* in Lake Abashiri, Hokkaido, Japan. *Marine Ecology Progress Series*, 1999, vol. 180, pp. 213–221. https://doi.org/10.3354/meps180213
29. Czekanowski J. Zur differential Diagnose der Neandertalgruppe. *Korrespondenzblatt der Deutschen Gesellschaft für Anthropologie, Ethnologie und Urgeschichte*, 1909, Bd 40, S. 44–47.

30. Kanaya G., Takagi Sh., Kikuchi E. Spatial dietary variations in *Laternula marilina* (Bivalva) and *Hediste* spp. (Polychaeta) along environmental gradients in two brackish lagoons. *Marine Ecology Progress Series*, 2008, vol. 359, pp. 133–144. https://doi.org/10.3354/meps07356
31. Macdonald T. A., Burd B. J., Macdonald V. I., van Roodselaar A. Taxonomic and feeding guild classification for the marine benthic macroinvertebrates of the Strait of Georgia, British Columbia. *Canadian Technical Report of Fisheries and Aquatic Sciences*, 2010, no. 2874, 63 p.
32. Meire P. M., Dereu J. Use of the abundance/biomass comparison method for detecting environmental stress: Some considerations based on intertidal macrozoobenthos and bird communities. *Journal of Applied Ecology*, 1990, vol. 27, no. 1, pp. 210–223. https://doi.org/10.2307/2403579
33. Nielsen A. M., Eriksen N. T., Iversen J. J. L., Riisgård H. U. Feeding, growth and respiration in the polychaetes *Nereis diversicolor* (facultative filter-feeder) and *N. virens* (omnivorous) – a comparative study. *Marine Ecology Progress Series*, 1995, vol. 125, pp. 149–158. https://doi.org/10.3354/meps125149
34. Riisgård H. U. Suspension feeding in the polychaete *Nereis diversicolor*. *Marine Ecology Progress Series*, 1991, vol. 70, pp. 29–37. https://doi.org/10.3354/meps070029
35. Sörensen T. A method of establishing groups of equal amplitude in plant sociology based on similarity of species content. *Biologiske Skrifter/Kongelige Danske Videnskabernes Selskab*, 1948, Bd 5, no. 4, S. 1–34.
36. Shannon C. E. A mathematical theory of communication. *Bell System Technical Journal*, 1948, vol. 27, iss. 3, pp. 379–423. https://doi.org/10.1002/j.1538-7305.1948.tb01338.x
37. Shannon C. E., Weaver W. *The Mathematical Theory of Communication.* Vol. 1. Urbana, IL : University of Illinois Press, 1949, 117 p.
38. Toba Y., Sato M. Filter-feeding behavior of three Asian *Hediste* species (Polychaeta: Nereididae). *Plankton and Benthos Research*, 2013, vol. 8, iss. 4, pp. 159–165. https://doi.org/10.3800/pbr.8.159
39. Vedel A., Riisgård H. U. Filter-feeding in the polychaete *Nereis diversicolor*: Growth and bioenergetics. *Marine Ecology Progress Series*, 1993, vol. 100, pp. 145–152. https://doi.org/10.3354/meps100145
40. Warwick R. M. A new method for detecting pollution effects on marine macrobenthic communities. *Marine Biology*, 1986, vol. 92, iss. 4, pp. 557–562. https://doi.org/10.1007/BF00392515

МАКРОЗООБЕНТОС ЭСТУАРИЯ РЕКИ СУСУЯ (ОСТРОВ САХАЛИН): II. ДОННЫЕ СООБЩЕСТВА И РАСПРЕДЕЛЕНИЕ КЛЮЧЕВЫХ ВИДОВ

В. С. Лабай, Е. С. Корнеев, Е. В. Абрамова, О. Н. Березова, А. И. Водопьянова, К. М. Костюченко, О. Б. Шарлай, Т. С. Шпилько

Сахалинский филиал ФГБНУ «Всероссийский научно-исследовательский институт рыбного хозяйства и океанографии» (СахНИРО), Южно-Сахалинск, Российская Федерация
E-mail: *v.labaj@yandex.ru*

Сообщества макрозообентоса и их характеристики в эстуариях рек острова Сахалин изучены недостаточно. В большинстве коротких рек Сахалина состав донных сообществ сильно ограничен по сравнению с таковым эстуариев других рек Дальнего Востока России. В сентябре 2022 г. обследован эстуарий реки Сусуя — полноразмерный по сравнению с эстуариями малых рек

острова. Цель работы — описать основные закономерности распределения донных сообществ, их структуры, ключевых видов и трофических характеристик макрозообентоса вдоль градиента солёности в полноразмерном эстуарии реки Сусуя на острове Сахалин. Методами кластерного и ординационного анализа выделены донные сообщества эстуария. Описаны основные сообщества и трофическая характеристика, особенности распределения ключевых видов макрозообентоса вдоль русла эстуария реки Сусуя. Приведены главные закономерности распределения сообществ макрозообентоса, ключевых видов и трофических группировок в эстуарии реки Сусуя. Выделены 11 сообществ макрозообентоса, объединённых в пять типов: сообщество переката, ограничивающего эстуарий сверху, сообщества δ-хорогалинной зоны, сообщества среднеэстуарной олигогалинной зоны, сообщества нижнеэстуарной полигалинно-мезогалинной зоны и сообщество устья реки. Сообщество уреза воды локализовано в устье реки и полигалинно-мезогалинной зоне. Основные сообщества эстуария реки Сусуя — *Corbicula japonica*, *Macoma balthica* и *Fluviocingula nipponica* + *Macoma balthica*. Основными факторами среды, влияющими на распределение ключевых видов макрозообентоса, являются солёность воды и — в меньшей степени — глубина. Тип грунта не выступает как определяющий фактор.

Ключевые слова: эстуарий, макрозообентос, донное сообщество, трофическая характеристика, остров Сахалин

1871
ИнБЮМ – IBSS

Морской биологический журнал
Marine Biological Journal
2025, vol. 10, no. 3, pp. 47–66
https://marine-biology.ru

UDC 582.261.1-152.632.3(262.5.04)

BENTHIC DIATOMS (BACILLARIOPHYTA): DIVERSITY AND HIERARCHICAL STRUCTURE OF TAXOCENES ON SOFT BOTTOM OFF THE KRUGLAYA BAY (THE BLACK SEA, CRIMEA)

© 2025 **E. Nevrova**

A. O. Kovalevsky Institute of Biology of the Southern Seas of RAS, Sevastopol, Russian Federation
E-mail: *el_nevrova@mail.ru*

Received 04.10.2024; revised 18.02.2025;
accepted 12.08.2025.

The Kruglaya Bay (or the Omega Bay) holds high recreational value due to its sheltered location within the Sevastopol region, extensive beach area, and shallow waters with the soft bottom. These features necessitate monitoring of marine biota state. This work was aimed at determining the species richness and hierarchical structure of benthic diatoms (Bacillariophyta) in the Kruglaya Bay insufficiently studied before and at comparing them with coastal biotopes off the Crimea being under various anthropogenic load. Based on results of a benthic survey in 2004, we studied the species richness of Bacillariophyta off the Omega Bay and analyzed the taxonomic diversity applying floristic and formalized methods and using taxonomic distinctness indices: TaxDI (AvTD and VarTD). In total, 264 species and intraspecific taxa of benthic diatoms were identified: 256 species, 73 genera, 35 families, 21 orders, and 3 classes. We found 70 species and 5 genera previously recorded by us as new to the Bacillariophyta flora of the northern Black Sea shelf, along with 5 species of diatoms previously described by us as new to science. The greatest species similarity was revealed both between habitats with the lowest anthropogenic load (the Omega Bay – the Dvuyakornaya Bay and the Omega Bay – the Laspi Bay) and between heavily polluted water areas (the Sevastopol Bay – the Karantinnaya Bay and the Sevastopol Bay – the Balaklava Bay) regardless of their geographical proximity and differences in hydrological and hydrophysical conditions. Bacillariophyta taxocenes from heavily polluted sites feature low species richness and high proportion of mono- and oligospecies branches due to reduction of low pollution–sensitive taxa. AvTD values exceeded the average expected level for the Black Sea Bacillariophyta flora. In conditionally clean waters, diatom taxocenes exhibited high species richness, numerous polyspecies branches, and a low proportion of mono- and oligospecies branches aggregating at different levels of a hierarchical tree. AvTD values are below the average expected level for the Black Sea diatom flora. Features of diatom taxocene structure from the compared sites are mediated by a taxa-specific response to combined environmental stressors. Using TaxDI when analyzing Bacillariophyta taxonomic diversity allows for statistically reliable assessment of marine coastal waters under different pollution regimes.

Keywords: Omega Bay, TaxDI, species richness, anthropogenic load

Within the Sevastopol Bay system, the Kruglaya Bay (or the Omega Bay) holds high recreational value due to its location within the city, shallow soft bottom, and the lack of industrial facilities in the surrounding area. Its shores host extensive beaches and numerous cafes, resorts, and recreational areas. Such a heavy use of the coastline exerts substantial anthropogenic load on its waters necessitating evaluation of the state of its marine biota. The main tasks of the coastal ecosystem monitoring

are the inventory and comprehensive assessment of biota. The resulting data makes it possible to track changes in the marine environment. Benthic diatoms (Bacillariophyta) are the key link in the functioning of coastal ecosystems. The assessment of their species richness is required for bioindication and analysis of the aquatic environment [Barinova et al., 2006; Blanco et al., 2012; Borja et al., 2013; Keck et al., 2016; Stenger-Kovács et al., 2016; Tokatli et al., 2020]. The study of benthic diatom diversity is of fundamental importance for the Black Sea shelf: there, increasing technogenic pollution and anthropogenic load affect the structure of taxocenes, and consequently reduce Bacillariophyta species richness [Guidelines, 2015; Nevrova, 2022; Petrov, Nevrova, 2004, 2007; Petrov et al., 2005, 2010]. To reveal aspects of Bacillariophyta taxonomic diversity, generalization of results and a comprehensive analysis based on both floristic and formalized methods are needed. In this regard, the aim of our work was to carry out a comparative assessment of current diversity and hierarchical structure of benthic diatom taxocenes in the previously insufficiently surveyed Kruglaya Bay and in Crimean coastal habitats subject to varying technogenic pollution involving taxonomic distinctness indices: TaxDI [Nevrova, 2022; Warwick, Clarke, 1998, 2001].

MATERIAL AND METHODS

Benthic diatoms were studied in the Omega Bay located in the northwestern Sevastopol within the Sevastopol Bay system (Fig. 1). Its low-gradient and abrasion-accumulative coasts composed of Sarmatian limestones and layers of marl form a leveled shoreline with alternating abrasion-erosion and accumulative sections [Agarkova-Lyakh, Lyakh, 2019; Ignatov et al., 2014]. Mean depths are approximately 0.5–1 m in the bay innermost part, about 5 m in the central area, and 16 m at the mouth. Bottom sediments are predominantly silt, fine-grained sand, and shells, both broken and unbroken [Zenkovich, 1960]. Compared to the open coast, the bay area is characterized by a calm wave regime, due to its enclosed type and mouth narrowing. The Kruglaya Bay is about 1 km long. It is characterized by a relatively weak water exchange and shallowness, thus promoting rapid summer heating of water. Since the bay's shores are among the most popular beaches in Sevastopol, and its coastline hosts dozens of tourist infrastructure facilities, the water area is subject to intensive recreational pressure during summer. This necessitates monitoring of the state of the biota.

Biological material was sampled on 28.07.2004 within a comprehensive survey conducted by IBSS Department of Benthos Ecology. Sampling covered sandy-silty sediments of the Omega Bay (44°35′N, 33°26′E) at depths ranging 1.5–16 m. Ten samples from five stations were processed. During a previous prognostic estimation of the diatom species richness, depending on the number of samples processed within a study area with similar biotopic conditions, it was revealed as follows: an analysis of only one station allows for accounting for approximately 35% of the total species richness, while an analysis of five stations, for 80% [Petrov, Nevrova, 2013, 2014]. Preliminary results of the study of diatom species richness in the Omega Bay are presented in the monograph [Nevrova, 2022]. In this paper, with the use of additional illustrative material, new data is discussed, and a further comparative analysis of Bacillariophyta hierarchical diversity in other biotopes of the Crimean coast is carried out.

The map of the study area was built using the digital sources https://d-maps.com/ [2024] and https://www.sasgis.org/ [2023], and then edited involving SAS.Planet and Adobe Photoshop software (Fig. 1).

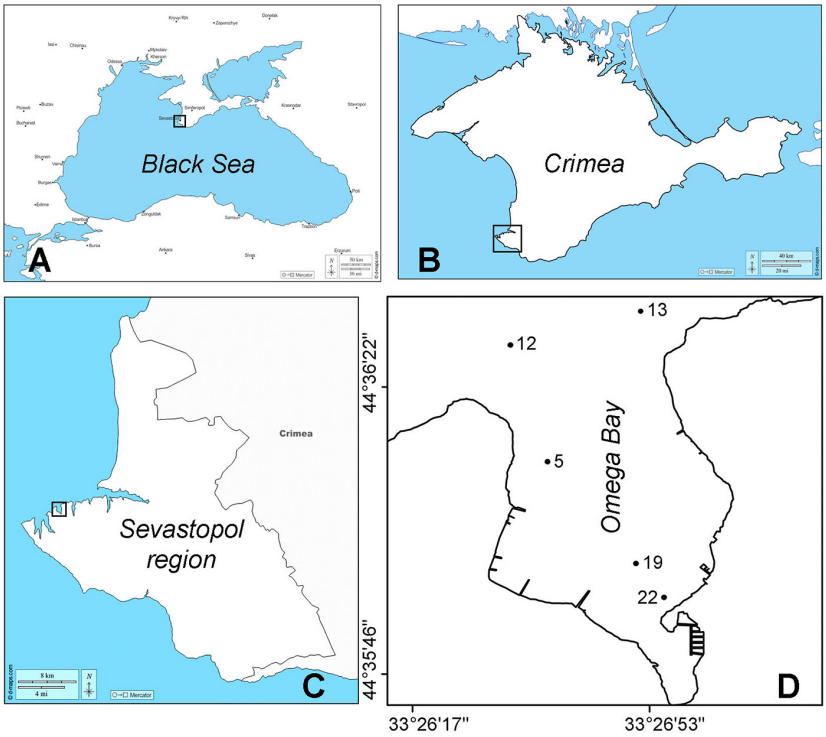

Fig. 1. Map of the study area: A, the Black Sea; B, the Crimean Peninsula; C, the Sevastopol region; D, sampling sites off the Omega Bay

Biological material was sampled by a diver with a meiobenthos core tube (S = 15.9 cm^2): the upper layer of soft bottom substrate was collected. To separate epipelon and epipsammon, the sediment was treated with ultrasound for 20 min. Permanent slides for a light and scanning electron microscopes (hereinafter LM and SEM, respectively) were prepared according to a standard method described in [Nevrova, 2022].

Microphotographs of valves were taken, and species in each sample were identified from permanent slides under a LM Nikon Eclipse E600 equipped with a PlanAPO ×100 objective and a digital camera Nikon DS-Fi1 at the Institute of Marine and Coastal Sciences (University of Szczecin, Poland) by the author. Ultrastructural microphotography was performed under a SEM Hitachi S-4500 (Japan) at the Goethe University (Frankfurt, Germany) by Professor H. Lange-Bertalot and master engineer M. Ruppel, and also under a SEM Hitachi SU3500 (Japan) (IBSS, Sevastopol, Russia) by the author and V. Lishaev, head of the Microscopy Laboratory.

Permanent slides for a LM are deposited in the collection of E. Nevrova in IBSS Department of Benthos Ecology, and partially in the collection of Professor A. Witkowski in the Department of Paleoceanology of the Institute of Marine and Coastal Sciences. Permanent stubs for a SEM are stored in the collection of Professor H. Lange-Bertalot at the Goethe University, and partially in the collection of E. Nevrova at IBSS.

We used the guides [Guslyakov et al., 1992; Levkov, 2009; Proshkina-Lavrenko, 1963; Witkowski et al., 2000] and other publications. The systematic position of benthic diatoms is based on [Round et al., 1990], with resent additions [AlgaeBase, 2024; Catalogue of Diatom Names, 2011; Guslyakov et al., 1992; Nevrova, 2013b; Witkowski et al., 2000*; etc.*]. Nomenclatural data is given in accordance with the International Plant Names Index [2024].

Morphometrics measurements of Bacillariophyta cells were performed using ImageJ software (v1.4.3.67) [2025].

During summer, near-bottom water of the Kruglaya Bay exhibits elevated concentrations of ammonium nitrogen, phosphorus, nitrates, and BOD_5 (biochemical oxygen demand) [Pavlova et al., 2001]. Bottom sediments are characterized by low-level technogenic pollution from urban runoff, high content of ammonium nitrates and phosphorus, and elevated values of BOD_5: the latter ones were approximately ten times higher in open waters at some stations [Mironov et al., 2003]. During hot season, intensive recreational load mediates oxygen depletion in near-bottom water and upper layer of bottom sediments. Nevertheless, in terms of technogenic pollution, the Omega Bay can be classified as a relatively unpolluted area, similar to the Dvuyakornaya and Laspi bays. These bays contrast sharply with heavily polluted ones: the Karantinnaya, Sevastopol, and Balaklava bays, where mean concentrations of heavy metals and organic pollutants in soft bottom sediments exceed background levels by 2–10 times [Nevrova, 2022]. The above-mentioned water areas were selected for comparative analysis precisely based on their pollution levels.

The hierarchical structure of diatom taxocenes in the Kruglaya Bay and in other areas along the Crimean coast of the Black Sea was analyzed in PRIMER v6 [Clarke, Gorley, 2006] using TaxDI. We applied the average taxonomic distinctness index (AvTD, Δ^+) and variation in taxonomic distinctness index (VarTD, Λ^+). Those were calculated according to a methodology described in [Nevrova, 2022; Warwick, Clarke, 1998, 2001].

RESULTS AND DISCUSSION

Species richness of benthic diatoms in the Omega Bay. The taxocene of benthic Bacillariophyta included 264 species and intraspecific taxa (hereinafter IST). Those were represented by 256 species, 73 genera, 35 families, 21 orders, and 3 classes (Table 1).

Table 1. Benthic diatoms on soft bottom off the Omega Bay

Taxon	Species
Class Coscinodiscophyceae Orders, 6 Families, 8 Genera, 14 Species, 20 Species and IST — 20	*Actinocyclus subtilis* (W. Greg.) Ralfs; *Amphitetras antediluvianum* Ehrenb.; *Auliscus sculptus* (W. Sm.) Ralfs; *Biddulphia rostrata* var. *alata* Proschk.-Lavr.; *Coscinodiscus radiatus* Ehrenb.; *Cyclotella choctawhatcheeana* Prasad*; *C. comensis* Grunow; *C. meneghiniana* Kütz.; *C. operculata* (C. Agardh) Kütz.; *Dimeregramma fulvum* (W. Greg.) Ralfs; *D. minor* (W. Greg.) Ralfs; *Glyphodesmis distans* (W. Greg.) Grunow; *Hyalodiscus scoticus* (Kütz.) Grunow; *Paralia sulcata* (Ehrenb.) Cleve; *Plagiogramma* sp.; *Puncticulata radiosa* (Lemmerm.) Håk.; *Stephanodiscus hantzschii* Grunow; *Thalassiosira eccentrica* (Ehrenb.) Cleve; *T. parva* Proschk.-Lavr.; *T. parvula* I. V. Makarova
Class Fragilariophyceae Orders, 7 Families, 7 Genera, 11 Species, 18 Species and IST, 18	*Ardissonea baculus* (W. Greg.) Grunow; *A. crystallina* (C. Agardh) Grunow; *Fragilaria* sp. 1; *Grammatophora marina* (Lyngbye) Kütz.; *G. oceanica* Ehrenb.; *Hyalosira aberrans* (Giffen) Navarro*; *Licmophora abbreviata* C. Agardh; *L. gracilis* (Ehrenb.) Grunow; *Microtabella delicatula* (Kütz.) Round; *Opephora krumbeinii* Witkowski, Witak et Stachura*; *O. marina* (W. Greg.) Petit; *O. mutabilis* (Grunow) Sabbe et Vyverman*; *O. pacifica* (Grunow) Petit*; *Psammodiscus nitidus* (W. Greg.) Round et D. G. Mann; *Rhabdonema minutum* Kütz.; *Tabularia gaillonii* (Bory) Bukht.; *T. tabulata* (C. Agardh) P. J. M. Snoeijs; *Thalassionema nitzschioides* (Grunow) Mereschk.

Continued on the next page…

Taxon	Species
Class Bacillariophyceae Orders, 8 Families, 20 Genera, 48 Species, 217 Species and IST, 226	*Achnanthes brockmannii* Hust.; *A. longipes* C. Agardh; *A. fimbriata* (Grunow) R. Ross; *Achnanthes* sp. O1; *Achnanthidium glyphos* Riaux-Gob., Compère et Witkowski*; *Amphora acuta* W. Greg.; *A. arcus* W. Greg.; *A. bigibba* Grunow ex A. Schmidt; *A. caroliniana* Giffen; *A.* cf. *abludens* Simonsen*; *A. crassa* W. Greg.; *A. cuneata* Cleve; *A. exigua* W. Greg.; *A. exilitata* Giffen*; *A. graeffeana* Hendey; *A. helenensis* Giffen*; *A. laevis* W. Greg.; *A. lineolata* Ehrenb.; *A. marina* W. Sm.; *A. obtusa* W. Greg.; *A. ocellata* Donkin; *A. ostrearia* Bréb.; *A. proteus* W. Greg.; *A. staurophora* Jahlin-Dannfelt; *A. subacutiuscula* Schoemann; *A. wisei* (Salah) Simonsen; *Amphora* sp. O1; *Amphora* sp. O2; *Aneumastus* sp. 1; *Anorthoneis excentrica* (Donkin) Grunow; *Astartiella bahusiensis* (Grunow) Witkowski, Lange-Bert. et Metzeltin*; *Astartiella* sp. O1; *Bacillaria paxillifera* (O. F. Müll.) Hendey; *Berkeleya scopulorum* (Bréb. et Kütz.) E. J. Cox; *Biremis ambigua* (Cleve) D. G. Mann; *B. lucens* (Hust.) Sabbe, Witkowski et Vyverman*; *B. ridicula* (Giffen) D. G. Mann*; *Caloneis densestriata* (Proschk.-Lavr.) Gusl.; *C. liber* (W. Sm.) Cleve; *Campylodiscus parvulus* W. Sm.; *C. thuretii* Bréb.; *Campylodiscus* sp. 1; *Catenula adhaerens* Mereschk.; *Chamaepinnularia alexandrowiczii* Witkowski, Lange-Bert. et Metzeltin*; *Chamaepinnularia* cf. *alexandrowiczii* Witkowski, Lange-Bert. et Metzeltin; *Ch. clamans* (Hust.) Witkowski, Lange-Bert. et Metzeltin*; *Ch. margaritiana* (Witkowski) Witkowski*; *Ch. truncata* (König) Witkowski, Lange-Bert. et Metzeltin*; *Climaconeis inflexa* (Bréb. ex Kütz.) E. J. Cox; *Cocconeiopsis breviata* (Hust.) Witkowski, Lange-Bert. et Metzeltin*; *C. fraudulenta* (A. W. F. Schmidt) Witkowski, Lange-Bert. et Metzeltin*; *C. patrickae* (Hust.) Witkowski, Lange-Bert. et Metzeltin*; *Cocconeis crispa* Edsbagge*; *C. clandestina* A. W. F. Schmidt*; *C. diminuta* Pant.*; *C. dirupta* var. *flexella* (Janisch et Rabenh.) Grunow; *C. discrepans* A. W. F. Schmidt*; *C. distans* W. Greg.; *C. engelbrechtii* Cholnoky; *C. euglypta* Ehrenb.; *C. guttata* Hust. et Aleem*; *C. molesta* var. *crucifera* Grunow; *C. pediculus* Ehrenb.; *C. pelta* A. W. F. Schmidt*; *C. peltoides* Hust.*; *C. placentula* Ehrenb.; *C. pseudocostata* Romero*; *C. scutellum* Ehrenb.; *C. scutellum* var. *parva* (Grunow) Cleve; *C. speciosa* W. Greg.; *C. stauroneiformis* (Rabenh.) Okuno; *Cocconeis* sp. O1; *Cocconeis* sp. O2; *Cocconeis* sp. 5W; *Cylindrotheca closterium* (Ehrenb.) Reimann et Lewin; *Dickieia resistans* Witkowski, Lange-Bert. et Metzeltin; *D. subinflata* (Grunow ex Cleve et J. D. Möller) D. G. Mann; *Diploneis bombus* (Ehrenb.) Cleve-Euler ex Backman et Cleve-Euler; *D. chersonensis* (Grunow) Cleve; *D. coffaeiformis* (A. W. F. Schmidt) Cleve*; *D. crabro* Ehrenb.; *D. didyma* Ehrenb.; *D. fusca* (W. Greg.) Cleve; *D. notabilis* (Grev.) Cleve; *D. notabilis* var. *tenera* Proschk.-Lavr.; *D. rex* Droop; *D. smithii* (Bréb.) Cleve; *D. smithii* var. *pumila* (Grunow) Hust.; *D. stroemii* Hust.*; *D. suborbicularis* (W. Greg.) Cleve; *D. vacillans* (A. W. F. Schmidt) Cleve; *D. vetula* (A. W. F. Schmidt) Cleve*; *Diploneis* sp. 1F; *Diploneis* sp. 1VS; *Entomoneis gigantea* var. *sulcata* (O'Meara) Gusl.; *Eolimna* sp. 2O*; *Fallacia cassubiae* Witkowski; *F. escorialis* (Simonsen) Sabbe et Vyverman*; *F. florinae* (Moeller) Witkowski*; *F. forcipata* (Grev.) A. Stickle et D. G. Mann; *F. margino-punctata* Sabbe et Vyverman*; *F. ny* (Cleve) D. G. Mann*; *F. oculiformis* (Hust.) D. G. Mann*; *F. schaeferae* (Hust.) D. G. Mann*; *F. subforcipata* (Hust.) D. G. Mann; *Fallacia* sp. 1F; *Fallacia* sp. 9O; *Gyrosigma attenuatum* (Kütz.) Cleve; *Halamphora acutiuscula* (Kütz.) Levkov; *H. angularis* (W. Greg.) Levkov; *H. coffeaeformis* (C. Agardh) Levkov; *H. eunotia* (Cleve) Levkov; *H. tenerrima* (Aleem et Hust.) Levkov*; *H. turgida* (W. Greg.) Levkov; *Hantzschia amphioxys* f. *capitata* O. Müll.; *H. marina* Donkin*; *H. virgata* (Roper) Grunow*; *Hantzschia* cf. 177-1; *Hantzschia* sp. O1; *Hippodonta* sp. 2; *Hippodonta* sp. 3; *Hippodonta* sp. 6; *Hippodonta* sp. 9; *Hippodonta* sp. O1; *Karayevia amoena* (Hust.) Bukht.; *Lunella ghalebii* Witkowski, Lange-Bert. et Metzeltin*; *Lyrella abruptapontica* Nevrova, Witkowski, Kulikovskiy & Lange-Bert.; *L. atlantica* (A. W. F. Schmidt) D. G. Mann; *L. barbara* (Heiden) D. G. Mann*; *L. clavata* (W. Greg.) D. G. Mann; *L. dilatata* (A. W. F. Schmidt) Nevrova, Witkowski, Kulikovskiy et Lange-Bert.**; *L. fogedii* Witkowski, Lange-Bert. et Metzeltin*;

Continued on the next page…

Taxon	Species
	L. hennedyi (W. Sm.) A. Stickle et D. G. Mann; *L. karayevae* Nevrova, Witkowski, Kulikovskiy et Lange-Bert.**; *L. lyroides* (Hendey) D. G. Mann; *L. majuscula* (Hust.) Witkowski*; *L. pontieuxini* Nevrova, Witkowski, Kulikovskiy et Lange-Bert.**; *L. pseudolyra* Nevrova, Witkowski, Kulikovskiy et Lange-Bert.**; *Mastogloia cuneata* (Meister) Simonsen*; *M. lanceolata* Cleve; *M. pumila* (Cleve et Möller) Cleve; *Navicula aleksandrae* Lange-Bert., Witkowski, Bogaczewicz-Adamczak et Zgrundo*; *N. arenaria* Donkin*; *N. bozenae* Lange-Bert., Witkowski, Bogaczewicz-Adamczak et Zgrundo*; *N. cancellata* Donkin; *Navicula* cf. *cancellata*; *N. capillata* Giffen*; *Navicula* cf. *opima* (Grunow) Grunow*; *N. cincta* (Ehrenb.) Ralfs; *N. digitoradiata* (W. Greg.) Ralfs; *N. flagellifera* Hust.*; *Navicula* cf. *flagellifera* Hust.; *N. germanopolonica* Lange-Bert., Witkowski, Bogaczewicz-Adamchak et Zgrundo*; *N. glabriuscula* var. *elipsoidales* Proschk.-Lavr.***; *N. gregaria* Donkin; *N. northumbrica* Donkin*; *N. palpebralis* Bréb.; *N. palpebralis* var. *angulosa* (W. Greg.) Van Heurck; *N. palpebralis* var. *minor* Grunow; *N. palpebralis* var. *semiplena* (W. Greg.) Cleve; *N. palpebrulum* Cholnoky*; *N. parapontica* Witkowski, Kulikovskiy, Nevrova et Lange-Bert.**; *N. perminuta* Grunow; *N. petrovii* Nevrova, Witkowski, Kociolek et Lange-Bert.** (syn. *N. scabriuscula* (Cleve et Grove) Mereschk.***); *N. phyllepta* Kütz.*; *N. phylleptosoma* Lange-Bert.*; *N. ramosissima* (C. Agardh) Cleve; *N. salinarum* Grunow; *N. salinicola* Hust.; *N. veneta* Kütz.; *N. viminoides* var. *cosmomarina* Lange-Bert., Witkowski, Bogaczewicz-Adamchak et Zgrundo*; *Navicula* sp. O1; *Navicula* sp. O2; *Nitzschia acuminata* (W. Sm.) Grunow; *N. aequorea* Hust.*; *N. agnita* Hust.*; *N. angularis* var. *affinis* (Grunow) Grunow; *Nitzschia* cf. *coarctata* Grunow; *N. compressa* (J. W. Bailey) Boyer; *N. constricta* (Kütz.) Ralfs; *N. dissipata* (Kütz.) Grunow; *N. frequens* Hust.*; *N. frustulum* (Kütz.) Grunow; *N. hybrida* Grunow; *N. inconspicua* Grunow; *N. insignis* W. Greg.; *N. liebetruthii* Rabenh.; *N. lorenziana* Grunow; *N. miserabilis* Cholnoky*; *N. pellucida* Grunow; *N. perindistincta* Cholnoky*; *N. persuadens* Cholnoky*; *N. rorida* Giffen*; *N. sigma* (Kütz.) W. Sm.; *N. spathulata* Bréb.; *N. spathulata* var. *hyalina* W. Greg.; *N. vidovichii* (Grunow) Grunow; *Oestrupia powellii* (Lewis) Heiden*; *Parlibellus delognei* (Van Heurck) E. J. Cox; *P. hamulifer* (Grunow) E. J. Cox; *P. plicatus* (Donkin) E. J. Cox; *Parlibellus* sp. O2; *Petroneis humerosa* (Bréb.) A. Stickle et D. G. Mann; *Pinnularia claviculus* (W. Greg.) Rabenh.*; *P. cruciformis* (Donkin) Cleve; *P. trevelyana* (Donkin) Rabenh.***; *Placoneis* sp. 1; *Plagiotropis elegans* (W. Sm.) Grunow; *P. lepidoptera* (W. Greg.) Kuntze; *P. pusilla* (W. Greg.) Kuntze*; *Planothidium delicatulum* (Kütz.) Round et Bukht.; *P. deperditum* (Giffen) Witkowski, Lange-Bert. et Metzeltin*; *P. quarnerensis* (Grunow) Witkowski, Lange-Bert. et Metzeltin; *Planothidium* sp. 2F; *Pleurosigma aestuarii* (Bréb.) W. Sm.; *P. angulatum* (Queckett) W. Sm.; *Psammodictyon panduriforme* (W. Greg.) D. G. Mann; *P. panduriforme* var. *continua* (Grunow) P. J. M. Snoeijs*; *Rhoicosphenia abbreviata* (C. Agardh) Lange-Bert.; *Seminavis* sp. 1; *Stauronella indubitabilis* Lange-Bert. et Genkal; *Staurophora salina* (W. Sm.) Mereschk.; *Surirella fastuosa* (Ehrenb.) Kütz.; *S. pandura* H. Perag. et Perag.; *Toxonidea insignis* Donkin***; *Trachyneis aspera* (Ehrenb.) Cleve

Note: *, species previously recorded by us as a new to the Black Sea flora; **, species previously described by us as a new to science; ***, species not registered within the last 50 or 100 years in the Black Sea.

Investigations in the Kruglaya Bay allowed revealing 70 species newly found for the Bacillariophyta flora of the northern Black Sea shelf, and 5 species described as new to science. Also, we noted 4 species not registered in the Black Sea within approximately 50 years of surveys [*Navicula glabriuscula* var. *elipsoidales*] or even 100 years [*Navicula petrovii* (syn. *N. scabriuscula*), *Toxonidea insignis*, and *Pinnularia trevelyana*]. Five genera are new for the Bacillariophyta flora of the Black Sea: *Astartiella* Witkowski, Lange-Bert. et Metzeltin, *Chamaepinnularia* Lange-Bert. et Krammer,

Cocconeiopsis Witkowski, Lange-Bert. et Metzeltin, *Eolimna* Lange-Bert. et Schiller, and *Lunella* P. J. M. Snoeijs. Those are represented by the species *Astartiella bahusiensis*, *Astartiella* sp. O1, *Chamaepinnularia alexandrowiczii*, *Ch. clamans*, *Ch. margaritiana*, *Ch. truncata*, *Cocconeiopsis breviata*, *C. fraudulenta*, *C. patrickae*, *Eolimna* sp. 2O, and *Lunella ghalebii* [Nevrova, 2022].

Representatives of the classes Coscinodiscophyceae and Fragilariophyceae are few in number, and their shares are 7.5 and 6.8%, respectively. The contribution of taxa of the class Bacillariophyceae is 85.6%. The order Naviculales is the most diverse in terms of taxonomy: 9 families, 22 genera, and 101 species and ITS. Within the order Achnanthales, we report 3 families, 7 genera, and 35 species and IST. The order Thalassiophysales comprises 1 family, 4 genera, and 32 species and IST, while the order Bacillariales, 1 family, 5 genera, and 33 species and IST. In the Omega Bay water area, the most species-rich genera are *Navicula* (32 species and IST), *Nitzschia* (23), *Cocconeis* (22), *Amphora* (21), *Diploneis* (17), *Lyrella* (11), and *Fallacia* (11).

Several species could not be identified using the literature available. However, we included them in the general list for analysis based on their morphological differences from known diatoms. Micrographs of non-identified species and new and rare taxa are provided in Figs 2–6.

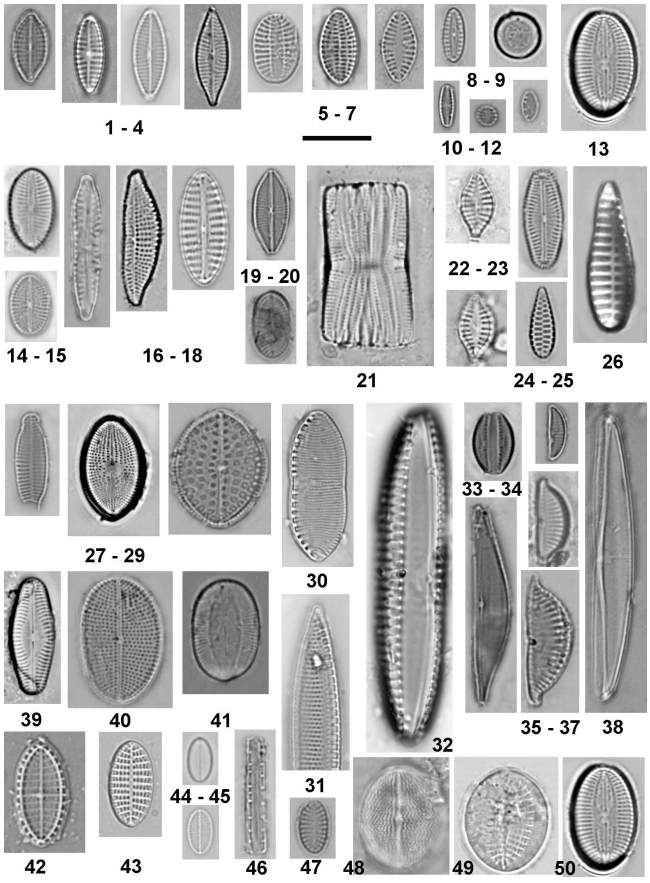

Fig. 2. Newly found for the Black Sea, rare, and non-identified species of benthic diatoms registered off the Omega Bay (a light microscope): 1, *Navicula viminoides* var. *cosmomarina*; 2, *N. bozenae*; 3, *N. aleksandrae*; 4, *N. phylleptosoma*; 5, *Cocconeis peltoides*; 6, *C. discrepans*; 7, *Planothidium deperditum*; 8, *Biremis lucens*; 9, *Cyclotella choctawhatcheeana*; 10, *Chamaepinnularia margaritiana*; 11, *Opephora krumbeinii*; 12, *Nitzschia inconspicua*; 13, *Fallacia oculiformis*; 14, *Diploneis* sp. 1; 15, *Cocconeiopsis breviata*; 16, *Hippodonta* sp. 6; 17, *Lunella ghalebii*; 18, *Hippodonta* sp. O1; 19, *Astartiella bahusiensis*; 20, *Astartiella* sp. O1; 21, *Hyalosira aberrans*; 22, 23, *Achnanthidium glyphos* [raphe valve (RV) and rapheless valve (RLV)]; 24, *Chamaepinnularia clamans*; 25, *Opephora mutabilis*; 26, *O. pacifica*; 27, *Karayevia amoena*; 28, *Cocconeiopsis fraudulenta*; 29, *Cocconeis guttata*; 30, *Nitzschia persuadens*; 31, *Hantzschia* cf. 177-1; 32, *Biremis ridicula*; 33, *Amphora helenensis*; 34, *Amphora* sp. O1; 35, *A. exilitata*; 36, *A. wisei*; 37, *Halamphora turgida*; 38, *Amphora* cf. *abludens*; 39, *Chamaepinnularia truncata*; 40, *Cocconeiopsis patrickae*; 41, *Cocconeis pelta*; 42, 43, *C. pseudocostata* (RV and RLV); 44, 45, *Cocconeis* sp. 5W (RV and RLV); 46, *Cocconeis* sp. O1; 47, *Nitzschia miserabilis*; 48, 49, *Cocconeis* sp. O2 (RV and RLV); 50, *Fallacia ny*. Scale bar is 10 μm

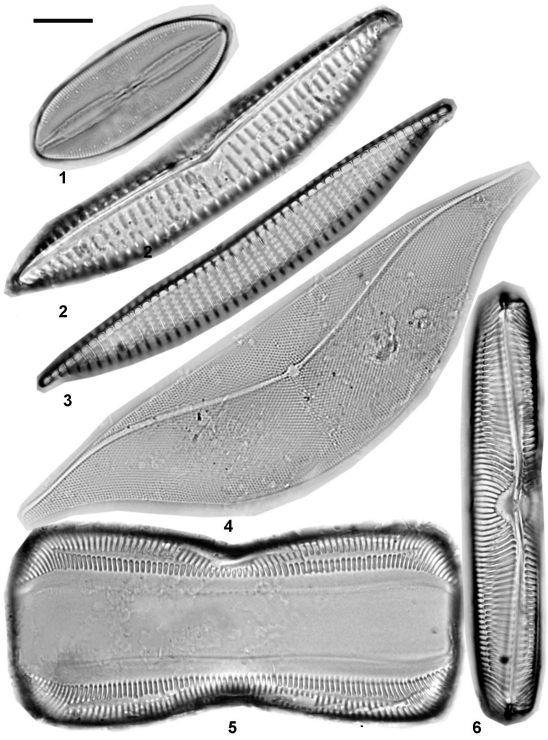

Fig. 3. Diatom species not recorded in the Black Sea within the last 100 years (a light microscope): 1, *Navicula glabriuscula* var. *elipsoidales*; 2, *N. petrovii* (syn. *N. scabriuscula*); 4, *Toxonidea insignis*; 5, 6, *Pinnularia trevelyana* (girdle and valve). Newly found species for the Black Sea: 3, *Hantzschia marina*. Scale bar is 10 μm

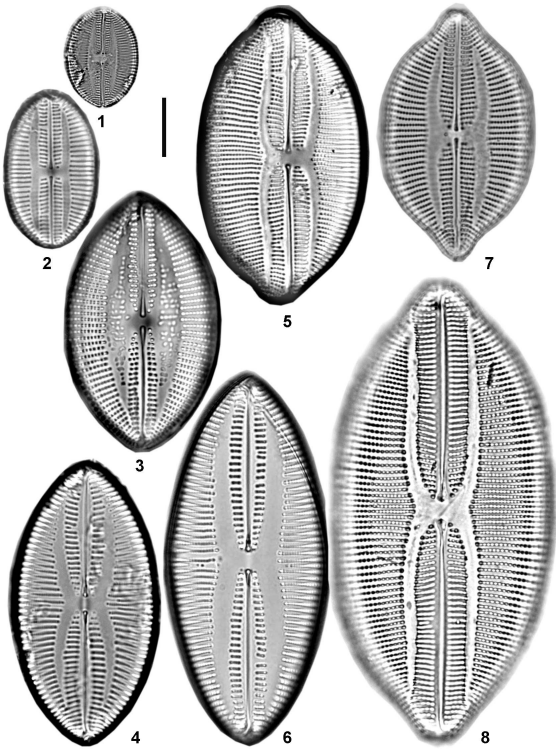

Fig. 4. Diatom species new for science (previously described by us) found off the Omega Bay (a light microscope): 1, *Lyrella fogedii*; 2, *L. majuscula*; 3, *L. abruptapontica*; 4, *L. karayevae*; 5, *L. dilatata*; 6, *L. pontieuxini*; 7, *L. barbara*; 8, *L. pseudolyra*. Scale bar is 10 μm

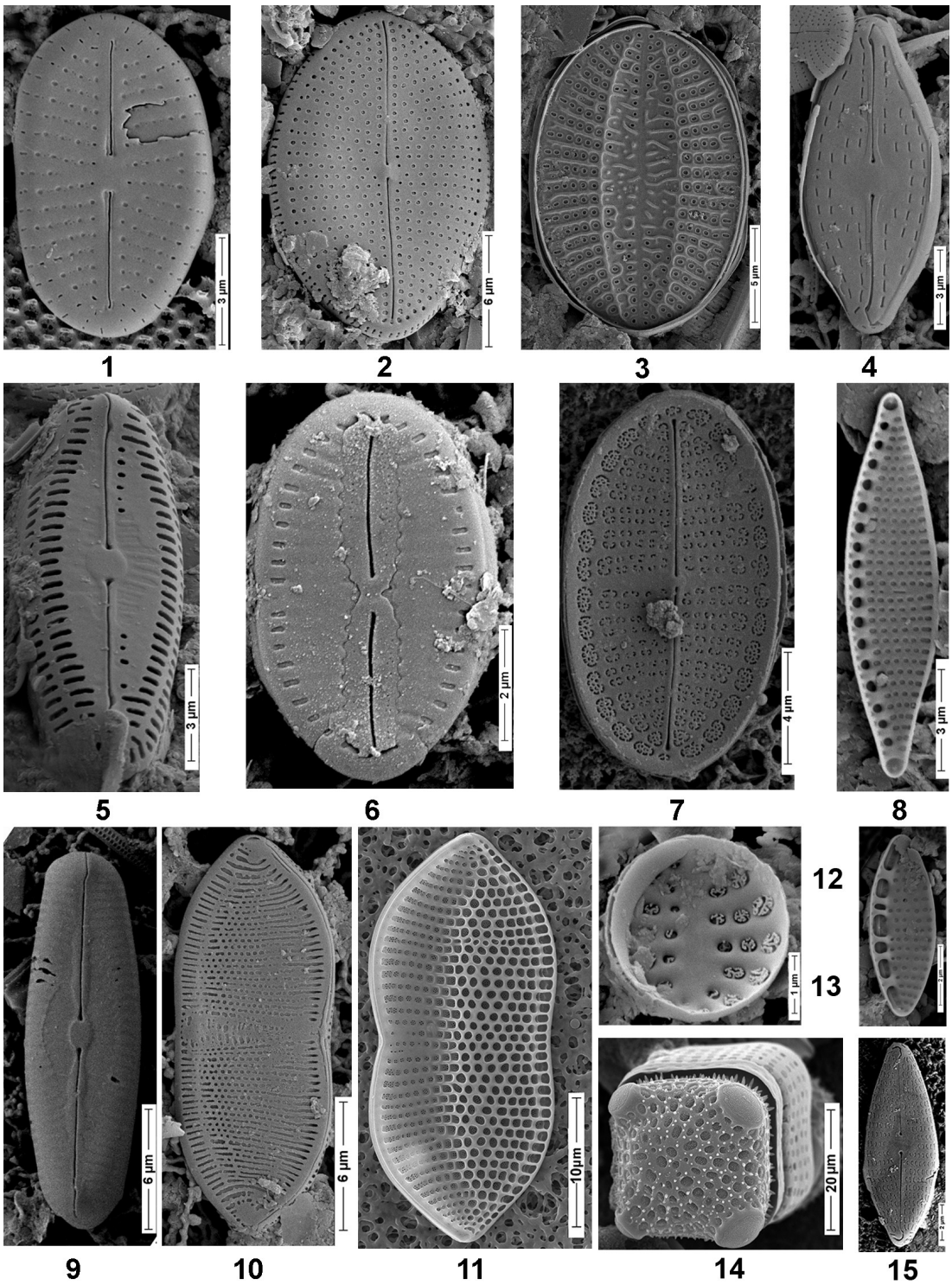

Fig. 5. Newly found to the Black Sea and rare species of benthic diatoms registered off the Omega Bay (a scanning electron microscope): 1, *Cocconeiopsis breviata*; 2, *Cocconeis clandestina*; 3, *C. pelta*; 4, *Navicula viminoides* var. *cosmomarina*; 5, *Chamaepinnularia alexandrowiczii*; 6, *Fallacia margino-punctata*; 7, *Cocconeis pseudocostata*; 8, *Nitzschia aequorea*; 9, *Chamaepinnularia truncata*; 10, *Nitzschia persuadens*; 11, *Psammodictyon panduriforme* var. *continua*; 12, *Opephora krumbeinii*; 13, *Nitzschia inconspicua*; 14, *Amphitetras antediluvianum*; 15, *Navicula aleksandrae*. Scale bars are 3 μm (1, 4, 5, 8); 6 μm (2, 9, 10); 5 μm (3); 10 μm (6, 11); 4 μm (7); 1 μm (12); 2 μm (13); 20 μm (14); 2 μm (15)

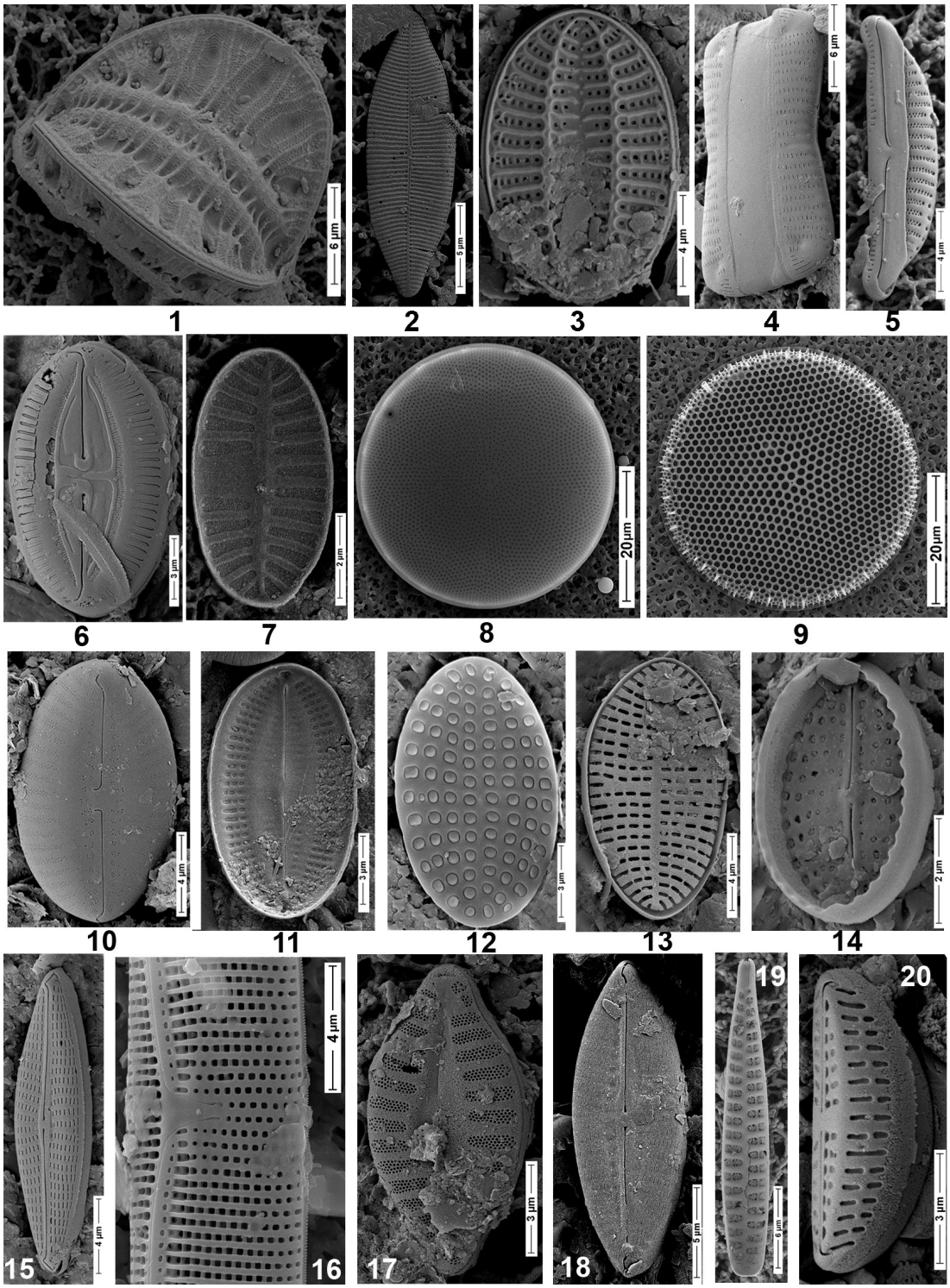

Fig. 6. Newly found for the Black Sea and rare species of benthic diatoms recorded off the Omega Bay (a scanning electron microscope): 1, *Campylodiscus* sp. 1; 2, *Astartiella bahusiensis*; 3, *Cocconeis peltoides*; 4, *Hippodonta* sp. 6; 5, *Halamphora tenerrima*; 6, *Fallacia florinae*; 7, *Planothidium deperditum*; 8, *Actinocyclus subtilis*; 9, *Thalassiosira eccentrica*; 10, *Diploneis coffaeiformis*; 11, *Fallacia oculiformis* (internal); 12, *Cocconeis guttata*; 13, *Cocconeis crispa*; 14, *C. diminuta*; 15, *Navicula phylleptosoma*; 16, *Nitzschia vidovichii* (central nodule); 17, *Planothidium delicatulum*; 18, *Navicula palpebrulum*; 19, *Opephora mutabilis*; 20, *Amphora helenensis*. Scale bars are 6 μm (1, 4, 19); 5 μm (2, 18); 4 μm (3, 5, 10, 13, 15, 16); 3 μm (6, 11, 12, 17, 20); 2 μm (7, 14); 20 μm (8, 9)

The biota of the Omega Bay has been studied in considerable detail regarding macrozoobenthic taxonomic richness, structure, and spatial distribution [Boltachova et al., 2022; Mironov et al., 2003], whilst microphytobenthos has been investigated only partially. Benthic diatom richness in the bay was surveyed by A. Proshkina-Lavrenko in October 1950 [1963], L. Ryabushko in the summer of 1990 [1994], and by a team of researchers in October 2016 [Ryabushko et al., 2022]. In the monograph authored by A. Proshkina-Lavrenko [1963], the registered diatom taxa are included in a general list, and this does not allow for determining which species were found in this biotope. L. Ryabushko reported 42 species and IST of benthic diatoms in the epiphyton [Ryabushko, 1994] and 14 species in the epipsammon [Ryabushko et al., 2022].

Importantly, among the 14 species listed in [Ryabushko et al., 2022], several are misidentified at the genus level. Thus, the one reported by the authors as *Pseudostaurosira medliniae* D. M. Williams et E. A Morales, 2010 [Ryabushko et al., 2022, Fig. 3D, E] and named the first record for the Kruglaya Bay and for the whole Black Sea, is misidentified, according to [Williams, Morales, 2010]. As the authors initially presumed, the species belongs to the *Planothidium delicatulum* (Kützing) Round & Bukhtiyarova, 1996 complex based on the following traits: valve shape with slightly rostrate ends, absence of spines on valve margins, striae density (18 in 10 μm), and multiseriate areolae within striae [Van de Vijver et al., 2018]. Species from this complex are common and abundant in the Black Sea [Guslyakov et al., 1992; Nevrova, Revkov, 2003].

The species the authors identified as *Cocconeis pinnata* Gregory ex Greville, 1859 [Ryabushko et al., 2022, Fig. 5A, B] is *Planothidium deperditum* (Giffen) A. Witkowski, H. Lange-Bertalot & D. Metzeltin, 2000 in accordance with valve shape, striae density (30 in 10 μm), and multiseriate areolae within striae. This diatom was previously reported as new to the Black Sea [Nevrova, 2022].

The species identified as *Diplomenora cocconeiformis* (Schmidt) Blazé, 1984 [Ryabushko et al., 2022, Fig. 3A–C] does not belong to the indicated genus due to the absence of a raphe on both valves. The micrograph of a raphe valve provided by the authors illustrates the genus *Cocconeis* Ehrenberg.

The species identified as *Coscinodiscus concinnus* W. Smith, 1856 [Ryabushko et al., 2022, Fig. 1A] is *Actinocyclus subtilis* (W. Greg.) Ralfs, 1861 based on the presence of a pseudonodulus, numerous labiate processes, and striae density (17–18 in 10 μm) [Andersen et al., 1986]. Additionally, *C. concinnus*, indicated by the authors as new to the Black Sea flora, has already been repeatedly reported as a rare species in various areas of the Black Sea [Bodeanu, 1987; Guidelines, 2015; Guslyakov, Nevrova, 1987; Nevrova, 2013b; Proshkina-Lavrenko, 1963].

The species assigned to *Anorthoneis dulcis* M. K. Hein, 1991 [Ryabushko et al., 2022, Fig. 3F–H] and reported as a new find for the Black Sea is *Cocconeiopsis pullus* (Hustedt) Witkowski, Lange-Bertalot et Metzeltin, 2000 based on the shape of valve and a hyaline area on its inner part, arrangement of striae and their density, and the shape of terminal and central raphe fissures. These are a new genus and a new species for the Black Sea already discovered by us for the first time for this basin at two sites (Cape Fiolent and Dvuyakornaya Bay) [Nevrova, 2016; Nevrova, Petrov, 2019a].

Also, there was an error concerning the priority of the record for the Black Sea: *Cocconeis guttata* Hustedt et Aleem, 1951 [Ryabushko et al., 2022, Fig. 4H–K] indicated as a new species to the flora has already been found in at least seven areas of the Black Sea (the estuary of the Belbek River, the Zernov's *Phyllophora* Field, Balaklava Bay, Karadag coast, Cape Fiolent, Dvuyakornaya Bay, and Omega Bay), as reported in [Nevrova, 2013a, 2014a, b, 2015, 2016; Nevrova, Petrov, 2019a].

A comparative assessment of total richness of flora of benthic Bacillariophyta in the Omega Bay and previously surveyed areas off the Crimean coast (based on the Bray–Curtis dissimilarity) revealed the greatest similarity in species composition between biotopes of the Omega Bay and the Dvuyakornaya Bay (53.3) and the Omega Bay and the Laspi Bay (45.3) characterized by the lowest technogenic pollution (Table 2). The maximum values were registered for the bays strongly polluted with salts of heavy metals and petroleum hydrocarbons: the Sevastopol Bay and the Karantinnaya Bay (64.6) and the Sevastopol Bay and the Balaklava Bay (57.8).

Table 2. Similarity in species composition of benthic diatoms in the study areas (based on Bray–Curtis dissimilarity)

Areas off the Crimean coast and species richness (IST)	Omega Bay	Laspi Bay	Dvuyakornaya Bay	Karantinnaya Bay	Sevastopol Bay
Omega Bay (264)	*	*	*	*	*
Laspi Bay (217)	45.3	*	*	*	*
Dvuyakornaya Bay (304)	53.2	44.9	*	*	*
Karantinnaya Bay (136)	38.9	64.6	36.8	*	*
Sevastopol Bay (186)	39.9	64.1	36.3	64.6	*
Balaklava Bay (191)	43.0	56.4	42.4	53.8	57.8

Subsequently, we analyzed the taxonomic diversity and structure of Bacillariophyta taxocenes in the Kruglaya Bay in comparison with those of previously studied biotopes along the Crimean coast. We calculated mean values of TaxDI (Δ^+) and its variability (Λ^+), as well as its deviation from the expected level for the whole Black Sea (Fig. 7). The method was properly described before [Nevrova, 2022].

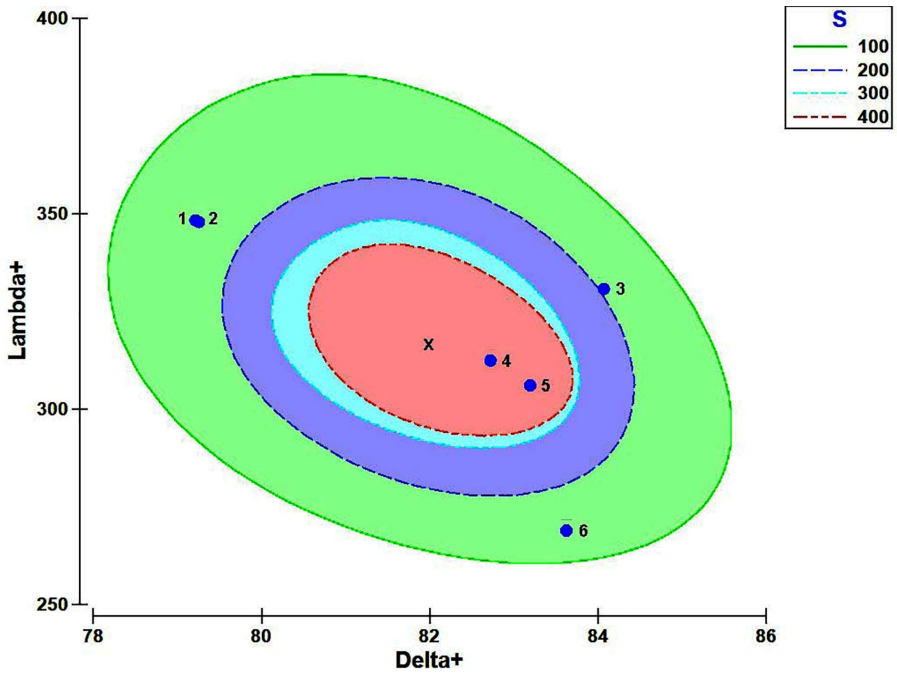

Fig. 7. Comparative assessment using TaxDI – AvTD (Δ^+) and VarTD (Λ^+) – of taxonomical diversity of benthic diatoms in various biotopes with different anthropogenic load off the Crimean coast: 1, the Omega Bay; 2, the Dvuyakornaya Bay; 3, the Balaklava Bay; 4, the Laspi Bay; 5, the Karantinnaya Bay; 6, the Sevastopol Bay; ×, average expected level for the Black Sea diatom flora. A 95% confidence ellipse

As already mentioned, the diversity of diatom taxocenes in the study areas was assessed by taxonomic distinctness indices: AvTD (Δ^+) and VarTD (Λ^+) [Clarke, Gorley, 2006; Clarke, Warwick, 2001; Warwick, Clarke, 1998, 2001]. Δ^+ represents the mean path length between every pair of species, randomly chosen from the list of a site, to a phylogenetically common node on a hierarchical tree of the taxocene. The index characterizes the vertical taxonomic evenness of the taxocene in the study area. Λ^+ describes the variability of pairwise distances (ω_{ij}) between pairs of species *i* and *j* relative to their mean value Δ^+. The value of Λ^+ shows the representation of taxa at increasing hierarchical levels and characterizes the horizontal asymmetry of the taxonomic tree [Warwick, Clarke, 1998, 2001]. The calculation algorithm allows for a reliable assessment of differences in taxonomic diversity and for recording deviations in the structure of diatoms in compared areas from the expected value for the Bacillariophyta flora of the whole Black Sea [Nevrova, 2022]. Despite the convenience of applying this method, the taxonomic diversity in marine microphytobenthos still has not been assessed (there are just a few works on freshwater microflora [Izsak et al., 2002; Leira et al., 2009]). For marine benthic Bacillariophyta, TaxDI is used for the first time [Nevrova, 2022].

TaxDI points corresponding to the biotopes with the highest technogenic pollution in the Karantinnaya, Balaklava, and Sevastopol bays are located in the lower right quadrant of the confidence ellipse. This is caused by high AvTD values and low VarTD variability, which reflect reduced taxonomic structure and decreased diversity within diatom taxocenes [Warwick et al., 2002]. The index values for these taxocenes are significantly above the expected value for the whole Black Sea flora ($\Delta^+ = 82.09$; $\Lambda^+ = 316.83$).

The structure of diatom taxocenes in heavily polluted bays shows low species richness and the disappearance of taxa with low resistance to technogenic contaminants; this reduces the species saturation of clades on the hierarchical tree and mediates an increase in taxonomic distances when calculating the index. Compared to the average expected level of TaxDI, a lower degree of vertical hierarchical evenness in the taxocene structure is characteristic of communities exposed to severe anthropogenic pollution. Such changes in the structure have been reported repeatedly [Ellingsen et al., 2005; Gottschalk, Kahlert, 2012; Heino et al., 2007; Masouras et al., 2021; Petrov et al., 2010; Stenger-Kovács et al., 2016].

TaxDI points corresponding to relatively unpolluted areas of the Omega and Dvuyakornaya bays are located in the upper left quadrant of the confidence ellipse. This is determined by the lowest AvTD values and the highest VarTD variability. The values of the indices fall below the expected ones for the Black Sea diatom flora. Such a taxocene structure is a reflection of high species richness and a large number of taxonomic clades of varying species saturation, which 'converge into nodes' at different hierarchical levels. The tree architecture is dominated by polyspecific clades closing at the genus level. Also, there are mono- and oligospecific clades: those aggregating at higher taxonomic levels (family and even order ones). Low Δ^+ and high Λ^+ values indicate vertical evenness and high variability in taxonomic distances between clades. A similar pattern has previously been described for pristine or minimally disturbed biotopes [Keck et al., 2016; Nevrova, Petrov, 2019b; Rimet, Bouchez, 2012].

For the diatom taxocene of the Laspi Bay (a relatively unpolluted site), AvTD and VarTD values are near the average expected level for the whole Black Sea. For the taxocene of the Balaklava Bay (a heavily polluted site), AvTD value is close to that of the Sevastopol Bay, but the variability is noticeably higher. Importantly, the values of all calculated indices lie within the 95% confidence ellipse.

TaxDI application for assessing taxonomic diversity allows for a deeper understanding of its aspects. The differences in the structure of the hierarchical tree of Bacillariophyta for the compared sites are largely driven by a response of benthic diatom taxocenes to combined factors and varying degrees of anthropogenic load. The greatest similarity in species richness and structure of Bacillariophyta taxocenes was revealed both between relatively unpolluted biotopes and between the most heavily polluted ones, indicating, regardless of the geographical distance between these sites, the heterogeneity of bottom substrates, and differences under hydrological conditions.

Conclusions:

1. The benthic diatom taxocene of the Kruglaya Bay (the Omega Bay) comprises 264 species and infraspecific taxa: 256 species, 73 genera, 35 families, 21 orders, and 3 classes. Representatives of the class Bacillariophyceae dominate. These include 70 species and 5 genera previously noted by us as new to the Bacillariophyta flora for the Black Sea northern shelf, as well as 5 diatom species we described as new to science before.
2. The similarity in species composition was registered both between biotopes with the lowest level of technogenic pollution (the Omega Bay – the Dvuyakornaya Bay and the Omega Bay – the Laspi Bay) and between areas strongly polluted with salts of heavy metals and petroleum hydrocarbons (the Sevastopol Bay – the Karantinnaya Bay and the Sevastopol Bay – the Balaklava Bay), regardless of their distance from each other and differences in hydrological and hydrophysical conditions.
3. Benthic diatom taxocenes in heavily polluted areas are characterized by low species richness and a predominance of mono- and oligospecific clades due to the elimination of taxa with low resistance to pollutants. AvTD values exceed the average expected level for the Bacillariophyta flora of the Black Sea.
4. In relatively unpolluted water areas, Bacillariophyta taxocenes are characterized by high species richness, a large number of polyspecific clades, and the presence of mono- and oligospecific clades aggregating at high levels of the hierarchical tree. AvTD values are lower as compared to the average expected level for the Black Sea benthic diatom flora.

This work was carried out in the Department of Benthos Ecology within the framework of IBSS state research assignment "Biodiversity as the basis for the sustainable functioning of marine ecosystems, criteria and scientific principles for its conservation" (No. 124022400148-4).

Acknowledgments. I express my deep gratitude to PhD A. Petrov (IBSS) for assistance with TaxDI calculations, to Professor A. Witkowski (University of Szczecin, Poland) for providing equipment for LM microphotography and his consultation on identification, to Professor H. Lange-Bertalot and master engineer M. Ruppel (Goethe University, Germany) for SEM microphotography and their taxonomic consultations, and to head of the Microscopy Laboratory V. Lishaev (IBSS) for his assistance with microphotography on a SEM Hitachi SU3500.

REFERENCES

1. Agarkova-Lyakh I. V., Lyakh A. M. State of the coasts and exogenous geological processes between Cape Konstantinovskiy and Cape Vinogradniy on the south-western coast of Crimea. *Uchenye zapiski Krymskogo federal'nogo universiteta imeni*

V. I. Vernadskogo. Geografiya. Geologiya, 2019, vol. 5 (71), no. 2, pp. 118–133. (in Russ.). https://elibrary.ru/jaycko

2. Barinova S. S., Medvedeva L. A., Anisimova O. V. *Bioraznoobrazie vodoroslei-indikatorov okruzhayushchei sredy*. Tel Aviv : Pilies Studio, 2006, 498 p. (in Russ.)
3. Boltachova N. A., Revkov N. K., Bondarenko L. V., Makarov M. V., Nadolny A. A. Benthic fauna of the Kruglaya Bay (Black Sea, Crimea). Part II: Taxonomic composition and quantitative characteristics of macrozoobenthos in the soft-bottom biotope. *Trudy Karadagskoi nauchnoi stantsii imeni T. I. Vyazemskogo – prirodnogo zapovednika RAN*, 2022, vol. 7, no. 2 (22), pp. 3–22. (in Russ.). https://elibrary.ru/qnkkey
4. Guslyakov N. E., Zakordonets O. A., Gerasimyuk V. P. *Atlas diatomovykh vodoroslei bentosa severo-zapadnoi chasti Chernogo morya i prilegayushchikh vodoemov*. Kyiv : Naukova dumka, 1992, 115 p. (in Russ.)
5. Guslyakov N. E., Nevrova E. L. *Sostav diatomovykh vodoroslei na tverdykh substratakh v raione Sevastopol'skoi bukhty* / Institut biologii yuzhnykh morei im. A. O. Kovalevskogo AN USSR. Sevastopol, 1987, 14 p. Dep. v VINITI 29.04.87, No. 3019-V87. (in Russ.)
6. Zenkovich V. P. *Morfologiya i dinamika sovetskikh beregov Chernogo morya.* Vol. 2. *Severo-zapadnaya chast'*. Moscow : AN SSSR, 1960, 216 p. (in Russ.)
7. Ignatov E. I., Orlova M. S., Sanin A. Yu. *Beregovye morfosistemy Kryma.* Sevastopol : EKOSI-Gidrofizika, 2014, 266 p. (in Russ.)
8. Mironov O. G., Kirjukhina L. N., Alyomov S. V. *Sanitary-Biological Aspects of the Sevastopol Bays Ecology in XX Century* / NAS of Ukraine, the Institute of Biology of Southern Seas. Sevastopol : EKOSI-Gidrofizika, 2003, 185 p. (in Russ.). https://repository.marine-research.ru/handle/299011/1466
9. Nevrova E. L. Benthic diatoms (Bacillariophyta) at Zernov's *Phyllophora* field (northern-western part of the Black Sea): Taxonomic diversity and structure of taxocene. *Morskoj ekologicheskij zhurnal*, 2014a, vol. 3, no. 13, pp. 47–58. (in Russ.). https://repository.marine-research.ru/handle/299011/1370
10. Nevrova E. L. Evaluation of benthic diatoms diversity (Bacillariophyta) near Karadag shore. In: *100 Years of the T. I. Vyazemsky Karadag Scientific Station* : issue of scientific papers / A. V. Gaevskaya, A. L. Morozova (Eds). Simferopol : N.Orianda, 2015, pp. 462–492. (in Russ.). https://repository.marine-research.ru/handle/299011/545
11. Nevrova E. L. The composition and structure of the benthic diatom taxocene (Bacillariophyra) near Cape Fiolent (the Crimea, the Black Sea). *Biologiya morya*, 2016, vol. 42, no. 5, pp. 334–342. (in Russ.). https://elibrary.ru/wwwgtn
12. Nevrova E. L. Structure and taxonomical diversity of benthic diatom at estuarines of rivers Belbek and Chernaya (South-West Crimea, Ukraine). *Al'gologiya*, 2013a, vol. 23, no. 4, pp. 471–492. (in Russ.). https://elibrary.ru/zqfoil
13. Nevrova E. L. Taxonomic diversity and structure of benthic diatom taxocene (Bacillariophyta) at Sevastopol Bay (the Black Sea). *Morskoj ekologicheskij zhurnal*, 2013b, vol. 12, no. 3, pp. 55–67. (in Russ.). https://repository.marine-research.ru/handle/299011/1296
14. Nevrova E. L. Taxonomic diversity and environmental assessment of benthic diatoms at Balaklava Bay (South-Western Crimea, the Black Sea, Ukraine). *Al'gologiya*, 2014b, vol. 24, no. 1, pp. 47–66. (in Russ.). https://elibrary.ru/zqfold
15. Nevrova E. L., Revkov N. K. Species composition of taxocene of benthic

diatoms (Bacillariophyta) of Laspi Bay (the Black Sea, Ukraine). *Al'gologiya*, 2003, vol. 13, no. 3, pp. 269–282. (in Russ.). https://elibrary.ru/zqfohr

16. Nevrova E. L. *Diversity and Structure of Benthic Diatom Taxocenes (Bacillariophyta) of the Black Sea* / A. V. Gaevskaya (Ed.) ; A. O. Kovalevsky Institute of Biology of the Southern Seas RAS. Sevastopol : IBSS, 2022, 329 p. (in Russ.). https://repository.marine-research.ru/handle/299011/12192
17. Pavlova E. V., Murina V. V., Kuftarkova E. A. Chemical and biological studies in the Omega Bay (the Black Sea, Sevastopol). In: *Ekologicheskaya bezopasnost' pribrezhnoi i shel'fovoi zon i kompleksnoe issledovanie resursov shel'fa* : sbornik nauchnykh trudov / NAN Ukrainy ; Morskoi gidrofizicheskii institut. Sevastopol : [EKOSI-Gidrofizika], 2001, iss. 2, pp. 159–176. (in Russ.). https://elibrary.ru/ebesuv
18. Petrov A. N., Nevrova E. L. Comparative analysis of taxocene structures of benthic diatoms (Bacillariophyta) in regions with different level of technogenic pollution (the Black Sea, Crimea). *Morskoj ekologicheskij zhurnal*, 2004, vol. 3, no. 2, pp. 72–83. (in Russ.). https://repository.marine-research.ru/handle/299011/748
19. Petrov A. N., Nevrova E. L., Malakhova L. V. Multivariate analysis of benthic diatoms distribution across the multidimensional space of the environmental factors gradient in Sevastopol Bay (the Black Sea, Crimea). *Morskoj ekologicheskij zhurnal*, 2005, vol. 4, no. 3, pp. 65–77. (in Russ.). https://repository.marine-research.ru/handle/299011/812
20. Proshkina-Lavrenko A. I. *Diatomovye vodorosli bentosa Chernogo morya.* Moscow : Izd-vo AN SSSR, 1963, 243 p. (in Russ.). https://repository.marine-research.ru/handle/299011/12747
21. *Guidelines for Quality Control of the Black Sea. Microphytobenthos* / E. L. Nevrova, A. A. Snigireva, A. N. Petrov, G. V. Kovaleva ; A. V. Gaevskaya (Ed.). Sevastopol ; Simferopol : N.Orianda, 2015, 176 p. (in Russ.). https://repository.marine-research.ru/handle/299011/1395
22. Ryabushko L. I. Fouling diatoms of the benthic plants of the Black Sea by Cape Omega. *Al'gologiya*, 1994, vol. 4, no. 1, pp. 62–71. (in Russ.). https://repository.marine-research.ru/handle/299011/9934
23. *AlgaeBase.* World-wide electronic publication, National University of Ireland, Galway / M. D. Guiry, G. M. Guiry (Eds) : [site], 2024. URL: http://www.algaebase.org [accessed: 10.07.2024].
24. Andersen R. A., Medlin L. K., Crawford R. M. An investigation of the cell wall components of *Actinocyclus subtilis* (Bacillariophyceae). *Journal of Phycology*, 1986, vol. 22, iss. 4, pp. 466–479. https://doi.org/10.1111/j.1529-8817.1986.tb02490.x
25. Blanco S., Cejudo-Figueiras C., Tudesque L., Bécares E., Hoffmann L., Ector L. Are diatom diversity indices reliable monitoring metrics? *Hydrobiologia*, 2012, vol. 695, iss. 1, pp. 199–206. https://doi.org/10.1007/s10750-012-1113-1
26. Bodeanu N. Structure et dynamique de l'algoflore unicellulaire dans les eaux du littoral Roumain de la mer Noire. *Cercetari Marine "Recherches Marines"*, 1987–1988, no. 20/21, pp. 19–251.
27. Borja A., Elliott M., Andersen J. H., Cardoso A. C., Carstensen J., Ferreira J. G., Heiskanen A.-S., Marques J. C., Neto J. M., Teixeira H., Uusitalo L., Uyarra M. C., Zampoukas N. Good Environmental Status of marine ecosystems: What is it and how do we know when we have attained it? *Marine Pollution Bulletin*, 2013, vol. 76,

iss. 1–2, pp. 16–27. https://doi.org/10.1016/j.marpolbul.2013.08.042

28. Catalogue of Diatom Names : database / E. Fourtanier, J. P. Kociolek (Comps). In: *California Academy of Sciences* : [site]. San Francisco, CA, 2011. URL: https://researcharchive.calacademy.org/research/diatoms/names/index.asp [accessed: 10.07.2024].
29. Clarke K. R., Gorley R. N. *PRIMER v6: User Manual. Tutorial.* Plymouth : PRIMER-E, 2006, 190 p.
30. Clarke K. R., Warwick R. M. *Change in Marine Communities: An Approach to Statistical Analysis and Interpretation.* 2nd edition. Plymouth : PRIMER-E Ltd., 2001, 176 p.
31. Ellingsen K. E., Clarke K. R., Somerfield P. J., Warwick R. M. Taxonomic distinctness as a measure of diversity applied over a large scale: The benthos of the Norwegian continental shelf. *Journal of Animal Ecology*, 2005, vol. 74, iss. 6, pp. 1069–1079. https://doi.org/10.1111/j.1365-2656.2005.01004.x
32. *Free Maps. D-maps.com* : [site], 2024. URL: https://d-maps.com/m/mediterranean/mernoire/mernoire03.pdf [accessed: 10.07.2024].
33. Gottschalk S., Kahlert M. Shifts in taxonomical and guild composition of littoral diatom assemblages along environmental gradients. *Hydrobiologia*, 2012, vol. 694, iss. 1, pp. 41–56. https://doi.org/10.1007/s10750-012-1128-7
34. Heino J., Mykrä H., Hämäläinen H., Aroviita J., Muotka T. Responses of taxonomic distinctness and species diversity indices to anthropogenic impacts and natural environmental gradients in stream macroinvertebrates. *Freshwater Biology*, 2007, vol. 52, iss. 9, pp. 1846–1861. https://doi.org/10.1111/j.1365-2427.2007.01801.x
35. *ImageJ (Image Processing and Analysis in Java)* : [site], 2025. URL: https://imagej.net/ij/ [accessed: 05.03.2025].
36. *International Plant Names Index (IPNI)* / Royal Botanic Gardens, Kew : [site], 2024. URL: https://www.ipni.org/ [accessed: 10.07.2024].
37. Izsak C., Price A. R. G., Hardy J. T., Basson P. W. Biodiversity of periphyton (diatoms) and echinoderms around a refinery effluent, and possible associations with stability. *Aquatic Ecosystem Health & Management*, 2002, vol. 5, iss. 1, pp. 61–70. https://doi.org/10.1080/14634980260199963
38. Keck F., Rimet F., Franc A. Phylogenetic signal in diatom ecology: Perspectives for aquatic ecosystems biomonitoring. *Ecological Applications*, 2016, vol. 26, iss. 3, pp. 861–872. https://doi.org/10.1890/14-1966
39. Leira M., Chen G., Dalton C., Irvine K., Taylor D. Patterns in freshwater diatom taxonomic distinctness along a eutrophication gradient. *Freshwater Biology*, 2009, vol. 54, iss. 1, pp. 1–14. https://doi.org/10.1111/j.1365-2427.2008.02086.x
40. Levkov Z. *Amphora sensu lato.* Ruggell : A. R. G. Gantner Verlag K. G., 2009, 916 p. (Diatoms of Europe : Diatoms of the European inland waters and comparable habitats / H. Lange-Bertalot (Ed.) ; vol. 5).
41. Masouras A., Karaouzas I., Dimitriou E., Tsirtsis G., Smeti E. Benthic diatoms in river biomonitoring – present and future perspectives within the Water Framework Directive. *Water*, 2021, vol. 13, iss. 4, art. no. 478 (15 p.). https://doi.org/10.3390/w13040478
42. Nevrova E., Witkowski A., Kulikovskiy M., Lange-Bertalot H., Kociolek J.-P. A revision of the diatom genus *Lyrella* Karayeva (Bacillariophyta: Lyrellaceae) from the Black Sea, with descriptions of five new species. *Phytotaxa*, 2013, vol. 83, no. 1, pp. 1–38. https://doi.org/10.11646/phytotaxa.83.1.1

43. Nevrova E., Petrov A. Benthic diatoms species richness at Dvuyakornaya Bay and other coastal sites of Crimea (the Black Sea) under various environments. *Mediterranean Marine Science*, 2019a, vol. 20, no. 3, pp. 506–520. https://doi.org/10.12681/mms.20319
44. Nevrova E., Petrov A. Assessment of benthic diatoms taxonomic diversity at coastal biotopes with different anthropogenic impact (Crimea, the Black Sea). *Turkish Journal of Botany*, 2019b, vol. 43, no. 5, pp. 608–618. https://doi.org/10.3906/bot-1903-43
45. Petrov A., Nevrova E. Database on Black Sea benthic diatoms (Bacillariophyta): Its use for a comparative study of diversity peculiarities under technogenic pollution impacts. In: *Ocean Biodiversity Informatics* : proceeding of the International Conference of Marine Biodiversity Data Management, Hamburg, Germany, 29 Nov. – 1 Dec., 2004 / E. Vanden Berghe, W. Appeltans, M. J. Costello, P. Pissierssens (Eds). Paris : UNESCO/IOC, VLIZ, BSH, 2007, pp. 153–165. (IOC Workshop Report ; no. 202 ; VLIZ Special Publication ; no. 37).
46. Petrov A., Nevrova E., Terletskaya A., Milyukin M., Demchenko V. Structure and taxonomic diversity of benthic diatoms assemblage in a polluted marine environment (Balaklava Bay, Black Sea). *Polish Botanical Journal*, 2010, vol. 55, no. 1, pp. 183–197.
47. Petrov A. N., Nevrova E. L. Prognostic estimation of species richness of benthic Bacillariophyta. *International Journal on Algae*, 2013, vol. 15, iss. 1, pp. 5–25. https://doi.org/10.1615/InterJAlgae.v15.i1.10
48. Petrov A. N., Nevrova E. L. Numerical analysis of the structure of benthic diatom assemblages in replicate samples (Crimea, the Black Sea). In: *Diatom Research Over Time and Space* / J. P. Kociolek, M. S. Kulikovskiy, J. Witkowski, D. M. Harwood (Eds). Stattgard, Germany : J. Cramer in der Gebruder Borntraeger Verlagsbuchhandlung, 2014, pp. 245–253. (Nova Hedwigia : Beiheft 143).
49. Rimet F., Bouchez A. Biomonitoring river diatoms: Implications of taxonomic resolution. *Ecological Indicators*, 2012, vol. 15, iss. 1, pp. 92–99. https://doi.org/10.1016/j.ecolind.2011.09.014
50. Round F. E., Crawford R. M., Mann D. G. *The Diatoms. Biology and Morphology of the Genera.* Cambridge, UK : Cambridge University Press, 1990, 747 p.
51. Ryabushko L. I., Begun A. A., Barinova S. S., Balycheva D. S. The epipsammon diatoms of Kruglaya Bay (the Black Sea). I. Centric, araphid and monoraphid. *Botanica Pacifica. A Journal of Plant Science and Conservation*, 2022, vol. 11, no. 1, pp. 87–97. https://doi.org/10.17581/bp.2022.11116
52. SAS.Planet : [program]. In: *SASGIS* : [site], 2023. URL: https://www.sasgis.org/sasplaneta/ [accessed: 10.07.2024].
53. Stenger-Kovács C., Hajnal É., Lengyel E., Buczkó K., Padisák J. A test of traditional diversity measures and taxonomic distinctness indices on benthic diatoms of soda pans in the Carpathian basin. *Ecological Indicators*, 2016, vol. 64, pp. 1–8. https://doi.org/10.1016/j.ecolind.2015.12.018
54. Tokatli C., Solak C. N., Yılmaz E. Water quality assessment by means of bio-indication: A case study of Ergene River using biological diatom index. *Aquatic Sciences and Engineering*, 2020, vol. 35, iss. 2, pp. 43–51. https://doi.org/10.26650/ASE2020646725
55. Van de Vijver B., Wetzel C. E., Ector L. Analysis of the type material of *Planothidium delicatulum* (Bacillariophyta) with the description of two new *Planothidium* species from the sub-Antarctic Region. *Fottea*, 2018, vol. 18, iss. 2, pp. 200–211. https://doi.org/10.5507/fot.2018.006

56. Warwick R. M., Clarke K. R. Taxonomic distinctness and environmental assessment. *Journal of Applied Ecology*, 1998, vol. 35, iss. 4, pp. 532–543. https://doi.org/10.1046/j.1365-2664.1998.3540523.x
57. Warwick R. M., Clarke K. R. Practical measures of marine biodiversity based on relatedness of species. *Oceanography and Marine Biology: An Annual Review*, 2001, vol. 39, pp. 201–231.
58. Warwick R. M., Ashman C. M., Brown A. R., Clarke K. R., Dowell B., Hart B., Lewis R. E., Shillabeer N., Somerfield P. J., Tapp J. F. Inter-annual changes in the biodiversity and community structure of the macrobenthos in Tees Bay and the Tees estuary, UK, associated with local and regional environmental events. *Marine Ecology Progress Series*, 2002, vol. 234, pp. 1–13. https://doi.org/10.3354/meps234001
59. Williams D. M., Morales E. A. *Pseudostaurosira medliniae* a new name for *Pseudostaurosira elliptica* (Gasse) Jung et Medlin. *Diatom Research*, 2010, vol. 25, iss. 1, pp. 225–226. https://doi.org/10.1080/0269249X.2010.9705843
60. Witkowski A., Lange-Bertalot H., Metzeltin D. *Diatom Flora of Marine Coasts. 1.* Ruggell ; Königstein : Gantner Verlag : Koeltz Scientific Books, 2000, 925 p. (Iconographia Diatomologica : Annotated Diatom Micrographs ; vol. 7: Diversity – Taxonomy – Identification / H. Lange-Bertalot (Ed.))

БЕНТОСНЫЕ ДИАТОМОВЫЕ ВОДОРОСЛИ (BACILLARIOPHYTA): РАЗНООБРАЗИЕ И ИЕРАРХИЧЕСКАЯ СТРУКТУРА ТАКСОЦЕНОВ НА РЫХЛЫХ ГРУНТАХ БУХТЫ КРУГЛАЯ (ЧЁРНОЕ МОРЕ, КРЫМ)

Е. Л. Неврова

ФГБУН ФИЦ «Институт биологии южных морей имени А. О. Ковалевского РАН»,
Севастополь, Российская Федерация
E-mail: *el_nevrova@mail.ru*

Бухта Круглая, или бухта Омега, имеет большое рекреационное значение в связи со своим внутренним расположением в регионе Севастополя, протяжённой пляжной зоной и мелководной акваторией с песчаным дном. Эти особенности определяют необходимость контроля состояния морской биоты. Целью работы стало выявление видового богатства и иерархической структуры таксоценов бентосных диатомовых водорослей (Bacillariophyta) в недостаточно изученной ранее бухте Круглая и сравнительный анализ с прибрежными биотопами Крыма, находящимися под антропогенным влиянием различного уровня. По результатам пробоотбора 2004 г. исследовано видовое богатство бентосных диатомовых водорослей бухты Круглая и проанализировано таксономическое разнообразие на основе флористических и формализованных методов с использованием индексов таксономической отличительности TaxDI (AvTD и VarTD). Выявлено 264 вида и внутривидовых таксона донных диатомовых водорослей, представленных 256 видами, 73 родами, 35 семействами, 21 порядком и 3 классами. Обнаружено 70 видов и 5 родов, ранее отмеченных нами как новые для флоры Bacillariophyta северного шельфа Чёрного моря, а также 5 видов, описанных нами ранее как новые для науки. Наибольшее сходство видового состава зарегистрировано как между биотопами с наименьшим уровнем техногенного воздействия (бухта Омега — бухта Двуякорная и бухта Омега — бухта Ласпи), так и между акваториями, сильно загрязнёнными техногенными поллютантами (Севастопольская бухта — бухта Карантинная и Севастопольская бухта — Балаклавская бухта), независимо от их удалённости и различий в гидрологических и гидрофизических условиях. Таксоцены Bacillariophyta сильно загрязнённых полигонов характеризуются невысоким богатством видов и большой долей моно- и олиговидовых ветвей вследствие редуцирования низкорезистентных к поллютантам

таксонов. Показатели AvTD превышают среднеожидаемый уровень для черноморской флоры Bacillariophyta. В условно чистых акваториях таксоцены диатомовых водорослей характеризуются высоким видовым богатством, большим количеством поливидовых ветвей и малой долей моно- и олиговидовых ветвей, агрегирующихся на разных уровнях иерархического древа. Значения AvTD находятся ниже среднеожидаемого уровня для флоры диатомовых водорослей Чёрного моря. Особенности структуры таксоценов Bacillariophyta сравниваемых полигонов обусловлены видоспецифической реакцией различных таксонов на сочетанные факторы влияния среды. Использование TaxDI при анализе таксономического разнообразия Bacillariophyta позволяет статистически достоверно оценивать состояние морских прибрежных акваторий с различным статусом загрязнения.

Ключевые слова: бухта Омега, TaxDI, видовое богатство, антропогенное воздействие

1871
ИнБЮМ – IBSS

Морской биологический журнал
Marine Biological Journal
2025, vol. 10, no. 3, pp. 67–79
https://marine-biology.ru

UDC 595.34(261.24)

SOME FEATURES OF DISTRIBUTION AND POPULATION STRUCTURE OF *PSEUDOCALANUS ACUSPES* (GIESBRECHT, 1881) (COPEPODA, CRUSTACEA) IN THE SOUTHEASTERN BALTIC SEA

© 2025 **Ju. Polunina[1], D. Kazakova[1,2], and A. Kondrashov[1]**

[1]Shirshov Institute of Oceanology of RAS, Moscow, Russian Federation
[2]Immanuel Kant Baltic Federal University, Kaliningrad, Russian Federation
E-mail: *jul_polunina@mail.ru*

Received 21.03.2024; revised 28.03.2025;
accepted 12.08.2025.

Based on plankton samples collected in the southeastern Baltic Sea (SEB) during research cruises of the Shirshov Institute of Oceanology of RAS, the occurrence, spatial distribution, and size and age structure of the key copepod species, *Pseudocalanus acuspes*, were studied. The current state of the *P. acuspes* population in the SEB remains insufficiently described. Sampling was carried out with a WP2 plankton net (Ø = 56 cm, mesh size of 100 μm) in different seasons by vertical stratified haul method. The size and age structure of the *P. acuspes* population was evaluated under microscopes, and specimens were measured from the anterior margin of the cephalothorax to the tip of the caudal rami. Quantitative indicators, especially abundance, were 10-fold higher in the early spring than in summer and autumn. There was a direct positive correlation between the species abundance and salinity of the bottom water layer in the SEB. On the slope of Gdansk Deep, the highest abundance and biomass of this crustacean were noted, while in the coastal zone (down to a depth of 30 m), the species was practically not found, with the exception of single nauplii. Features of the vertical distribution were revealed: in spring and autumn, abundance and biomass of *P. acuspes* were the highest in a water layer below the halocline upper boundary, whereas in summer, in a cold intermediate layer. In different years and seasons, its population was represented by all developmental stages: juveniles (nauplii and copepodites) and adult individuals, mainly females. The proportion of nauplii was the highest in early spring (70% on average). It indicates active reproduction during this season, at water temperature of +4…+7 °C preferred by this arctic species. The size of adult individuals ranged 1.03 to 1.63 mm, and *P. acuspes* were smaller than copepods of other reported populations inhabiting various areas of the World Ocean.

Keywords: *Pseudocalanus*, abundance, biomass, population structure, zooplankton, southeastern Baltic Sea

Planktonic copepods *Pseudocalanus* Boeck, 1873 are widely distributed in the neritic zone of Arctic and boreal waters throughout the Northern Hemisphere. Calanoids of this genus often dominate zooplankton communities and are important in pelagic ecosystems as a key food source for many commercially valuable fish. Noteworthy, there are *Pseudocalanus* species exhibiting similar morphology, and this complicates species-level identification. This difficulty is compounded by the fact that several species frequently co-occur within one water area. In many studies, researchers do not differentiate between individual species and limit identification down to the genus level to avoid confusion.

The genus *Pseudocalanus* was previously considered to comprise six species [Corkett, McLaren, 1979]. Three were reported from Eurasian waters: *Pseudocalanus elongatus* (Brady, 1865), *P. gracilis* Sars G. O., 1903, and *P. major* Sars G. O., 1900 [Brodsky et al., 1983]. Following a revision by B. W. Frost [1989], the genus is considered to cover seven species. In the Atlantic Ocean basin, five *Pseudocalanus* species have been identified; in the North Sea, two, *P. elongatus* and *P. acuspes* Giesbrecht, 1881; and in the southern Baltic Sea, *P. acuspes* alone [Frost, 1989]. The species inhabiting the Baltic Sea was classified as *P. elongatus* [Aleksandrov et al., 2009; Flinkman et al., 1998; Möllmann et al., 2000; Polunina et al., 2021; Shchuka, 2002]. Morphological studies of the Baltic Sea specimens failed to provide a definitive assessment of crustacean composition in its different areas. The genetic analysis of *Pseudocalanus* copepods in the Arkona basin of the Baltic Sea confirmed the occurrence of *P. acuspes* [Bucklin et al., 2003]. For the Bornholm basin, two species were reported: *P. elongatus* and *P. acuspes*, with the latter prevailing in abundance [Grabbert et al., 2010; Renz, 2006]. In the Gulf of Finland and the central Baltic, only the occurrence of *P. acuspes* was confirmed [Holmborn et al., 2011].

The occurrence of *P. elongatus* in the southern Baltic Sea cannot be ruled out: this species may enter the Baltic Sea from the North Sea *via* bottom water advection or surface currents driven by strong westerly and northwesterly winds, primarily autumn and winter ones. Considering the ratio of these two species in the Bornholm basin, where only 2 *P. elongatus* specimens were identified among 262 copepods examined [Grabbert et al., 2010], its proportion in the southeastern Baltic Sea (hereinafter SEB) is expected to be negligible. *P. acuspes* and *P. elongatus* are morphologically and morphometrically similar. In the North Sea and the Arkona and Bornholm basins of the Baltic Sea, differentiating characteristics cover their reproductive timing, number of generations, egg production rates, *etc.* [Renz, 2006; Renz et al., 2007, 2008].

Contemporary data on *P. acuspes* population structure, sizes, and spatial distribution in SEB are still scarce. The aim of this work is to reveal features of *Pseudocalanus acuspes* horizontal and vertical distribution and describe its population structure in SEB.

MATERIAL AND METHODS

Material was sampled during research cruises conducted by the Shirshov Institute of Oceanology of RAS: the 135th cruise of the RV "Professor Shtokman," 03.04.2017–07.04.2017; the 48th cruise of the RV "Akademik Boris Petrov," 01.11.2021–11.11.2021; and the 61st cruise of the RV "Akademik Ioffe," 28.06.2022–12.07.2022. The study area encompassed both open-sea area (depths down to 110 m) and the coastal zone (depths < 30 m) within the exclusive economic zone of Russia, in SEB (Fig. 1).

Water temperature and salinity were measured by multiparameter probes Idronaut Ocean Seven 316S Plus and Sea & Sun CTD 90Mc having similar characteristics. At each station, while selecting zooplankton sampling layers, vertical profiles of several hydrological parameters were obtained with the CTD to determine positions of the thermocline and halocline.

Zooplankton was sampled during daylight hours with a WP2 plankton net (Ø = 56 cm, mesh size of 100 μm). The sampling strategies differed between the years. In 2017, sampling covered the following layers: 1) the upper mixed layer (hereinafter UML) (from the upper boundary of the thermocline to the surface); 2) the layer from the upper boundary of the halocline to the surface; 3) the layer from the bottom to the surface (full-depth haul). In 2021 and 2022, samples were taken

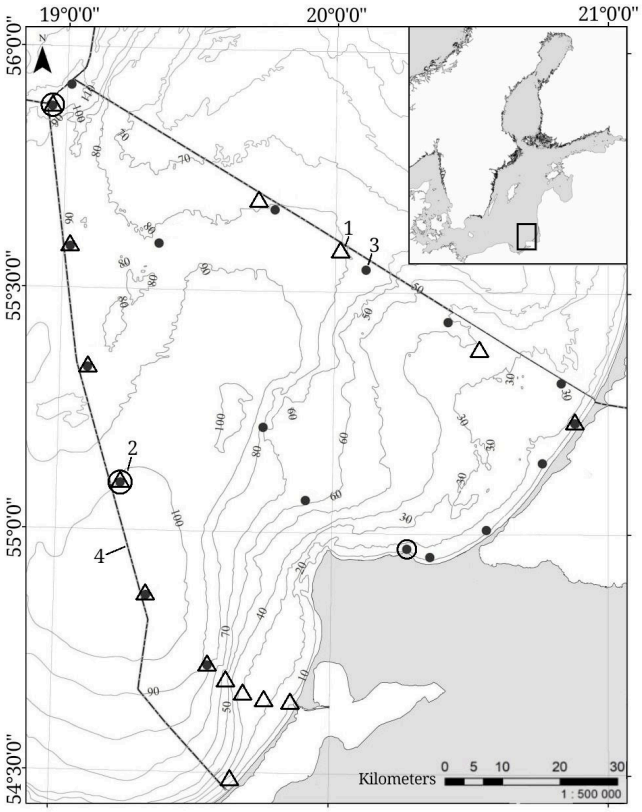

Fig. 1. Zooplankton sampling stations in the southeastern Baltic Sea. The research area is highlighted on the Baltic Sea map in the upper right corner. 1, stations in April 2017; 2, stations in July 2022; 3, stations in November 2021; 4, the borders of the exclusive economic zone of Russia

with a plankton catcher from the following layers: 1) UML; 2) the intermediate layer (from the upper boundary of the thermocline to the upper boundary of the halocline); 3) the layer below the halocline (from the bottom to the upper boundary of the halocline). Samples were preserved in a 4% formaldehyde solution. Their subsequent laboratory processing and statistical analysis followed standard procedures [Metodicheskie rekomendatsii, 1984]; biomass of copepods was calculated using length–weight regressions [Recommendations on Methods, 1985; Vinogradov, Shushkina, 1987]. In total, 77 samples were processed: 37 in 2017, 33 in 2021, and 7 in 2022.

To analyze *P. acuspes* size and age structure, 360 ind. were examined and classified into nauplii, copepodites (early ones, stages I–III; late ones, stages IV–V), and mature females and males. All specimens were measured under microscopes MBS-10 (Russia) at ×32 magnification and Olympus CX41 (Japan) at ×100 magnification. Total length of copepodites and adults was measured from the anterior end of the cephalosome to the posterior end of the urosome, excluding the caudal setae.

Data analysis involved MS Office Excel 2010 and SPSS Statistics 23.0. Spearman's rank correlation coefficient (R) was calculated, and one-way analysis of variance (ANOVA) was performed to compare size and age groups across all seasons and years. Chaddock scale was applied to evaluate the strength (the tightness) of correlations. Distribution maps were built in CorelDRAW Standard 2020 based on a map constructed in ArcGIS.

RESULTS

Hydrological conditions. In SEB waters, the upper layer began to warm in spring, and at depths of 10–20 m, a seasonal thermocline and UML were formed (Fig. 2). Water temperature in UML ranged within +4.2…+7.1 °C averaging +5.2 °C: this is indicative of the early spring biological season (winter-to-spring transition). The highest temperatures were recorded near the shore. The cold intermediate layer (hereinafter CIL) occurred at depths of 16–55 m, with the core at 45–46 m and water temperature of +3.4 °C. Above the halocline, water was weakly stratified. There, salinity ranged 7.2–8.7 psu (2a in Fig. 2). The upper boundary of the halocline was located at depths of 55–65 m. Within the halocline, water temperature varied +3.9 to +7.3 °C, and salinity increased with depth. On the slopes of the Gdansk Deep, near-bottom temperature and salinity were +7.5…+7.7 °C and 13.7 psu, respectively; on the slopes of the Gotland Deep, the values were of +6.8 °C and 12.4 psu.

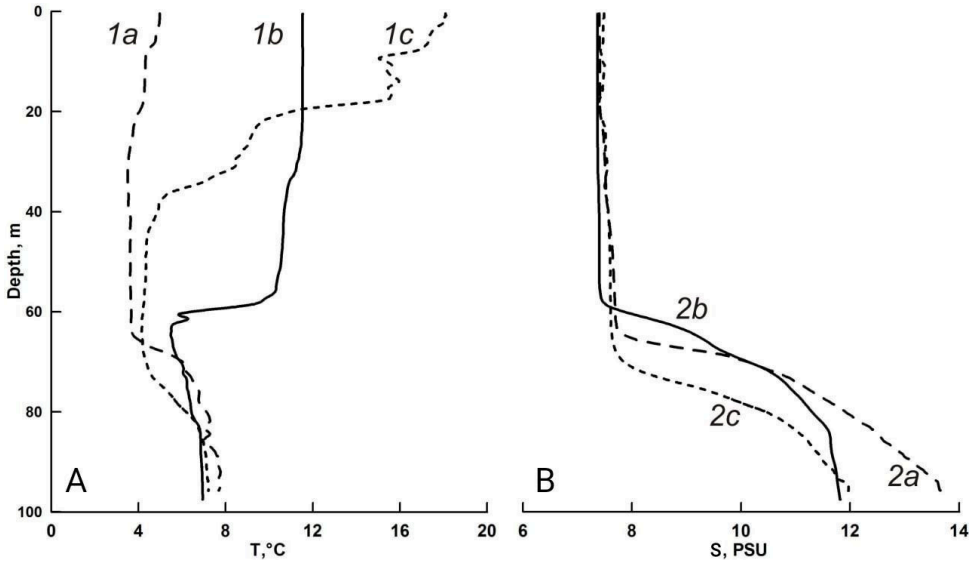

Fig. 2. Vertical distribution of thermohaline indicators on the northeastern slope of the Gdansk Deep in different seasons of the study. A, water temperature, °C; B, water salinity, psu. 1a, 2a, spring 2017; 1b, 2b, autumn 2021; 1c, 2c, summer 2022

In summer, stepped stratification was observed in the upper layer of water (Fig. 2A) suggesting the pulsed nature of the warming. The thickness of UML on the northern slope of the Gdansk Deep did not exceed 10 m; the temperature was of +18.1 °C, and salinity was of 7.5 psu. The most pronounced temperature gradients were associated with a well-defined CIL: a remnant of autumn and winter cooling. The core of CIL was located at 65 m; the water temperature was of 4.1 °C, and the salinity value was similar to that for UML, 7.6 psu. In the bottom layer, the temperature reached +6.0…+7.0 °C, and the salinity increased to 12.0 psu (2c in Fig. 2).

In autumn, cooling of UML and deepening of the seasonal thermocline down to the depth of the permanent halocline were recorded (Fig. 2). Although temperature variations within this layer were minor, a detailed analysis of the data allowed us to identify UML with a lower boundary of 35–47 m, temperature values of +9.8…+11.8 °C, and salinity of 7.1–7.4 psu. CIL was relatively thin (about 10 m); its core was located at 48–58 m, and thermohaline indicators were +4.4…+4.6 °C and 7.6–8.5 psu. The halocline depths ranged within 55–65 m, water temperature and salinity were of +5.8…+11 °C and 6.8–9.0 psu, respectively (Fig. 2). The bottom layer, from a depth of 65–75 m, had the temperature of +5.4…+6.8 °C and salinity of 9.0–11.7 psu.

On the slope of the Gdansk Deep, bottom water temperatures were consistent across all seasons and years: +7…+8 °C. Bottom salinity in April 2017 was approximately 2 psu higher than in subsequent years (Fig. 2).

Quantitative indicators and distribution patterns. Substantial seasonal variations were observed in quantitative indicators of *P. acuspes* in SEB. In spring, the abundance of this copepod ranged within 0.01–57.9 thousand ind.·m^{-3} averaging 17.1 thousand ind.·m^{-3}, *i. e.*, about 13% of the total zooplankton abundance. Its biomass ranged within 0.1–521.3 mg·m^{-3} averaging 152.4 mg·m^{-3}, *i. e.*, 21% of the total zooplankton biomass. In summer, the abundance of all *P. acuspes* stages in the open sea ranged 1.3–1.9 thousand ind.·m^{-3} (1.6 thousand ind.·m^{-3} on average), whereas the biomass ranged within 27–53 mg·m^{-3} (40 mg·m^{-3} on average). In autumn, the abundance reached a peak of 7.2 thousand ind.·m^{-3} averaging 1.4 thousand ind.·m^{-3}, *i. e.*, 13.3% of the total zooplankton abundance.

The biomass of this copepod ranged within 0.1–143.1 mg·m^{-3} averaging 32.1 mg·m^{-3}, *i. e.*, 16.6% of the total zooplankton biomass. Overall, the highest quantitative indicators for *P. acuspes* were recorded in spring. Across all seasons, this copepod comprised 13–24% of the total zooplankton abundance and 17–29% of the total zooplankton biomass in SEB; this allowed classifying the species as a subdominant one.

The analysis of *P. acuspes* spatial distribution revealed noticeable differences between the coastal zone and the open-sea area. In spring, high abundance, 13–58 thousand ind.·m^{-3}, was recorded at deep-water stations on the slopes of the Gdansk and Gotland deeps (Fig. 3A). This copepod accounted for approximately 15% of the total zooplankton abundance. In the coastal zone (at depth < 30 m), the abundance was significantly lower, 0.04–4 thousand ind.·m^{-3}, with a reduced contribution to the total zooplankton community, 2%. The coastal population of *P. acuspes* was dominated by juveniles: nauplii and early copepodites.

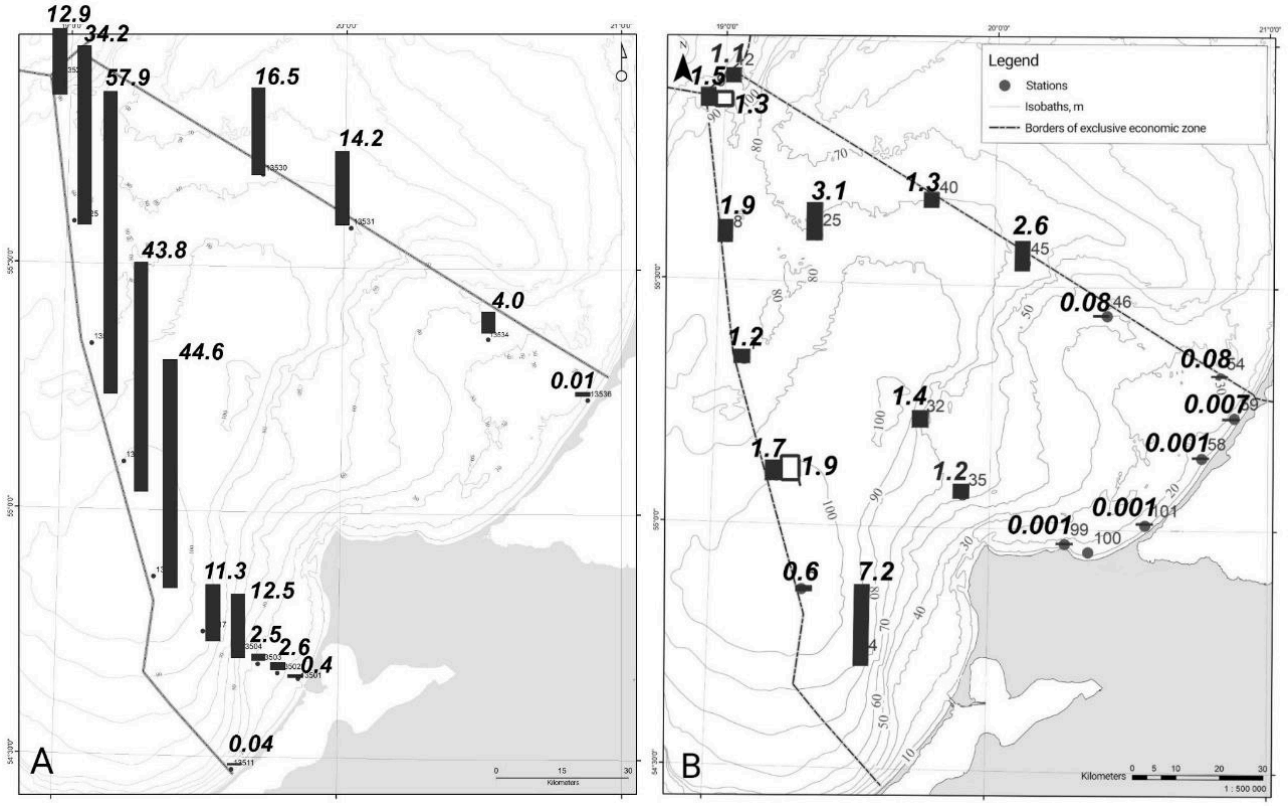

Fig. 3. Spatial distribution of *Pseudocalanus acuspes* (by abundance, thousand ind.·m^{-3}) in the southeastern Baltic Sea: A, April 2017; B, July 2022 (white columns) and November 2021 (black columns)

In summer, there were no *P. acuspes* at coastal stations. At deep-water stations in the Gdansk and Gotland deeps, the species accounted for 24% of the total zooplankton abundance and 21% of the total zooplankton biomass (Fig. 3B).

In autumn, the highest values (3.1–7.2 thousand ind.·m^{-3}) were noted at stations on the slopes of the Gdansk and Gotland deeps; *P. acuspes* constituted an average of 12% of the total zooplankton abundance. In the coastal zone, its abundance did not exceed 100 ind.·m^{-3}, and the proportion in zooplankton was only 0.2% (Fig. 3B).

The mean abundance of *P. acuspes* was more than 10 times lower in summer and autumn than in early spring.

The following features of seasonal vertical distribution were revealed: in spring and autumn, the maximum *P. acuspes* abundance and biomass were recorded in the layer below the halocline, whereas in summer, peaks were registered in CIL (Fig. 4).

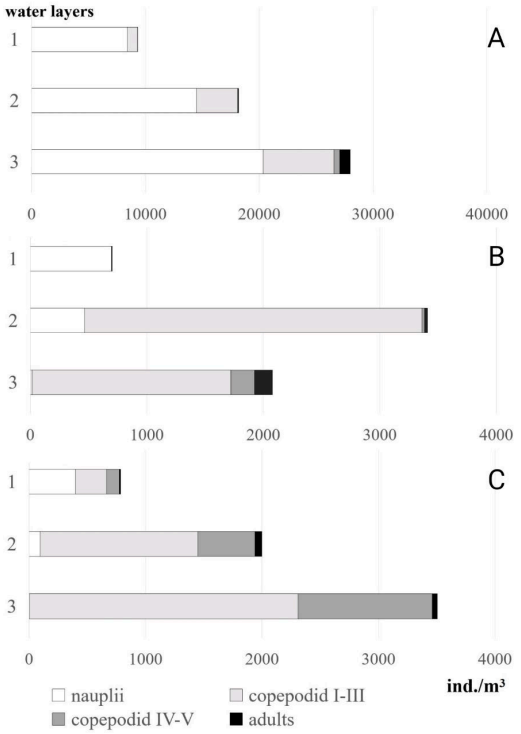

Fig. 4. The structure of *Pseudocalanus acuspes* population (by abundance, ind.·m^{-3}) in different water layers in the southeastern Baltic Sea in April 2017 (A), July 2022 (B), and November 2021 (C). A, B: 1, from the surface to the thermocline upper boundary; 2, from the surface to the halocline upper boundary; 3, from the surface to the bottom. C: 1, from the surface the thermocline upper boundary; 2, from the thermocline upper boundary to the halocline upper boundary; 3, from the halocline upper boundary to the bottom

Population structure. During the study period, the *P. acuspes* population comprised all developmental stages: nauplii, copepodites, and adult females and males. In spring, nauplii were predominant in UML (83–100%); the proportion of early copepodites did not exceed 17%, and proportions of late copepodites and adults constituted less than 1% (Fig. 4A). Throughout the water column, nauplii also prevailed accounting for 10–100% of the total population (67% on average). Proportions of early copepodites ranged within 5–41% (24% on average); late copepodites, within 0.2–11% (2% on average); and adults, within 0.6–37% (6% on average). Adult specimens consisted almost exclusively of females: the ratio was about 100% (males were exceptionally rare). In the coastal zone, the *P. acuspes* population was represented by nauplii alone (100%).

In summer, nauplii remained dominant in UML: 85 to 100% of the population (Fig. 4B). Within the thermocline, with a decrease in water temperature, the proportion of nauplii declined to 16%, while copepodites I–III reached 83% of the total population. The proportion of late copepodites and adults did not exceed 1% in these two layers. Below the upper boundary of the halocline, copepodites IV–V and adults appeared (10.5 and 8.5% on average, respectively). In this layer, the proportion of early copepodites was approximately 80%, while that of nauplii did not exceed 1% of the total abundance.

In autumn, *P. acuspes* nauplii were predominant in UML: 28 to 92% of the total population (52% on average) (Fig. 4C). The proportion of early copepodites averaged 33%, while that of the late ones was 13%. The presence of adults was recorded in this layer (approximately 3%): a phenomenon not observed

in previous seasons and likely resulting from the deepening of the thermocline and water mixing during autumn. Copepodites dominated the intermediate layer (early copepodites accounted for 47–86%, and late ones, for 12–43%); average proportions of nauplii and adults did not exceed 4%. Below the halocline peak, early copepodites prevailed: 62 to 74%. The proportion of late copepodites varied 24 to 38%, and that of nauplii did not exceed 0.3%. Adults constituted up to 3%, and females predominated (over 90%). In the coastal zone, nauplii prevailed: their proportion varied 60 to 100% (75% on average). The rest of the population consisted of early copepodites (late copepodites and adults were absent).

A significant positive correlation was found between the total species abundance and bottom water salinity in SEB across all three seasons ($R = 0.51$; $p = 0.002$; $n = 31$). In spring, when the surface water layer had not yet warmed and was cooler than the bottom layer (mean surface water temperature was +5.2 °C, and bottom water temperature was +6.0 °C), a strong positive correlation was established between the total species abundance and bottom salinity ($R = 0.70$; $p = 0.002$; $n = 15$), as well as between the total species abundance and bottom water temperature ($R = 0.60$; $p = 0.009$; $n = 15$). A feature of the *P. acuspes* vertical distribution was the fact that nauplii were highly abundant in the surface layer. Furthermore, a negative correlation was recorded between nauplii abundance and surface water temperature ($R = –0.64$; $p = 0.005$; $n = 15$). In summer, a strong positive correlation was registered between the abundance of late copepodites and adults and water salinity ($R = 0.83$; $p = 0.021$; $n = 7$). A strong negative correlation was revealed between the abundance of early copepodites and water temperature ($R = –0.87$; $p = 0.011$; $n = 7$). In autumn, there were no significant correlations between copepod abundance and thermohaline parameters in UML. Below the halocline, a negative correlation was observed between the total abundance of *P. acuspes* and bottom water temperature ($R = –0.54$; $p = 0.019$; $n = 15$), and a positive correlation was found between the total abundance and bottom salinity ($R = 0.48$; $p = 0.035$; $n = 15$).

Size structure. The population consisted of different developmental stages, with each characterized by its own size ranges. Body length of nauplii was of 0.18–0.43 mm, with the largest specimens recorded in spring (Table 1). Early copepodites (I–III) were of 0.45–0.70 mm, while late copepodites (IV–V) had the length of 0.88–1.38 mm (Table 1). Adults measured 1.01–1.63 mm. Importantly, females were significantly larger than males (Table 1), that is common for calanoids. All groups, except for early copepodites, were larger in spring than in summer and autumn.

Table 1. Mean body length and its range (in parentheses) in *Pseudocalanus acuspes* individuals of different age (mm) in April 2017, July 2022, and November 2021

Stage	April 2017	July 2022	November 2021
Nauplii	0.31 (0.20–0.43)	0.19 (0.15–0.25)	0.28 (0.18–0.38)
Copepodites I–III	0.61 (0.45–0.78)	0.81 (0.70–0.93)	0.69 (0.50–0.80)
Copepodites IV–V	1.19 (0.88–1.38)	1.10 (0.95–1.23)	0.95 (0.88–1.05)
Females	1.36 (1.20–1.63)	1.34 (1.18–1.55)	1.25 (1.03–1.49)
Males	1.25 (1.05–1.33)	1.19 (1.01–1.30)	1.24 (1.18–1.46)

Nauplii were noticeably smaller in summer than in spring and autumn ($F = 32.7$; $P < 0.001$), while sizes of spring and autumn nauplii did not differ much ($F = 32.7$; $P = 0.013$). Early copepodites were significantly smaller in spring than in summer and autumn ($F = 34.2$; $P < 0.001$). Sizes of late copepodites differed noticeably across all seasons; those were the largest in spring and the smallest

in autumn ($F = 13.0$; $P < 0.001$). In spring and summer, body lengths of females did not differ ($F = 6.2$; $P = 0.35$); in autumn, those were shorter than in spring ($F = 6.2$; $P = 0.002$), but these differences were not statistically significant ($F = 6.2$; $P = 0.098$). No noticeable differences in body length of males were established across all seasons ($F = 2.5$; $P = 0.092$).

DISCUSSION

Analysis of thermohaline conditions in SEB during our study revealed key patterns: below the halocline, the temperature in more saline layer remained stable across all seasons varying by less than 1 °C, and values of the surface salinity showed minimal fluctuations. The position and structure of the halocline varied only slightly. Strong density stratification in SEB restricts vertical water exchange and limits deep-water aeration. During the period analyzed, temperatures from the surface water layer down to the density gap (the upper boundary of the halocline) were primarily governed by convection and varied widely; temperatures below the halocline remained constant across all seasons. Vertical salinity distribution was similar in summer 2022 and autumn 2021, but different in spring 2017: bottom salinity reached 14 psu *vs.* ≤ 12 psu in other seasons. These features seem to be mediated by major inflows of North Sea water into the Baltic Sea in 2014–2016 [Naumann et al., 2016]. Such inflows are rare, but dense, oxygen-rich, and saline waters spread through Baltic Sea depressions [Matthäus et al., 2006]; apparently, this was observed in spring 2017.

P. acuspes abundance in SEB ranged 0.01 to 57.9 thousand ind.·m^{-3} during the study period. The fact that it was 13–29% of the total zooplankton abundance and biomass allowed referring the species to subdominant ones in the zooplankton community in SEB. Most specimens, particularly late copepodites and adults, occurred at depths exceeding 55 m, in the high-salinity layer, below the halocline. In contrast, the occurrence of this copepod in the coastal zone was limited to sporadic records of nauplii. So, in SEB, the highest *P. acuspes* abundance was registered deeper than 55 m.

A high proportion of juveniles, especially nauplii, was observed in spring, and this indicated active population reproduction during the season under low water temperatures (+4…+7 °C) preferred by this arctic-boreal species. The analysis of quantitative data from other Baltic Sea areas showed that the maximum values of the *P. acuspes* abundance in the Bornholm basin were reported for spring: 869 thousand ind.·m^{-3} in April 2003 and 618 thousand ind.·m^{-3} in May 2002 [Renz, 2006]. Similarly, a peak, 11 thousand ind.·m^{-3}, was recorded in the Gdansk Bay in March 2007 [Dzierzbicka-Glowacka et al., 2013]. In SEB during early spring, with water temperatures of +4…+7 °C, the abundance of this species was orders of magnitude higher than that during summer and autumn. It can be assumed that the high abundance of *P. acuspes* in spring 2017 is mediated by the inflow of North Sea water into SEB reported for 2014–2016 [Naumann et al., 2016]. A rise in bottom salinity in April 2017 seems to form specific conditions that could favorably affect the local development of the copepod. However, it cannot be excluded that individuals from the western sites of the sea were brought there with the inflow.

Analysis of data on the quantitative development of *P. acuspes* under thermohaline conditions of other water areas showed as follows. In the northern Pacific Ocean, in the Avacha Bay, this species was the dominant one across all seasons in 1988–1989 constituting 20–55% of the total copepod abundance. It was abundant in summer and autumn [Samatov, 2001], though the surface temperature fluctuated +11 to +21 °C in July–August [Potapov, 2014], and salinity varied 1 to 25 psu. The abundance of the species peaked at 32 psu in the bottom water layer [Lepskaya et al., 2014]. The Chukchi Sea is inhabited by four *Pseudocalanus* species, with *P. acuspes* comprising 50 to 90% of their total biomass.

Meanwhile, its abundance decreases in areas with water temperature higher than +10 °C [Ershova et al., 2017]. In the White Sea, two species were identified: *P. minutus* and *P. acuspes* [Markhaseva et al., 2012]. In the open White Sea, summer water temperature does not exceed +15 °C; in coastal areas, it reaches +20 °C; in winter, it drops to negative values. In the open sea, salinity is 28–30 psu, while in coastal areas, it decreases to 0–5 psu [Maksimova, Chugainova, 2014]. In the White Sea, the reproductive intensity of *P. acuspes* is the highest at +9 °C; both the reproductive rate and population production declined with the water temperature rise to +12 °C [Ershova et al., 2016]. Accordingly, the species inhabits waters with salinity from 1 to 30 psu and temperature from negative values to +20 °C.

SEB exhibits strong water stratification. Long-term data indicate that surface salinity typically ranges within 6–8 psu across all seasons, while water temperature varies within +3…+18 °C. A permanent halocline is formed at depths of 55–70 m; in the bottom water layer, salinity reaches 9–14 psu, and temperature is +3.2…+7.0 °C [Dubravin, 2017]. Thus, the salinity and temperature ranges in SEB correspond to the ranges of *P. acuspes* occurrence and reproduction.

During this study, the population comprised all age groups, including adults: both females and males. Previous research showed that in the southern Baltic Sea, only one generation of *P. acuspes* was formed within a year. The abundance of nauplii peaked in March; that of copepodites I, in May; the abundance of copepodites II, in July; and that of copepodites III–IV, in September and October. The overwintering group typically consisted of late copepodites and adults [Renz, Hirche, 2004]. In SEB, according to our data, the proportion of males was extremely low: it did not exceed 5% of the mature population in spring and summer and rose to 10% in autumn. Such a low proportion of males may be governed by their shorter lifespan: unlike females, males cease feeding upon reaching maturity [Corkett, McLaren, 1979; Renz, Hirche, 2004]. In the western Baltic Sea (the Arkona and Bornholm basins), the male-to-female ratio was 1 : 5 within April–July 2004 [Renz, Hirche, 2004]. The presence of all age stages, *inter alia* adults, allows this population in SEB to be classified as self-sustaining. More frequent sampling throughout a year is required to fully characterize the seasonal development and reproduction of the species in SEB. In spring, almost all age groups were larger than in summer and autumn. Copepods are known to exhibit pronounced seasonal and interannual variability in body size driven chiefly by key environmental factors, water temperature and food availability, both affecting the developmental duration and the growth of different age stages [Brodsky et al., 1983]. Water temperature alone can account for more than 90% of the variability in copepod growth rates [Huntley, Lopez, 1992]. Individuals are likely to grow large in spring, at low temperatures.

In SEB, body length of *P. acuspes* females ranged within 1.03–1.63 mm, while that of males, within 1.01–1.46 mm. The maximum sizes of specimens, 1.05–1.63 mm, were recorded in spring, when the temperature was low throughout the water column. In summer, in the Avacha Bay (the Pacific Ocean), *P. acuspes* adults reached 1.45–2.20 mm [Samatov, 2001], and in the White Sea, 0.95–1.81 mm [Markhaseva et al., 2012]. Thus, this copepod was the smallest in the Baltic Sea as compared to specimens of this species recorded in the other regions of the Northern Hemisphere.

P. acuspes distribution in SEB is patchy, with aggregations in terms of abundance and biomass deeper than 55–65 m in the open-sea area, where the halocline is well-developed. The smaller size of adults in the Baltic Sea than in other areas of the range of this species and low proportion of males in the population seem to result from the isolation of the Baltic population from the other ones. As hypothesized, this arctic-boreal species survived in the Baltic Sea as a component of a cold-water relict fauna, as a remnant of geological glacial processes that occurred approximately 10,000 years ago [Renz, 2006].

The hydrological conditions of the Baltic Sea and the specific ecology of *P. acuspes* have facilitated its survival at more southern latitudes, at the edge of its range. However, the revealed population structure and small size of individuals allow suggesting that the Baltic Sea population of this copepod exists under suboptimal conditions.

Conclusions:

1. Substantial interannual and seasonal variations in *Pseudocalanus acuspes* abundance and biomass were revealed in zooplankton of the southeastern Baltic Sea (SEB). On average, this species accounted for 17–29% of the total zooplankton biomass being a subdominant one in the planktonic community. In spring 2017, the quantitative indicators of *P. acuspes* were 4–10 times higher than in summer and autumn in subsequent years. This peak seemed to result from elevated near-bottom salinity which creates favorable conditions for the development of this species in the Baltic Sea.
2. In SEB, the highest abundance of *P. acuspes* was recorded on the northeastern slope of the Gdansk Deep. This species was rare in the coastal zone and primarily represented by early juvenile stages. The analysis of vertical distribution showed as follows: in spring and autumn, the maximum abundance and biomass of this copepod were registered below the upper boundary of the halocline (deeper than 55 m), while in summer, the highest value was recorded within the cold intermediate layer. A significant positive correlation was found between the total abundance of the species and the near-bottom salinity in SEB.
3. The *P. acuspes* population in SEB covered all developmental stages: nauplii, copepodites, and adults. In spring, the proportion of nauplii was the highest (70% on average) indicating active reproduction at low water temperature (it is preferable for arctic-boreal copepods). In other seasons, the population was dominated by copepodites, chiefly early one. In autumn, the proportion of older age groups increased. Adults were predominantly comprised of females (the proportion of males was low).
4. The size of adult specimens ranged within 1.01–1.63 mm, and *P. acuspes* were smaller than those reported from other water areas of the Northern Hemisphere.

The work was carried out within the framework of the state assignment of the Ministry of Education and Science of Russia for IO RAS (No. FMWE-2024-0025).

Acknowledgements. The authors are grateful to E. Ezhova, the head of the laboratory of marine ecology, for her support of this study, and to the laboratory staff for their assistance in sampling. The authors are deeply indebted to the reviewers for their valuable comments and suggestions.

REFERENCES

1. Aleksandrov S. V., Zhigalova N. N., Zezera A. S. Long-term dynamics of zooplankton in the southeastern Baltic Sea. *Biologiya morya*, 2009, vol. 35, no. 4, pp. 241–248. (in Russ.). https://elibrary.ru/owdxqb
2. Brodsky K. A., Vyshkvartseva N. V., Kos M. S., Markhaseva E. L. *Veslonogie rakoobraznye (Copepoda: Calanoida) morei SSSR i sopredel'nykh vod.* Leningrad : Nauka, 1983, 358 p. (Opredeliteli po faune SSSR, izdavaemye ZIN AN SSSR ; no. 135). (in Russ.)
3. Vinogradov M. E., Shushkina E. A. *Funktsionirovanie planktonnykh soobshchestv epipelagiali okeana.* Moscow : Nauka, 1987, 240 p. (in Russ.)
4. Dubravin V. F. *Evolution of the Thermohaline Structure of the Baltic Sea Waters* / P. P. Shirshov Institute of Oceanology RAS. Moscow : Pero, 2017, 438 p. (in Russ.). https://elibrary.ru/yagxfr
5. Ershova E. A., Kosobokova K. N., Vorobieva O. V. Changes in the egg production rate of two copepod species of the genus *Pseudocalanus*

in relation to temperature in the White Sea. *Okeanologiya*, 2016, vol. 56, no. 4, pp. 592–598. (in Russ.). https://doi.org/10.7868/S0030157416040031

6. Lepskaya E. V., Tepnin O. B., Kolomeitsev V. V., Ustimenko E. A., Sergeenko N. V., Vinogradova D. S., Sviridenko V. D., Pokhodina M. A., Schegolkova V. A., Maksimenkov V. V., Polyakova A. A., Galyamov R. S., Gorin S. L., Koval M. V. Historical review of studies of Avachinskaya Bay and principle results of complex ecological monitoring 2013. *Issledovaniya vodnykh biologicheskikh resursov Kamchatki i severo-zapadnoi chasti Tikhogo okeana*, 2014, no. 34, pp. 5–21. (in Russ.). https://elibrary.ru/stahaf
7. Maksimova M. P., Chugainova V. A. *Gidrokhimicheskii i gidrologicheskii rezhim pribrezhnoi zony Belogo morya. Marikul'tura.* Moscow : IIU MGOU, 2014, 200 p. (in Russ.). https://elibrary.ru/naedvs
8. *Metodicheskie rekomendatsii po sboru i obrabotke materialov pri gidrobiologicheskikh issledovaniyakh na presnovodnykh vodoemakh : zooplankton i ego produktsiya* / G. G. Vinberg, G. M. Lavrent'eva (Eds). Leningrad : Gos. NII ozernogo i rechnogo rybnogo khoz-va, 1984, 33 p. (in Russ.)
9. Polunina J. J., Krechik V. A., Paka V. T. Spatial variability of zooplankton and hydrological indicators of the waters of the southern and central Baltic Sea in late summer of 2016. *Okeanologiya*, 2021, vol. 61, no. 6, pp. 958–968. (in Russ.). https://doi.org/10.31857/S0030157421060113
10. Potapov V. V. Hydrological characteristics of Avachinskaya Bay. *Fundamental'nye issledovaniya*, 2014, no. 9–10, pp. 2227–2231. (in Russ.). https://elibrary.ru/socjuv
11. Shchuka T. A. *Kharakteristika sovremennogo sostoyaniya zooplanktona Baltiiskogo morya* : avtoref. dis. … kand. biol. nauk : 03.00.16. Moscow, 2002, 28 p. (in Russ.)
12. Bucklin A., Frost B., Bradford-Grieve J., Allen L., Copley N. Molecular systematic and phylogenetic assessment of 34 calanoid copepod species of the Calanidae and Clausocalanidae. *Marine Biology*, 2003, vol. 142, iss. 2, pp. 333–343. https://doi.org/10.1007/s00227-002-0943-1
13. Corkett C. J., McLaren I. A. The biology of *Pseudocalanus*. *Advances in Marine Biology*, 1979, vol. 15, pp. 1–231. https://doi.org/10.1016/S0065-2881(08)60404-6
14. Dzierzbicka-Glowacka L., Kalarus M., Janecki M., Musialik M., Mudrak S., Żmijewska M. I. Population dynamics of *Pseudocalanus minutus elongatus* in the Gulf of Gdansk (southern Baltic Sea) – experimental and numerical results. *Journal of Natural History*, 2013, vol. 47, iss. 5–12, pp. 715–738. https://doi.org/10.1080/00222933.2012.722698
15. Ershova E. A., Questel J. M., Kosobokova K., Hopcroft R. R. Population structure and production of four sibling species of *Pseudocalanus* spp. in the Chukchi Sea. *Journal of Plankton Research*, 2017, vol. 39, iss. 1, pp. 48–64. https://doi.org/10.1093/plankt/fbw078
16. Flinkman J., Aro E., Vuorinen I., Viitasalo M. Changes in northern Baltic zooplankton and herring nutrition from 1980s to 1990s: Top-down and bottom-up processes at work. *Marine Ecology Progress Series*, 1998, vol. 165, pp. 127–136. https://doi.org/10.3354/meps165127
17. Frost B. W. A taxonomy of the marine calanoid copepod genus *Pseudocalanus*. *Canadian Journal of Zoology*, 1989, vol. 67, no. 3, pp. 525–551. https://doi.org/10.1139/z89-077
18. Grabbert S., Renz J., Hirche H.-J., Bucklin A. Species-specific PCR discrimination of species of the calanoid copepod *Pseudocalanus*, *P. acuspes* and *P. elongatus*, in the Baltic and North seas. *Hydrobiologia*, 2010, vol. 652, iss. 1, pp. 289–297. https://doi.org/10.1007/s10750-010-0360-2
19. Holmborn T., Goetze E., Põllupüü M., Põllumäe A. Genetic species identification and low genetic diversity in *Pseudocalanus acuspes* of the Baltic Sea. *Journal of Plankton Research*, 2011, vol. 33, iss. 3, pp. 507–515. https://doi.org/10.1093/plankt/fbq113
20. Huntley M. E., Lopez M. D. G. Temperature-dependent production of marine copepods: A global synthesis. *The American Naturalist*, 1992, vol. 140, no. 2, pp. 201–242. https://doi.org/10.1086/285410
21. Markhaseva E. L., Abramova A. A.,

Mingazov N. D. *Pseudocalanus acuspes* (Crustacea: Copepoda) from the White Sea. *Proceedings of the Zoological Institute RAS*, 2012, vol. 316, no. 1, pp. 57–70. https://doi.org/10.31610/trudyzin/2012.316.1.57

22. Matthäus W., Nehring D., Feistel R., Nausch G., Mohrholz U., Lass H. The inflow of highly saline water into the Baltic Sea. In: *State and Evolution of the Baltic Sea, 1952–2005: A Detailed 50-year Survey of Meteorology and Climate, Physics, Chemistry, Biology, and Marine Environment* / R. Feistel, G. Nausch, N. Wasmund (Eds). Hoboken, NJ : Wiley, 2006, pp. 265–309. https://doi.org/10.1002/9780470283134.ch10
23. Möllmann C., Kornilovs G., Sidrevics L. Long-term dynamics of main mesozooplankton species in the central Baltic Sea. *Journal of Plankton Research*, 2000, vol. 22, iss. 11, pp. 2015–2038. https://doi.org/10.1093/plankt/22.11.2015
24. Naumann M., Nausch G., Mohrholz V. A succession of four major Baltic inflows in the period 2014–2016 – an overview of propagation and environmental change. In: *Multiple Drivers for Earth System Changes in the Baltic Sea Region* : proceedings of the 1st Baltic Earth Conference, 2016, pp. 13–17. (International Baltic Earth Secretariat Publication ; no. 9).
25. *Recommendations on Methods for Marine Biological Studies in the Baltic Sea. Mesozooplankton Biomass Assessment* / Working Group 14 ; L. Hernroth (Ed.). Uppsala : The Baltic Marine Biologists, 1985, 26 p. (The Baltic Marine Biologists Publ. ; no. 10).
26. Renz J. *Life Cycle and Population Dynamics of the Calanoid Copepod Pseudocalanus spp. in the Baltic Sea and North Sea* : PhD Thesis / Universität Bremen. Bremen, 2006, 134 p. https://epic.awi.de/id/eprint/15646/
27. Renz J., Hirche H.-J. Life cycle of *Pseudocalanus acuspes* in the Baltic Sea. In: *2004 ICES Annual Science Conference, Vigo, Spain*. ICES CM, 2004, L:20, pp. 1–11. https://doi.org/10.17895/ices.pub.25349554
28. Renz J., Mengedoht D., Hirche H.-J. Reproduction, growth and secondary production of *Pseudocalanus elongatus* Boeck (Copepoda, Calanoida) in the southern North Sea. *Journal of Plankton Research*, 2008, vol. 30, iss. 5, pp. 511–528. https://doi.org/10.1093/plankt/fbn016
29. Renz J., Peters J., Hirche H.-J. Life cycle of *Pseudocalanus acuspes* Giesbrecht (Copepoda, Calanoida) in the Central Baltic Sea: II. Reproduction, growth and secondary production. *Marine Biology*, 2007, vol. 151, iss. 2, pp. 515–527. https://doi.org/10.1007/s00227-006-0510-2
30. Samatov A. D. *Pseudocalanus* species (Copepoda: Calanoida) in Avachinskaya Bay, Southeastern Kamchatka. *Russian Journal of Marine Biology*, 2001, vol. 27, iss. 4, pp. 218–226. https://doi.org/10.1023/A:1011911319002

ОСОБЕННОСТИ РАСПРЕДЕЛЕНИЯ И СТРУКТУРА ПОПУЛЯЦИИ *PSEUDOCALANUS ACUSPES* (GIESBRECHT, 1881) (COPEPODA, CRUSTACEA) В ЮГО-ВОСТОЧНОЙ ЧАСТИ БАЛТИЙСКОГО МОРЯ

Ю. Ю. Полунина[1], Д. М. Казакова[1,2], А. А. Кондрашов[1]

[1]Институт океанологии имени П. П. Ширшова РАН, Москва, Российская Федерация

[2]Балтийский федеральный университет имени Иммануила Канта, Калининград, Российская Федерация

E-mail: *jul_polunina@mail.ru*

По материалам планктонных сборов, проведённых в юго-восточной части Балтийского моря (ЮВБ) на НИС Института океанологии имени П. П. Ширшова РАН, исследовали встречаемость, пространственное распределение и размерно-возрастную структуру популяции ключевого для экосистемы вида веслоногих ракообразных — *Pseudocalanus acuspes*. Современное состояние популяции *P. acuspes* в ЮВБ описано недостаточно полно. Пробы отбирали планктонной сетью WP2 (Ø = 56 см, размер ячеи 100 мкм) в разные сезоны методом вертикальных

послойных ловов. Размерно-возрастную структуру популяции *P. acuspes* оценивали с использованием микроскопов, измеряли длину особей от начала цефалоторакса до конца фуркальных ветвей. Установлено, что в ранневесенний период количественные показатели, особенно численность *P. acuspes*, были в десятки раз выше, чем летом и осенью. Выявлено наличие прямой положительной средней связи между общей численностью вида и придонной солёностью вод в ЮВБ. На склоне Гданьской впадины отмечена максимальная численность и биомасса особей, в то время как в прибрежной зоне (до глубины 30 м) этот вид практически не встречался, за исключением единичных науплиусов. Выявлены особенности вертикального распределения: в весенний и осенний периоды численность и биомасса *P. acuspes* были максимальными ниже верхней границы галоклина, тогда как летом — в холодном промежуточном слое. Популяция этого вида в разные годы и сезоны была представлена всеми возрастными стадиями — ювенильными (науплиусами и копеподитами) и взрослыми особями, преимущественно самками. Максимальная доля науплиусов отмечена ранней весной (в среднем 70 %), что указывает на активное размножение рачков при температуре воды +4…+7 °C, предпочтительной для этого аркто-бореального вида. Размеры половозрелых особей варьировали от 1,03 до 1,63 мм; рачки были мельче, чем в других районах Мирового океана.

Ключевые слова: *Pseudocalanus*, численность, биомасса, структура популяции, зоопланктон, юго-восточная часть Балтийского моря

1871
ИнБЮМ – IBSS

Морской биологический журнал
Marine Biological Journal
2025, vol. 10, no. 3, pp. 80–95
https://marine-biology.ru

UDC [594.133:575.2/.8](262.5+262.54)

GENETIC AND MORPHOLOGICAL VARIABILITY OF A BIVALVE *ANADARA KAGOSHIMENSIS* (TOKUNAGA, 1906) AS PROBABLE COMPONENTS OF ITS ADAPTIVE SUCCESS IN THE AZOV AND BLACK SEA REGION

© 2025 **E. Slynko[1,2], V. Ryabushko[2], A. Kozhara[3], I. Voroshilova[3], A. Slynko[1], A. Baimukhambetova[1], V. Pashaev[1], and A. Mironovsky[4]**

[1]Russian Biotechnological University, Moscow, Russian Federation
[2]A. O. Kovalevsky Institute of Biology of the Southern Seas of RAS, Sevastopol, Russian Federation
[3]Papanin Institute for Biology of Inland Waters Russian Academy of Sciences, Borok, Russian Federation
[4]Severtsov Institute of Ecology and Evolution, Russian Academy of Sciences, Moscow, Russian Federation
E-mail: *elena.slynko.76@mail.ru*

Received 10.09.2024; revised 31.03.2025;
accepted 12.08.2025.

An invasive population of a bivalve of the genus *Anadara* inhabiting the Kerch Strait of the Sea of Azov was investigated using methods of molecular genetics and multivariate morphometric analysis. These molluscs are highly successful invaders in the Azov–Black Sea region and have a significant effect on local biocenoses which underpins the relevance of this study. The aim of the work was to identify *Anadara* molluscs of the Kerch Strait down to the species level and analyze their genetic and phenotypic heterogeneity, with regard to their adaptability and invasion success. It was confirmed that the investigated population belongs to the species *Anadara kagoshimensis* (Tokunaga, 1906). Morphometric variability in 6 shell characters and polymorphism in a fragment of the cytochrome oxidase I gene in this population were examined. The genetic diversity in our sample appeared to be not lower than in some native populations of this species. At the same time, the analysis of morphological variations gives reason to believe that there are multiple ontogenetic channels in the individual development of the studied population of *A. kagoshimensis*. It is suggested that this condition contributed to the adaptive success of the ark shell in the Azov–Black Sea basin.

Keywords: *Anadara kagoshimensis*, cytochrome oxidase I, Black Sea, Kerch Strait, alien species, adaptation, genetic diversity

Since the second half of the 20th century, the Mediterranean basin, which includes the Sea of Azov and the Black Sea, is an arena for the mass distribution of alien molluscs. A significant part of these species is so-called Lessepsian migrants that penetrated the Mediterranean basin from the southeast *via* the Suez Canal. A prominent place in this category is occupied by *Anadara kagoshimensis* (Tokunaga, 1906): a large bivalve of the family Arcidae Lamarck, 1809, which noticeably affected benthic communities of the marine shelf during its expansion throughout the basin. This species is listed among 100 most dangerous invaders of the Mediterranean basin [Streftaris, Zenetos, 2006] and waters

of Russia [Soldatov et al., 2018]. It is mentioned along with successful invasive species: the rapa whelk *Rapana venosa* (Valenciennes, 1846), the Pacific oyster *Magallana gigas* (Thunberg, 1793), and the sand clam *Mya arenaria* Linnaeus, 1758 [Orlenko, 1994; Pereladov, 2013; Streftaris, Zenetos, 2006].

The current area of the anadara invasion outside its native range covers the Mediterranean, Marmara, and Black seas, the Sea of Azov (waters of Bulgaria, Romania, Ukraine, Russia, Georgia, and Turkey), and the Atlantic coast of Spain and France [Bañón et al., 2015]. Its introduction from the Indo-Pacific into recipient water bodies is usually associated with repeated unintentional transfer of free-swimming larvae *via* ballast water. The mollusc was first registered outside its native range in 1968 in the Black Sea [Kiseleva, 1992]; just a year later, it was recorded in the Adriatic Sea [Ghisotti, 1973]. The finds were initially identified as *Scapharca* cfr. *cornea* (Reeve, 1844) [accepted name *Anadara cornea* (Reeve, 1844)], *Scapharca inaequivalvis* (Bruguière, 1789) [accepted name *Anadara inaequivalvis* (Bruguière, 1789)], and *Cunearca cornea-inaequivalvis* [accepted name *Anadara inaequivalvis* (Bruguière, 1789)] [Ghisotti, 1973; Ghisotti, Rinaldi, 1976; Gomoiu, 1984; Ivanov, 1991; Kiseleva, 1992]. According to the results of genetic analysis [Krapal et al., 2014; Lee, Kim, 2003; Tanaka, Aranishi, 2014], molluscs noted in European waters under these species names should be attributed to *A. kagoshimensis*. However, V. Anistratenko and co-authors [2014], who studied the conchological variability of the Sea of Azov–Black Sea anadara, concluded that the nature and boundaries of these variations correspond to those of *A. inaequivalvis* from the type habitat: the Coromandel Coast (India).

Due to various adaptations, primarily to hypoxic environmental conditions, and wide ecological plasticity, this *Anadara* species can inhabit highly eutrophic waters; at the same time, the mollusc is found in areas characterized by a significant range of salinity [Anistratenko, Khaliman, 2006]. Forming settlements with high abundance and biomass, it acts as an ecosystem engineer creating the core of the consortium [Bondarev, 2020]. Already by 2013, in some areas of the Kerch Strait, the anadara has become one of the most common zoobenthic species [Revkov, 2016]. However, while competing for a substrate, *A. kagoshimensis* is capable of effective displacing of native species, chiefly representatives of the genus *Cerastoderma* Poli, 1795 [Anistratenko, Khaliman, 2006; Öztürk, 2021]. In the Azov–Black Sea basin, this species is also known to have a high morphological variability of both the shell and the soft body [Anistratenko et al., 2014; Finogenova et al., 2012].

The objectives of this work were to clarify the species affiliation and analyze the genetic and phenotypic polymorphism of this common invasive mollusc in the Azov–Black Sea basin in the context of its adaptive capabilities and invasive success.

MATERIAL AND METHODS

For molecular genetic analysis, 15 mature anadara specimens measuring 37 to 41 mm in length were sampled in the Kerch Strait in 2018. Immediately after delivery of live molluscs to a laboratory, those were removed from their shells, and samples were taken from the leg tissues fixed in 96% ethanol. Total DNA was isolated using the innuPREP DNA Mini Kit (Analytik Jena, Germany). Amplification of the mitochondrial gene fragment of the first subunit of cytochrome oxidase (COI), approximately 630 base pairs (bp), was performed using COI-4L primer (a forward one) 5’-GGTGTGTGTTTAAGATTTCACA-3’ [Lee, Kim, 2003] and HCO2198 primer (a reverse one) 5’-TAAACTTCAGGGTGACCAAAAAATCA-3’ [Folmer et al., 1994]. Ready-to-use lyophilized PCR mixtures (master mixes) for DNA amplification, in a volume of 20 μL, served as amplification mixtures.

The master mixes contained all the components required for a single reaction, including hot start Taq DNA polymerase, deoxyribonucleotides, and electrophoresis dye (manufactured by a research and production company "Genlab," Moscow, Russia). The polymerase chain reaction was carried out according to the protocol: +94 °C, 2 min 30 s; 35 cycles (+94 °C, 30 s; +58 °C, 1 min; +72 °C, 1 min; +72 °C, 10 min). PCR products were sequenced in both forward and reverse directions at "Evrogen" (Moscow). The resulting haplotypes have been deposited in the NCBI (National Center for Biotechnology Information) international database (https://www.ncbi.nlm.nih.gov/) under accession numbers MK992370 – MK992374.

The nucleotide sequences were viewed applying the MEGA6 software [Tamura et al., 2013]. To compare the sequences obtained with the sequences available in the NCBI database [2025], the BLAST program [Johnson et al., 2008] was used. Calculations of genetic variability parameters and neutrality tests [Fu, 1997; Tajima, 1989] were performed involving the DNASP 5.10 software [Librado, Rozas, 2009] and Arlequin ver 3.1 [Excoffier, Lischer, 2010].

The median network of COI haplotypes was constructed in the Network v. 10.2.0.0 program by the median joining [Bandelt et al., 1999]. During the analysis, the following *A. kagoshimensis* nucleotide sequences from the NCBI database were additionally used: MF426975 – MF426984, KM267562 – KM267563, KT266828, ON716108, AB854409 – AB854417, AB854403 – AB854408, AB854359 – AB854402, KF417435 – KF417440, KJ490940, and KJ490941. To construct the median network, all nucleotide sequences were shortened to 450 bp in accordance with the shortest fragment length presented in the international database for other invasive populations.

To analyze morphological variability in the same 15 molluscs that were used in the genetic analysis, 6 characters were measured (Fig. 1, Table 1).

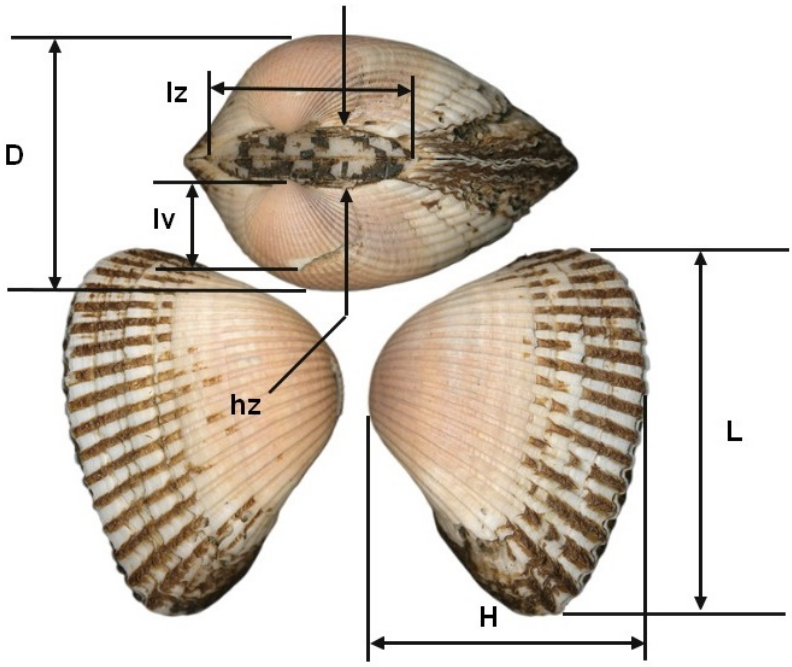

Fig. 1. Scheme of measurements of *Anadara kagoshimensis* specimens: L, shell length; H, shell height; D, shell width; lz, ligament length; hz, ligament width; lv, width of the top of the shell

Table 1. Absolute values of measurements of the characters for 15 *Anadara kagoshimensis* individuals

Specimen number	Measurements, mm					
	L	H	D	lz	hz	lv
1	41	33	28	25	4	13
2	41	32	27	21	4	9
3	40	31	28	21	5	11
4	39	32	27	23	4	11
5	40	31	26.5	20	5	9
6	38	28	26	21	4	12
7	34	28	25	17	5	10
8	40	31	26	19	5	12
9	39	31	27	20	5	11
10	38	31	27	18	4	10
11	37	29	25	19	4	11
12	39	32	28.5	23	5	13
13	37	31	24	20	4	10
14	37	30	25	19	4	12
15	38	32	27	18	5	9

Note: designation of the characters is the same as in Fig. 1.

The cluster analysis and principal component analysis (hereinafter PCA) were performed using the NTSYS 2.02k software package [Rohlf, 1998]. For the canonical discriminant analysis, including determining the probability of an individual's assignment to groups identified by the cluster analysis, the Statistica 6 package was applied. The *a priori* probability of assignment to the group was taken to be proportional to the group size. The calculations involved indices of the ratio of absolute values of measurements to the shell length (L). To assess similarity relationships among individuals, squared multidimensional Euclidean distances (E^2) were determined based on the standardized values of the indices. The cluster analysis of the matrices of morphological distances was performed by the complete linkage. In the PCA, the eigenvectors were calculated using the correlation matrix. The vector length was taken to be equal to 1. When constructing graphs illustrating the PCA results, along with the traditional technique (distribution of individuals in PC1 and PC2 coordinates), an approach known as the ontogenetic channels method was applied [Mina, 2001; Mina et al., 1996, 2010]. Its use in the analysis of the morphological diversity in ecological forms of large African barbs of the *Barbus intermedius* (sensu Banister, 1973) complex [Banister, 1973] and Altai osmans of the genus *Oreoleuciscus* Warpachowski, 1889 showed that each ecological form of the studied fish groups has its own corresponding ontogenetic channel [Mina, 2001; Mina et al., 1996; Mironovsky et al., 2014]. Later, the opposite was shown to be true: the identification of distinct ontogenetic channels in the morphological variability of individuals of a certain population may indicate high ecological plasticity of this population which can mediate the arising of morphological and ecological forms [Dgebuadze et al., 2017, 2020; Mironovsky et al., 2019].

RESULTS

Genetic diversity. In the sample of 15 analyzed specimens of the Kerch Strait anadara, for a 450-bp COI gene fragment, 5 haplotypes were identified differing by 1–2 nucleotide substitutions, which corresponds to difference levels of 0.22 and 0.44%, respectively (Fig. 2). More than half of the individuals

in the sample studied (8 specimens, or 53.3%) were carriers of the H1 haplotype (Table 2). The remaining haplotypes were represented by 1–3 specimens. The variants of nucleotide sequences that we recorded are identical to those from populations in the waters of Japan and South Korea. Two haplotypes, H3 and H4, were registered by us for the first time (Fig. 2, Table 2).

Table 2. Haplotype designations and nucleotide sequence numbers in NCBI

Haplotype	Number in NCBI	Nucleotide sequence numbers from the international database NCBI identical to those in the paper
H1	MK992371	AB854359, AB854381, AB854396, AB854379, AB854369
H2	MK992370	AB854408
H3	MK992373	–
H4	MK992372	–
H5	MK992374	AB854406, AB854370, AB854360

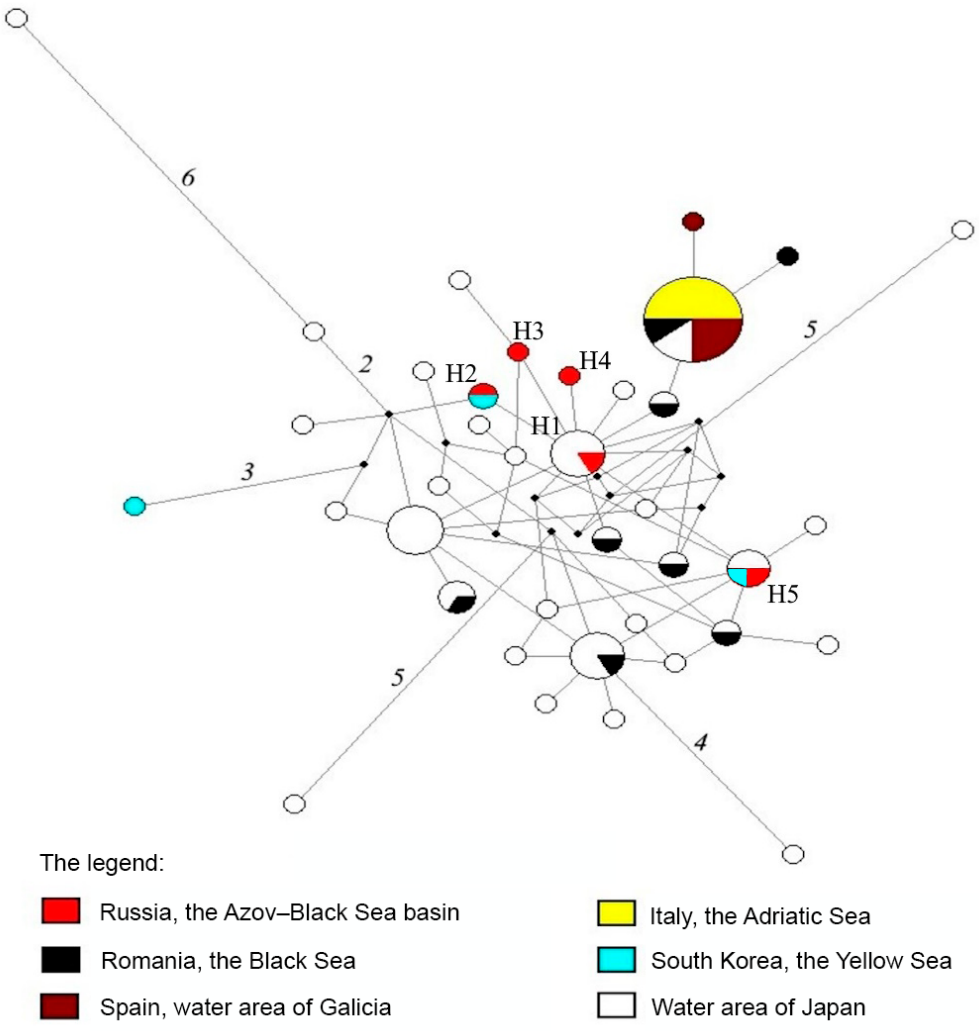

Fig. 2. Median haplotype network of the COI gene fragment (450 base pairs) of *Anadara kagoshimensis*. If the number of mutational substitutions between haplotypes exceeds 1, it is indicated above the segment connecting the haplotypes. The diameter of the circle denoting the haplotype is proportional to its frequency of occurrence. Black dots indicate median vectors – not yet discovered or disappeared sequence variants

In our sample, the nucleotide diversity and the number of haplotypes and nucleotide substitutions are somewhat lower, while the values of haplotype diversity are not lower than in several samples from native populations (Table 3).

Table 3. Indices of genetic diversity of the mitochondrial COI gene fragment in the invasive population of *Anadara kagoshimensis* of the Kerch Strait (Azov–Black Sea basin) and in samples from its native area

Population	*n*	h	Hd	π (%)	Ns
The Kerch Strait (Azov–Black Sea basin)	15	5	0.71 ± 0.11	0.16 ± 0.04	4
The Yellow Sea*	20	6	0.45 ± 0.14	0.19 ± 0.15	9
Water area of Japan*, min/max (8 samples)	14/36	7/15	0.65 ± 0.09 / 0.93 ± 0.02	0.22 ± 0.16 / 0.59 ± 0.36	7/17

Note: *n*, number of studied specimens; h, number of haplotypes; Hd, haplotypic diversity; π, nucleotide diversity; Ns, number of nucleotide substitutions between the sequences of individuals in the studied populations. *, data from [Tanaka, Aranishi, 2014].

The neutrality test values are negative, while their discrepancies with theoretically expected values are not significant ($p > 0.02$).

Morphological variability. On the dendrogram showing phenetic relationships of *A. kagoshimensis* individuals in terms of the set of considered characters, four clusters can be provisionally identified: **A**, **B**, **C**, and **D** (Fig. 3).

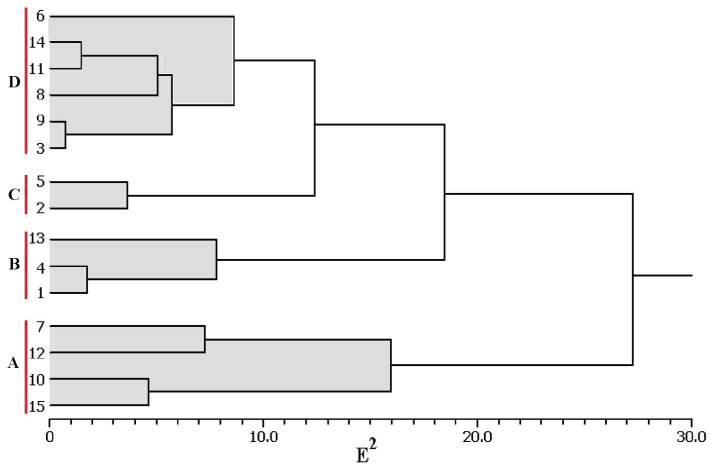

Fig. 3. A dendrogram of the similarity of *Anadara kagoshimensis* individuals of the Kerch Strait according to the set of morphological characters; 1–15, numbers of individuals; A–D, designations of clusters; E^2, squared Euclidean distance

These preliminary identified groups were subjected to the discriminant analysis. Its results showed that in the coordinates of the first two discriminant functions, individuals of the groups corresponding to four clusters of the dendrogram in Fig. 3 are clearly separated from each other (Fig. 4).

Calculations showed as follows. The posterior probability (*i. e.*, considering the determined values of the discriminant functions) of assigning each analyzed individual to a group corresponding to one of the dendrogram clusters in Fig. 3 tends to 1. The probability of erroneous assigning any individual to one of the clusters is noticeably lower than the significance level of $p = 0.05$ accepted in most biological studies (in most cases, the level of $p = 0.01$ as well) (Table 4).

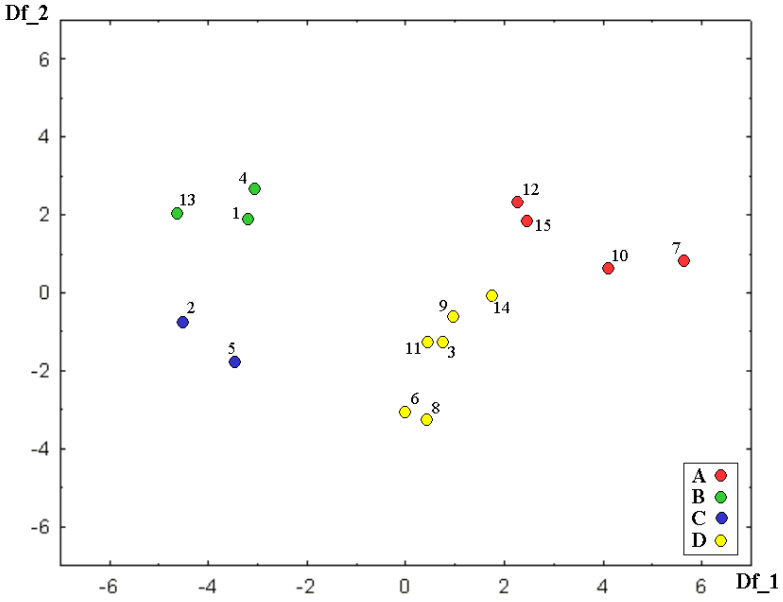

Fig. 4. Distribution of *Anadara kagoshimensis* individuals of the Kerch Strait in coordinates of the first (Df_1) and second (Df_2) discriminant functions. Numbering of individuals and group designations are the same as in Fig. 3

Table 4. Posterior probability of assigning *Anadara kagoshimensis* individuals to one of the dendrogram clusters (see Fig. 3)

Specimen of a group	Group A	Group B	Group C	Group D
A(7)	$p > 0.999$	$p < 0.001$	$p < 0.001$	$p < 0.001$
A(10)	$p > 0.999$	$p < 0.001$	$p < 0.001$	$p < 0.001$
A(12)	$p > 0.990$	$p < 0.001$	$p < 0.001$	$p = 0.003$
A(15)	$p > 0.999$	$p < 0.001$	$p < 0.001$	$p < 0.001$
B(1)	$p < 0.001$	$p > 0.999$	$p < 0.001$	$p < 0.001$
B(4)	$p < 0.001$	$p > 0.999$	$p < 0.001$	$p < 0.001$
B(13)	$p < 0.001$	$p > 0.999$	$p < 0.001$	$p < 0.001$
C(2)	$p < 0.001$	$p < 0.001$	$p > 0.999$	$p < 0.001$
C(5)	$p < 0.001$	$p < 0.001$	$p > 0.999$	$p < 0.001$
D(3)	$p < 0.001$	$p < 0.001$	$p < 0.001$	$p > 0.999$
D(8)	$p < 0.001$	$p < 0.001$	$p < 0.001$	$p > 0.999$
D(9)	$p = 0.005$	$p < 0.001$	$p < 0.001$	$p > 0.990$
D(11)	$p < 0.001$	$p < 0.001$	$p < 0.001$	$p > 0.999$
D(14)	$p = 0.013$	$p < 0.001$	$p < 0.001$	$p > 0.990$
D(6)	$p < 0.001$	$p < 0.001$	$p < 0.001$	$p > 0.999$

Note: the letters indicate the groups corresponding to the dendrogram clusters; the digits in parentheses are the numbers of the individuals.

All considered above gives good reason to assume that the division of 15 *Anadara* specimens into 4 morphologically distinct groups is not just an accident, but an objective reflection of the morphological heterogeneity of the population.

The results of the analysis of variation among the studied individuals using the PCA correspond to those described above (Fig. 5, Table 5).

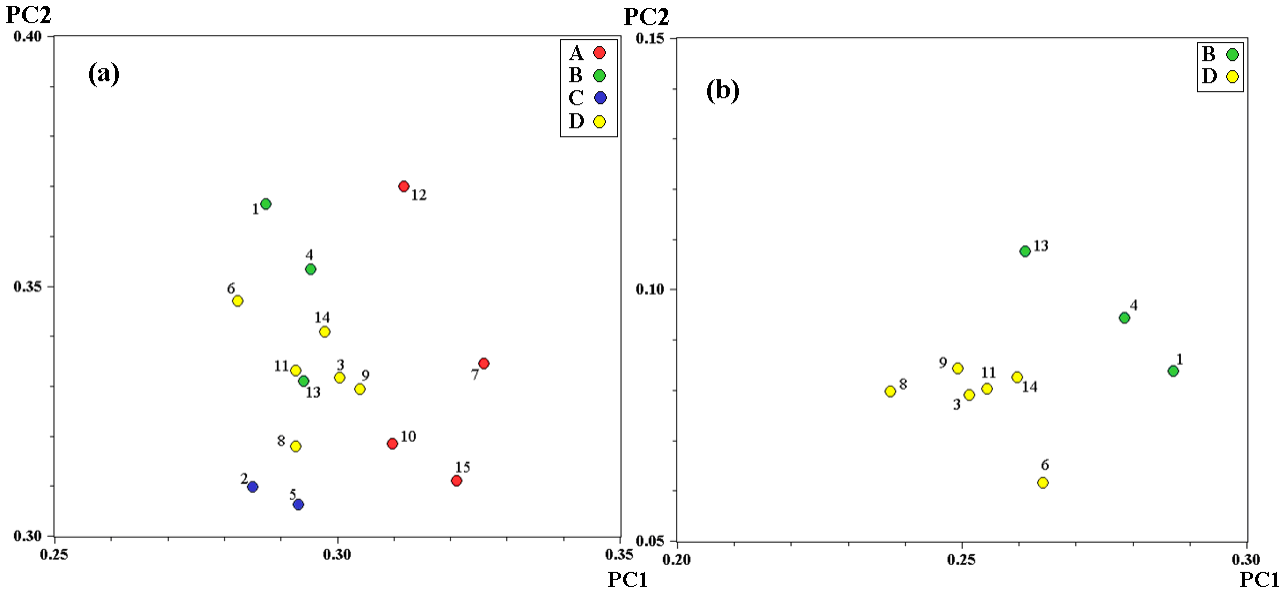

Fig. 5. Distribution of *Anadara kagoshimensis* individuals of the Kerch Strait in coordinates of the principal components: **a**, principal component analysis of 15 individuals of clusters A, B, C, and D; **b**, principal component analysis of 9 individuals of clusters B and D. Numbering of individuals and group designations are the same as in Figs 2 and 3

Table 5. Eigenvalues of the principal components and factor loadings of characters in principal component analysis of variability of *Anadara kagoshimensis* of the Kerch Strait

Character	Fig. 5a (15 specimens)		Fig. 5b (9 specimens)	
	PC1	PC2	PC1	PC2
H	0.442	0.116	0.207	0.745
D	0.607	0.301	0.175	–0.373
lz	–0.215	0.670	0.647	0.062
hz	0.625	–0.157	–0.658	–0.033
lv	0.014	0.650	0.274	–0.549
λ	1.77	1.63	2.01	1.41
Explained variance, %	35.30	32.61	40.16	28.3

Note: λ, eigenvalues of the principal components. Other designations are the same as in Figs 3–5.

Analysis of 15 specimens of the four previously identified clusters revealed that 4 specimens of cluster **A** and 2 specimens of cluster **C** are isolated from other ones (Fig. 5a). The distributions of individuals of clusters **B** and **D** overlap (see Fig. 5a). Let us, however, take into account that with incomplete separation of several sets (groups) in the coordinates of the principal components, individuals of the non-separated groups may become isolated at the next step of the analysis, when the already isolated groups are excluded from consideration. Let us exclude from analysis 4 specimens of cluster **A** and 2 specimens of cluster **C** and repeat the PCA for 9 specimens of clusters **B** and **D**. It is obvious that clusters **B** and **D** are clearly separated (Fig. 5b).

When using the discriminant analysis, one cycle of calculations was enough to sort 15 studied individuals into 4 clusters, and one graph was enough to visualize the results. When applying the PCA, two cycles and graphs were required. This fact is quite understandable if we take into account that PC1,

PC2… are the axes of the greatest variance between all individuals of the analyzed sample, without *a priori* division into groups, while the discriminant functions Df1_, Df_2… are the axes of the greatest differences between the centroids of **already specified** groups, previously identified by the cluster analysis.

For further consideration, it is important to note that two isolated clusters are clearly separated, each cluster by one of the two principal components: cluster **A**, by PC1, and cluster **C**, by PC2 (see Fig. 5a). The distributions of clusters **B** and **D** overlap both by PC1 and PC2 (see Fig. 5b). The division is clear and unambiguous only by the **combination** of the first two principal components: PC1 and PC2 (see Fig. 5b).

Thus, in the space of the considered characters, the studied specimens form 4 well-differentiated groups. Such heterogeneity can be interpreted differently reflecting several situations. One of them is a change in morphological proportions as the molluscs grow due to ontogenetic allometry. In this case, distances between clusters to one degree or another reflect the differences between individuals of various size groups. Specifically, positive allometry was revealed for the dependence of the anadara shell height and its width (convexity) on the length: $H = 0.730 \times L^{1.037 \pm 0.0184}$ and $D = 0.473 \times L^{1.103 \pm 0.022}$, respectively [Zhavoronkova, Zolotnitsky, 2014]. Although the molluscs in our sample differ little in the absolute size of their shells, this hypothesis requires verification.

Another possible situation is the presence of epigenetically determined channels (creodes) in the ontogeny of individuals of the analyzed *A. kagoshimensis* population. Creodes serve as attractors for the trajectories of individual development and are realized in the phenotype in the form of morphologically distinguishable groups of individuals. Each creode corresponds to a separate cluster.

The so-called ontogenetic channel method allows us to distinguish these two fundamentally different situations. The pattern is as follows. The values of one of the principal components reflecting the morphology of individuals are plotted on the ordinate axis (Y) of the graphs, and the parameter reflecting absolute sizes of individuals (in our case, it is the shell length, L, in mm) is plotted on the abscissa axis (X) [Mina et al., 1996]. This approach helps in estimating the ratio of differences mediated by allometric growth and differences related to polymorphism. In other words, it helps in separating differences of size groups in a single, monomorphic population from differences of morphological subunits of a polymorphic population. The results of this approach are shown in Fig. 6.

The distribution of specimens of cluster **A** along the ordinate axis (PC1) is clearly separated from the distribution of specimens of the other three clusters. So, each specimen of cluster **A** is morphologically different from all comparable-sized specimens of the other clusters of the sample (Fig. 6a).

It follows from the above that the observed isolation of 4 individuals of cluster **A** cannot be explained by the size difference: this is not allometry, but evidence of morphological subdivision of the population. The section highlighted in Fig. 6a by shading is usually considered in studies of this issue as an ‘ontogenetic channel’: a two-dimensional projection of the region of the multidimensional space of characters where individual ontogenetic trajectories are located [Mina, 2001; Mina et al., 1996]. Thus, there are grounds for a completely justified assumption that the development of individuals of cluster **A** occurs in a separate ontogenetic channel (see Fig. 6a).

Along the ordinate axis (here, it is no longer PC1, but PC2 of 15 specimens), two molluscs of cluster **C** also differ from all the same-sized ones (see Fig. 6b). The short size range and small number of individuals do not yet allow us to claim that it is an independent ontogenetic channel, but the phenetic isolation of this group can hardly be unambiguously explained by the effect of allometry.

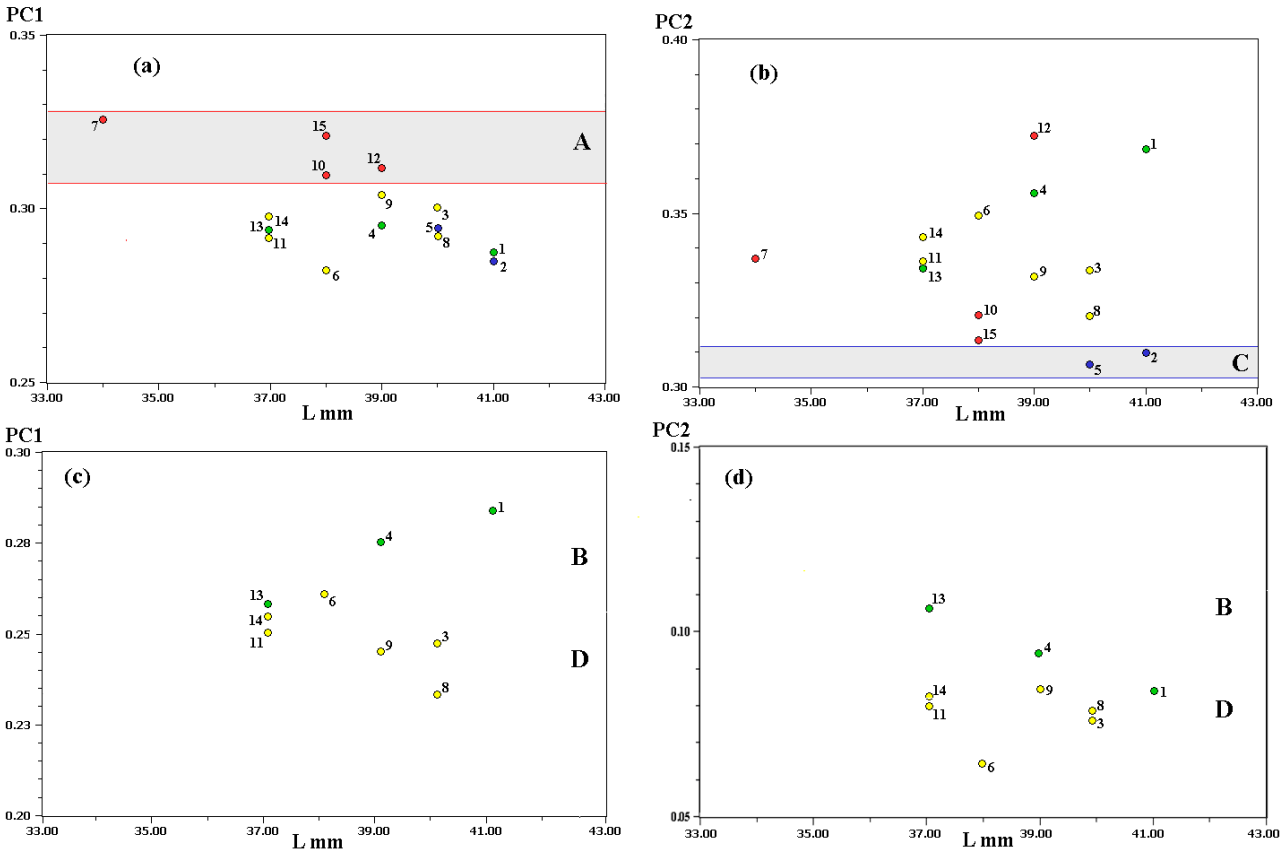

Fig. 6. Ontogenetic channels of *Anadara kagoshimensis* individuals of the Kerch Strait: **a**, individuals of cluster A, PC1 to the principal component analysis (PCA) of variability of 15 individuals of the studied sample; **b**, individuals of cluster C, PC2 to the PCA of variability of 15 individuals of the studied sample; **c**, individuals of clusters B and D, PC1 to the PCA of variability of 9 individuals of clusters B and D; **d**, individuals of clusters B and D, PC2 to the PCA of variability of 9 individuals of clusters B and D. Numbering of individuals and group designations are the same as in Figs 2–4

In Fig. 6c and 6d, the ordinate axes show the values of PC1 and PC2 of the PCA not for all 15 individuals studied, but only for 9 molluscs of clusters **B** and **D**. Obviously, the distributions of the compared groups slightly overlap, and, despite the almost complete coincidence of the size ranges, we would mistakenly come to a conclusion about just a tendency for the isolation of the channels analyzed. The graph in Fig. 5b helps to avoid such an error: there, clusters **B** and **D** are clearly separated, with a pronounced hiatus in the **combination** of PC1 and PC2. Thus, we do not deal with a tendency, but with a complete separation of the ontogenetic trajectories of these groups in the multidimensional space of the initial characters.

Let us summarize the results of the analysis of morphological variability:

1. Multivariate analysis of the variability of the sampled individuals shows that the studied population is heterogeneous and is divided into several clearly distinct groups based on the set of characters considered.
2. Analysis of the ratio of morphological differences of specimens of the identified groups with differences in their absolute sizes does not provide grounds for concluding that the identified differences are allometric in nature.

3. The above provides reasonable grounds to believe that there are several ontogenetic channels in the morphogenesis of individuals of the studied population of *A. kagoshimensis*. At the moment, the presence of such channels can be discussed at the level of a hypothesis, and its confirmation requires further research involving additional material.

DISCISSION

The presented results clearly indicate that all analyzed individuals belong to one species known both from the native range (Indo-Pacific region) and the area of invasion (waters of Spain, Italy, and Romania). The reduction in genetic diversity is not as significant as, for example, in the case of the rapa whelk and the Pacific oyster [Chandler et al., 2008; Slynko et al., 2018]. In the Azov–Black Sea basin, these invasive mollusc species (the anadara, the rapa whelk, and the Pacific oyster) have a similar origin (Indo-Pacific region), although the scenarios for their distribution are different.

In the case of the Pacific oyster, there was a deliberate introduction from the Sea of Japan and European oyster nurseries [Slynko et al., 2018]. Its low genetic diversity may be due to both intense inbreeding under mariculture conditions and the poor genetic diversity of donor populations. The low genetic diversity observed in the rapa whelk populations could be driven by the founder effect in the absence of repeated invasions. Apparently, as assumed by M. Pereladov [2013], there is a high mortality rate of both adult individuals attached to the surface of vessel bottoms and larvae in ballast water during long-term transportation.

The higher genetic diversity in the anadara invasive populations is mediated by the fact that both in the Atlantic and in the Mediterranean basin, they are permanently replenished with individuals from the native range due to the significantly increased cargo turnover with the Indochina countries [Ulman et al., 2017; Zenetos et al., 2010]. Surprisingly, the Kerch Strait sample does not contain haplotypes that are most common in populations from waters of Spain, Italy, and Romania. At the same time, there are haplotypes identical to those from the native range, but absent from the above-mentioned European populations. A relatively large number of haplotypes (13) in the Black Sea (5 in the Kerch Strait, and 8 in the waters of Romania) is likely to result from the absence of two effects, the founder one and the bottleneck one, during the invasion. The obtained data suggest that in the case of the anadara, we observe multiple expansion [Wilson et al., 2009]. However, applying the Tajima's test (*D*) and Fu's test (*Fs*) on our material, this hypothesis cannot be verified, since the test results are statistically insignificant.

Most ecological studies on the Black Sea anadara highlight stability and even prosperity of its populations [Anistratenko, Khaliman, 2006; Ivanov, 1991; Revkov, 2016; Revkov, Scherban, 2017; Zolotarev, Zolotarev, 1987]. In the area of its invasion, the mollusc demonstrates a wide range of salinity, respiratory, and trophic adaptations. A logical question arises: what ensures its adaptive success? A high level of morphological divergence of populations of this species in the northwestern Black Sea has been previously noted [Finogenova et al., 2012]. In this case, according to the classical concepts of I. Schmalhausen [1982] and A. Rasnitsyn [1987], multiple stable channels of ontogenetic development should be formed acting as attractors and ensuring pronounced morphological differentiation at the definitive stages. Apparently, this is exactly the pattern we observe when analyzing the morphological variability of the Kerch Strait anadara (the Sea of Azov). A similar pattern of subdivision by morphometric features was recently revealed for the anadara of the Black Sea and Sea of Azov [Mirzoeva, Zhukov, 2021]. The authors interpreted the clusters obtained after excluding dimensional variability as ecomorphotypes,

the formation of which contributes to more successful adaptation of molluscs to a heterogeneous environment. Despite the use of different terminology, we are likely to be talking about the same phenomenon: intrapopulation divergence related to the diversity of biotopes colonized by this species. The obtained results of the study of the anadara morphological variability are obviously preliminary and require further research.

Conclusions. Based on the analysis of the nucleotide sequences of the COI mtDNA gene fragment, it was possible to confirm that *Anadara kagoshimensis* (Tokunaga, 1906), originating from the Pacific basin, inhabits the Sea of Azov waters, namely the Kerch Strait. It is quite likely that we are dealing with repeated expansion with a classic anthropogenous type of distribution. The success of the introduction seems to be partly associated with the ability of this mollusc to form multiple trajectories of individual development in population ontogenesis, apparently corresponding to different ecological forms.

This work was carried out within the framework of IBSS state research assignment No. 124022400148-4 and 124022400152-1, IEE RAS state research assignment No. 1022061400194-8-1.6.19, and IBIW RAS state research assignment No. 124032100075-5 and 124032500016-4.

REFERENCES

1. Anistratenko V. V., Khaliman I. A. Bivalve mollusc *Anadara inaequivalvis* (Bivalvia, Arcidae) in the northern part of the Sea of Azov: Completion of colonization of the Azov – Black Sea Basin. *Vestnik zoologii*, 2006, vol. 40, no. 6, pp. 505–511. (in Russ.)
2. Bondarev I. P. Features of biocenotic relations of *Anadara kagoshimensis* (Bivalvia, Arcidae) in the Kazachya Bay of the Black Sea. *Rossiiskii zhurnal biologicheskikh invazii*, 2020, vol. 13, no. 2, pp. 10–22. (in Russ.). https://elibrary.ru/vrlyzp
3. Dgebuadze Y. Y., Mironovsky A. N., Mendsaikhan B., Slyn'ko Y. V. Rapid morphological diversification of the cyprinid fish *Oreoleuciscus potanini* (Cyprinidae) in the course of formation of a reservoir in a river of the semiarid zone. *Doklady Rossiiskoi akademii nauk. Nauki o zhizni*, 2020, vol. 490, no. 1, pp. 85–89. (in Russ.). https://doi.org/10.31857/S2686738920010060
4. Dgebuadze Y. Y., Mironovskii A. N., Mendsaikhan B., Slyn'ko Y. V. The first case of morphological differentiation of Altai osman *Oreoleuciscus potanini* (Cyprinidae, Actinopterigii) in a river. *Doklady Akademii nauk*, 2017, vol. 473, no. 2, pp. 250–253. (in Russ.). https://doi.org/10.7868/S0869565217080266
5. Zhavoronkova A. M., Zolotnitsky A. P. Characteristic of the allometric growth of bivalve mollusk anadara (*Anadara inaequivalvis*) of the Kerch Strait. *Ekosistemy, ikh optimizatsiya i okhrana*, 2014, iss. 10 (29), pp. 128–133. (in Russ.). https://elibrary.ru/tgnbrf
6. Zolotarev V. N., Zolotarev P. N. Bivalve *Cunearca cornea* – a new element of the fauna of the Black Sea. *Doklady Akademii nauk SSSR*, 1987, vol. 97, no. 2, pp. 501–502. (in Russ.)
7. Ivanov D. A. Autoacclimatization of the commercial bivalve *Cunearca cornea* in the Kerch Strait. *Biologiya morya*, 1991, no. 5, pp. 95–98. (in Russ.). https://elibrary.ru/czfivy
8. Kiseleva M. I. Sravnitel'naya kharakteristika donnykh soobshchestv u poberezh'ya Kavkaza. In: *Mnogoletnie izmeneniya zoobentosa Chernogo morya* / V. E. Zaika (Ed.). Kyiv : Naukova dumka, 1992, pp. 84–99.

(in Russ.). https://repository.marine-research.ru/handle/299011/5644

9. Mina M. V. Morphological diversification of fish as a consequence of the divergence of ontogenetic trajectories. *Ontogenez*, 2001, vol. 32, no. 6, pp. 471–476. (in Russ.). https://elibrary.ru/mpinsn
10. Mina M. V., Shkil F. N., Abdissa B. Individual ontogenetic trajectories and ontogenetic channels of three forms of large African barbs (*Barbus intermedius* complex). Analysis of experimental data. *Voprosy ikhtiologii*, 2010, vol. 50, no. 4, pp. 471–479. (in Russ.). https://elibrary.ru/mtjdpv
11. Mironovsky A. N., Dgebuadze Y. Y., Mendsaikhan B., Slyn'ko Y. V. Morphological differentiation of Altai osman *Oreoleuciscus humilis* (Cyprinidae) in the Tuin-Gol River, Lake Valley, Mongolia. *Voprosy ikhtiologii*, 2019, vol. 59, no. 1, pp. 105–109. (in Russ.). https://doi.org/10.1134/S0042875219010077
12. Mironovsky A. N., Dgebuadze Y. Y., Kas'yanov A. N., Slyn'ko Y. V. Phenetic relationships and multivariate ontogenetic channels of ecological forms of Altai osman *Oreoleuciscus potanini* (Cyprinidae) in Lake Nogon (Great Lakes Hollow, Mongolia). *Voprosy ikhtiologii*, 2014, vol. 54, no. 1, pp. 25–31. (in Russ.). https://doi.org/10.7868/S0042875214010081
13. Orlenko A. N. The acclimatization of giant oyster *Crassostrea gigas* (Bivalvia, Mytiliformes, Grassostreidae) and the principal stages of its introduction in the Black Sea. *Zoologicheskii zhurnal*, 1994, vol. 73, iss. 1, pp. 51–54. (in Russ.)
14. Pereladov M. V. Modern status and biological aspects of veined rapa whelk (*Rapana venosa*) in the north-east Black Sea. *Trudy VNIRO*, 2013, vol. 150, pp. 8–20. (in Russ.). https://elibrary.ru/tfsjnf
15. Rasnitsyn A. P. Tempy evolyutsii i evolyutsionnaya teoriya (gipoteza adaptivnogo kompromissa). In: *Evolyutsiya i biotsenoticheskie krizisy* : [sbornik statei] / L. P. Tatarinov, A. P. Rasnitsyn (Eds). Moscow : Nauka, 1987, pp. 46–64. (in Russ.)
16. Revkov N. K. Colonization's features of the Black Sea basin by recent invader *Anadara kagoshimensis* (Bivalvia: Arcidae). *Marine Biological Journal*, 2016, vol. 1, no. 2, pp. 3–17. (in Russ.). https://doi.org/10.21072/mbj.2016.01.2.01
17. Revkov N. K., Scherban S. A. The biology of the bivalve *Anadara kagoshimensis* in the Black Sea. *Ekosistemy*, 2017, iss. 9, pp. 47–56. (in Russ.). https://elibrary.ru/zxqxhz
18. Slynko Y. V., Slynko E. E., Pirkova A. V., Ladygina L. V., Ryabushko V. I Mitochondrial DNA barcoding of the Pacific oyster *Crassostrea gigas* (Thunberg, 1793) (Mollusca: Bivalvia: Ostreidae), cultivated in the Black Sea. *Genetika*, 2018, vol. 54, no. 12, pp. 1419–1425. (in Russ.) https://doi.org/10.1134/S0016675818120159
19. Soldatov A. A., Revkov N. K., Petrosyan V. G. 42. *Anadara kagoshimensis* (Tokunaga, 1906). In: *The Most Dangerous Invasive Species of Russia (Top 100)* / Yu. Yu. Dgebuadze, V. G. Petrosyan, L. A. Khlyap (Eds). Moscow : KMK Scientific Press, 2018, pp. 260–266. (in Russ.). https://elibrary.ru/rfivnx
20. Finogenova N. L., Kurakin A. P., Kovtun O. A. Morphological differentiation of *Anadara inaequivalves* (Bivalvia, Arcidae) in the Black Sea. *Gidrobiologicheskii zhurnal*, 2012, vol. 48, no. 5, pp. 3–10. (in Russ.). https://doi.org/10.1615/HydrobJ.v49.i1.10
21. Shmal'gauzen I. I. *Organizm kak tseloe v individual'nom i istoricheskom razvitii* : izbrannye trudy. Moscow : Nauka, 1982, 383 p. (in Russ.)
22. Anistratenko V. V., Anistratenko O. Yu., Khaliman I. A. Conchological variability of *Anadara inaequivalvis* (Bivalvia, Arcidae)

in the Black–Azov Sea Basin. *Vestnik zoologii*, 2014, vol. 48, no. 5, pp. 457–466.

23. Bandelt H.-J., Forster P., Röhl A. Median-joining networks for inferring intraspecific phylogenies. *Molecular Biology and Evolution*, 1999, vol. 16, iss. 1, pp. 37–48. https://doi.org/10.1093/oxfordjournals.molbev.a026036
24. Banister K. E. A revision of the large *Barbus* (Pisces, Cyprinidae) of east and central Africa. Studies on African Cyprinidae. Part 2. *Bulletin of the British Museum (Natural History). Zoology*, 1973, vol. 26, pp. 3–148. https://doi.org/10.5962/bhl.part.204
25. Bañón R., Trigo J. E., Pérez-Dieste J., Fernández J., Barros-García D., De Carlos A. Range expansion, biometric features and molecular identification of the exotic ark shell *Anadara kagoshimensis* from Galician waters, NW Spain. *Journal of the Marine Biological Association of the UK*, 2015, vol. 95, iss. 3, pp. 545–550. https://doi.org/10.1017/S0025315414002045
26. Chandler E. A., McDowell J. R., Graves J. E. Genetically monomorphic invasive populations of the rapa whelk, *Rapana venosa*. *Molecular Ecology*, 2008, vol. 17, no. 18, pp. 4079–4091. https://doi.org/10.1111/j.1365-294x.2008.03897.x
27. Folmer O., Black M., Hoeh W., Lutz R., Vrijenhoek R. DNA primers for amplification of mitochondrial cytochrome c oxidase subunit I from diverse metazoan invertebrates. *Molecular Marine Biology and Biotechnology*, 1994, vol. 3, no. 5, pp. 294–299.
28. Fu Y.-X. Statistical tests of neutrality against population growth, hitchhiking and background selection. *Genetics*, 1997, vol. 147, iss. 2, pp. 915–925. https://doi.org/10.1093/genetics/147.2.915
29. Excoffier L., Lischer H. E. L. Arlequin suite ver 3.5: A new series of programs to perform population genetics analyses under Linux and Windows. *Molecular Ecology Resources*, 2010, vol. 10, iss. 3, pp. 564–567. https://doi.org/10.1111/j.1755-0998.2010.02847.x
30. Ghisotti F. *Scapharca* cfr. *cornea* (Reeve), ospite nuova del Mediterraneo. *Conchiglie*, 1973, vol. 9, no. 3–4, pp. 1–68.
31. Ghisotti F., Rinaldi E. Osservazioni sulla popolazione di Scapharca, insediatasi in questi ultimi anni su un tratto del litorale Romagnolo. *Conchiglie*, 1976, vol. 12, no. 9–10, pp. 183–195.
32. Gomoiu M.-T. *Scapharca inaequivalvis* (Bruguière) – a new species in the Black Sea. *Cercetări marine – Recherches marines*, 1984, vol. 17, pp. 131–141.
33. Johnson M., Zaretskaya I., Raytselis Y., Merezhuk Y., McGinnis S., Madden T. L. NCBI BLAST: A better web interface. *Nucleic Acids Research*, 2008, vol. 36, suppl. 2, pp. w5–w9. https://doi.org/10.1093/nar/gkn201
34. Krapal A.-M., Popa O. P., Levarda A. F., Iorgu E. I., Costache M., Crocetta F., Popa L. O. Molecular confirmation on the presence of *Anadara kagoshimensis* (Tokunaga, 1906) (Mollusca: Bivalvia: Arcidae) in the Black Sea. *Travaux du Museum National d'Histoire Naturelle "Grigore Antipa"*, 2014, vol. 57, iss. 1, pp. 9–12. https://doi.org/10.2478/travmu-2014-0001
35. Lee S. Y., Kim S. H. Genetic variation and discrimination of Korean arkshell *Scapharca* species (Bivalvia, Arcoida) based on mitochondrial COI gene sequences and PCR-RFLP. *Korean Journal of Genetics*, 2003, vol. 25, no. 4, pp. 309–315.
36. Librado P., Rozas J. DnaSP v5: A software for comprehensive analysis of DNA polymorphism data. *Bioinformatics*, 2009, vol. 25, iss. 11, pp. 1451–1452. https://doi.org/10.1093/bioinformatics/btp187
37. Mina M. V., Mironovsky A. N.,

Dgebuadze Yu. Yu. Morphometry of barbel of lake Tana, Ethiopia: Multivariate ontogenetic channels. *Folia Zoologica*, 1996, vol. 45, suppl. 1, pp. 109–116.

38. Mirzoeva A., Zhukov O. Conchological variability of *Anadara kagoshimensis* (Bivalvia: Arcidae) in the northern part of the Black–Azov Sea basin. *Biologia*, 2021, vol. 76, iss. 12, pp. 3671–3684. https://doi.org/10.1007/s11756-021-00844-4
39. National Center for Biotechnology Information [databases]. In: *National Library of Medicine* : [site]. Bethesda, MD, 2025. URL: https://www.ncbi.nlm.nih.gov/ [accessed: 03.01.2025].
40. Öztürk B. *Non-indigenous Species in the Mediterranean and the Black Sea* / General Fisheries Commission for the Mediterranean. Rome : FAO, 2021, 92 p. (Studies and Reviews ; no. 87). https://doi.org/10.4060/cb5949en
41. Rohlf F. J. *NTSYS-pc: Numerical Taxonomy and Multivariate Analysis System. Version 2.02. Getting Started Guide.* New York : Applied Biostatistics Inc., 1998, 43 p.
42. Streftaris N., Zenetos A. Alien marine species in the Mediterranean – the 100 'worst invasives' and their impact. *Mediterranean Marine Science*, 2006, vol. 7, no. 1, pp. 87–118. https://doi.org/10.12681/MMS.180
43. Tajima F. Statistical method for testing the neutral mutation hypothesis by DNA polymorphism. *Genetics*, 1989, vol. 123, no. 3, pp. 585–595. https://doi.org/10.1093/genetics/123.3.585
44. Tamura K., Stecher G., Peterson D., Filipski A., Kumar S. MEGA6: Molecular Evolutionary Genetics Analysis version 6.0. *Molecular Phylogenetics and Evolution*, 2013, vol. 30, iss. 12, pp. 2725–2729. https://doi.org/10.1093/molbev/mst197
45. Tanaka T., Aranishi F. Genetic variability and population structure of ark shell in Japan. *Open Journal of Marine Science*, 2014, vol. 4, no. 1, pp. 8–17. https://doi.org/10.4236/ojms.2014.41002
46. Ulman A., Ferrario J., Occhpinti-Ambrogi A., Arvanitidis C., Bandi A., Bertolino M., Bogi C., Chatzigeorgiou G., Ali Çiçek B., Deidun A., Ramos-Espla A., Koçak C., Lorenti M., Martinez-Laiz G., Merlo G., Princisgh E., Scribano G., Marchini A. A massive update of non-indigenous species records in Mediterranean marinas. *PeerJ*, 2017, vol. 5, art. no. e3954 (60 p.). https://doi.org/10.7717/peerj.3954
47. Wilson J. R. U., Dormontt E. E., Prentis P. J., Lowe A. J., Richardson D. M. Something in the way you move: Dispersal pathways affect invasion success. *Trends in Ecology and Evolution*, 2009, vol. 24, iss. 3, pp. 136–144. https://doi.org/10.1016/j.tree.2008.10.007
48. Zenetos A., Gofas S., Verlaque M., Cinar M. E., Garcia Raso J. E., Bianchi C. N., Morri C., Azzurro E., Bilecenoglu M., Froglia C., Siokou I., Violanti D., Sfriso A., San Martin G., Giangrande A., Katagan T., Ballesteros E., Ramos Espla A., Mastrototaro F., Ocana O., Zingone A., Gambi M. C., Streftaris N. Alien species in the Mediterranean Sea by 2010. A contribution to the application of European Union's Marine Strategy Framework Directive (MSFD). Part I. Spatial distribution. *Mediterranean Marine Science*, 2010, vol. 11, no. 2, pp. 381–493. https://doi.org/10.12681/mms.87

ГЕНЕТИЧЕСКАЯ И МОРФОЛОГИЧЕСКАЯ ИЗМЕНЧИВОСТЬ МОЛЛЮСКА *ANADARA KAGOSHIMENSIS* (TOKUNAGA, 1906) КАК ВЕРОЯТНЫЕ СОСТАВЛЯЮЩИЕ АДАПТИВНОГО УСПЕХА ЭТОГО ВИДА В АЗОВО-ЧЕРНОМОРСКОМ РЕГИОНЕ

Е. Е. Слынько[1,2], В. И. Рябушко[2], А. В. Кожара[3], И. С. Ворошилова[3], А. Ю. Слынько[1], А. С. Баймухамбетова[1], В. Ш. Пашаев[1], А. Н. Мироновский[4]

[1]ФГБОУ ВО «Российский биотехнологический университет (РОСБИОТЕХ)», Москва, Российская Федерация

[2]ФГБУН ФИЦ «Институт биологии южных морей имени А. О. Ковалевского РАН», Севастополь, Российская Федерация

[3]ФГБУН «Институт биологии внутренних вод имени И. Д. Папанина РАН», Борок, Российская Федерация

[4]Институт проблем экологии и эволюции имени А. Н. Северцова РАН, Москва, Российская Федерация

E-mail: *elena.slynko.76@mail.ru*

Методами молекулярно-генетического и многомерного морфометрического анализа исследована инвазийная популяция двустворчатого моллюска рода *Anadara*, обитающая в Керченском проливе Азовского моря. Моллюски этого рода являются весьма успешными вселенцами в Азово-Черноморском бассейне, оказывая значительное влияние на местные биоценозы, что определяет актуальность исследования. Задачей работы было уточнить видовую принадлежность и проанализировать генетический и фенотипический полиморфизм анадары в Керченском проливе в контексте её адаптивных возможностей и инвазионного успеха. Подтверждена принадлежность исследованной популяции к виду *Anadara kagoshimensis* (Tokunaga, 1906). Для представителей этой популяции изучена изменчивость 6 морфометрических признаков раковины и полиморфизм фрагмента гена цитохромоксидазы I. Генетическое разнообразие в исследуемой выборке оказалось не ниже, чем в некоторых нативных популяциях анадары. Анализ морфологической изменчивости даёт основания полагать, что в индивидуальном развитии особей рассматриваемой популяции *A. kagoshimensis* имеет место несколько каналов онтогенеза. Высказано предположение, что это обстоятельство способствовало адаптивному успеху анадары в Азово-Черноморском бассейне.

Ключевые слова: *Anadara kagoshimensis*, цитохромоксидаза I, Чёрное море, Керченский пролив, чужеродный вид, адаптация, генетическое разнообразие

1871
ИнБЮМ – IBSS

Морской биологический журнал
Marine Biological Journal
2025, vol. 10, no. 3, pp. 96–104
https://marine-biology.ru

UDC [504.5:665.71](262.54.04)

OIL POLLUTION IN THE KERCH STRAIT AFTER THE "VOLGONEFT" TANKER ACCIDENT IN DECEMBER 2024

© 2025 **O. Soloveva, E. Tikhonova, and K. Zaripova**

A. O. Kovalevsky Institute of Biology of the Southern Seas of RAS, Sevastopol, Russian Federation
E-mail: *zaripova_km@ibss-ras.ru*

Received 29.05.2025; revised 13.06.2025;
accepted 12.08.2025.

In December 2024, up to 4,000 tons of petroleum products entered the marine environment of the Kerch Strait as a result of an accident involving two tankers carrying fuel oil. Considering intensive shipping in the region and chronic hydrocarbon (HC) loading there, the task of determining the extent of pollution and assessing the state of waters has become urgent. The aim of this study was to evaluate the qualitative and quantitative composition of HC in the Kerch Strait waters after the accident. Sampling was carried out in spring 2025 during the 134th cruise of the RV "Professor Vodyanitsky." HC and n-alkane concentrations were determined by gas chromatography. Physicochemical parameters of waters were also assessed (pH, Eh, dissolved oxygen, temperature, and salinity). HC content ranged 0.01 to 0.27 mg·L^{-1}, with the maximum permissible concentration (0.05 mg·L^{-1}) exceeded at 6 stations out of 13. The highest values were recorded in the pre-strait area of the Black Sea. At stations with elevated HC levels, signs of biodegraded oil pollution were recorded. Physicochemical parameters of waters remained within normal limits. The distribution of n-alkanes and HC composition provide evidence for actively occurring self-purification processes.

Keywords: pollution, water, hydrocarbons, Kerch Strait, Black Sea

Oil products remain one of the key pollutants of marine ecosystems. Tanker accidents significantly contribute to their release into the marine environment [Avarii i posledstviya, 2025]. The first large-scale accident occurred in March 1957: over 120 thousand tons of oil entered waters off the coast of Great Britain as a result of the "Torrey Canyon" oil spill. The Kerch Strait is also considered to be an impact area due to intensive shipping, activity of Kavkaz and Krym ports, and the operation of the roadstead transshipment complex in the southern strait [Matishov et al., 2013]. On 11 November, 2007, during a storm, the oil tanker "Volgoneft-139" sank there with 5 thousand tons of fuel oil, and about 1.3 thousand tons entered the water area [Tikhonova et al., 2021]. The second accident occurred in 2017: the bulk carrier "Geroi Arsenala" split in two with 19 tons of diesel fuel and 1.5 tons of motor oil on board [Krushenie sukhogruza, 2020]. On 15 December, 2024, there was another shipwreck in the strait: two tankers, "Volgoneft-212" and "Volgoneft-239," both with a cargo of fuel oil, were caught in a storm. One tanker split in two, and another ran aground. This resulted in a spill of 2.4 to 4 thousand tons of fuel oil out of a total volume of 9.2 thousand tons [Yunusov, 2025].

Due to active water circulation from both the Sea of Azov and Black Sea, pollutants are relatively quickly carried beyond the strait. Currents from the Sea of Azov prevail over the Black Sea ones. River runoff is important in the formation of surge phenomena and water level fluctuations at the ends of the strait and affects the water balance of both seas [Eremeev et al., 2003; The Oil Spill Accident, 2008]. Studies provide evidence that the pre-strait area of the Black Sea is subject to the greatest pollution, while currents from the Sea of Azov mainly transport organic matter of allochthonous and autochthonous origin [Nemirovskaya et al., 2022a]. According to previously obtained data, on 13 November, 2007, the concentration of oil products in the surface water layer at the tanker wreck site was 2.5 mg·L^{-1}, *i. e.*, it reached 50 MPC (maximum permissible concentration) [Matishov et al., 2013]. It was 8 times higher than the mean content of oil products in the strait waters in 1985–1988 [Klenkin et al., 2007]. In the first months after the accident, values of 3–14 thousand MPC of oil products were recorded in water, and clots of fresh fuel oil were found in bottom sediments. By May 2008, the situation with oil pollution of the strait waters and bottom had stabilized; by August 2008, the strait was completely cleared of the consequences of the accidental fuel oil spill [Fashchuk et al., 2010].

Thus, given the high technogenic load, the issue of assessing the state of water masses of the Kerch Strait and adjacent areas of the Black Sea and Sea of Azov is of particular relevance. The aim of this work was to determine the qualitative and quantitative composition of hydrocarbons in the Kerch Strait waters after the tanker accident in December 2024.

MATERIAL AND METHODS

Water from the Kerch Strait surface layer was sampled in glass containers with a bathometer on 15–16 March, 2025 (the 134th cruise of the RV "Professor Vodyanitsky") along a grid of stations (Fig. 1). The work was carried out at a wind speed of 2.4–9.4 m·s^{-1}, wave height of 0.3–1.2 m, and air temperature of +10.1…+11.9 °C. Physical and chemical parameters of water (temperature, salinity, pH, Eh, and dissolved oxygen content) were measured with a verified portable logging multiparameter meter HI-98194 (Hanna Instruments, Germany). This tool provides measurements in the following ranges:

- temperature, 0.0 to +50.0 °C (resolution 0.1 °C, and error ±0.1 °C);
- salinity, 0.00 to 70.00 psu (resolution 0.01 psu, and error ±0.01 psu);
- pH, 0.0 to 14.0 (resolution 0.01, and error ±0.02);
- Eh (redox potential), –2,000 to +2,000 mV (resolution 0.1 mV, and error ±1.0 mV);
- dissolved oxygen, 0.00 to 50.00 mg·L^{-1} (resolution 0.01 mg·L^{-1}, and error ±0.10 mg·L^{-1}).

Extracts with hexane were prepared according to the state standard GOST R 52406-2005 directly onboard the research vessel (IBSS core facility RV "Professor Vodyanitsky"). The content of hydrocarbons (hereinafter HC) and n-alkanes in water was determined by gas chromatography on a Crystal 5000.2 chromatograph ("Chromatec," Russia) with a flame ionization detector at the IBSS core facility "Spectrometry and Chromatography." The method ensures obtaining results with an accuracy not exceeding the following values (with a confidence probability P of 0.95): at an oil product concentration 0.02 to 0.5 mg·dm^{-3} inclusive, the relative standard deviation of reproducibility is 25%, and at a concentration over 0.5 mg·dm^{-3}, 13%. To process the results, Chromatec Analytic 3.0 software was used, and absolute calibration and percentage normalization were applied. HC origin was determined based on the chromatogram character, n-alkane distribution, and biogeochemical markers. The difference in means of two samples was assessed based on box plots (MS Office Excel) with outliers showing the distribution of data by quartiles; the median and outliers were highlighted.

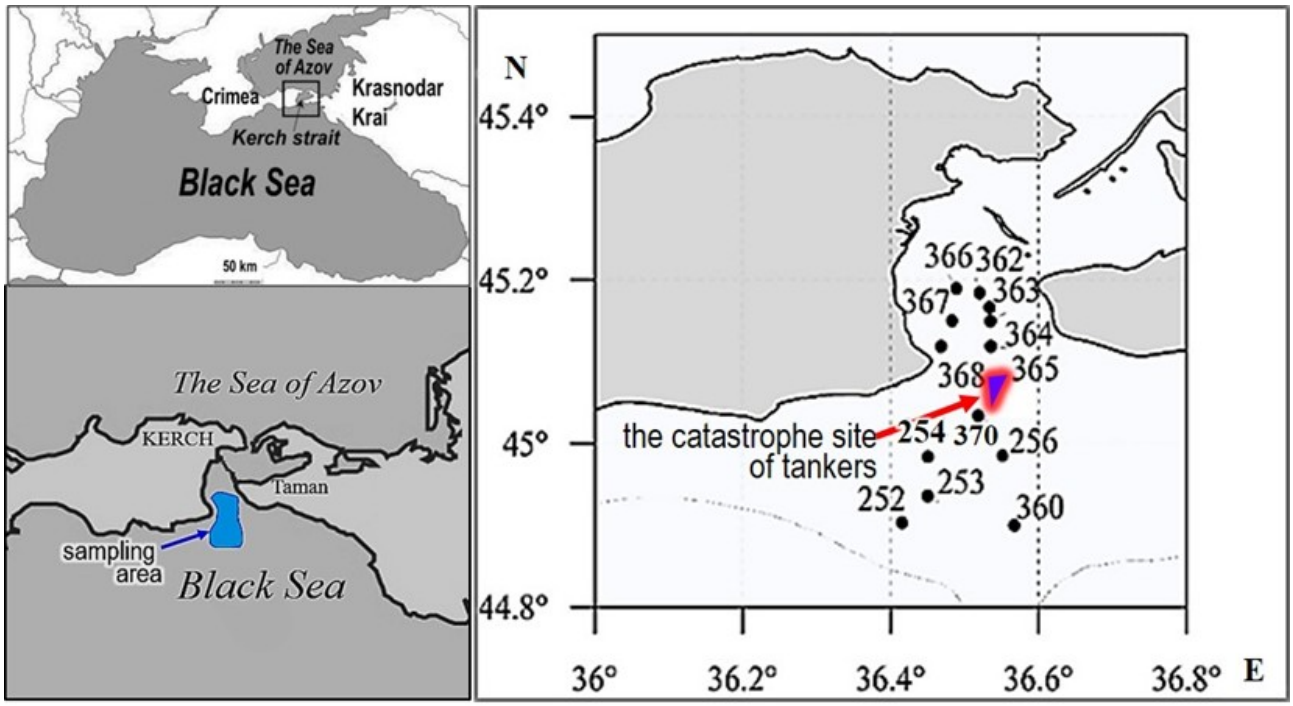

Fig. 1. Schematic map of water sampling from the surface layer in the Kerch Strait water area (the 134th cruise of the RV "Professor Vodyanitsky," March 2025)

RESULTS AND DISCUSSION

The physical and chemical parameters of water (Table 1) are sensitive indicators of pollution, including fuel oil one, and allow for the rapid detection of deviations from the natural state of seawater in the ecosystem. The values of pH in the surface layer at the stations surveyed varied 8.2 to 8.4 indicating a slight alkaline reaction of the aquatic environment. No dependence of water pH on HC concentration in it was revealed. The values of Eh varied +85 to +134 mV; this characterizes the aquatic environment as an oxidizing one. The lowest values of Eh were recorded in water of shallow stations (*e. g.*, +85 mV at sta. 366); higher values were registered at deeper stations (+134 mV at sta. 256). Oxygen saturation ranged 101 to 105%, and the concentration of dissolved oxygen ranged 9.6 to 10.9 mg·L^{-1}. The highest values (105% and 10.9 mg·L^{-1}) were revealed at sta. 366 and 367, while the minimum one, at sta. 254 (101%). Water masses of the surveyed area were characterized by saturation and slight supersaturation with oxygen. At all the stations, the content of dissolved oxygen was above the standard value of 6 mg·L^{-1}. According to the Order of the State Fisheries Committee of Russia No. 96 of 28.04.1999, this may indicate optimal aeration. In case of fuel oil pollution, a sharp decrease in these parameters is usually observed due to oxygen consumption for HC oxidation and toxic effects on phytoplankton and microfauna. In this case, the recorded levels of dissolved oxygen may indirectly evidence the lack of large-scale fuel oil pollution in water. In the surface layers, salinity varied 18.52 to 18.74 psu. These values are typical for the water area surveyed. Water temperature in the surface layer varied +8.5 to +10.0 °C. In terms of organoleptic properties, *inter alia* the absence of a film on the surface and the lack of changes in color, odor, and turbidity, no traces of fuel oil were registered in the surface water layer.

Table 1. Physical and chemical parameters of the surface water in the Kerch Strait, March 2025

Station number	t, °C	pH	Eh, mV	DO, %	DO, mg·L^{-1}	S, psu
366	+8.81	8.3	+85	104.5	10.9	18.54
362	+9.47	8.4	+88	103.9	10.6	18.67
363	+9.70	8.2	+96	102.0	9.6	18.67
364	+9.73	8.2	+102	104.4	10.5	18.73
365	+9.88	8.2	+88	103.6	10.5	18.73
368	+9.19	8.2	+103	103.5	10.6	18.69
367	+8.71	8.2	+113	105.0	10.9	18.52
252	+9.57	8.2	+100	104.8	10.7	18.74
253	+9.32	8.2	+117	102.7	10.5	18.48
254	+10.63	8.2	+132	100.5	10.3	18.60
370	+9.72	8.2	+120	101.6	10.2	18.49
256	+9.94	8.2	+134	101.2	10.2	18.65
360	+10.00	8.2	+130	101.4	10.3	18.65

Note: DO, dissolved oxygen; S, salinity.

HC concentration in the water area surveyed varied within the range of 0.01–0.27 mg·L^{-1} (Fig. 2A). At 6 stations out of 13, HC content in water exceeded the MPC (0.05 mg·L^{-1}) or was at its level. Stations with a slight excess of sanitary standards (1 to 1.6 MPC) were grouped near the western coast of the strait (Kerch area). At stations located in the eastern strait, the values were within the MPC. A significant excess was revealed at 2 stations in the pre-strait area of the Black Sea, southward of the tanker wreck site (Fig. 2A).

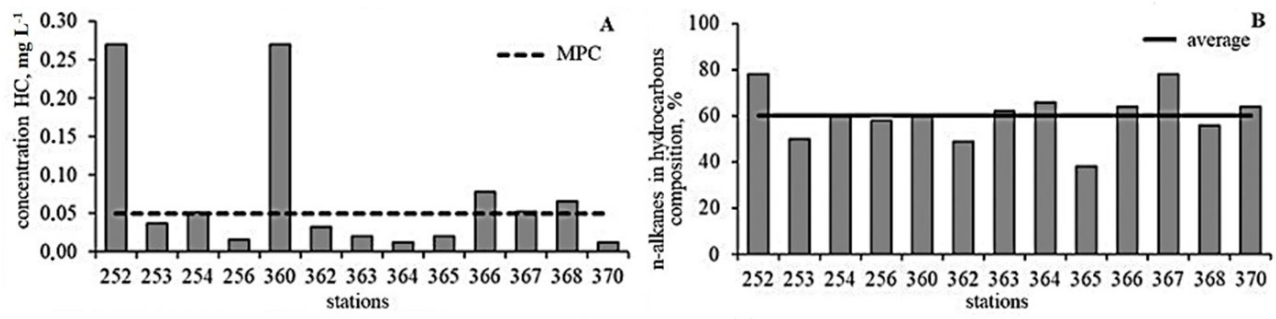

Fig. 2. Hydrocarbon concentration (A) and n-alkanes/hydrocarbons ratio (B) in the surface layer of the Kerch Strait waters (the 134th cruise of the RV “Professor Vodyanitsky,” March 2025)

In the surface water layer, the n-alkanes/hydrocarbons ratio varied 38 to 78% averaging 60% (Fig. 2B). These values are elevated and provide evidence for an intensive flow of n-alkanes into the strait water area.

Statistical analysis (Fig. 3a–c) showed the presence of outliers among the obtained values of HC concentration, unresolved complex mixture (hereinafter UCM), and n-alkanes/hydrocarbons ratio. Thus, we revealed stations with indicators significantly exceeding HC values characteristic of the water area surveyed.

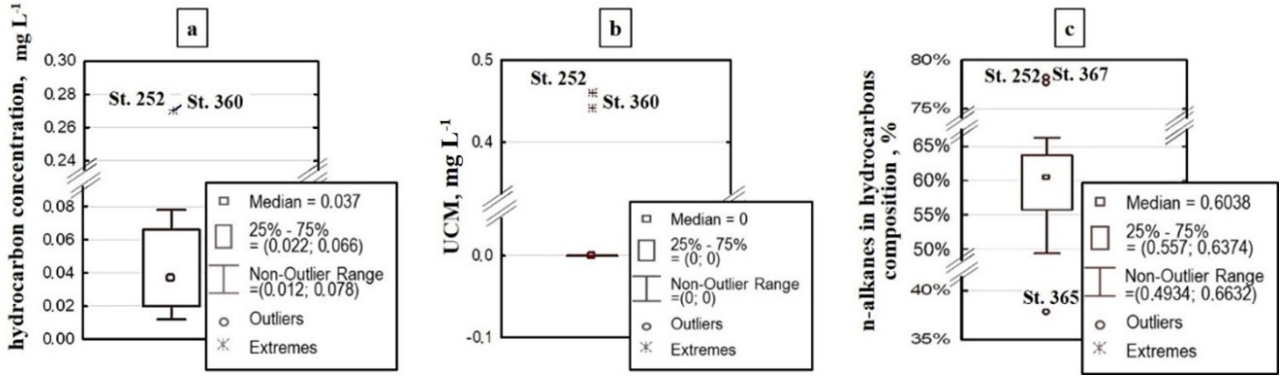

Fig. 3. Box plots showing the presence of statistical outliers in the data: a, hydrocarbon concentration; b, unresolved complex mixture (UCM); c, n-alkanes/hydrocarbons ratio

As noted above, sta. 252 and 360 were characterized by elevated HC values. At these stations, HC concentration significantly exceeded the MPC: by 5.4 times. In terms of n-alkanes/hydrocarbons ratio, elevated values were recorded at sta. 252 and 367, and reduced ones, at sta. 365 (Fig. 3c). HC content noted at other stations was typical for this area [Nemirovskaya et al., 2022a]. Furthermore, at sta. 252 and 360, UCM was determined: 0.46 and 0.44 mg·L^{-1}, respectively. The presence of UCM in water indicates oil pollution [Wang et al., 2015]. In this area, similar values were observed before (in 2019–2021): oil pollution reached 0.25 mg·L^{-1} [Nemirovskaya et al., 2022b], while the presence of UCM was not recorded at that time. There was no UCM at other sites surveyed.

UCM accumulation is also possible as a result of biodegradation of saturated oil components [Hu et al., 2018]. The "hump" on chromatograms is shifted to the high-molecular weight region (Fig. 4), which also provides evidence for the oil nature of UCM [Nemirovskaya, 2013] and, consequently, the presence of oil pollution in water.

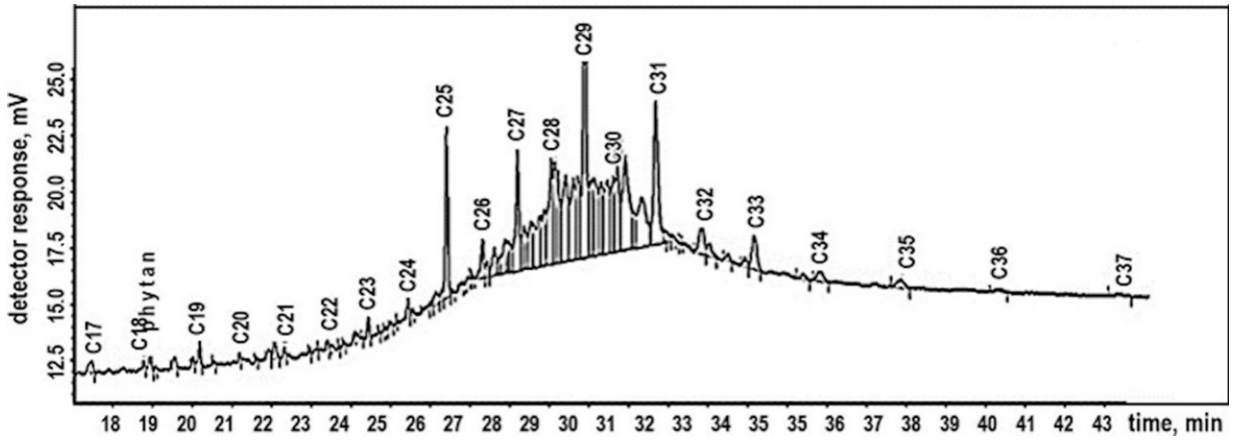

Fig. 4. Example of a chromatogram showing the presence of an unresolved complex mixture (UCM) in the surface layer of the Kerch Strait waters (sta. 360) (the 134th cruise of the RV "Professor Vodyanitsky," March 2025)

In water studied, n-alkanes were identified within the range of C_{17}–C_{37}, with C_{36} and C_{37} recorded at sta. 252 and 360. At other sites, n-alkanes were found within C_{17}–C_{35}; this range is typical for coastal waters.

Based on the data obtained, a significant difference in the content of oil products at sta. 252 and 360 was established compared to that at other stations surveyed. Due to this fact, the composition of n-alkanes was analyzed for selected groups of stations separately. The stations were divided into two groups: G1 (sta. 252 and 360) and G2 (stations 363, 365, 367, 368, 353, 352, 370, and 356). At the stations with low and moderate HC content (G2), the distribution of n-alkanes was of a bimodal character (Fig. 5a). For G2, the peaks in the low-molecular weight region fell on autochthonous C_{17} (10%) and C_{19} (8%) [Nemirovskaya, 2013]. Allochthonous n-alkanes, C_{27} (8%), C_{29} (14%), and C_{31} (13%), dominated over autochthonous ones and formed the second maximum. The revealed pattern of the distribution of n-alkanes corresponds to that in coastal waters, where natural sources of HC prevail. However, given the sampling area where chronic oil pollution was recorded (a shipping artery) [Nemirovskaya et al., 2022b], it can be assumed that in this case, traces of oil products that underwent biotransformation were also present. Thus, active self-purification processes are taking place in the studied components in waters of the Kerch Strait ecosystem.

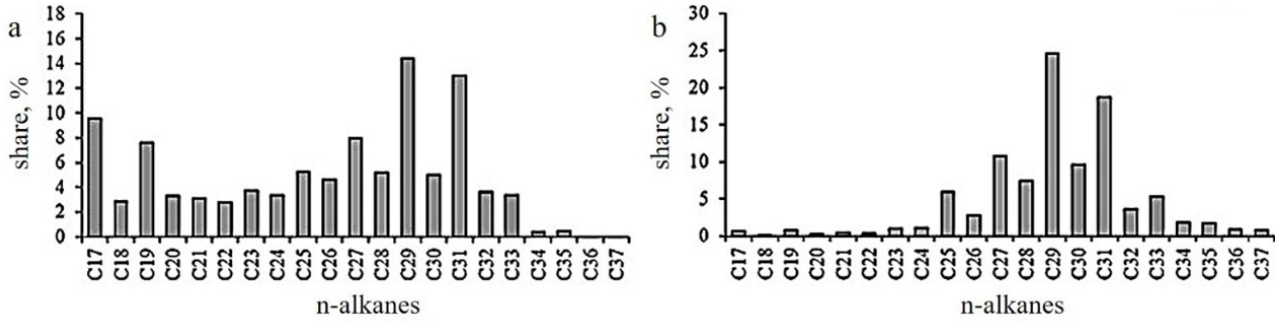

Fig. 5. Distribution of n-alkanes in water at stations with low and moderate hydrocarbon content (a) and high hydrocarbon content (b) in the Kerch Strait (the 134th cruise of the RV "Professor Vodyanitsky," March 2025)

At stations with high HC concentration (G1), the distribution of n-alkanes differed significantly from that for G2. The content of autochthonous C_{17} and C_{19} was minor (lower than 1%). The distribution was unimodal, with maximums of C_{27}, C_{29}, and C_{31} (Fig. 5b) and with a fairly high proportion of C_{28} and C_{30}. The distribution pattern is similar to that recorded in biodegraded oil aggregates [Nemirovskaya, 2013]. The distribution of n-alkanes during biodegradation was characterized by the absence of peaks in the low-molecular weight region, typical of oil pollution, and the predominance of peaks of C_{26}–C_{29}, which may indicate a high degree of HC weathering. The predominance of odd n-alkanes, typical of allochthonous matter, seems to be related to the active decomposition of even high-molecular weight homologues [Nemirovskaya, 2013]. As established before, in some cases, after oil spills, allochthonous homologues predominated in the composition of n-alkanes [Wang, Fingas, 2003].

To clarify HC origin, additional parameters were also considered, in particular, the CPI_2 marker (carbon preference index). It is the key one for revealing the presence of oil products and is described by the ratio of the number of odd homologues in the high-molecular weight region to even ones [Peters, Moldowan, 1993]. In the presence of fresh oil pollution, the marker values are close to 1. At stations of G1, its values were 2.3 and 2.8, which corresponds to those for a biogenic

substance [Ficken et al., 2000]. If we assume the influx of fuel oil, we can conclude as follows: its relatively light components are likely to have degraded after two months; a trace of its presence could be the "hump" on the chromatogram (see Fig. 4).

UCM/n-alkanes ratio for stations of G1 was 2.1 and 2.75 (> 2), and this is typical for degraded oil products [Shirneshan et al., 2016]. As already noted, the "hump" is shifted to the high-molecular weight region and is located under the dominant peaks; it is typical for oil pollution.

Based on the nature of the chromatograms and the values of individual markers of HC origin at stations of G1, it can be assumed that elevated HC concentrations in water masses of these sites are related to the presence of biodegraded oil components.

Thus, traces of oil pollution were recorded in the Black Sea water area adjacent to the Kerch Strait. Importantly, its components were heavily biodegraded, which may indicate active self-purification processes.

Conclusions. The values of hydrocarbon (HC) concentration in the surveyed water area, the Kerch Strait, fluctuated within the range of 0.01 to 0.27 mg·L^{-1}. At 6 stations out of 13 analyzed, HC content in the surface water layer exceeded the MPC (0.05 mg·L^{-1}) or was at its level. Stations with a slight excess of sanitary standards (1–1.6 MPC) were grouped near the western coast of the strait (Kerch area). At the stations situated in the eastern Kerch Strait, the values were within the MPC. A significant excess of the MPC for the HC content was registered at two stations in the pre-strait area of the Black Sea.

At the stations with low and moderate HC pollution, the distribution pattern of n-alkanes corresponds to that in coastal waters, where natural sources of HC prevail. However, given the intensity of shipping in the sampling area, where chronic oil pollution was recorded, it can be assumed as follows: in this case, there were traces of oil products that underwent biotransformation.

At the stations with an increased HC content – in the Black Sea water area adjacent to the Kerch Strait – traces of oil pollution were revealed based on the presence of an unresolved complex mixture. The origin of this pollution remains unclear, as it is impossible to clarify the composition of the fuel oil by the methods used. Strong biodegradation of oil components was recorded, which may evidence active self-purification processes in this water area.

This work was carried out within the framework of IBSS state research assignment "Assessment of oil pollution of coastal marine waters of the Crimean Peninsula resulting from the Kerch Strait disaster in December 2024 and development of recommendations for improving coastal waters by stimulating natural self-purification processes" (No. 125050605819-8).

REFERENCES

1. *Avarii i posledstviya tankernoi perevozki mazuta (Kerchenskii proliv – 2007 g., g. Anapa – 2024 g.)* / G. G. Matishov, A. V. Kleshchenkov, V. V. Kulygin, S. V. Berdnikov. Rostov-on-Don : Izd-vo YuNTs RAN, 2025, 152 p. (in Russ.)
2. Eremeev V. N., Ivanov V. A., Ilyin Yu. P. Oceanographic conditions and ecological problems in the Kerch Strait. *Morskoj ekologicheskij zhurnal*, 2003, vol. 2, no. 3, pp. 27–40. (in Russ.). https://repository.marine-research.ru/handle/299011/717
3. *The Oil Spill Accident in the Kerch Strait: Its Effects on the Water Ecosystems* / I. G. Korpakov, S. A. Agapov (Eds). Rostov-on-Don : FSUE AzNIIRKh, 2008, 229 p. (in Russ.). https://elibrary.ru/llwdzy
4. Klenkin A. A., Pavlenko L. F., Skripnik G. V., Korpakova I. G. Characteristic of oil pollution of the Sea of Azov and regularities in its dynamics.

Vodnye resursy, 2007, vol. 34, no. 6, pp. 731–736. (in Russ.). https://elibrary.ru/ibcenb

5. Krushenie sukhogruza v Chernom more: spasateli nashli tela trekh pogibshikh. In: *RIA Novosti* : [site]. Moscow, 2020. (in Russ.). URL: https://ria.ru/incidents/20170419/1492605203.html [accessed: 12.04.2025].
6. Matishov G. G., Inzhebeikin Y. I., Savitskii R. M. The environmental and biotic impact of the oil spill in Kerch Strait in November 2007. *Vodnye resursy*, 2013, vol. 40, no. 3, pp. 259–273. (in Russ.). https://elibrary.ru/pyskph
7. Nemirovskaya I. A. *Oil in the Ocean (Pollution and Natural Flow)*. Moscow : Nauchnyi mir, 2013, 432 p. (in Russ.). https://elibrary.ru/ymmlmd
8. Nemirovskaya I. A., Khaustov A. P., Redina M. M. Distribution and genesis of hydrocarbons in water and sediments of the Kerch Strait. *Geokhimiya*, 2022a, vol. 67, no. 1, pp. 47–56. (in Russ.). https://doi.org/10.31857/S0016752522010095
9. Fashchuk D. Ya., Flint M. V., Ivanova A. A., Tkachenko Yu. Yu. Kerch Strait oil pollution by the results of 2007–2009 researches. *Izvestiya Rossiiskoi akademii nauk. Seriya geograficheskaya*, 2010, no. 4, pp. 86–97. (in Russ.). https://elibrary.ru/mtcpdd
10. Yunusov R. Razliv mazuta v Kerchenskom prolive: polnaya khronologiya katastrofy. In: *Federal Press* : [site]. Moscow, 2025. (in Russ.). URL: https://fedpress.ru/article/3372475 [accessed: 01.05.2025].
11. Ficken K. J., Li B., Swain D. L., Eglinton G. An n-alkane proxy for the sedimentary input of submerged/floating freshwater aquatic macrophytes. *Organic Geochemistry*, 2000, vol. 31, iss. 7–8, pp. 745–749. https://doi.org/10.1016/S0146-6380(00)00081-4
12. Hu S.-z., Li S.-f., Wang J.-h., Cao J. Origin of unresolved complex mixtures (UCMs) in biodegraded oils: Insights from artificial biodegradation experiments. *Fuel*, 2018, vol. 231, pp. 53–60. https://doi.org/10.1016/j.fuel.2018.05.073
13. Nemirovskaya I. A., Zavialov P. O., Khramtsova A. V. Hydrocarbon pollution in the waters and sediments of the Kerch Strait. *Marine Pollution Bulletin*, 2022b, vol. 180, art. no. 113760 (13 p.). https://doi.org/10.1016/j.marpolbul.2022.113760
14. Peters K. E., Moldowan J. M. *The Biomarker Guide: Interpreting Molecular Fossils in Petroleum and Ancient Sediments*. New Jersey : Prentice Hall, 1993, 363 p.
15. Tikhonova E. A., Soloveva O. V., Burdiyan N. V. Assessment of the pollution by organic substances of water and sea bottom sediments of the Kerch Strait and the adjacent Azov–Black Sea water area. In: *Processes in GeoMedia* – vol. 3 / T. Chaplina (Ed.). Cham, Switzerland : Springer Nature Switzerland AG, 2021, pp. 285–293. (Series : Springer Geology). https://doi.org/10.1007/978-3-030-69040-3_27
16. Shirneshan G., Bakhtiari A. R., Memariani M. Distribution and origins of n-alkanes, hopanes, and steranes in rivers and marine sediments from Southwest Caspian coast, Iran: Implications for identifying petroleum hydrocarbon inputs. *Environmental Science and Pollution Research*, 2016, vol. 23, iss. 17, pp. 17484–17495. https://doi.org/10.1007/s11356-016-6825-8
17. Wang Z., Fingas M. F. Development of oil hydrocarbon fingerprinting and identification techniques. *Marine Pollution Bulletin*, 2003, vol. 47, iss. 9–12, pp. 423–452. https://doi.org/10.1016/S0025-326X(03)00215-7
18. Wang M., Wang C., Hu X., Zhang H., He S., Lv S. Distributions and sources of petroleum, aliphatic hydrocarbons and polycyclic aromatic hydrocarbons (PAHs) in surface sediments from Bohai Bay and its adjacent river, China. *Marine Pollution Bulletin*, 2015, vol. 90, iss. 1–2, pp. 88–94.

НЕФТЯНОЕ ЗАГРЯЗНЕНИЕ КЕРЧЕНСКОГО ПРОЛИВА ПОСЛЕ АВАРИИ ТАНКЕРОВ «ВОЛГОНЕФТЬ» В ДЕКАБРЕ 2024 Г.

О. В. Соловьёва, Е. А. Тихонова, К. М. Зарипова

ФГБУН ФИЦ «Институт биологии южных морей имени А. О. Ковалевского РАН»,
Севастополь, Российская Федерация
E-mail: *zaripova_km@ibss-ras.ru*

В декабре 2024 г. в результате аварии двух танкеров, перевозивших мазут, в Керченском проливе в морскую среду поступило до 4 тыс. т нефтепродуктов. С учётом судоходного характера региона и хронической нагрузки углеводородами (УВ) актуальными задачами стали выявление масштабов загрязнения и анализ состояния воды. Цель работы — определить качественный и количественный состав УВ в воде Керченского пролива после аварии. Пробоотбор проведён весной 2025 г. в рамках 134-го рейса НИС «Профессор Водяницкий». Концентрации УВ и н-алканов определены методом газовой хроматографии. Оценены физико-химические параметры воды (pH, Eh, содержание растворённого кислорода, температура и солёность). Значения концентрации УВ колебались от 0,01 до 0,27 мг·л$^{-1}$, при этом на 6 из 13 станций была превышена ПДК (0,05 мг·л$^{-1}$). Максимальные величины зафиксированы в акватории Чёрного моря, прилегающей к проливу. На станциях с высокими уровнями содержания УВ в воде обнаружены признаки биодеградированного нефтяного загрязнения. Физико-химические показатели воды оставались в пределах нормы. Распределение н-алканов и состав УВ указывают на активно происходящие процессы самоочищения.

Ключевые слова: загрязнение, вода, углеводороды, Керченский пролив, Чёрное море

1871
ИнБЮМ – IBSS

Морской биологический журнал
Marine Biological Journal
2025, vol. 10, no. 3, pp. 105–119
https://marine-biology.ru

UDC [582.261.1:551.326.7](265.54.04)

SPECIES COMPOSITION OF THE MICROALGAL COMMUNITY IN SEA ICE AND UNDER-ICE WATER IN BAYS OF RUSSKY ISLAND (PETER THE GREAT BAY, SEA OF JAPAN)

© 2025 **E. Yurikova and A. Begun**

A. V. Zhirmunsky National Scientific Center of Marine Biology FEB RAS, Vladivostok, Russian Federation
E-mail: *komcitykat@mail.ru*

Received 22.02.2024; revised 12.04.2024;
accepted 12.08.2025.

Sea ice can serve as a habitat for microalgae which can adapt to its unique conditions and successfully reproduce in it. This paper continues the analysis of material obtained for the first time from sea ice in two bays of Russky Island (the Sea of Japan) in 2020–2021 aimed at studying layer-by-layer distribution of the qualitative and quantitative composition of inhabiting microalgae. The taxonomic analysis allowed for identifying 87 species of microalgae from 48 genera and 7 divisions. The maximum species richness was characteristic of the Bacillariophyta division (57–100% of the species number in an ice layer). Algal flora of sea ice and under-ice water was formed mainly by benthic cosmopolites. The composition of dominant species varied depending on year, bay, and depth of an ice layer; the prevailing species were *Chaetoceros socialis* f. *radians*, *Cylindrotheca closterium*, *Navicula septentrionalis*, *Nitzschia frigida*, *Thalassiosira gravida*, *T. nordenskioeldii*, and *Plagioselmis* sp. Species composition varied most significantly between years of the study. Differences in species composition were also noted between bays and biotopes, as well as depending on the position of the layer in the ice column.

Keywords: ice algal flora, diatoms, Sea of Japan

Sea ice is a combination of rather harsh ecological factors. Nevertheless, some microalgae species are capable of adapting to this environment and successfully colonizing ice thereby affecting its physical and chemical properties. In turn, the state of ice, including its thickness and breakup timing, affects the ecosystem and the productivity of the entire water area during winter and early spring. Across this period, microalgae extensively developing within ice serve as a critical source of primary production.

Peter the Great Bay (the Sea of Japan) is one of the southernmost areas in the Northern Hemisphere capable of sustaining a stable ice cover for several months. However, research on its ice biota has been limited to the analysis of chlorophyll content and the value of primary production of microalgae [Kuznetsov, 1980], as well as production characteristics within ice of the Razdolnaya River estuary [Zvalinsky et al., 2010]. In the Voevoda and Novik bays of Russky Island, hydrological, hydrochemical, and ecological studies have been carried out [Barabanshchikov et al., 2015, 2018; Khristoforova et al., 2016, 2017; Mel'nichenko et al., 2014, 2017]. The sea-ice biotope in Peter the Great Bay has not been covered by algological surveys *prior* to this work, likely due to methodological challenges of sampling. In contrast,

the under-ice phytoplankton community in the bay has been extensively investigated in terms of species richness and abundance [Orlova et al., 2009; Ponomareva, 2017; Semkin et al., 2022; Shevchenko et al., 2020; Sorokin, Konovalova, 1973; Stonik, 2018].

The first research of sea-ice microalgae in two bays of Russky Island, the Voevoda and Novik bays, was conducted in 2020–2021, and the findings on the quantitative characteristics of ice microalgae were published [Yurikova, Begun, 2022]. This work is a continuation of the study, and its aim is to analyze microalgae species composition in both sea ice and under-ice water in the Voevoda and Novik bays of Russky Island during winter of 2020 and 2021.

MATERIAL AND METHODS

The study was carried out in February 2020 and 2021 in the Voevoda and Novik bays (Russky Island, the Sea of Japan) (Fig. 1). The environmental conditions during the field surveys and the sampling methodology were described in detail by E. Yurikova and A. Begun earlier [2022].

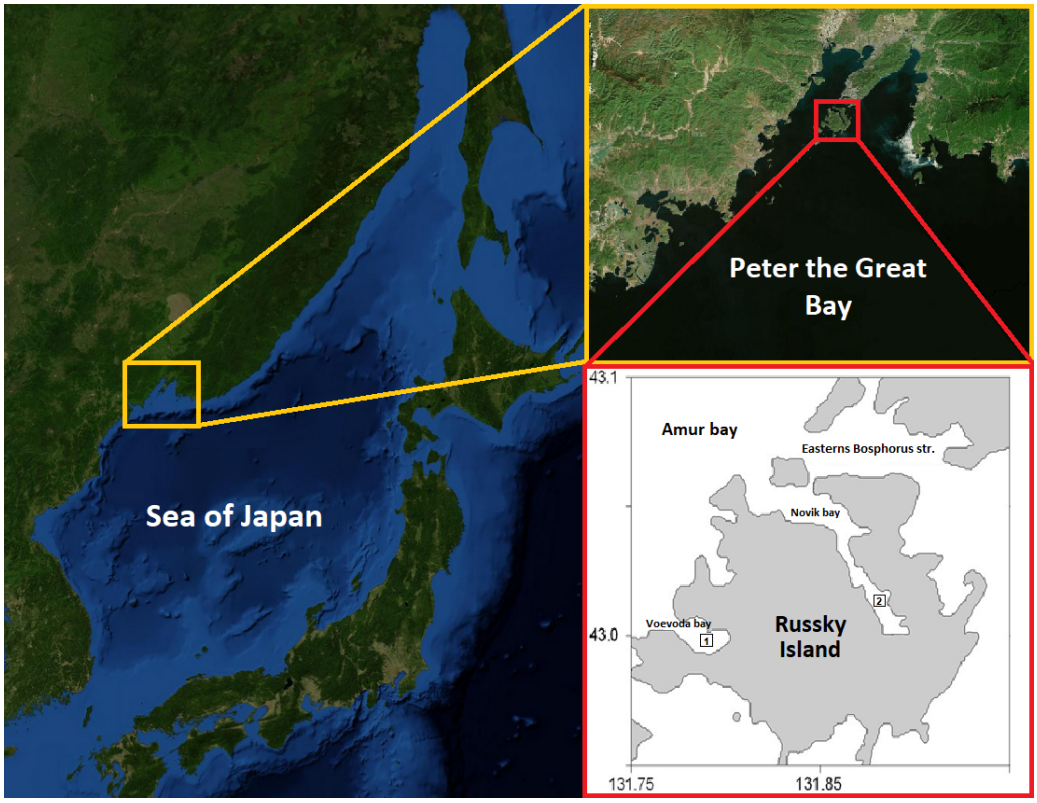

Fig. 1. Sampling sites in bays of Russky Island (the Sea of Japan): 1, the Voevoda Bay; 2, the Novik Bay

In 2020, ice thickness was approximately 40 cm in both bays; in 2021, it was about 60 cm. In 2020, 4 ice and 1 under-ice water samples were taken in each bay, while in 2021, 6 ice samples and 1 under-ice water sample were taken. Samples were fixed with Utermöhl's solution to a pale-yellow color [Utermöhl, 1958]. Following a method for sedimentation [Radchenko et al., 2010], after 12 days, the supernatant was decanted from each sample, and a residue of 100–200 mL was left.

For scanning electron microscopy, samples were prepared by boiling in 98% sulfuric acid for 40 min and then rinsed with distilled water. The material was analyzed in the laboratory of marine microbiota of NSCMB FEB RAS. For species identification of microalgae, we used a transmitted light

microscope Olympus BX41 equipped with a UPLanF1 100×/1.30 objective (Japan). Taxonomic identification was verified under a Zeiss Sigma 300 VP scanning electron microscope (the UK). Microalgal classification follows the system of [Konovalova et al., 1989] updated with nomenclatural revisions over the past 10 years. For identification, we used the guides [Hoppenrath et al., 2009; Identifying Marine Phytoplankton, 1997; Konovalova, 1998; Konovalova et al., 1989; Ryabushko, Begun, 2015].

Similarity analysis was performed in PRIMER v7.0.21 [Clarke, Gorley, 2015; Clarke, Warwick, 2001]. Non-metric multidimensional scaling was applied to ordinate algal communities based on species composition for different ice layers and under-ice water. The Sørensen coefficient was used as the distance measure.

RESULTS

In sea ice and under-ice water samples of 2020–2021, 87 taxa (species, varieties, and forms) from 48 genera and 7 divisions were identified (Table 1): Ochrophyta (2 species), Bacillariophyta (67), Cryptophyta (1), Dinophyta (13), Chlorophyta (2), Euglenophyta (1), and Haptophyta (1). Sixteen taxa could not be identified down to the species level. In ice, 79 species were recorded; out of them, 46 were exclusive to this biotope. In under-ice water, 41 species were registered, with only 8 being exclusive to it.

In 2020, 52 species from 31 genera and 4 divisions were noted for both bays, with 36 species out of them inhabiting the Voevoda Bay, and 37, the Novik Bay. Twenty-one species were common to two bays. In 2021, 63 species representing 41 genera and 7 divisions were found, with 50 species out of them inhabiting the Voevoda Bay, and 43, the Novik Bay. Thirty-one species were common for these two bays.

Ecological characteristic was determined for 66 out of 87 taxa revealed, and phytogeographical one, for 62. Benthic species dominated accounting for 50% (51% of recorded in sea ice, and 45% of registered in under-ice water). Benthic-planktonic species constituted 9%. Out of planktonic species, neritic ones accounted for 24%; oceanic for 8%; panthalassic for 8%; and freshwater for 1%. Phytogeographical analysis showed that cosmopolitans were the largest group comprising 40% of species (40% of noted in sea ice, and 48% of found in under-ice water). Out of the total number of species with known phytogeographic characteristic, tropical-arctic-boreal algae comprised 19%; tropical-boreal, 18%; arctic-boreal, 15%; boreal, 5%; and bipolar, 3%.

Table 1. Species composition of microalgae in sea ice (I) and under-ice water (UIW) of two bays of Russky Island in 2020–2021

Taxon	Ecological characteristic	Phytogeographical characteristic	2020				2021			
			Voevoda Bay		Novik Bay		Voevoda Bay		Novik Bay	
			I	UIW	I	UIW	I	UIW	I	UIW
Ochrophyta										
Ebria tripartita (Schumann) Lemmermann, 1899	N	B	–	–	–	–	–	–	+	–
Octactis speculum (Ehrenberg) F. H. Chang, J. M. Grieve et J. E. Sutherland, 2017	O	C	+	–	+	–	+	–	+	–

Continued on the next page…

Taxon	Ecological characteristic	Phytogeographical characteristic	2020				2021			
			Voevoda Bay		Novik Bay		Voevoda Bay		Novik Bay	
			I	UIW	I	UIW	I	UIW	I	UIW
Bacillariophyta										
Actinoptychus senarius (Ehrenberg) Ehrenberg, 1843	BP	C	–	–	–	–	+	–	–	–
Amphora proteus Gregory, 1857	Ben	C	–	–	–	–	+	–	–	–
Asterionella formosa Hassall, 1850	Fw	–	–	–	–	+	–	–	–	–
Caloneis liber (W. Smith) Cleve, 1894	Ben	C	–	–	–	–	–	–	–	+
Chaetoceros socialis f. *radians* (F. Schütt) A. I. Proshkina-Lavrenko, 1963	N	TAB	+	–	+	–	+	–	+	–
Cocconeis costata Gregory, 1855	Ben	C	–	–	–	–	+	–	+	–
Cocconeis scutellum Ehrenberg, 1838	Ben	C	+	–	–	–	+	+	+	–
Coscinodiscus oculus-iridis (Ehrenberg) Ehrenberg, 1840	P	AB	+	–	+	–	–	–	–	–
Coscinodiscus sp.	–	–	–	+	+	+	–	–	–	–
Cyclotella choctawhatcheeana Prasad, 1990	N	TB	–	–	+	–	+	–	–	–
Cylindrotheca closterium (Ehrenberg) Reimann et J. C. Lewin, 1964	BP	C	+	+	+	–	+	–	+	+
Cymbellafalsa diluviana (Krasske) Lange-Bertalot et Metzeltin, 2009	Ben	B	–	–	–	–	+	–	–	–
Detonula confervacea (Cleve) Gran, 1896	N	AB	+	–	–	–	+	–	+	–
Diploneis chersonensis (Grunow) Cleve, 1894	Ben	TAB	–	–	+	–	–	–	–	–
Diploneis lineata (Donkin) Cleve, 1894	Ben	TB	+	–	–	–	+	–	+	–
Diploneis smithii (Brébisson) Cleve, 1894	Ben	C	–	–	–	+	+	–	–	–
Entomoneis gigantea var. *decussata* (Grunow) Nizamuddin, 1982	BP	B	–	–	–	–	+	–	+	+
Grammatophora marina (Lyngbye) Kützing, 1844	Ben	C	+	–	–	+	+	–	+	–

Continued on the next page…

Taxon	Ecological characteristic	Phytogeographical characteristic	2020				2021			
			Voevoda Bay		Novik Bay		Voevoda Bay		Novik Bay	
			I	UIW	I	UIW	I	UIW	I	UIW
Gyrosigma arcuatum (Donkin) Sterrenburg, 2005	Ben	C	–	–	–	–	+	–	–	–
Gyrosigma fasciola (Ehrenberg) J. W. Griffith et Henfrey, 1856	Ben	–	–	–	–	–	+	–	–	–
Gyrosigma tenuissimum (W. Smith) Griffith et Henfrey, 1856	Ben	TB	–	–	–	–	–	–	+	–
Halamphora costata (W. Smith) Levkov, 2009	Ben	TB	+	–	–	–	+	–	+	–
Halamphora cymbifera (Gregory) Levkov, 2009	Ben	TB	+	–	–	–	+	–	–	–
Haslea ostrearia (Gaillon) Simonsen, 1974	Ben	TB	–	–	–	–	+	–	–	–
Leptocylindrus minimus Gran, 1915	N	TAB	+	–	–	–	–	–	–	–
Licmophora abbreviata C. Agardh, 1831	Ben	C	–	–	–	–	–	–	+	–
Licmophora communis (Heiberg) Grunow, 1881	Ben	AB	–	–	–	–	+	–	–	–
Melosira moniliformis (O. F. Müller) C. Agardh, 1824	BP	TAB	–	–	–	–	–	–	+	–
Melosira moniliformis var. *subglobosa* (Grunow) Hustedt, 1927	BP	AB	–	–	–	–	+	–	–	–
Navicula distans (W. Smith) Ralfs, 1861	Ben	TAB	–	–	–	–	+	+	–	+
Navicula granii (Jørgensen) Gran, 1908	N	AB	–	–	–	–	+	+	–	+
Navicula johanrossii Giffen, 1967	Ben	TB	–	–	–	–	+	–	–	–
Navicula ramosissima (C. Agardh) Cleve, 1895	Ben	TAB	–	–	–	–	+	+	–	+
Navicula septentrionalis Cleve, 1896	N	AB	+	+	–	–	+	–	+	+
Navicula sp. 1	–	–	+	+	+	+	–	–	–	–
Navicula sp. 2	–	–	+	–	–	–	–	–	–	–
Navicula sp. 3	–	–	–	–	–	–	+	–	–	–
Navicula transitans var. *derasa* (Grunow) Cleve, 1883	–	–	–	–	–	+	+	+	+	+

Continued on the next page…

Taxon	Ecological characteristic	Phytogeographical characteristic	2020				2021			
			Voevoda Bay		Novik Bay		Voevoda Bay		Novik Bay	
			I	UIW	I	UIW	I	UIW	I	UIW
Navicula transitans var. *derasa* f. *delicatula* Heimdal, 1970	–	–	–	–	–	+	+	+	+	+
Nitzschia angularis W. Smith, 1853	Ben	C	–	–	–	+	–	–	–	–
Nitzschia distans W. Gregory, 1857	Ben	TB	–	–	+	–	–	–	–	–
Nitzschia frigida Grunow, 1880	–	–	+	+	+	+	+	–	+	+
Nitzschia sp. 1	–	–	–	–	–	–	+	–	–	–
Nitzschia sp. 2	–	–	–	+	+	+	–	–	–	–
Nitzschia sp. 3	–	–	–	–	–	+	–	–	–	–
Nitzschia sp. 4	–	–	–	–	–	–	+	+	+	+
Odontella aurita (Lyngbye) C. Agardh, 1832	BP	TAB	+	+	+	–	+	+	+	+
Parlibellus delognei (Van Heurck) E. J. Cox, 1988	Ben	C	–	–	–	–	+	+	–	+
Pinnularia sp.	–	–	–	–	–	–	+	–	–	–
Pleurosigma elongatum W. Smith, 1852	Ben	C	–	–	–	–	+	+	+	+
Pleurosigma formosum W. Smith, 1852	Ben	TAB	+	–	–	–	–	–	–	–
Pleurosigma inflatum Shadbolt, 1854	Ben	TB	+	+	–	–	–	–	–	–
Pleurosigma intermedium W. Smith, 1853	Ben	TAB	+	–	–	–	–	–	–	–
Pseudo-nitzschia fraudulenta (Cleve) Hasle, 1993	P	C	–	–	+	–	–	–	–	–
Pseudo-nitzschia pungens (Grunow ex Cleve) G. R. Hasle, 1993	P	C	–	–	+	–	–	–	–	–
Rhaphoneis amphiceros (Ehrenberg) Ehrenberg, 1844	Ben	TB	–	–	–	–	–	–	+	–
Rhoicosphenia marina (Kützing) M. Schmidt, 1889	Ben	TAB	–	–	–	–	+	–	–	–
Skeletonema sp.	–	–	+	–	+	–	+	–	–	–
Tabularia fasciculata (C. Agardh) D. M. Williams et Round, 1986	Ben	C	+	+	+	+	+	–	+	–

Continued on the next page…

Taxon	Ecological characteristic	Phytogeographical characteristic	2020				2021			
			Voevoda Bay		Novik Bay		Voevoda Bay		Novik Bay	
			I	UIW	I	UIW	I	UIW	I	UIW
Tabularia tabulata (C. Agardh) Snoeijs, 1992	Ben	C	+	–	–	–	+	+	+	–
Thalassionema nitzschioides (Grunow) Mereschkowsky, 1902	P	TAB	+	+	+	–	–	–	–	–
Thalassiosira gravida Cleve, 1896	P	Bip	–	–	–	+	+	–	–	–
Thalassiosira nordenskioeldii Cleve, 1873	N	AB	+	+	+	–	+	+	+	+
Thalassiosira punctigera (Castracane) Hasle, 1983	N	TB	–	–	–	–	+	+	+	–
Thalassiosira sp.	–	–	+	–	–	–	–	–	–	–
Trachyneis aspera (Ehrenberg) Cleve, 1894	Ben	C	+	–	+	–	+	–	+	+
Ulnaria ulna (Nitzsch) P. Compère, 2001	Ben	C	–	–	–	–	–	–	+	–
Cryptophyta										
Plagioselmis sp.	–	–	–	–	–	–	–	+	–	+
Dinophyta										
Alexandrium sp.	–	–	–	–	–	+	–	–	–	–
Amphidinium sphenoides Wulff, 1919	O	AB	–	–	–	+	–	–	–	+
Dinophysis acuminata Claparède et Lachmann, 1859	N	C	+	–	+	–	–	–	–	–
Gyrodinium fusiforme Kofoid et Swezy, 1921	N	TAB	–	–	+	+	–	–	–	+
Gyrodinium lacryma (Meunier) Kofoid et Swezy, 1921	O	AB	–	–	–	–	–	–	–	+
Oblea rotunda (Lebour) Balech ex Sournia, 1973	O	–	+	–	+	–	–	–	–	–
Protoceratium reticulatum (Claparède et Lachmann) Bütschli, 1885	N	C	+	–	–	–	–	–	–	–
Protoperidinium brevipes (Paulsen, 1908) Balech, 1974	N	C	+	–	–	+	–	–	+	–
Protoperidinium depressum (Bailey, 1854) Balech, 1974	O	C	+	–	+	–	–	–	–	–
Protoperidinium granii (Ostenfeld) Balech, 1974	N	–	–	–	–	–	–	–	+	+

Continued on the next page…

Taxon	Ecological characteristic	Phytogeographical characteristic	2020				2021			
			Voevoda Bay		Novik Bay		Voevoda Bay		Novik Bay	
			I	UIW	I	UIW	I	UIW	I	UIW
Protoperidinium pellucidum Bergh, 1881	N	C	+	+	+	+	+	–	–	–
Protoperidinium pentagonum (Gran) Balech, 1974	N	Bip	+	–	+	–	–	–	–	–
Protoperidinium sp.	–	–	+	–	–	–	+	+	–	–
Chlorophyta										
Carteria sp.	–	–	–	–	–	–	+	–	+	–
Chlamydomonas sp.	–	–	–	–	–	–	+	–	+	–
Euglenophyta										
Eutreptiella braarudii Throndsen, 1969	–	–	–	–	+	+	+	+	+	+
Haptophyta										
Unidentified species	–	–	–	–	–	–	+	–	+	–

Note: N, neritic; O, oceanic; P, panthalassic; Ben, benthic; BP, bentic-planktonic; FW, freshwater; B, boreal; C, cosmopolite; AB, arctic-boreal; TB, tropical-boreal; TAB, tropical-arctic-boreal; Bip, bipolar.

In the Voevoda Bay in 2020, the highest species number was revealed for ice layers of 0–10 and 10–20 cm (22 species each), and in 2021, for the layer of 10–20 cm (28 species) (Fig. 2). Conversely, in the Novik Bay in both years, the highest species richness was found in under-ice water (19 and 22 species). Diatoms dominated the microalgal community in both biotopes accounting for 100% in one of ice layers. Pennate diatoms were significantly more diverse (53 species) than centric ones (14 species), with mean pennate-to-centric ratios of 3 : 1 and 6 : 1 in ice and under-ice water, respectively. In 2020, the diversity of centric diatoms peaked in ice layers of 0–10 and 10–20 cm in both bays (5 and 4 species); in 2021, in the lower ice layer of the Voevoda Bay, 50–62 cm (6 species), and in the mid-ice layer of the Novik Bay, 30–40 cm (4 species).

The sea-ice algal community was dominated by neritic planktonic species, primarily arctic-boreal ones (Fig. 3). The prevailing taxa varied by location, year, biotope, and sampling depth. Thus, in 2020, sea ice in the Voevoda Bay was co-dominated by *Nitzschia frigida* (up to 94% of total abundance in an ice layer) and *Thalassiosira nordenskioeldii* (up to 41%). In under-ice water, the prevailing taxa were *Nitzschia* sp. 2 (up to 41%) and *Cylindrotheca closterium* (up to 31%). In the Novik Bay, the ice community was dominated by *C. closterium* (up to 63%), *T. nordenskioeldii* (up to 55%), and *N. frigida* (up to 28%), while under-ice water was dominated by *Thalassiosira gravida* (up to 88%). In 2021, in the Voevoda Bay ice, the prevailing taxa were *Navicula septentrionalis* (up to 59%), *Nitzschia* sp. 4 (up to 46%), *Navicula granii* (up to 41%), and *Chaetoceros socialis* f. *radians* (up to 76%). Under-ice water was dominated by *Plagioselmis* sp. (up to 67%). In the Novik Bay, the ice community was characterized by the high abundance of *Nitzschia* sp. 4 (up to 72%), *N. frigida* (up to 40%), and *C. socialis* f. *radians* (up to 27%), and under-ice water community, by the high abundance of *T. nordenskioeldii* (up to 34%) and *Plagioselmis* sp. (up to 25%).

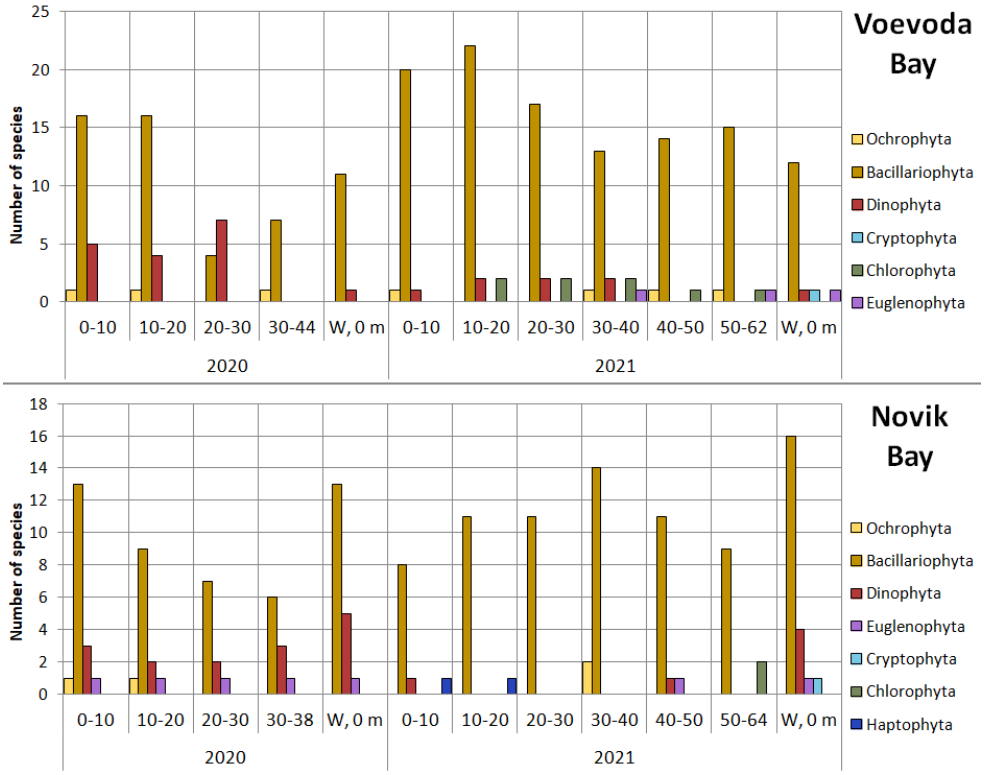

Fig. 2. Species number in samples of ice and under-ice water in the Voevoda and Novik bays

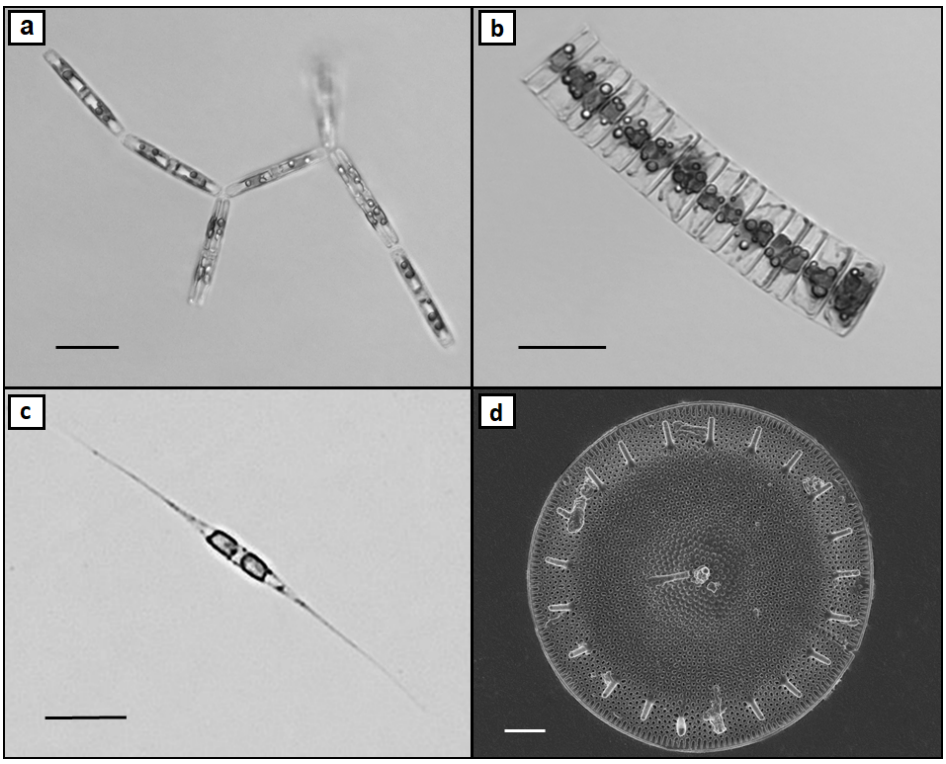

Fig. 3. Dominant microalgal species: a, *Nitzschia frigida*; b, *Navicula septentrionalis*; c, *Cylindrotheca closterium* (a light microscope); d, *Thalassiosira nordenskioeldii* (a scanning electron microscope). Scale bars are 20 µm (a–c) and 4 µm (d)

Statistical analysis revealed that microalgal community structure varied noticeably across ice layers and under-ice water, with the key drivers being biotope, sampling depth, location, and year (Fig. 4). Inter-annual variation was the most significant factor, with similarity between samples from the same year of 25% only. In 2021, communities showed pronounced spatial segregation clustering by bay, with within-bay similarity of 40%. In contrast, in 2020, there was no clear spatial pattern. The highest similarity, 65%, was recorded between several neighboring ice layers: in 2020, between those of 20–40 cm in the Novik Bay, and in 2021, between those of 30–50 cm in the Voevoda Bay and 0–20 cm in the Novik Bay.

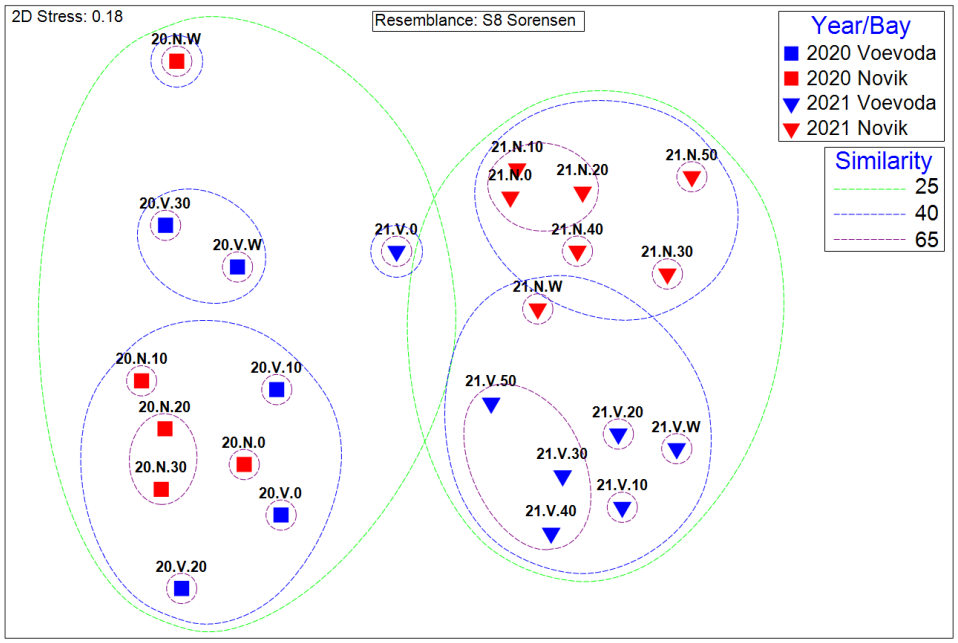

Fig. 4. Non-metric multidimensional scaling of algal flora ordination for samples of ice and under-ice water. Samples are signed according to a "year.bay.layer" pattern; a digit in a layer index indicates its upper boundary; W denotes a sample of under-ice water

DISCUSSION

The sea-ice algal communities in the Voevoda and Novik bays exhibited similar taxonomic structure, with diatoms dominating both species composition and richness [Yurikova, Begun, 2022]. Within 2020–2021, 45 species were common for two bays (52% of their total number). The similarity in algal flora in the bays can be traced through the revealed most species-rich genera. Moreover, in the Novik Bay, a higher number of represented groups were identified in each year of the study. While species richness of sea-ice microalgae was similar between two bays in 2020, the Voevoda Bay showed 1.3-fold higher richness in 2021 than the Novik Bay. The similarity in species composition likely reflects the close geographical proximity of these bays, as well as their connection with the semi-enclosed Amur Bay which features restricted water circulation. Differences in taxonomic structure are mediated by location of the bays. The Novik Bay deeply embays Russky Island, and its mouth is substantially isolated from the Eastern Bosphorus Strait; this results in the highly isolated nature of its biotope. The more exposed Voevoda Bay experiences freshwater inflow from the Russkaya River that mediates the formation of distinct microalgal community as compared to that in the Novik Bay.

Statistical analysis revealed the most significant variability in the species composition of sea ice and under-ice water samples between years of the study. In 2021, the microalgal composition in the bays was richer than in 2020, and this aligns with the data on their quantitative development [Yurikova, Begun, 2022]. This phenomenon may be attributed to specific meteorological conditions that favored the formation of a thicker ice cover than in the previous year. Differences in species composition were also affected by location (sampling site), biotope, and depth of the ice layer.

The majority of diatoms registered in sea ice of the Voevoda and Novik bays are well-documented constituents of the under-ice phytoplankton in Peter the Great Bay; it develops at sub-zero water temperatures and can attain bloom concentrations in winter and early spring [Begun et al., 2003, 2011; Konovalova et al., 1989; Orlova et al., 2009; Ponomareva, 2017; Ryabushko et al., 2019; Shevchenko et al., 2020; Stonik, 2018]. A study of microphytobenthos on rocky substrates within the ice sheet of Vostok Bay in January 1980 recorded a peak diatom biomass (2,576 mg·m^{-2}) at a water temperature of −1.2 °C, and the dominant species was a benthic-planktonic one: *Odontella aurita* (Lyngbye) C. Agardh, 1832 [Ryabushko, 1986; Ryabushko, Begun, 2015]. Interestingly, this species also occurred in the Voevoda and Novik bays. Furthermore, several species we registered have been previously reported in studies of sea-ice biota across polar regions [Buinitskii, 1973; Kauko et al., 2009; Mel'nikov, 1989; Usachev, 1949].

The common taxa in the ice algal flora of the bays of Russky Island are neritic planktonic species. However, a significant proportion of other species covered benthic (49%) and benthic-planktonic (10%) forms. Those are typical for sediment habitats or for fouling of various underwater substrates, and this can be governed by the shallow nature of the bays and the proximity of the benthic biotope. Due to wave action and uplift to the water surface, benthic species can colonize the underside of an ice cover using it as a substrate and serving as cryoperiphyton [Buinitskii, 1973; Ewert, Deming, 2013; Mel'nikov, Bondarchuk, 1987]. As known [Kauko et al., 2009], due to turbulent mixing of pelagic waters, microalgae cells are incorporated into sea ice during its formation. However, according to some researchers [Olsen et al., 2017; Ratkova, Wassmann, 2005], microphytobenthos is another source for the replenishment of the ice biotope with algal flora.

The microalgal community of Russky Island bays is a mixed planktonic diatom assemblage comprising both centric forms (predominantly pelagic) and pennate ones (usually benthic-affiliated). This reflects patterns observed in under-ice phytoplankton communities of Peter the Great Bay [Begun et al., 2011; Ponomareva, 2017; Shevchenko et al., 2020; Sorokin, Konovalova, 1973]. Pennate species outnumbered centric ones by 4 times, and such a greater diversity aligns with documented successional patterns during ice algae bloom [Leu et al., 2015; Van Leeuwe et al., 2018].

Our study of sea ice in the bays of Russky Island revealed that the ice algal flora consists of both planktonic and benthic microalgae. Such a composition is mediated by the fact as follows. During the characteristic winter bloom of under-ice phytoplankton, abundant species become incorporated into the ice community with varying degrees of intensity during sea-ice formation. The intensity is associated with several complex meteorological and hydrochemical processes occurring in the water area during this period. This is reflected in the distinct species composition and quantitative abundance of microalgae [Yurikova, Begun, 2022] within each specific layer of an ice cover.

Conclusions. This survey substantially expanded data on microalgal flora of sea ice and under-ice water in Peter the Great Bay. The first comprehensive species list of cryophilic microalgae is provided. It comprises 87 taxa from 48 genera and 7 divisions. The algal flora was dominated by ben-

thic cosmopolitan species. The more exposed Voevoda Bay exhibited higher species richness but lower divisional diversity than the enclosed Novik Bay.

In 2020, 52 species from 31 genera and 4 divisions were recorded in both bays. Out of these, 36 species were noted in the Voevoda Bay, and 37, in the Novik Bay; 21 species were common for two bays. In 2021, 63 species from 41 genera and 7 divisions were registered. Out of these, 50 species were found in the Voevoda Bay, and 43, in the Novik Bay; 31 species were common. Community composition showed pronounced vertical stratification. The species composition in ice and under-ice water samples was found to vary most significantly in different years of the study.

This research was supported by the Federal Service for Hydrometeorology and Environmental Monitoring of the Russian Federation (agreement No. 169-15-2023-002).

Acknowledgements. The authors thank P. Tishchenko, P. Semkin, Yu. Barabanshchikov, and S. Sagalaev (V. I. Il'ichev Pacific Oceanological Institute FEB RAS) for field assistance. The authors are grateful to A. Lazaryuk for scientific consultation. This work was carried out at the core facility "Marine Biobank" (NSCMB FEB RAS).

REFERENCES

1. Barabanshchikov Yu. A., Tishchenko P. Ya., Semkin P. Yu., Volkova T. I., Zvalinsky V. I., Mikhailik T. A., Sagalaev S. G., Sergeev A. F., Tishchenko P. P., Shvetsova M. G., Shkirnikova E. M. Seasonal hydrological and hydrochemical surveys in the Voevoda Bay (Amur Bay, Japan Sea). *Izvestiya TINRO*, 2015, vol. 180, pp. 161–178. (in Russ.). https://doi.org/10.26428/1606-9919-2015-180-161-178
2. Barabanshchikov Yu. A., Tishchenko P. Ya., Semkin P. Yu., Mikhailik T. A., Kosyanenko A. A. Conditions of forming for therapeutic mud in the Voevoda Bay (Amur Bay, Japan Sea). *Izvestiya TINRO*, 2018, vol. 192, pp. 167–176. (in Russ.). https://doi.org/10.26428/1606-9919-2018-192-167-176
3. Begun A. A., Orlova T. Yu., Zvyagintsev A. Yu. Phytoplankton of Amur Bay in the Sea of Japan near Vladivostok. *Al'gologiya*, 2003, vol. 13, no. 2, pp. 204–215. (in Russ.). https://elibrary.ru/ahnogo
4. Begun A. A., Maslennikov S. I., Zvyagintsev A. Yu. Phytoplankton in treatment facilities area near Vladivostok (Amurskii Bay, Japan Sea). *Nauchnye trudy Dal'rybvtuza*, 2011, vol. 24, pp. 3–12. (in Russ.). https://elibrary.ru/oirajb
5. Boychenko T. V., Khristoforova N. K., Emelyanov A. A. Microbial indication of pollution for the surface waters in the Novik Bay (Russky Island, Peter the Great Bay, Japan Sea). *Izvestiya TINRO*, 2019, vol. 198, pp. 186–194. (in Russ.). https://doi.org/10.26428/1606-9919-2019-198-186-194
6. Buinitskii V. Kh. *Morskie l'dy i aisbergi Antarktiki.* Leningrad : Izd-vo LGU, 1973, 256 p. (in Russ.)
7. Zvalinsky V. I., Maryash A. A., Shvetsova M. G., Sagalaev S. G., Tishchenko P. Y., Stonik I. V., Begun A. A. Production and hydrochemical characteristics of ice, under-ice water and sediments in the Razdolnaya River estuary (Amursky Bay, Sea of Japan) during the ice cover period. *Biologiya morya*, 2010, vol. 36, no. 3, pp. 186–195. (in Russ.). https://elibrary.ru/ouiphz
8. Konovalova G. V. *Dinoflagellyaty (Dinophyta) dal'nevostochnykh morei Rossii i sopredel'nykh akvatorii Tikhogo okeana.* Vladivostok : Dal'nauka, 1998, 300 p. (in Russ.)
9. Konovalova G. V., Orlova T. Yu., Pautova L. A. *Atlas morskogo fitoplanktona Yaponskogo morya.* Leningrad : Nauka, 1989, 160 p. (in Russ.)
10. Kuznetsov L. L. Chlorophylls and primary production of microalgae connected with ice of the Amur Bay (Sea of Japan). *Biologiya morya*, 1980, no. 5, pp. 72–74. (in Russ.)
11. Mel'nikov I. A. *Ekosistema arkticheskogo morskogo l'da.* Moscow : AN SSSR, 1989, 192 p. (in Russ.)
12. Mel'nikov I. A, Bondarchuk L. L. To the ecology

of the mass aggregations of colonial diatom algae under the arctic drifting sea ice. *Okeanologiya*, 1987, iss. 2, pp. 317–321. (in Russ.)

13. Mel'nichenko N. A., Tyuveev A. V., Lazaryuk A. Yu., Savchenko V. G., Kustova E. V. Particular features of forming sea ice vertical structure in the Novik Bay (the Russian Island) by NMR and MRT. *Vestnik Dal'nevostochnogo otdeleniya Rossiiskoi akademii nauk*, 2017, no. 4 (194), pp. 70–80. (in Russ.). https://elibrary.ru/zndttz
14. Mel'nichenko N. A., Tyuveev A. V., Lazaryuk A. Yu., Savchenko V. G., Kharlamov P. O., Yurtsev A. Yu., Mar'yina E. N. Vertical distribution of brine content, temperature and salinity in land fast ice of the Novik Bay (Russky Island) of Peter the Great Bay. *Vestnik Dal'nevostochnogo otdeleniya Rossiiskoi akademii nauk*, 2014, no. 5 (177), pp. 32–38. (in Russ.). https://elibrary.ru/tndocn
15. Orlova T. Yu., Stonik I. V., Shevchenko O. G. Flora of planktonic microalgae of Amursky Bay, Sea of Japan. *Biologiya morya*, 2009, vol. 35, no. 1, pp. 48–61. (in Russ.). https://doi.org/10.1134/S106307400901009X
16. Ponomareva A. A. *Struktura i dinamika fitoplanktona v bukhte Paris (zaliv Petra Velikogo, Yaponskoe more).* [dissertation]. Vladivostok : NNTsMB DVO RAN, 2017, 171 p. (in Russ.). https://elibrary.ru/zqepgn
17. Radchenko I. G., Kapkov V. I., Fedorov V. D. *Prakticheskoe rukovodstvo po sboru i analizu prob morskogo fitoplanktona* : uchebno-metodicheskoe posobie dlya studentov biologicheskikh spetsial'nostei universitetov. Moscow : Mordvintsev, 2010, 60 p. (in Russ.)
18. Ryabushko L. I. *Diatomovye vodorosli verkhnei sublitorali severo-zapadnoi chasti Yaponskogo morya.* [dissertation]. Sevastopol, 1986, 244 p. (in Russ.)
19. Ryabushko L. I., Begun A. A. *Diatoms of Microphytobenthos of the Sea of Japan* : in 2 vols. Simferopol ; Sevastopol : N.Orianda, 2015, vol. 1, 288 p. (in Russ.). https://repository.marine-research.ru/handle/299011/7924
20. Stonik I. V. Qualitative and quantitative composition of phytoplankton in the Golden Horn Bay, Japan Sea. *Izvestiya TINRO*, 2018, vol. 194, pp. 167–174. (in Russ.). https://doi.org/10.26428/1606-9919-2018-194-167-174
21. Usachev P. I. Mikroflora polyarnykh l'dov. *Trudy Instituta okeanologii*, 1949, vol. 3, pp. 216–259. (in Russ.)
22. Khristoforova N. K., Boychenko T. V., Emelyanov A. A., Popova A. V. Microbiological control of the water condition in the Novik Bay (Peter the Great Bay, Japan Sea). *Izvestiya TINRO*, 2017, vol. 189, pp. 121–130. (in Russ.). https://doi.org/10.26428/1606-9919-2017-189-121-130
23. Khristoforova N. K., Degteva Yu. E., Berdasova K. S., Emelyanov A. A., Lazaryuk A. Yu. Chemical and ecological state of the waters in the Novik Bay (Russky Island, Peter the Great Bay, Japan Sea). *Izvestiya TINRO*, 2016, vol. 186, pp. 135–144. (in Russ.). https://doi.org/10.26428/1606-9919-2016-186-135-144
24. Shevchenko O. G., Tevs K. O., Shul'kin V. M. Integrated monitoring of phytoplankton in a shallow inlet of Peter the Great Bay (Japan Sea): Dynamics of chlorophyll *a* and nutrients. *Izvestiya TINRO*, 2020, vol. 200, iss. 1, pp. 141–154. (in Russ.). https://doi.org/10.26428/1606-9919-2020-200-141-154
25. Yurikova E. A., Begun A. A. Quantitative structure of the sea ice microalgae community (Russky Island, Peter the Great Bay, Sea of Japan). *Marine Biological Journal*, 2022, vol. 7, no. 2, pp. 98–112. (in Russ.). https://doi.org/10.21072/mbj.2022.07.2.08
26. *Identifying Marine Phytoplankton* / T. R. Carmelo (Ed.). San Diego, CA : Academic Press, 1997, 874 p. https://doi.org/10.1016/B978-0-12-693018-4.X5000-9
27. Clarke K. R., Gorley R. N. *PRIMER version 7: User Manual / Tutorial.* Plymouth, UK : PRIMER-E, 2015, 296 p.
28. Clarke K. R., Warwick R. M. *Change in Marine Communities: An Approach to Statistical Analysis and Interpretation.* 2nd edition. Plymouth : PRIMER-E, 2001, 176 p.

29. Ewert M., Deming J. W. Sea ice microorganisms: Environmental constraints and extracellular responses. *Biology*, 2013, vol. 2, iss. 2, pp. 603–628. https://doi.org/10.3390/biology2020603
30. Hoppenrath M., Elbrächter M., Drebes G. *Marine Phytoplankton: Selected Microphytoplankton Species from the North Sea Around Helgoland and Sylt.* Stuttgart : E. Schweizerbart'sche Verlagsbuchhandlung, 2009, 264 p.
31. Kauko H. M., Olsen L. M., Duarte P., Peeken I., Granskog M. A., Johnsen G., Fernández-Méndez M., Pavlov A. K., Mundy Ch. J., Assmy Ph. Algal colonization of young Arctic sea ice in spring. *Frontiers in Marine Science*, 2018, no. 5, art. no. 199 (20 p.). https://doi.org/10.3389/fmars.2018.00199
32. Leu E., Mundy Ch. J., Assmy Ph., Campbell K., Gabrielsen T. M., Gosselin M. Arctic spring awakening – steering principles behind the phenology of vernal ice algal blooms. *Progress in Oceanography*, 2015, vol. 139, pp. 151–170. https://doi.org/10.1016/j.pocean.2015.07.012
33. Olsen L. M., Laney S. R., Duarte P., Kauko H. M., Fernández-Méndez M., Mundy Ch. J., Rösel A., Meyer A., Itkin P., Cohen L., Peeken I., Tatarek A., Różańska-Pluta M., Wiktor J., Taskjelle T., Pavlov A. K., Hudson S. R., Granskog M. A., Hop H., Assmy Ph. The seeding of ice algal blooms in Arctic pack ice: The multiyear ice seed repository hypothesis. *Journal of Geophysical Research: Biogeosciences*, 2017, vol. 122, iss. 7, pp. 1529–1548. https://doi.org/10.1002/2016JG003668
34. Ratkova T. N., Wassmann P. Sea ice algae in the White and Barents seas: Composition and origin. *Polar Research*, 2005, vol. 24, no. 1–2, pp. 95–110. https://doi.org/10.3402/polar.v24i1.6256
35. Ryabushko L. I., Balycheva D. S., Bondarenko A. V., Zheleznova S. N., Begun A. A., Stonik I. V. Different aspects of studying a diatom *Cylindrotheca closterium* (Ehrenberg) Reimann et Lewin, 1964 in natural and laboratory conditions. *Marine Biological Journal*, 2019, vol. 4, no. 2, pp. 52–62. https://doi.org/10.21072/mbj.2019.04.2.06
36. Semkin P., Tishchenko P., Pavlova G., Barabanshchikov Yu., Tishchenko P., Shvetsova M., Shkirnikova E., Fedorets Yu. O_2 and CO_2 responses of the synaptic period to under-ice phytoplankton bloom in the eutrophic Razdolnaya River estuary of Amur Bay, the Sea of Japan. *Journal of Marine Science and Engineering*, 2022, vol. 10, iss. 12, art. no. 1798 (17 p.). https://doi.org/10.3390/jmse10121798
37. Sorokin Y. I., Konovalova G. V. Production and decomposition of organic matter in a bay of the Japan Sea during the winter diatom bloom. *Limnology and Oceanography*, 1973, vol. 18, iss. 6, pp. 962–967. https://doi.org/10.4319/lo.1973.18.6.0962
38. Utermöhl H. Zur Vervollkommnung der quantitativen Phytoplankton-Methodik. *Internationale Vereinigung für theoretische und angewandte Limnologie: Mitteilungen*, 1958, vol. 9, iss. 1, pp. 1–38. https://doi.org/10.1080/05384680.1958.11904091
39. Van Leeuwe M. A., Tedesco L., Arrigo K. R., Assmy Ph., Campbell K., Meiners K. M. Microalgal community structure and primary production in Arctic and Antarctic sea ice: A synthesis. *Elementa: Science of the Anthropocene*, 2018, vol. 6, art. no. 4 (25 p.). https://doi.org/10.1525/elementa.267

ВИДОВОЙ СОСТАВ СООБЩЕСТВА МИКРОВОДОРОСЛЕЙ МОРСКОГО ЛЬДА И ПОДЛЁДНОЙ ВОДЫ В БУХТАХ ОСТРОВА РУССКИЙ (ЗАЛИВ ПЕТРА ВЕЛИКОГО, ЯПОНСКОЕ МОРЕ)

Е. А. Юрикова, А. А. Бегун

Национальный научный центр морской биологии имени А. В. Жирмунского ДВО РАН, Владивосток, Российская Федерация

E-mail: *komcitykat@mail.ru*

Морской лёд способен выступать в качестве местообитания для микроводорослей, которые могут приспосабливаться к его уникальным условиям и успешно размножаться в нём. В настоящей работе продолжен анализ материала, впервые полученного при исследовании морского льда двух бухт острова Русский (Японское море) в 2020–2021 гг., с целью изучить послойное распределение качественного и количественного состава микроводорослей, населяющих его. В результате таксономического анализа идентифицировано 87 видов из 48 родов и 7 отделов микроводорослей. Максимальное видовое богатство представлено видами отдела Bacillariophyta (57–100 % числа видов в слое льда). Альгофлора морского льда и подлёдной воды была сформирована в основном бентосными видами, относящимися к группе космополитов. Состав доминирующих видов изменялся в зависимости от года, бухты и глубины изучаемого слоя льда; в число превалирующих видов входили *Chaetoceros socialis* f. *radians*, *Cylindrotheca closterium*, *Navicula septentrionalis*, *Nitzschia frigida*, *Thalassiosira gravida*, *T. nordenskioeldii* и *Plagioselmis* sp. Наиболее значительно видовой состав различался между годами исследования, а также в зависимости от бухты, биотопа и расположения слоя в толще льда.

Ключевые слова: ледовая альгофлора, диатомовые водоросли, Японское море

1871
ИнБЮМ – IBSS

Морской биологический журнал
Marine Biological Journal
2025, vol. 10, no. 3, pp. 120–124
https://marine-biology.ru

NOTES

UDC 582.26/.27-114.328:549

THE EFFECT OF HEAVY METALS ON THE GROWTH RATE OF MICROALGAE *HETEROSIGMA AKASHIWO*, *ALEXANDRIUM AFFINE*, AND *PROROCENTRUM FORAMINOSUM*

© 2025 **Zh. Markina[1] and A. Ognistaya[1,2]**

[1]A. V. Zhirmunsky National Scientific Center of Marine Biology, FEB RAS, Vladivostok, Russian Federation
[2]Far Eastern Federal University, Vladivostok, Russian Federation
E-mail: *alya_lokshina@mail.ru*

Received 18.11.2022; revised 14.04.2023;
accepted 12.08.2025.

A rise in the frequency of harmful algal blooms is associated with increasing environmental pollution, in particular with a gain in heavy metal content in waters. The aim of the study was to assess the effect of heavy metals on the growth rate of microalgae causing such blooms. The effect of heavy metals on the growth rate of microalgae *Heterosigma akashiwo*, *Alexandrium affine*, and *Prorocentrum foraminosum* was investigated: cadmium Cd^{2+}, nickel Ni^{2+}, and lead Pb^{2+} at concentrations of 10 and 20 μg·L^{-1}, as well as zinc Zn^{2+} and iron Fe^{3+} at 50 and 100 μg·L^{-1}. The evaluation was carried out on the third and seventh days of the experiment. These heavy metals were found to affect all investigated algae species. On the third day, the growth rate of *H. akashiwo* increased with the addition of Cd^{2+}, Pb^{2+}, Ni^{2+}, and Fe^{3+}; the growth was suppressed with the addition of Zn^{2+}. On the seventh day, the microalga inhibition was recorded at 10 and 20 μg·L^{-1} of Cd^{2+}, 10 μg·L^{-1} of Pb^{2+} and Ni^{2+}, and 100 μg·L^{-1} of Zn^{2+}. *H. akashiwo* stimulation occurred at 20 μg·L^{-1} of Pb^{2+} and Ni^{2+}, as well as at 50 and 100 μg·L^{-1} of Fe^{3+}. The growth rate of *A. affine* on the third day rose at 20 μg·L^{-1} of Cd^{2+}, 10 and 20 μg·L^{-1} of Pb^{2+} and Ni^{2+}, and 100 μg·L^{-1} of Fe^{2+} and Zn^{2+}. On the seventh day, the growth rate dropped because of the negative effect of 10 and 20 μg·L^{-1} of Cd^{2+} and Pb^{2+}, as well as 20 μg·L^{-1} of Ni^{2+}. Stimulation of *A. affine* growth was registered at 10 μg·L^{-1} of Ni^{2+} and at both concentrations of Fe^{3+} and Zn^{2+}. *P. foraminosum* was the least resistant to heavy metals. Its growth rate decreased when exposed to all toxicants, except for Fe^{3+}: in this case, stimulation of the microalga growth occurred on the seventh day of the experiment.

Keywords: *Heterosigma akashiwo*, *Alexandrium affine*, *Prorocentrum foraminosum*, cadmium, nickel, lead, zinc, iron, heavy metals

In recent decades, in various areas of the World Ocean, a considerable rise in harmful blooms of algae has been registered caused by a raphidophyte *Heterosigma akashiwo* (Y. Hada) Y. Hada ex Y. Hara, M. Chihara [Dursun et al., 2016; Heisler et al., 2008] and by dinoflagellates of the genera *Alexandrium* Halim, 1960 [Anderson et al., 2012] and *Prorocentrum* Ehrenberg, 1834 [Li et al., 2021; Shin et al., 2019]. Some researchers relate a gain in frequency of such events with increasing pollution of the environment [Heisler et al., 2008]. Heavy metals are regularly recorded in waters of Russian seas [Marine Water Pollution, 2020], and they are more and more often being revealed in other areas

of the World Ocean. Effects of these toxicants on plant organisms have been studied for a long time, but most investigations are focused on sublethal and lethal concentrations, while metal content corresponding to a natural one is analyzed less and less [Nagajoti et al., 2010].

Due to the above, the aim of this work was to assess the effect of cadmium, nickel, lead, zinc, and iron on the growth rate of three microalgae: *Heterosigma akashiwo*, *Alexandrium affine* H. Inoue & Y. Fukuyo Balech, and *Prorocentrum foraminosum* Faust.

MATERIAL AND METHODS

Plant material. The objects of the study were cultures of unicellular algae *H. akashiwo* (strain MBRU_HAK-SR11) (Raphidophyceae), *A. affine* (strain AFRU-12) (Dinophyta), and *P. foraminosum* (strain MBRU_PrRUS_16) (Dinophyta). All the algae were provided by the "Marine Biobank" core facility of the A. V. Zhirmunsky National Scientific Center of Marine Biology, FEB RAS (https://marbank.dvo.ru/).

Experimental conditions. The algae were cultured on *f* medium [Guillard, Ryther, 1962] in 250-mL Erlenmeyer flasks. A culture medium volume was 100 mL; temperature was +18 °C; light intensity was 70 μmol·m^{-2}·s^{-1}; and a light/dark cycle was 14 h : 10 h (light : dark). There was no air bubbling. A culture at the exponential growth stage was used as an inoculum. The initial cell concentration was 20,000 cells·mL^{-1} for *H. akashiwo*, 300 cells·mL^{-1} for *P. foraminosum*, and 1,000 cells·mL^{-1} for *A. affine*. Experiments lasted for seven days.

Samples of 1 mL were taken with a pipette dispenser (Tomanalit, Russia). Cells were counted on the third and seventh days in a 50-mL Nageotte chamber under an EVOS M5000 microscope (Thermo Fisher Scientific, the USA) at 10× magnification. A total of six replicates were counted for each variant of the experiment. The investigations were carried out in three biological replicates [Rukovodstvo, 2002].

Toxicants and their concentrations. Cd^{2+} was added as $3CdSO_4 \times 8H_2O$; Ni^{2+}, $NiSO_4 \times 7H_2O$; Pb^{2+}, $PbCl_2$; Zn^{2+}, $ZnSO_4 \times 7H_2O$; and Fe^{3+}, $FeCl_3 \times 6H_2O$, with recalculation into metal ions on the day of the experiment. Concentrations were chosen based on data on the content of these heavy metals in coastal waters of Russia and their maximum permissible concentrations (MPC). Analyzed values correspond to MPC and 2MPC [Marine Water Pollution, 2020].

The growth rate was calculated by the standard formula [Guillard, Ryther, 1962] The reliability of differences between samples was assessed using the Mann–Whitney test at a significance level of $p < 0.05$.

RESULTS AND DISCUSSION

The growth rate of *H. akashiwo* was higher on the third day than the control when exposed to Pb^{2+} and Ni^{2+} at a concentration of 10 μg·L^{-1} and Fe^{2+} at 50 and 100 μg·L^{-1} (Table 1). In other cases, the value did not differ significantly from the control. On the seventh day, the growth rate at 10 μg·L^{-1} of Cd^{2+} was noticeably lower than that in the control.

The growth rate of *A. affine* increased significantly on the third day under the effect of Cd^{2+} at a concentration of 20 μg·L^{-1}, as well as Pb^{2+} and Ni^{2+} (Table 2). The addition of 50 μg·L^{-1} of Fe^{2+} and Zn^{2+} governed a decrease in the studied parameter. On the seventh day, with 10 and 20 μg·L^{-1} of Cd^{2+} and Pb^{2+} in a medium, the alga growth was inhibited. At the same time, 10 μg·L^{-1} of Ni^{2+}, 50 μg·L^{-1} of Fe^{2+}, and 100 μg·L^{-1} of Zn^{2+} stimulated the growth.

Table 1. Mean values of the growth rate (div.·day^{-1}) of *Heterosigma akashiwo* when exposed to heavy metals at different concentrations (μg·L^{-1})

Day	0	Cd^{2+}		Pb^{2+}		Ni^{2+}		Fe^{2+}		Zn^{2+}	
		10	20	10	20	10	20	50	100	50	100
The third	0.31	0.34	0.31	**0.39**	0.35	**0.39**	0.35	**0.42**	**0.40**	0.27	0.28
The seventh	0.23	*0.17*	0.20	0.21	0.26	0.21	0.26	0.24	0.25	0.23	0.22

Note: values significantly higher than the control level ($p < 0.05$) are highlighted in bold; a value significantly lower than the control level is highlighted in italics.

Table 2. Mean values of the growth rate (div.·day^{-1}) of *Alexandrium affine* when exposed to heavy metals at different concentrations (μg·L^{-1})

Day	0	Cd^{2+}		Pb^{2+}		Ni^{2+}		Fe^{2+}		Zn^{2+}	
		10	20	10	20	10	20	50	100	50	100
The third	0.21	0.18	**0.33**	**0.36**	**0.36**	**0.45**	**0.37**	*0.03*	0.24	*0.11*	**0.41**
The seventh	0.13	*−0.16*	*−0.29*	*−0.01*	*0.05*	**0.21**	0.12	**0.27**	0.14	0.13	**0.23**

Note: values significantly higher than the control level ($p < 0.05$) are highlighted in bold; values significantly lower than the control level are highlighted in italics.

The growth rate of *P. foraminosum* at all analyzed metal concentrations was lower both on the third and seventh days compared to the control. However, on the seventh day of the experiment, with the addition of Fe^{2+}, stimulation of the microalga growth was recorded (Table 3).

Table 3. Mean values of the growth rate (div.·day^{-1}) of *Prorocentrum foraminosum* when exposed to heavy metals at different concentrations (μg·L^{-1})

Day	0	Cd^{2+}		Pb^{2+}		Ni^{2+}		Fe^{2+}		Zn^{2+}	
		10	20	10	20	10	20	50	100	50	100
The third	0.24	*0.05*	0.21	*0.12*	*0.10*	*0.08*	0.20	*−0.20*	*−0.33*	*−0.11*	*0.10*
The seventh	0.13	*0.05*	*0.01*	0.12	0.10	*0.01*	*−0.03*	0.16	0.24	0.13	0.06

Note: values significantly lower than the control level ($p < 0.05$) are highlighted in italics.

The toxicity of heavy metals for microalgae of different divisions has been shown repeatedly. It is related mostly to the fact that they cause oxidative stress resulting from an increase in abundance of free radicals. Due to damage to molecules by free radicals, physiological processes are violated, and this ultimately affects the viability of cells [Nagajoti et al., 2010].

Heavy metals are non-degradable; accordingly, their interaction with organisms remains constant throughout an experiment. In this case, a toxic effect may occur, and it was registered for *P. foraminosum* in our study. However, we recorded stimulation of growth with a further decrease in its intensity, *i. e.*, hormesis effect, for *H. akashiwo* in a medium containing lead, nickel, and iron and for *A. affine* in a medium containing cadmium, lead, nickel, and zinc. Hormesis is a two-phase, sometimes multi-phase, dose-dependent response of an organism to the effect of a chemical substance; it is characterized by periods of stimulation and suppression of various biological functions (growth intensity of the population of organisms changes as well). The manifestation of hormesis is driven by physiological characteristics of an organism. Usually, it occurs under the effect of concentrations lower than lethal ones [Calabrese, Mattson, 2011; Cedergreen et al., 2007].

In general, the studied species were more sensitive to the effect of all metals than other representatives of microalgae. Thus, inhibition of the growth rate in *Phaeocystis antarctica* population by 10% was revealed at a concentration of 135 μg·L^{-1} of Cd^{2+} and 260 μg·L^{-1} of Pb^{2+} [Gissi et al., 2015]. The growth rate of *Isochrysis galbana* rose at 50–100 μg·L^{-1} of Pb^{2+} [Ahmadi et al., 2021]. At the same time, *Ankistrodesmus falcatus* turned out to be a species close in its resistance to the effect of Ni^{2+}: its cell abundance decreased at metal concentrations of 15–30 μg·L^{-1} after just 24 h of the experiment [Martínez-Ruiz, Martínez-Jeronimo, 2015].

Conclusion. Heavy metals we tested affected all analyzed microalgae species. The most sensitive one was *Prorocentrum foraminosum*, and the least sensitive one was *Heterosigma akashiwo*. The growth rate of *H. akashiwo* increased with the addition of Cd^{2+}, Pb^{2+}, Ni^{2+}, and Fe^{2+}; the growth rate of *Alexandrium affine* rose in a medium containing Cd^{2+}, Pb^{2+}, Ni^{2+}, Fe^{2+}, and Zn^{2+}. Therefore, it can be assumed that the listed metals can affect the forming of blooms of these species.

This work was financed by the A. V. Zhirmunsky National Scientific Center of Marine Biology, FEB RAS, state research assignment FWFE-2024-0004 "Dynamics of marine ecosystems, adaptation of marine organisms and communities to environmental factors."

REFERENCES

1. *Marine Water Pollution.* Annual Report 2020 / A. Korshenko (Ed.). Moscow : Nauka, 2020, 200 p. (in Russ.)
2. *Rukovodstvo po opredeleniyu metodom biotestirovaniya toksichnosti vod, donnykh otlozhenii, zagryaznyayushchikh veshchestv i burovykh rastvorov* / Ministerstvo prirodnykh resursov Rossiiskoi Federatsii. Moscow : REFIA : NIA-Priroda, 2002, [60] p. (in Russ.)
3. Ahmadi Z. B., Taherizadeh M. R., Zadi M. Y. Effects of different concentrations of lead on growth, photosynthetic pigmentation and protein in micro alga *Isochrysis galbana*. *Journal of Oceanography*, 2021, vol. 12, iss. 46, pp. 109–116.
4. Anderson D. M., Alpermann T. J., Cembella A. D., Collos Y., Masseret E., Montresor M. The globally distributed genus *Alexandrium*: Multifaceted roles in marine ecosystems and impacts on human health. *Harmful Algae*, 2012, vol. 14, pp. 10–35. https://doi.org/10.1016/j.hal.2011.10.012
5. Calabrese E. J., Mattson M. P. Hormesis provides a generalized quantitative estimate of biological plasticity. *Journal of Cell Communication and Signaling*, 2011, vol. 5, iss. 1, pp. 25–38. https://doi.org/10.1007/s12079-011-0119-1
6. Cedergreen N., Streibig J. C., Kudsk P., Mathiassen S. K., Duke S. O. The occurrence of hormesis in plants and algae. *Dose-Response*, 2007, vol. 5, iss. 2, pp. 150–162. https://doi.org/10.2203/dose-response.06-008.Cedergreen
7. Dursun F., Taş S., Koray T. Spring bloom of the raphidophycean *Heterosigma akashiwo* in the Golden Horn Estuary at the northeast of Sea of Marmara. *Ege Journal of Fisheries and Aquatic Sciences*, 2016, vol. 33, iss. 3, pp. 201–207. https://doi.org/10.12714/egejfas.2016.33.3.03
8. Guillard R. R. L., Ryther J. H. Studies of marine planktonic diatoms. I. *Cyclotella nana* Hustedt, and *Detonula confervacea* (Cleve) Gran. *Canadian Journal of Microbiology*, 1962, vol. 8, no. 2, pp. 229–239. https://doi.org/10.1139/m62-029
9. Gissi F., Adams M. S., King C. K., Jolley D. F. A robust bioassay to assess the toxicity of metals to the Antarctic marine microalga *Phaeocystis antarctica*. *Environmental Toxicology and Chemistry*, 2015, vol. 34, iss. 7, pp. 1578–1587. https://doi.org/10.1002/etc.2949
10. Heisler J., Glibert P. M., Burkholder J. M., Anderson D. M., Cochlan W., Dennison W. C., Dortch Q., Gobler C. J., Heil C. A., Humphries E., Lewitus A., Magnien R., Marshall H. G.,

Sellner K., Stockwell D. A., Stoecker D. K., Suddleson M. Eutrophication and harmful algal blooms: A scientific consensus. *Harmful Algae*, 2008, vol. 8, iss. 1, pp. 3–13. https://doi.org/10.1016/j.hal.2008.08.006

11. Li M., Zhang F., Glibert P. M. Seasonal life strategy of *Prorocentrum minimum* in Chesapeake Bay, USA: Validation of the role of physical transport using a coupled physical–biogeochemical–harmful algal bloom model. *Limnology and Oceanography*, 2021, vol. 66, iss. 11, pp. 3873–3886. https://doi.org/10.1002/lno.11925
12. Martínez-Ruiz E. B., Martínez-Jeronimo F. Nickel has biochemical, physiological, and structural effects on the green microalga *Ankistrodesmus falcatus*: An integrative study. *Aquatic Toxicology*, 2015, vol. 169, pp. 27–36. https://doi.org/10.1016/j.aquatox.2015.10.007
13. Nagajoti P. C., Lee K. D., Sreekanth T. V. M. Heavy metals, occurrence and toxicity for plants: A review. *Environmental Chemistry Letters*, 2010, vol. 8, iss. 3, pp. 199–216. https://doi.org/10.1007/s10311-010-0297-8
14. Shin H. H., Li Z., Mertens K. N., Seo M. H., Gu H., Lim W. A., Yoon Y. H., Soh H. Y., Matsuoka K. *Prorocentrum shikokuense* Hada and *P. donghaiense* Lu are junior synonyms of *P. obtusidens* Schiller, but not of *P. dentatum* Stein (Prorocentrales, Dinophyceae). *Harmful Algae*, 2019, vol. 89, art. no. 101686 (14 p.). https://doi.org/10.1016/j.hal.2019.101686

ДЕЙСТВИЕ ТЯЖЁЛЫХ МЕТАЛЛОВ НА СКОРОСТЬ РОСТА МИКРОВОДОРОСЛЕЙ *HETEROSIGMA AKASHIWO*, *ALEXANDRIUM AFFINE* И *PROROCENTRUM FORAMINOSUM*

Ж. В. Маркина[1], А. В. Огнистая[1,2]

[1]Национальный научный центр морской биологии имени А. В. Жирмунского, Владивосток, Российская Федерация

[2]Дальневосточный федеральный университет, Владивосток, Российская Федерация

E-mail: *alya_lokshina@mail.ru*

Увеличение частоты вредоносных цветений водорослей связывают с растущим загрязнением окружающей среды, в частности с повышением содержания тяжёлых металлов в водах. Цель работы — оценить влияние тяжёлых металлов на скорость роста микроводорослей, вызывающих такие цветения. Изучено действие ионов кадмия Cd^{2+}, свинца Pb^{2+} и никеля Ni^{2+} в концентрациях 10 и 20 мкг·л$^{-1}$, а также цинка Zn^{2+} и железа Fe^{3+} в концентрациях 50 и 100 мкг·л$^{-1}$ на скорость роста микроводорослей *Heterosigma akashiwo*, *Alexandrium affine* и *Prorocentrum foraminosum*. Оценка выполнена на третьи и седьмые сутки опыта. Выявлено, что эти тяжёлые металлы оказывали влияние на все изученные виды водорослей. На третьи сутки скорость роста *H. akashiwo* увеличивалась при добавлении Cd^{2+}, Pb^{2+}, Ni^{2+} и Fe^{3+}; подавление роста обнаружено при внесении Zn^{2+}. На седьмые сутки ингибирование микроводоросли выявлено при содержании 10 и 20 мкг·л$^{-1}$ Cd^{2+}, 10 мкг·л$^{-1}$ Pb^{2+} и Ni^{2+}, а также 100 мкг·л$^{-1}$ Zn^{2+}. Стимуляция *H. akashiwo* происходила при 20 мкг·л$^{-1}$ Pb^{2+} и Ni^{2+}, 50 и 100 мкг·л$^{-1}$ Fe^{3+}. Скорость роста *A. affine* на третьи сутки увеличивалась при 20 мкг·л$^{-1}$ Cd^{2+}, 10 и 20 мкг·л$^{-1}$ Pb^{2+} и Ni^{2+}, а также 100 мкг·л$^{-1}$ Fe^{2+} и Zn^{2+}. На седьмые сутки рост уменьшался в результате негативного влияния 10 и 20 мкг·л$^{-1}$ Cd^{2+} и Pb^{2+} и 20 мкг·л$^{-1}$ Ni^{2+}. Стимуляция роста водоросли зафиксирована при 10 мкг·л$^{-1}$ Ni^{2+}, а также при обеих концентрациях Fe^{3+} и Zn^{2+}. Наименее устойчивым к тяжёлым металлам оказался вид *P. foraminosum*. Его скорость роста снижалась при воздействии всех токсикантов, за исключением Fe^{3+}: в данном случае происходила стимуляция роста микроводоросли на седьмой день эксперимента.

Ключевые слова: *Heterosigma akashiwo*, *Alexandrium affine*, *Prorocentrum foraminosum*, кадмий, никель, свинец, цинк, железо, тяжёлые металлы

ISSN 2499-9768
25003
9 772499 976005 >

Вниманию читателей!

Зоологический институт РАН,
Институт биологии южных морей
имени А. О. Ковалевского РАН

издают
научный журнал

Морской биологический журнал
Marine Biological Journal

- МБЖ — периодическое издание открытого доступа. Подаваемые материалы проходят независимое двойное слепое рецензирование. Журнал публикует обзорные и оригинальные научные статьи, краткие сообщения и заметки, содержащие новые данные теоретических и экспериментальных исследований в области морской биологии, материалы по разнообразию морских организмов, их популяций и сообществ, закономерностям распределения живых организмов в Мировом океане, результаты комплексного изучения морских и океанических экосистем, антропогенного воздействия на морские организмы и экосистемы.
- Целевая аудитория: биологи, экологи, биофизики, гидро- и радиобиологи, океанологи, географы, учёные других смежных специальностей, аспиранты и студенты соответствующих научных и отраслевых профилей.
- Статьи публикуются на русском и английском языках.
- Периодичность — четыре раза в год.
- Подписной индекс в каталоге «Пресса России» — Е38872. Цена свободная.

Заказать журнал

можно в научно-информационном отделе ИнБЮМ.
Адрес: ФГБУН ФИЦ «Институт биологии южных морей имени А. О. Ковалевского РАН», пр-т Нахимова, 2, г. Севастополь, 299011, Российская Федерация.
Тел.: +7 8692 54-06-49.
E-mail: *mbj@imbr-ras.ru*.

Zoological Institute of RAS,
A. O. Kovalevsky Institute of Biology
of the Southern Seas of RAS

publish
scientific journal

Морской биологический журнал
Marine Biological Journal

- MBJ is an open access, peer reviewed (double-blind) journal. The journal publishes original articles as well as reviews and brief reports and notes focused on new data of theoretical and experimental research in the fields of marine biology, diversity of marine organisms and their populations and communities, patterns of distribution of animals and plants in the World Ocean, the results of a comprehensive studies of marine and oceanic ecosystems, anthropogenic impact on marine organisms and on the ecosystems.
- Intended audience: biologists, ecologists, biophysicists, hydrobiologists, radiobiologists, oceanologists, geographers, scientists of other related specialties, graduate students, and students of relevant scientific profiles.
- The articles are published in Russian and English.
- The journal is published four times a year.
- The subscription index in the “Russian Press” catalogue is E38872. The price is free.

You may order the journal

in the scientific information department of IBSS.
Address: A. O. Kovalevsky Institute of Biology of the Southern Seas of RAS, 2 Nakhimov avenue, Sevastopol, 299011, Russian Federation.
Tel.: +7 8692 54-06-49.
E-mail: *mbj@imbr-ras.ru*.